frontiers | Research Topics

Pathogenesis, diagnostics, treatments of *Mycobacterium tuberculosis* and its co-infection with HIV or SARS-CoV-2

Edited by
Amit Singh and Divakar Sharma

Published in
Frontiers in Cellular and Infection Microbiology
Frontiers in Immunology

ISSN 1664-8714
ISBN 978-2-8325-4388-7
DOI 10.3389/978-2-8325-4388-7

About Frontiers

Frontiers is more than just an open access publisher of scholarly articles: it is a pioneering approach to the world of academia, radically improving the way scholarly research is managed. The grand vision of Frontiers is a world where all people have an equal opportunity to seek, share and generate knowledge. Frontiers provides immediate and permanent online open access to all its publications, but this alone is not enough to realize our grand goals.

Frontiers journal series

The Frontiers journal series is a multi-tier and interdisciplinary set of open-access, online journals, promising a paradigm shift from the current review, selection and dissemination processes in academic publishing. All Frontiers journals are driven by researchers for researchers; therefore, they constitute a service to the scholarly community. At the same time, the *Frontiers journal series* operates on a revolutionary invention, the tiered publishing system, initially addressing specific communities of scholars, and gradually climbing up to broader public understanding, thus serving the interests of the lay society, too.

Dedication to quality

Each Frontiers article is a landmark of the highest quality, thanks to genuinely collaborative interactions between authors and review editors, who include some of the world's best academicians. Research must be certified by peers before entering a stream of knowledge that may eventually reach the public - and shape society; therefore, Frontiers only applies the most rigorous and unbiased reviews. Frontiers revolutionizes research publishing by freely delivering the most outstanding research, evaluated with no bias from both the academic and social point of view. By applying the most advanced information technologies, Frontiers is catapulting scholarly publishing into a new generation.

What are Frontiers Research Topics?

Frontiers Research Topics are very popular trademarks of the *Frontiers journals series*: they are collections of at least ten articles, all centered on a particular subject. With their unique mix of varied contributions from Original Research to Review Articles, Frontiers Research Topics unify the most influential researchers, the latest key findings and historical advances in a hot research area.

Find out more on how to host your own Frontiers Research Topic or contribute to one as an author by contacting the Frontiers editorial office: frontiersin.org/about/contact

Pathogenesis, diagnostics, treatments of *Mycobacterium tuberculosis* and its co-infection with HIV or SARS-CoV-2

Topic editors
Amit Singh — Central University of Punjab, India
Divakar Sharma — University of Delhi, India

Citation
Singh, A., Sharma, D., eds. (2024). *Pathogenesis, diagnostics, treatments of Mycobacterium tuberculosis and its co-infection with HIV or SARS-CoV-2*. Lausanne: Frontiers Media SA. doi: 10.3389/978-2-8325-4388-7

Table of contents

frontiers | Frontiers in Cellular and Infection Microbiology

TYPE Editorial
PUBLISHED 18 January 2024
DOI 10.3389/fcimb.2024.1359356

OPEN ACCESS

EDITED AND REVIEWED BY
Nahed Ismail,
University of Illinois Chicago, United States

*CORRESPONDENCE
Divakar Sharma
divakarsharma88@gmail.com
Amit Singh
amit.singh@cup.edu.in

RECEIVED 21 December 2023
ACCEPTED 10 January 2024
PUBLISHED 18 January 2024

CITATION
Sharma D and Singh A (2024) Editorial: Pathogenesis, diagnostics, treatments of *Mycobacterium tuberculosis* and its co-infection with HIV or SARS-CoV-2. *Front. Cell. Infect. Microbiol.* 14:1359356. doi: 10.3389/fcimb.2024.1359356

Editorial: Pathogenesis, diagnostics, treatments of *Mycobacterium tuberculosis* and its co-infection with HIV or SARS-CoV-2

Divakar Sharma[1]* and Amit Singh[2]*

[1]Department of Microbiology, Lady Hardinge Medical College, Delhi University, Delhi, India, [2]Department of Microbiology, Central University of Punjab, Bathinda, Punjab, India

KEYWORDS

antimicrobial resistance, tuberculosis, co-infection, HIV, SARS-CoV-2

Editorial on the Research Topic

Pathogenesis, diagnostics, treatments of *Mycobacterium tuberculosis* and its co-infection with HIV or SARS-CoV-2

In this Research Topic of Frontiers in Cellular and Infection Microbiology and Frontiers in Immunology, we edited a collection of eight original research articles and one case report within the theme "*Pathogenesis, Diagnostics, Treatments of Mycobacterium tuberculosis and It's Co-Infection with HIV or SARS-CoV-2*." The major goal of this Research Topic was to gather the updated view of the modern approaches used for the early diagnosis, treatment and pathogenesis mechanisms of *M. tuberculosis* and its co-infection with HIV or SARS-CoV-2, which ultimately delivered the updated view on technologies and their applications for the management of these co-infections. *Mycobacterium tuberculosis* is the major cause of tuberculosis (TB) disease across the globe. One-fourth of the world's population is infected with TB asymptomatically. Longer regimen of anti-TB drugs (leading to poor adherence and treatment), interrupted anti-TB drugs treatment (incomplete anti-TB treatment), and ineffectiveness of the anti-TB drugs due to the re-emergence of latent TB infections are major issues that hindrance to achieving the end of the global TB epidemic by 2035 as WHO plans. The emergence of drug-resistant *Mycobacterium tuberculosis* and co-infections with HIV as well as SARS-CoV-2 poses a serious threat to global health agencies. It was reported that the TB cases in India and other endemic countries are 2-3 times higher than in the last few years. Bacteria have acquired different mechanisms and became multidrug-resistant by various mechanisms like alternation in the target site, over expression of efflux pumps, inactivation of drugs by enzymes and biofilms (Singh et al., 2015). These mechanisms adopted by bacteria and longer anti-tuberculosis treatment regimens are the greatest threat in TB control programs especially in malnourished, immune-compromised, *Mycobacterium tuberculosis* co-infection with HIV and SARS-CoV-2 in developing countries. The incidence of infectious diseases like Tuberculosis & its drug resistant forms, and co-infection with HIV & SARS-CoV-2 are high and often cause critical illness, which seriously threatens human life and health. In this editorial, we have focus on this thematic issue and discussed the edited papers, which help to culminate this serious problem.

Early diagnosis of mycobacterium is crucial for the management of clinical tuberculosis. Li et al. evaluated and validated the diagnostic performance like sensitivity, specificity, and accuracy of the nucleotide matrix-assisted laser desorption time-of-flight mass spectrometry (MALDI-TOF-MS) for identification of mycobacterium species. They analyzed 108 samples, and found the 96.91% sensitivity, and 100% specificity of the nucleotide MALDI-TOF-MS in mycobacterial identification and the lower limit of detection was 50 bacteria/mL. For validation of *Mycobacterium tuberculosis* diagnosis they have compared the sensitivity and specificity of MALDI-TOF-MS (72.7%, 100%), to the Gene-Xpert (63.6%, 100%), culture (54.5%, 100%), and AFS (27.3%, 100%). Further they have suggested that the optimized nucleotide MALDI-TOF-MS has higher sensitivity, and specificity at lower limit of detection in mycobacterial identification, and would considered as a potential assay for identification.

Tang et al. evaluated the Interferon-inducible protein 10 (IP-10) m-RNA release assay for the diagnosis of TB in patients with HIV co-infection and efficacy compared to the Interferon gamma release assays (IGRAs) test (QFT-GIT). The IP-10 mRNA release assay was significantly higher sensitive than that of QFT-GIT test, because IP-10 mRNA release assay is less dependent on CD4+ T cells count (a well stated attribute of HIV-infected patients) than QFT-GIT test. Therefore, this study suggested that *M.tuberculosis* specific IP-10 mRNA is considered as a better biomarker for diagnosis of TB in patients with HIV co-infection.

Xu et al. compared the diagnostic performance of laboratory assays like GeneXpert, culture, and T-SPOT.TB (T-SPOT) on the ultrasound-guided core needle biopsy samples for diagnosis of extra-pulmonary tuberculosis (EPTB) in HIV-positive and HIV-negative patients. For ultrasound-guided core needle biopsy samples, GeneXpert (Xpert) showed higher sensitivity and specificity than culture and T-SPOT.TB (T-SPOT), which suggested the superior performance of GeneXpert as compared to other method in diagnosing EPTB across HIV status and sample types.

Hu et al. reported the diagnostic efficacy of the QuantiFERON-TB Gold In-Tube (QFT-GIT) test for the preoperative differential diagnosis of spinal tuberculosis. They have analyzed the patients with spinal tuberculosis by the QFT-GIT test and found the sensitivity and the specificity were 92.16% and 67.14% respectively. They have increased the accuracy of diagnostic QFT-GIT test from 77.42% to 80.65% when a new threshold (1.58 IU/mL) assigned for the study cohort and suggested that the intensity of the QFT-GIT test findings in spinal tuberculosis may be related to the duration of a patient's disease.

In a study, Singh et al. accessed the distribution of *M.tuberculosis* genotypes among HIV-positive and HIV-negative patients suspected to tuberculosis at the National Institute of Tuberculosis and Respiratory Diseases, New Delhi, a tertiary care dedicated TB hospital. They screened the 503 subjects for pulmonary and extra-pulmonary tuberculosis, and found 276 *M. tuberculosis* culture positive. Genotyping data revealed that most prevalent lineage was Central Asian Strain (CAS) genotype followed by Beijing genotype among HIV-positive and HIV-negative patients. Through in this study they reported that predominance of Beijing genotype was almost double (22.5%) in HIV-positive as compare to the HIV-negative (10.9%), which suggest the high transmissibility of these genotypes in the community.

In another study, de Sa et al. investigated the relationship between from single nucleotide polymorphisms (SNPs) of the NLRP3, CARD8, AIM2, CASP-1, IFI16, and IL-1b inflammasome genes, as well as the profiles of secreted pro-inflammatory cytokines (e.g., IL-1b, IL-18, IL-33, and IL-6) with the TB clinical profiles, TB-HIV co-infection, and IRIS onset. TT genotype in NLRP3 rs4612666 and C-C-T-G-C NLRP3 haplotype polymorphisms were associated with the increased risk for EPTB, however increased levels of IL-6 or IL-33 and IL-18 or IL-33 were found in TB patients both without and with HIV carrying the minor frequency allele NLRP3 polymorphisms. Therefore, this study depicted the association of genetic polymorphisms (Single or multiple) of crucial genes of innate immunity as well as pro-inflammatory cytokines in the clinical outcomes related to co-infections like TB-HIV.

Weng et al. presented a case report on disseminated tuberculosis in a child during the COVID-19 pandemic and hypothesized that COVID-19 infection created immunosuppressive effect with possible implications for tuberculosis dissemination. Further they suggested that more significant research to be needed for better diagnosis and treatment options for the co-infection of *M. tuberculosis* and SARS-CoV-2.

Huang et al. elucidated the common processes and pathways between COVID-19 and TB pathogenesis through bioinformatics and system biology approaches. They used RNA-seq datasets (GSE196822 and GSE126614) and identified differentially expressed genes (DEGs) IFI44L, ISG15, MX1, IFI44, OASL, RSAD2, GBP1, OAS1, IFI6, and HERC5. Further they identified some potential drugs (suloctidil, prenylamine, acetohexamide, terfenadine, prochlorperazine, 3′-azido-3′-deoxythymidine, chlorophyllin, etoposide, clioquinol, and propofol), which to be proposed as alternative treatment strategy for TB and COVID-19, after their validation by future research.

In conclusion, this Research Topic includes several excellent studies summarizing the latest advances in the diagnosis and therapeutics of pulmonary tuberculosis, extra-pulmonary tuberculosis co-infection with HIV and SARS-CoV-2. This Research Topic will promote the integration of the advanced approaches (genomics, transcriptomics, proteomics and bioinformatics) for the development of superior diagnostics and therapeutics, in future, which would be used in the management of tuberculosis, and co-infection with HIV and SARS-CoV-2 (Sharma et al, 2020). Finally, to fight with these pandemics (TB, COVID-19 and HIV) developing new diagnostic approaches should consider the economic component of low and middle-income countries for universal equality and one health world.

Author contributions

DS: Conceptualization, Supervision, Writing – original draft, Writing – review & editing. AS: Writing – review & editing.

Acknowledgments

Editors are highly thankful to frontiers for accepting our proposal and providing an opportunity to edit the manuscripts in the journal of international repute. Such a platform will encourage the upcoming researchers to contribute to TB-HIV and COVID-19 research and create awareness about the disease proposal.

Conflict of interest

The authors declare that the research was conducted in the absence of any commercial or financial relationships that could be construed as a potential conflict of interest.

Publisher's note

References

Sharma, D., Sharma, S., and Sharma, J. (2020). Potential strategies for the management of drug-resistant tuberculosis. *J. Global Antimicrobial Resistance* 22, 210–214.

Singh, A., Gopinath, K., Sharma, P., Bisht, D., Sharma, P., Singh, N., et al. (2015). Comparative proteomic analysis of sequential isolates of Mycobacterium tuberculosis from a patient with pulmonary tuberculosis turning from drug sensitive to multidrug resistant. *Indian J. Med. Res.* 141, 27–45.

frontiers | Frontiers in Cellular and Infection Microbiology

TYPE Original Research
PUBLISHED 20 September 2022
DOI 10.3389/fcimb.2022.983579

OPEN ACCESS

EDITED BY
Amit Singh,
All India Institute of Medical Sciences, India

REVIEWED BY
Manjunatha Venkataswamy,
National Institute of Mental Health and Neurosciences (NIMHANS), India
Ritesh Thakare,
Brown University, United States

*CORRESPONDENCE
Qile Gao
gaoql@csu.edu.cn

SPECIALTY SECTION
This article was submitted to Clinical Microbiology, a section of the journal Frontiers in Cellular and Infection Microbiology

RECEIVED 01 July 2022
ACCEPTED 05 September 2022
PUBLISHED 20 September 2022

CITATION
Hu X, Zhang H, Li Y, Zhang G, Tang B, Xu D, Tang M, Guo C, Liu S and Gao Q (2022) Analysis of the diagnostic efficacy of the QuantiFERON-TB Gold In-Tube assay for preoperative differential diagnosis of spinal tuberculosis. *Front. Cell. Infect. Microbiol.* 12:983579. doi: 10.3389/fcimb.2022.983579

Analysis of the diagnostic efficacy of the QuantiFERON-TB Gold In-Tube assay for preoperative differential diagnosis of spinal tuberculosis

Xiaojiang Hu[1,2], Hongqi Zhang[1,2], Yanbin Li[2,3], Guang Zhang[1,2], Bo Tang[1,2], Dongcheng Xu[1,2], Mingxing Tang[1,2], Chaofeng Guo[1,2], Shaohua Liu[1,2] and Qile Gao[1,2]*

[1]Department of Spine Surgery and Orthopaedics, Xiangya Hospital, Central South University, Changsha, China, [2]National Clinical Research Center for Geriatric Disorders, Xiangya Hospital, Central South University, Changsha, China, [3]Department of Clinical Laboratory, Xiangya Hospital, Central South University, Changsha, China

Background: Differential diagnosis of spinal tuberculosis is important for the clinical management of patients, especially in populations with spinal bone destruction. There are few effective tools for preoperative differential diagnosis in these populations. The QuantiFERON-TB Gold In-Tube (QFT-GIT) test has good sensitivity and specificity for the diagnosis of tuberculosis, but its efficacy in preoperative diagnosis of spinal tuberculosis has rarely been investigated.

Method: A total of 123 consecutive patients with suspected spinal tuberculosis hospitalized from March 20, 2020, to April 10, 2022, were included, and the QFT-GIT test was performed on each patient. We retrospectively collected clinical data from these patients. A receiver operating characteristic (ROC) curve was plotted with the TB Ag-Nil values. The cutoff point was calculated from the ROC curve of 61 patients in the study cohort, and the diagnostic validity of the cutoff point was verified in a new cohort of 62 patients. The correlations between TB Ag-Nil values and other clinical characteristics of the patients were analyzed.

Results: Of the 123 patients included in the study, 51 had confirmed tuberculosis, and 72 had non-tuberculosis disease (AUC=0.866, 95% CI: 0.798-0.933, P<0.0001). In patients with spinal tuberculosis, the QFT-GIT test sensitivity was 92.16% (95% CI: 80.25%-97.46%), and the specificity was 67.14% (95% CI: 54.77%-77.62%). The accuracy of diagnostic tests in the validation cohort increased from 77.42% to 80.65% when a new cutoff point was selected (1.58 IU/mL) from the ROC curve of the study cohort. The TB Ag-Nil values in tuberculosis patients were correlated with the duration of the patients' disease (r=0.4148, P=0.0025).

Conclusion: The QFT-GIT test is an important test for preoperative differential diagnosis of spinal tuberculosis with high sensitivity but low specificity. The

diagnostic efficacy of the QFT-GIT test can be significantly improved *via* application of a new threshold (1.58 IU/mL), and the intensity of the QFT-GIT test findings in spinal tuberculosis may be related to the duration of a patient's disease.

KEYWORDS

spinal tuberculosis, QuantiFERON-TB Gold In-Tube (QFT-GIT), QFT-GIT, interferon-gamma release tests, IGRAs. ROC curve, disease duration, T-SPOT.TB

1 Introduction

Spinal tuberculosis is a secondary infection caused by *Mycobacterium tuberculosis* and accounts for approximately 50% of all bone tuberculosis cases. *M.tuberculosis* can be transmitted to the spine by blood and lymphatic transmission from pulmonary tuberculosis, but it is also commonly seen in the spread of tuberculosis of the bladder, kidney, etc. More than 100,000 people are diagnosed with spinal tuberculosis each year worldwide, and China is a high-burden country for tuberculosis (Dunn and Ben Husien, 2018; Harding, 2020). The symptoms of spinal tuberculosis are often not obvious in the early stages and therefore often do not attract the attention of patients. Spinal tuberculosis can have serious consequences, such as kyphosis, spinal cord injury, and, in 10-30% of patients, even paraplegia. Therefore, early diagnosis and regular antituberculosis treatment are of great importance for improving the prognosis of patients with spinal tuberculosis (Go et al., 2012; Wang et al., 2020). Currently, spinal tuberculosis is often diagnosed on the basis of postoperative microbial culture (Perronne et al., 1994), the GeneXpert MTB/RIF system (Patel et al., 2020; Qi et al., 2022), and metagenomic next-generation sequencing (mNGS) (Shi et al., 2020; Sun et al., 2021). These diagnostic techniques require invasive tests or open surgery to obtain specimens, often delaying the patient's confirmation of the diagnosis. The diagnostic efficacy of many preoperative tests is unsatisfactory: the CT, MRI, and other imaging techniques used are very similar to those used for pyogenic spinal infections, spinal brucellosis, and spinal tumors, and it is often difficult to distinguish these diseases by imaging (Kanna et al., 2019; Miyamoto and Akagi, 2019; Shroyer et al., 2021). While serologic indices such as white blood cell count (WBC), erythrocyte sedimentation rate (ESR), C-reactive protein (CRP), and procalcitonin (PCT) have been shown to play significant roles in differentiating active tuberculosis from non-tuberculosis, they lack specificity in differential diagnosis of spinal tuberculosis. Therefore, there is an urgent clinical need for a valuable diagnostic method for differential diagnosis of spinal tuberculosis in the preoperative period (Chen et al., 2016).

Currently, early diagnosis of *M. Tuberculosis* infection can be made using the tuberculin skin test (TST), which determines the status of tuberculosis *via* intradermal injection of purified protein derivatives from *M. Tuberculosis* strains. However, the TST has its limitations: age, smoking, diabetes, and BCG vaccination can cause false-positives in the TST and affect the determination of the results (Lu et al., 2021). In addition, interferon-gamma (IFN-γ) release assays (IGRAs) can be used to diagnose tuberculosis (Cho et al., 2010). IGRAs include common assays such as the T-SPOT.TB test, the QuantiFERON-TB Gold In-Tube (QFT-GIT) test, and the QuantiFERON-TB Gold Plus assay (Hamada et al., 2021). In China, a relatively widely used method is the T-SPOT.TB test, which assesses the presence of tuberculosis by stimulating T cells with the *M. Tuberculosis*-specific antigens ESAT-6 and CFP-10 and determining the numbers of spots obtained by the reaction. The QFT-GIT has demonstrated higher sensitivity than the T-SPOT.TB test in many studies (Harada et al., 2008). The QFT-GIT test is an immunological method for the diagnosis of tuberculosis that uses an enzyme-linked immunosorbent assay (ELISA) to detect the levels of IFN-γ produced upon stimulation with the tuberculosis-specific antigens ESAT-6, CFP-10, and TB7.7, which are specifically expressed by *M.tuberculosis* and all BCG strains and the majority of non-tubercle bacteria do not contain these antigens. The immune response to *M. Tuberculosis* is calculated by subtracting the background level from the stimulation level (TB Ag-Nil), which informs the diagnosis of tuberculosis (Shafeque et al., 2020)

The QFT-GIT test has been widely used in the clinical diagnosis of pulmonary tuberculosis (Lu et al., 2021) and has shown good sensitivity and specificity for this application, but its diagnostic efficacy for spinal tuberculosis is unclear (Harada et al., 2008). Unlike pulmonary tuberculosis, spinal tuberculosis is mainly caused by hematogenous dissemination of tuberculosis bacilli and needs to be clinically differentiated from pyogenic infection of the spine, brucellosis infection of the spine, and spinal tumors (Perronne et al., 1994). Studies have shown that diseases such as septic infections and cancers may also cause a nonspecific increase in INF-γ, resulting in false-positive results

in the T-SPOT.TB and QFT-GIT tests (Choi et al., 2018). Therefore, the sensitivity and specificity of the QFT-GIT test in the diagnosis of spinal tuberculosis differs from that in the diagnosis of pulmonary tuberculosis, and a more appropriate diagnostic threshold is needed for differential diagnosis of spinal tuberculosis using the QFT-GIT test. In this study, we analyzed 123 patients with suspected spinal tuberculosis through a multicenter retrospective study. Based on the final diagnoses of the patients, we analyzed the sensitivity and specificity of the QFT-GIT test, plotted receiver operating characteristic (ROC) curves from the TB Ag-Nil values to find a suitable cutoff point for spinal tuberculosis, and analyzed the diagnostic efficacy of the adjusted cutoff point to improve the diagnostic efficacy of the QFT-GIT test in spinal tuberculosis. Finally, we correlated the TB Ag-Nil values of the QFT-GIT test with other clinical data of the patients to find a clinical indicator that may be correlated with the results of the QFT-GIT test in tuberculosis patients. We hope that this study will provide a relevant basis for the early diagnosis of patients with spinal tuberculosis.

2 Method

2.1 Study design

2.1.1 Inclusion and exclusion criteria

A total of 123 patients with suspected spinal tuberculosis who were hospitalized at Xiangya Hospital, Xiangya Boai Hospital, Changsha First Hospital and Hunan Chest Hospital from March 20, 2020, to the present were selected. The inclusion criteria were as follows: 1. patients who were able to be diagnosed with tuberculosis or non-tuberculosis according to diagnostic criteria, and **2**. patients who were admitted for QFT-GIT testing. The exclusion criteria were as follows: 1. patients without QFT-GIT testing, 2. patients with autoimmune diseases, 3. patients with HIV infection, 4. patients with multiple infections, and 5. patients with severe underlying comorbid diseases. The Ethics Committee of Xiangya Hospital, Central South University, approved the implementation of this study (Ethical review number:201303232), and all enrolled subjects and their families gave written informed consent to the conduct of the study.

2.1.2 Diagnostic criteria

According to the 2021 WHO guidelines for tuberculosis, the criteria for diagnosing spinal tuberculosis in this study were 1. a positive culture for *M. Tuberculosis*, 2. a positive Xpert result, 3. presence in an area with a high prevalence of tuberculosis meeting the appropriate histological features (containing at least one of the following three characteristics: caseous necrosis, granulomatous inflammation, and positive antacid staining) and effective antituberculosis treatment, and 4. detection of *M. Tuberculosis* genes in patient lesion specimens *via* mNGS (Sun et al., 2021). The criteria for diagnosing non-tuberculosis were as follows: 1. proof of other types of microbial infection by microbiological culture, PCR or mNGS; 2. pathological diagnosis of cancer or chronic septic inflammation (Coleman, 2006); and 3. no combination of pulmonary or other extrapulmonary tuberculosis.

2.2 QuantiFERON-TB Gold In-Tube test

A QFT-GIT test kit was purchased from QIAGEN (USA). The QFT-GIT test is used for *in vitro* qualitative detection of *M. Tuberculosis*-specific T-cell immunoreactivity in fresh anticoagulated human peripheral venous blood. After collecting a patient's venous blood with an anticoagulation tube according to the kit instructions, the whole blood was added to three blood culture tubes, a blank control tube (Nil), a tuberculosis antigen tube (TB Ag) and a mitogen-positive control tube (Mitogen), each containing the *Mycobacterium tuberculosis*-specific antigens ESAT-6, CFP-10 and TB7.7 (p4). The whole blood was incubated in blood culture tubes at 37°C for 16-24 hours. Subsequently, the blood culture tubes were centrifuged, the plasma was collected, and the IFN-γ (IU/mL) content was determined by ELISA. The IFN-γ content of the TB Ag tube was subtracted from that of the Nil control tube and was determined to be positive if TB Ag-Nil ≥ 0.35 IU/mL. Due to the limited linear range of the ELISA standard curve, values greater than 10 IU/mL were defined as 10 IU/mL (Nikitina et al., 2016). The Mitogen and Nil wells were used for quality control of the results.

2.3 Statistical analysis

The sample data were statistically analyzed using SPSS 20.0 software and GraphPad Prism 9. The gender compositions and the proportions of patients with other comorbid diseases in the two groups were compared by chi-square test. The patients' ages, BMI values, and WBC values conforming to a normal distribution are described using the mean ± standard deviation and were compared between groups *via* independent-sample t test. The duration of patients' disease and the variables with nonnormal distributions such as patient course and C-reactive protein (CRP), erythrocyte sedimentation rate(ESR), and TB Ag-Nil values are described using the median and percentiles and were compared between groups *via* nonparametric rank sum test. Correlation analysis was performed using Spearman's rho test. The results of the tests are expressed as P values, and $P < 0.05$ indicated a significant difference between the two groups. The results of the diagnostic tests were calculated on the website http://vassarstats.net/clin1.html#return. All figures in this paper were drawn using GraphPad Prism 9.0.

3 Results

3.1 Patient characteristics

We retrospectively collected data on 123 patients with suspected preoperative spinal tuberculosis from March 20, 2020, to April 10, 2022, at Xiangya Hospital, Xiangya Boai Hospital, Changsha First Hospital and Hunan Chest Hospital and identified 51 patients with tuberculosis and 72 patients without tuberculosis according to our diagnostic criteria. We used all patients in the period from March 20, 2020, to April 1, 2021, as the study cohort and used the patients admitted from April 2, 2021, to April 10, 2022, as the validation cohort. The study cohort contained 28 patients with tuberculosis and 33 patients with non-tuberculosis disease; the validation cohort contained 23 patients with tuberculosis and 39 patients with non-tuberculosis disease. The general characteristics of the two groups of patients are shown in Table 1; there were no significant differences in any characteristics between the study cohort patients and the validation cohort patients.

3.2 QFT-GIT test diagnostic efficacy

We plotted a ROC curve according to the final diagnosis and TB Ag-Nil values in 123 patients (Figure 1A) and found that the QFT-GIT test showed good diagnostic efficacy with an area under the curve (AUC)=0.866 (95% CI: 0.798-0.933, P<0.0001) in patients with spinal tuberculosis. The specific results are shown in Table 2. The sensitivity of the QFT-GIT test was 92.16% (95% CI: 80.25%-97.46%), the specificity was 67.14% (95% CI: 54.77%-77.62%), the positive predictive value was 67.14% (95% CI: 54.77%-77.62%), the negative predictive value was 92.45% (95% CI. 80.93%-97.55%), the positive likelihood ratio was 2.885 (95% CI: 2.040-4.080), the negative likelihood ratio was 0.115 (95% CI: 0.044-0.299), and the accuracy of the diagnostic test was 78.05%. We divided the 123 patients into a learning cohort and a validation cohort according to time, and the results and ROC curves of the respective diagnostic tests for both cohorts are also shown in Table 2 and Figure 1. We observed significantly higher TB Ag-Nil values in the tuberculosis group than in the NTB group for all patients and for the two cohorts (learning and validation) (Figures 1B–D).

3.3 Diagnostic efficacy based on an adjusted cutoff point

We found a new cutoff point (1.58 IU/mL) from the ROC curve of 61 patients in the study cohort and determined whether the QFT-GIT test result was negative or positive based on the adjusted cutoff point in 62 patients in the validation cohort. The results of the diagnostic test are shown in Table 2. The sensitivity was reduced from 86.96% (95% CI: 65.33% -96.57%) -96.57%) to 73.91% (95% CI: 51.31%-88.92%); however, at the same time, the specificity increased from 71.79% (95% CI: 54.90%-84.45%) to 84.62% (95% CI: 68.79%-93.59). Using the adjusted cutoff value, the accuracy of the diagnostic test increased from 77.42% to 80.65% (Table 2).

TABLE 1 The clinical characteristics of recruited patients in two independent cohorts.

	Study cohort		P#	Validation cohort		P&	P$
	TB (28)	NTB (33)		TB (23)	NTB (39)		
Age, years	53.93 ± 16.51	56.67 ± 13.41	0.478	53.57 ± 16.28	53.33 ± 13.58	0.952	0.454
Sex, male, %	16 (57)	19 (58)	0.973	14 (61)	25 (64)	0.799	0.531
Course, days	105 (45,180)	60 (42,135)	0.382	90 (30,210)	60 (30,150)	0.542	0.345
BMI, kg/m^2	22.71 ± 3.06	22.72 ± 3.72	0.989	21.51 ± 4.26	22.06 ± 3.99	0.689	0.256
Diabetes	1	4	0.363	0	5	0.148	1.000
Hypohepatia	2	3	1.000	3	2	0.350	1,000
Renal Insufficiency	0	1	1.000	0	1	1.000	1.000
Cancer	0	3	0.243	0	10	0.010	0.075
pulmonary tuberculosis	9	0	0.000	4	0	0.016	0.154
WBC, $*10^9$/L	6.07 ± 2.26	6.73 ± 2.32	0.263	6.14 ± 2.20	7.08 ± 3.36	0.239	0.525
CRP, mg/L	11.34 (4.20,31.96)	17.95 (3.12,61.80)	0.733	25.58 (10.63,77.11)	13.83 (1.30,38.78)	0.133	0.326
ESR, mm/h	55.00 (29.25,81.00)	74.00 (33.00,112.50)	0.173	74.00 (63.00,107.00)	50.00 (35.00,104.00)	0.244	0.542
TB antigen positive, %	5 (18)	1 (3)	0.085	8 (35)	0 (0)	0.000	0.592
QFT-GIT positive, %	27 (96)	12 (36)	0.000	20 (87)	11 (28)	0.000	0.119

TB, spinal tuberculosis; NTB, non-tuberculosis;
#Comparisons were conducted between TB and NTB in study cohort.
&Comparisons were conducted between TB and NTB in validation cohort.
$Comparisons were conducted between the study cohort and validation cohort.

TABLE 2 Diagnosis performance of the QFT-GIT and adjusted QFT-GIT.

	AUC (95%CI)	Sensitive (95%CI)	Specificity (95%CI)	PPV (95%CI)	NPV (95%CI)	PLR (95%CI)	NLR (95%CI)	Accuracy
All patients (n=123)	0.866 (0.798-0.933)	92.16% (80.25%-97.46%)	68.06% (55.89%-78.28%)	67.14% (54.77%-77.62%)	92.45% (80.93%-97.55%)	2.885 (2.040-4.080)	0.115 (0.044-0.299)	78.05%
Study cohort (n=61)	0.864 (0.761-0.966)	96.43% (79.76%-99.81%)	63.64% (45.14%-79.04%)	69.23% (52.27%-82.45%)	95.45% (75.12%-99.76%)	2.652 (1.679-4.188)	0.056 (0.008-0.398)	78.69%
Validation cohort (n=62)	0.860 (0.764-0.955)	86.96% (65.33%-96.57%)	71.79% (54.90%-84.45%)	64.52% (45.38%-80.17%)	90.32% (73.10%-97.47%)	3.083 (1.824-5.212)	0.182 (0.062-0.532)	77.42%
Validation cohort (Based on adjusted cutoff point*)	0.860 (0.764-0.955)	73.91% (51.31%-88.92%)	84.62% (68.79%-93.59)	73.91% (51.31%-88.92%)	84.62% (68.79%-93.59%)	4.804 (2.213-10.428)	0.308 (0.154-0.619)	80.65%

TB, spinal tuberculosis; NTB, non-tuberculosis; AUC, the area under the curve; PPV, positive predictive value; NPV, negative predictive value; PLR, positive likelihood ratio; NLR, negative likelihood ratio; CI, confidence interval.
*adjusted cutoff point=1.58IU/mL

3.4 Correlation analysis between the QFT-GIT test result and other indications

We analyzed the correlations between TB Ag-Nil and WBC, ESR, CRP and disease duration in a sample of 51 tuberculosis patients and 72 non-tuberculosis patients, respectively, by Spearman's rho test. We found no correlations between TB Ag-Nil values and patients' WBC, ESR and CRP in either the tuberculosis or non-tuberculosis groups (Figures 2A–F). Notably, our results showed a significant correlation between TB Ag-Nil and the duration of disease in tuberculosis patients (r=0.4148, P=0.0025) (Figure 2G) but not in non-tuberculosis patients (r=0.1168, P=0.3286) (Figure 2H).

4 Discussion

In this study, we enrolled 51 patients with tuberculosis and 72 patients with non-tuberculosis disease and assigned them to either the study cohort or the validation cohort according to the time of admission. There were no significant differences in age, sex, BMI, or duration of disease between the two cohorts. Nine patients in the non-tuberculosis group had a combined or final diagnosis of spinal tumor; notably, differential diagnosis between spinal tumors and spinal tuberculosis *via* imaging is sometimes difficult (Du et al., 2021). All these patients presented with vertebral bone destruction, and some spinal tumors were even visible on imaging as features consistent with spinal tuberculosis, such as abscesses of the psoas major muscle. Tuberculosis of the spine is often secondary to tuberculosis of other sites, most often pulmonary tuberculosis (Dunn and Ben Husien, 2018). In addition, patients with combined pulmonary or extrapulmonary tuberculosis were excluded from the non-tuberculosis group to avoid effects of these conditions on the QFT-GIT test. Our study also confirmed the inability to differentiate spinal tuberculosis from other diseases on the basis of ESR, CRP, and WBC. For comparison of these indicators between the two groups of patients, a nonparametric test was used, because the data for ESR and CRP did not conform to a normal distribution; in contrast, an independent-sample t test was used to analyze the differences in WBC between the two groups. As another challenge to differential diagnosis of spinal tuberculosis, septic and brucellosis infections are infectious diseases like tuberculosis, so these diseases also lead to increases in serum infection indicators (Ghassibi et al., 2021). Tumors can also sometimes cause the release of inflammatory substances, leading to increases in serum inflammatory marker levels in patients (Allin and Nordestgaard, 2011). Several of the above serologic indicators are not tuberculosis specific, and we did not see differences in these serologic indicators between patients with spinal tuberculosis and patients with non-tuberculosis disease in our data; therefore, early diagnosis of spinal tuberculosis by conventional inflammatory indicators is very difficult.

Our results showed that the QFT-GIT test showed high sensitivity (92.16%) in the diagnosis of spinal tuberculosis, and a high sensitivity can reduce underdiagnosis of spinal tuberculosis. However, the specificity of the QFT-GIT test was only 68.06%. The relatively low specificity may have been related to pyogenic infections of the spine caused by other pathogens, which can be caused by a variety of nonspecific microorganisms; certain nontuberculous mycobacterial infections, such as *Mycobacterium kansasii* (Johnston et al., 2017), *Mycobacterium szulgai* (Weng et al., 2020) and *Mycobacterium marinum* (Arend et al., 2002), may also cause positive test results in patients. The results of tests with low specificity can mislead physicians, causing them to use antituberculosis therapies for patients without tuberculosis. This has led to the treatment of misdiagnosed patients with unnecessary antituberculosis drugs with considerable adverse effects, including hepatotoxicity, optic

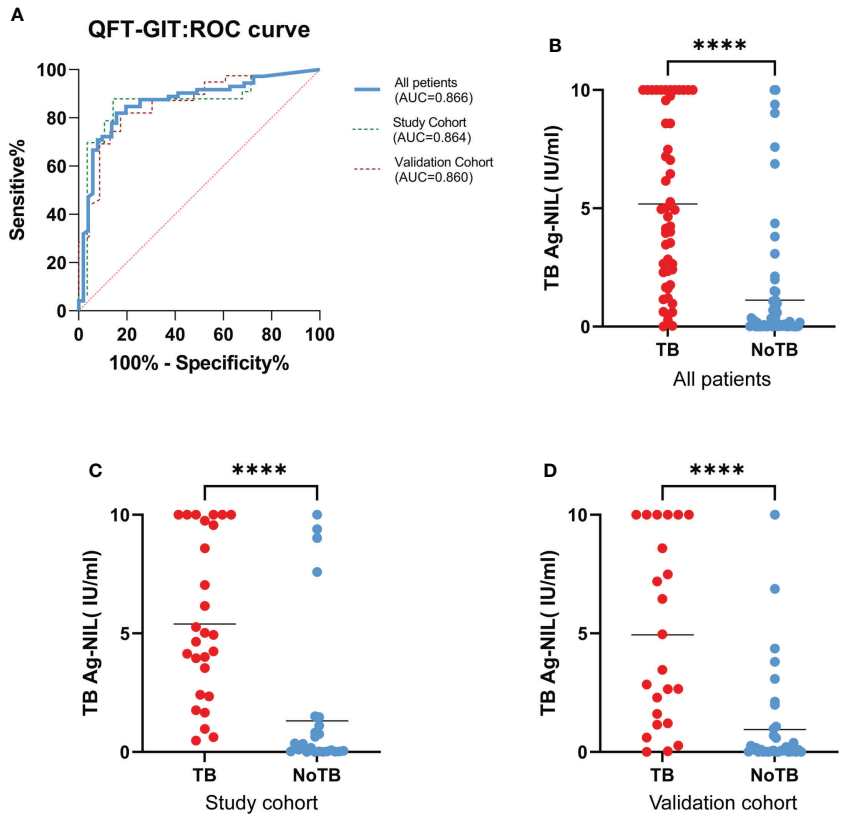

FIGURE 1
QFT-GIT diagnostic effectiveness. **(A)**. ROC curve by final diagnosis and TB Ag-Nil values in all 123 patients, study cohort and validation cohort; **(B, C, D)**. TB Ag-Nil values in the TB group than in patients in the NTB group, both in all patients, in the study cohort and in the validation. (**** means P ≤ 0.0001).

nerve damage, and hearing loss (Yew et al., 2018; Ghassibi et al., 2021). In addition, incorrect antituberculosis treatment may lead to the emergence of drug-resistant bacteria (Nagel et al., 2017). Targeted anti-infective therapies can significantly shorten the course of the disease and improve the prognosis of patients (Kim et al., 2012).

To improve the specificity of the diagnostic test, we attempted to plot a ROC curve (AUC=0.866) with the continuous variable TB Ag-Nil, and we found that the QFT-GIT test showed good efficacy in the diagnosis of spinal tuberculosis. We further found a more appropriate cutoff point (1.58 IU/mL) in the study cohort for the diagnosis of spinal tuberculosis. We used this new cutoff point as a diagnostic criterion, specifying ≥1.58 IU/mL as positive in the QFT-GIT test. We reclassified the diagnostic test results in the validation cohort as being different from those in the study cohort and found that the QFT-GIT test showed better accuracy for the diagnosis of spinal tuberculosis with this new cutoff. The sensitivity was reduced to a certain degree, but the specificity of the diagnosis was improved.

We analyzed the correlations between TB Ag-Nil and WBC, ESR, CRP and disease duration in 51 tuberculosis patients and 72 non-tuberculosis patients in our sample and found that TB Ag-Nil was significantly positively correlated with patient course in the tuberculosis group. Previous studies have also shown that the intensity of the QFT-GIT test result is not related to the severity of tuberculosis but may be related to the activity of tuberculosis (Nikitina et al., 2016). The relationship between the intensity of the QFT-GIT test result and the duration of a patient's disease has rarely been reported; however, a study of the intensity of the QFT-GIT test results at different periods of tuberculosis could not be performed because the present study was not designed as a follow-up investigation. This topic may deserve further study.

Clinical studies related to the QFT-GIT test have primarily focused on pulmonary tuberculosis, and a Japanese study showed that the sensitivity and specificity of the QFT-GIT test for the diagnosis of tuberculosis reached 92.6% and 98.8%, respectively (Harada et al., 2008). The QFT-GIT test shows high sensitivity and specificity in pulmonary tuberculosis. In

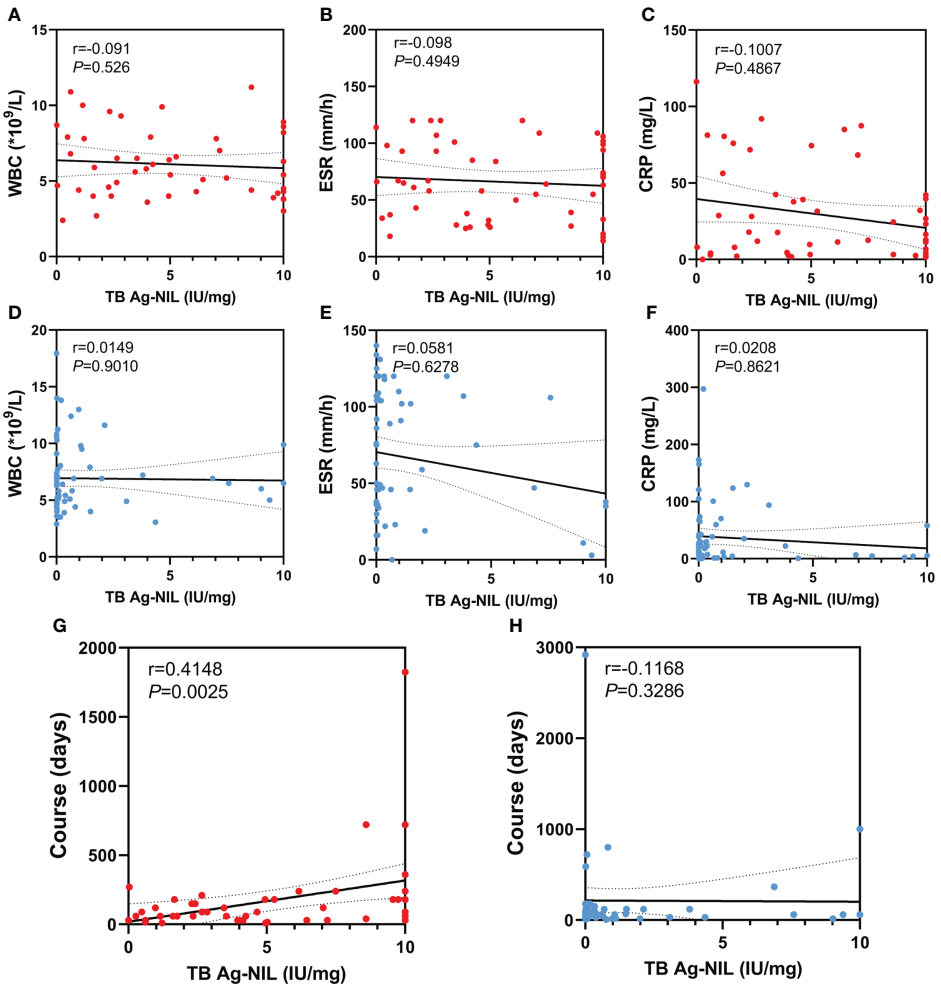

FIGURE 2
Correlation analysis between QFT-GIT and other indication: The red dots represent TB patients and the blue dots represent NTB patients. **(A, D)** Correlation analysis between TB Ag-Nil and WBC in TB patients or NTB patients; **(B, E)** Correlation analysis between TB Ag-Nil and ESR in TB patients or NTB patients; **(C, F)** Correlation analysis between TB Ag-Nil and CRP in TB patients or NTB patients; **(G, H)** Correlation analysis between TB Ag-Nil and course in TB patients or NTB patients;

2018, Sungim Choi et al. (Choi et al., 2018) reported a clinical study on the QFT-GIT test in spinal tuberculosis in Korea. Their results of QFT-GIT test sensitivity (91%) and specificity (65%) were similar to our results showing both high sensitivity and low specificity. However, our study differed from theirs in several ways. First, our study included 51 patients with confirmed spinal tuberculosis, which is a relatively large sample size compared to those in other studies on osteoarticular tuberculosis and spinal tuberculosis. Second, our study was a multicenter study, and new patients will continue to be enrolled. Third, we plotted the ROC curve according to TB Ag-Nil values, divided patients into a study cohort and a validation cohort by admission time, found a new appropriate cutoff point from the ROC curve of the study cohort, and validated this new cutoff point in the validation cohort, demonstrating the improved diagnostic accuracy of this new cutoff point. Fourth, we found a correlation between TB Ag-Nil values and the duration of disease in patients with spinal tuberculosis *via* correlation analysis, providing a reference for preoperative differential diagnosis of spinal tuberculosis.

Notably, our study has some limitations. First, although the QFT-GIT examination was completed for all cases included in the study, a small amount of other biochemical examination data was missing for some cases due to refusal of some of the examinations, and some patients were missing BMI data because many patients with mobility problems could not cooperate to complete the height and weight measurements. Second, the present study was a preliminary study; we will correlate multiple indicators in later

experiments, which may further improve the diagnostic efficacy. Based on the results of the current study, we will also conduct further prospective studies to improve the accuracy of preoperative differential diagnosis of spinal tuberculosis.

5 Conclusion

The QFT-GIT test is an important test for preoperative differential diagnosis of spinal tuberculosis with high sensitivity but low specificity. The diagnostic efficacy of the QFT-GIT test can be significantly improved *via* application of a new threshold (1.58 IU/mL), and the intensity of the QFT-GIT test findings in spinal tuberculosis may be related to the duration of a patient's disease.

Data availability statement

The original contributions presented in the study are included in the article/supplementary material. Further inquiries can be directed to the corresponding author.

Author contributions

XH and QG designed research, performed research, analyzed data, and wrote the paper. HZ and YL developed the idea for the study. GZ, BT, DX collected the data. MT, CG and SL revised the paper. All authors contributed to the article and approved the submitted version.

Funding

This study was supported by National Natural Science Foundation of China (No. 82072460,No. 82170901) and Natural Science Foundation of Hunan Province, China (No.2020JJ4892, No.2020JJ4908).

Acknowledgments

I would particularly like to acknowledge the spine surgery of Xiangya Boai Hospital, Changsha First Hospital and Hunan Chest Hospital, for their wonderful collaboration and patient support.

Conflict of interest

The authors declare that the research was conducted in the absence of any commercial or financial relationships that could be construed as a potential conflict of interest.

Publisher's note

All claims expressed in this article are solely those of the authors and do not necessarily represent those of their affiliated organizations, or those of the publisher, the editors and the reviewers. Any product that may be evaluated in this article, or claim that may be made by its manufacturer, is not guaranteed or endorsed by the publisher.

References

Allin, K. H., and Nordestgaard, B. G. (2011). Elevated c-reactive protein in the diagnosis, prognosis, and cause of cancer. *Crit. Rev. Clin. Lab. Sci.* 48, 155–170. doi: 10.3109/10408363.2011.599831

Arend, S. M., Van Meijgaarden, K. E., De Boer, K., De Palou, E. C., Van Soolingen, D., Ottenhoff, T. H., et al. (2002). Tuberculin skin testing and *in vitro* T cell responses to ESAT-6 and culture filtrate protein 10 after infection with mycobacterium marinum or m. *kansasii. J. Infect. Dis.* 186, 1797–1807. doi: 10.1086/345760

Chen, C. H., Chen, Y. M., Lee, C. W., Chang, Y. J., Cheng, C. Y., and Hung, J. K. (2016). Early diagnosis of spinal tuberculosis. *J. Formos Med. Assoc.* 115, 825–836. doi: 10.1016/j.jfma.2016.07.001

Choi, S., Jung, K. H., Son, H. J., Lee, S. H., Hong, J. M., Kim, M. C., et al. (2018). Diagnostic usefulness of the QuantiFERON-TB gold in-tube test (QFT-GIT) for tuberculous vertebral osteomyelitis. *Infect. Dis. (Lond)* 50, 346–351. doi: 10.1080/23744235.2017.1410282

Cho, O. H., Park, S. J., Park, K. H., Chong, Y. P., Sung, H., Kim, M. N., et al. (2010). Diagnostic usefulness of a T-cell-based assay for osteoarticular tuberculosis. *J. Infect.* 61, 228–234. doi: 10.1016/j.jinf.2010.06.015

Coleman, R. E. (2006). Clinical features of metastatic bone disease and risk of skeletal morbidity. *Clin. Cancer Res.* 12, 6243s–6249s. doi: 10.1158/1078-0432.CCR-06-0931

Dunn, R. N., and Ben Husien, M. (2018). Spinal tuberculosis: review of current management. *Bone Joint J.* 100-b, 425–431. doi: 10.1302/0301-620X.100B4.BJJ-2017-1040.R1

Du, X., She, Y., Ou, Y., Zhu, Y., Luo, W., and Jiang, D. (2021). A scoring system for outpatient orthopedist to preliminarily distinguish spinal metastasis from spinal tuberculosis: A retrospective analysis of 141 patients. *Dis. Markers* 2021, 6640254. doi: 10.1155/2021/6640254

Ghassibi, M., Yen, T. C., Harris, S., Si, Z., Leary, E., and Choma, T. J. (2021). Responsiveness of routine diagnostic tests for vertebral osteomyelitis may be influenced by the infecting organism. *Spine J.* 21, 1479–1488. doi: 10.1016/j.spinee.2021.04.001

Go, J. L., Rothman, S., Prosper, A., Silbergleit, R., and Lerner, A. (2012). Spine infections. *Neuroimaging Clin. N Am.* 22, 755–772. doi: 10.1016/j.nic.2012.06.002

Hamada, Y., Cirillo, D. M., Matteelli, A., Penn-Nicholson, A., Rangaka, M. X., and Ruhwald, M. (2021). Tests for tuberculosis infection: landscape analysis. *Eur. Respir. J.* 58 (5), 2100167. doi: 10.1183/13993003.00167-2021

Harada, N., Higuchi, K., Yoshiyama, T., Kawabe, Y., Fujita, A., Sasaki, Y., et al. (2008). Comparison of the sensitivity and specificity of two whole blood interferon-gamma assays for m. *tuberculosis infection. J. Infect.* 56, 348–353. doi: 10.1016/j.jinf.2008.02.011

Harding, E. (2020). WHO global progress report on tuberculosis elimination. *Lancet Respir. Med.* 8, 19. doi: 10.1016/S2213-2600(19)30418-7

Johnston, J. C., Chiang, L., and Elwood, K. (2017). Mycobacterium kansasii. *Microbiol. Spectr.* 5 (1), TNMI7-0011–2016. doi: 10.1128/9781555819866.ch42

Kanna, R. M., Babu, N., Kannan, M., Shetty, A. P., and Rajasekaran, S. (2019). Diagnostic accuracy of whole spine magnetic resonance imaging in spinal tuberculosis validated through tissue studies. *Eur. Spine J.* 28, 3003–3010. doi: 10.1007/s00586-019-06031-z

Kim, C. J., Song, K. H., Park, W. B., Kim, E. S., Park, S. W., Kim, H. B., et al. (2012). Microbiologically and clinically diagnosed vertebral osteomyelitis: impact of prior antibiotic exposure. *Antimicrob. Agents Chemother.* 56, 2122–2124. doi: 10.1128/AAC.05953-11

Lu, P., Liu, Q., Zhou, Y., Martinez, L., Kong, W., Ding, X., et al. (2021). Predictors of discordant tuberculin skin test and QuantiFERON-TB gold in-tube results in Eastern China: A population-based, cohort study. *Clin. Infect. Dis.* 72, 2006–2015. doi: 10.1093/cid/ciaa519

Miyamoto, H., and Akagi, M. (2019). Usefulness of dynamic contrast-enhanced magnetic resonance images for distinguishing between pyogenic spondylitis and tuberculous spondylitis. *Eur. Spine J.* 28, 3011–3017. doi: 10.1007/s00586-019-06057-3

Nagel, S., Streicher, E. M., Klopper, M., Warren, R. M., and Van Helden, P. D. (2017). Isoniazid resistance and dosage as treatment for patients with tuberculosis. *Curr. Drug Metab.* 18, 1030–1039. doi: 10.2174/1389200218666171031121905

Nikitina, I. Y., Panteleev, A. V., Sosunova, E. V., Karpina, N. L., Bagdasarian, T. R., Burmistrova, I. A., et al. (2016). Antigen-specific IFN-γ responses correlate with the activity of m. tuberculosis infection but are not associated with the severity of tuberculosis disease. *J. Immunol. Res.* 2016, 7249369. doi: 10.1155/2016/7249369

Patel, J., Upadhyay, M., Kundnani, V., Merchant, Z., Jain, S., and Kire, N. (2020). Diagnostic efficacy, sensitivity, and specificity of xpert MTB/RIF assay for spinal tuberculosis and rifampicin resistance. *Spine (Phila Pa 1976)* 45, 163–169. doi: 10.1097/BRS.0000000000003225

Perronne, C., Saba, J., Behloul, Z., Salmon-Céron, D., Leport, C., Vildé, J. L., et al. (1994). Pyogenic and tuberculous spondylodiskitis (vertebral osteomyelitis) in 80 adult patients. *Clin. Infect. Dis.* 19, 746–750. doi: 10.1093/clinids/19.4.746

Qi, Y., Liu, Z., Liu, X., Fang, Z., Liu, Y., and Li, F. (2022). Tuberculosis-specific Antigen/Phytohemagglutinin ratio combined with GeneXpert MTB/RIF for early diagnosis of spinal tuberculosis: A prospective cohort study. *Front. Cell Infect. Microbiol.* 12, 781315. doi: 10.3389/fcimb.2022.781315

Shafeque, A., Bigio, J., Hogan, C. A., Pai, M., and Banaei, N. (2020). Fourth-generation QuantiFERON-TB gold plus: What is the evidence? *J. Clin. Microbiol.* 58 (9), e01950-19. doi: 10.1128/JCM.01950-19

Shi, C. L., Han, P., Tang, P. J., Chen, M. M., Ye, Z. J., Wu, M. Y., et al. (2020). Clinical metagenomic sequencing for diagnosis of pulmonary tuberculosis. *J. Infect.* 81, 567–574. doi: 10.1016/j.jinf.2020.08.004

Shroyer, S. R., Davis, W. T., April, M. D., Long, B., Boys, G., Mehta, S. G., et al. (2021). A clinical prediction tool for MRI in emergency department patients with spinal infection. *West J. Emerg. Med.* 22, 1156–1166. doi: 10.5811/westjem.2021.5.52007

Sun, W., Lu, Z., and Yan, L. (2021). Clinical efficacy of metagenomic next-generation sequencing for rapid detection of mycobacterium tuberculosis in smear-negative extrapulmonary specimens in a high tuberculosis burden area. *Int. J. Infect. Dis.* 103, 91–96. doi: 10.1016/j.ijid.2020.11.165

Wang, B., Gao, W., and Hao, D. (2020). Current study of the detection and treatment targets of spinal tuberculosis. *Curr. Drug Targets* 21, 320–327. doi: 10.2174/1389450120666191002151637

Weng, T. P., Syue, L. S., and Lee, N. Y. (2020). Disseminated mycobacterium szulgai infection in a patient with anti-interferon-gamma autoantibodies. *IDCases* 21, e00848. doi: 10.1016/j.idcr.2020.e00848

Yew, W. W., Chang, K. C., and Chan, D. P. (2018). Oxidative stress and first-line antituberculosis drug-induced hepatotoxicity. *Antimicrob. Agents Chemother.* 62 (8), e02637-17. doi: 10.1128/AAC.02637-17

frontiers | Frontiers in Cellular and Infection Microbiology

TYPE Original Research
PUBLISHED 20 September 2022
DOI 10.3389/fcimb.2022.962059

OPEN ACCESS

EDITED BY
Divakar Sharma,
University of Delhi, India

REVIEWED BY
Maura Manion,
National Institute of Allergy and Infectious Diseases (NIH), United States
Esaki M. Shankar,
Central University of Tamil Nadu, India

*CORRESPONDENCE
Mariza Gonçalves Morgado
mmorgado@ioc.fiocruz.br
Nathalia Beatriz Ramos de Sá
nathalia.beatriz2008@gmail.com

SPECIALTY SECTION
This article was submitted to Clinical Microbiology, a section of the journal Frontiers in Cellular and Infection Microbiology

RECEIVED 05 June 2022
ACCEPTED 30 August 2022
PUBLISHED 20 September 2022

CITATION
de Sá NBR, de Souza NCS, Neira-Goulart M, Ribeiro-Alves M, Da Silva TP, Pilotto JH, Rolla VC, Giacoia-Gripp CBW, de Oliveira Pinto LM, Scott-Algara D, Morgado MG and Teixeira SLM (2022) Inflammasome genetic variants are associated with tuberculosis, HIV-1 infection, and TB/HIV-immune reconstitution inflammatory syndrome outcomes. *Front. Cell. Infect. Microbiol.* 12:962059. doi: 10.3389/fcimb.2022.962059

Inflammasome genetic variants are associated with tuberculosis, HIV-1 infection, and TB/HIV-immune reconstitution inflammatory syndrome outcomes

Nathalia Beatriz Ramos de Sá[1]*, Nara Cristina Silva de Souza[1], Milena Neira-Goulart[1], Marcelo Ribeiro-Alves[2], Tatiana Pereira Da Silva[1], Jose Henrique Pilotto[1,3], Valeria Cavalcanti Rolla[4], Carmem B. W. Giacoia-Gripp[1], Luzia Maria de Oliveira Pinto[5], Daniel Scott-Algara[6], Mariza Gonçalves Morgado[1]* and Sylvia Lopes Maia Teixeira[1]

[1]1Laboratory of AIDS & Molecular Immunology, Oswaldo Cruz Institute, FIOCRUZ, Rio de Janeiro, Brazil, [2]Laboratory of Clinical Research on STD/AIDS, National Institute of Infectious Diseases Evandro Chagas, FIOCRUZ, Rio de Janeiro, Brazil, [3]Nova Iguaçu General Hospital, Nova Iguaçu, Rio de Janeiro, Brazil, [4]Clinical Research Laboratory on Mycobacteria, National Institute of Infectious Diseases Evandro Chagas, FIOCRUZ, Rio de Janeiro, Brazil, [5]Laboratory of Viral Immunology, Oswaldo Cruz Institute, FIOCRUZ, Rio de Janeiro, Brazil, [6]Unité de Biologie Cellulaire des Lymphocytes, Institut Pasteur, Paris, France

Background: Tuberculosis (TB) and AIDS are the leading causes of infectious diseases death worldwide. Here, we investigated the relationship between from single nucleotide polymorphisms (SNPs) of the NLRP3, CARD8, AIM2, CASP-1, IFI16, and IL-1β inflammasome genes, as well as the profiles of secreted proinflammatory cytokines (e.g., IL-1β, IL-18, IL-33, and IL-6) with the TB clinical profiles, TB-HIV coinfection, and IRIS onset.

Methods: The individuals were divided into four groups: TB-HIV group (n=88; 11 of them with IRIS), HIV-1 group (n=20), TB group (n=24) and healthy volunteers (HC) group (n=10), and were followed up at INI/FIOCRUZ and HGNI (Rio de Janeiro/Brazil) from 2006 to 2016. Real-time PCR was used to determine the genotypes of the Single Nucleotide Polymorphism (SNPs), and ELISA was used to measure the plasma cytokine levels. Unconditional logistic regression models were used to perform risk estimations.

Results: A higher risk for extrapulmonary TB was associated with the TT genotype (aOR=6.76; P=0.026) in the NLRP3 rs4612666 Single Nucleotide Polymorphism (SNP) and the C-C-T-G-C haplotype (aOR=4.99; P= 0.017) in the NLRP3 variants. This same Single Nucleotide Polymorphism (SNP) was associated with lower risk against extrapulmonary TB when the carrier allele C (aOR=0.15; P=0.021) was present. Among those with HIV-1 infections, a higher risk for TB onset was associated with the GA genotype (aOR=5.5; P=0.044) in

the IL1-β rs1143634 Single Nucleotide Polymorphism (SNP). In contrast, lower risk against TB onset was associated with the A-G haplotype (aOR=0.17; P= 0.026) in the CARD8 variants. Higher IL-6 and IL-33 levels were observed in individuals with TB. A higher risk for IRIS onset was associated with CD8 counts ≤ 500 cells/mm^3 (aOR=12.32; P=0.010), the presence of extrapulmonary TB (aOR=6.6; P=0.038), and the CT genotype (aOR=61.06; P=0.026) or carrier allele T (aOR=61.06; P=0.026) in the AIM2 rs2276405 Single Nucleotide Polymorphism (SNP), whereas lower risk against IRIS onset was associated with the AT genotype (aOR=0.02; P=0.033) or carrier allele T (aOR=0.02; P=0.029) in the CARD8 rs2043211 Single Nucleotide Polymorphism (SNP) and the T-G haplotype (aOR=0.07; P= 0.033) in the CARD8 variants. No other significant associations were observed.

Conclusions: Our results depict the involvement of genetic polymorphisms of crucial innate immunity genes and proinflammatory cytokines in the clinical outcomes related to TB-HIV coinfection.

KEYWORDS

tuberculosis, HIV-1, TB-HIV/IRIS, inflammasome Single Nucleotide Polymorphism (SNP), proinflammatory cytokines

Introduction

Tuberculosis (TB) and AIDS are the major causes of death from infectious diseases worldwide. In 2020, 10 million TB cases were estimated globally, including 815,000 cases among people living with HIV (PLWH) (World Health Organization, 2020), making TB the most common comorbidity leading to death among PLWH (World Health Organization, 2020). In 2019, 16% of all cases of TB that were reported to the World Health Organization (WHO) were extrapulmonary TB (EPTB) (World Health Organization, 2020). Combined antiretroviral therapy (cART) during TB treatment improves survival by restoring immune functions (Müller et al., 2010). However, treatment with anti-TB drugs followed by cART initiation can lead to a paradoxical immune reconstitution inflammatory syndrome (IRIS) (Shelburne et al., 2005). Current research has established some pathological mechanisms that are related to IRIS development, such as high viral loads, low baseline CD4+ T-cell counts (<50–100 cells/mm3) (Antonelli et al., 2010; Luetkemeyer et al., 2014) with high levels of CD4 activation and replication (Tibúrcio et al., 2021), and short time intervals between TB treatment and cART (French et al., 2004; Chang et al., 2014; Tan et al., 2016). The genetic basis of host susceptibility to infectious diseases has received enormous attention (Fellay et al., 2009; Seaby et al., 2016; Wu et al., 2017). Highly polymorphic class I and II human leukocyte antigens (HLAs), killer-cell immunoglobulin-like receptor (KIR), cytokine genes, and genes involved in inflammation (inflammasome genes) are actively contributing factors that are associated with susceptibility and/or resistance to TB and HIV-1 infection (Kulkarni et al., 2008; Levy, 2009; Martin and Carrington, 2013; Pontillo et al., 2013; De Lima et al., 2016; Naranbhai and Carrington, 2017; Tsiara et al., 2018; de Sá et al., 2020). However, studies linking host genetics to the pathogenesis of IRIS are still scarce (Narendran et al., 2016; de Sá et al., 2020).

Inflammasomes are cytosolic multiprotein oligomers of the innate immune system that are responsible for the activation of inflammatory responses, including toll-like receptors (TLRs) and nod-like receptors (NLRs) that interact with several adaptor proteins, which leads to the activation of caspase-1 and induces the release of the proinflammatory cytokines such as IL-1ß and IL-18 (Rathinam and Fitzgerald, 2016). Different pattern-recognizing receptors (e.g., NLRP1 and NLRP3) can activate inflammasome assembly in response to specific stimuli, which leads to inflammation and the innate immune response (Man and Kanneganti, 2015). Dysregulation of the inflammasome has been associated with susceptibility to TB-HIV coinfection and TB-HIV/IRIS (Lai et al., 2015; Tan et al., 2015; Tan et al., 2016). In this regard, some investigations have found that TB-HIV/IRIS is associated with changes in the expression of cytokines that are related to the inflammasome activation pathway and other proinflammatory cytokines, such as IL-1β, IL-18, IL-33, IL-6, IL-17, IL-22, TNF, and IFN-γ, which suggests a key role in the development of TB-HIV/IRIS

(Tadokera et al., 2011; Conesa-Botella et al., 2012; Tan et al., 2015; Tan et al., 2016; Ravimohan et al., 2018).

Although some studies have already observed the relationships among inflammasome coding genes and inflammasome activation-related cytokines with TB-HIV coinfected individuals, these studies are still scarce, especially for TB-HIV/IRIS individuals (Tan et al., 2016; Marais et al., 2017; Ravimohan et al., 2018; Ravimohan et al., 2020). In a previous study, we evaluated the role of host genetic markers (e.g., HLA-B, HLA-C, and KIR) in the risk and/or protection of TB-HIV coinfection outcomes, including the increased risk for TB-HIV/IRIS (de Sá et al., 2020). Considering the highly inflammatory profiles observed in TB-HIV coinfections, which increase during TB-HIV/IRIS, in the present study, we investigated the distributions of 11 single nucleotide polymorphisms (SNPs) of the major inflammasome pathway genes (e.g., NLRP3, CARD8, AIM2, CASP-1, IFI16, and IL-1β), cytokine levels (e.g., IL-1β, IL-6, IL-18, and IL-33), and their potential influence on the susceptibility to TB and/or HIV-1 as well as on the occurrence of TB-HIV/IRIS.

Materials and methods

Patient enrollment and study design

This study nested two clinical and immunological follow-up studies conducted in the Laboratory of AIDS & Molecular Immunology (IOC/FIOCRUZ) from 2006 to 2016, as previously described (da Silva et al., 2013; da Silva et al., 2017; Giacoia-Gripp et al., 2019). All participants signed an informed consent form, and the local ethics committee approved the studies. The study participants consisted of 142 individuals, who were divided into four groups as follows: individuals with TB and infected with HIV-1 (TB-HIV group, n=88; 11 of them with paradoxical TB-HIV/IRIS); individuals infected with HIV-1 without a diagnosis of TB (HIV-1 group, n=20); individuals with TB and seronegative for HIV-1 infection (TB group, n=24); and healthy controls with neither HIV-1 infection nor TB (HC, group, n=10).

The individuals were enrolled and followed up at the Clinical Research Laboratory on Mycobacteria (LAPCLINTB) of the National Institute of Infectious Diseases Evandro Chagas, Oswaldo Cruz Foundation (INI/FIOCRUZ), Rio de Janeiro, Brazil (2006-2011/2014-2016) and at the Nova Iguaçu General Hospital (HGNI), Rio de Janeiro, Brazil (2014-2016). The details regarding patient eligibility, enrollment, inclusion/exclusion criteria, anti-TB and cART treatments, study design, demographic and clinical data at the study entry visit, and availability of blood samples were previously described (de Sá et al., 2020). All TB-HIV coinfected individuals were investigated for the identification of IRIS development in both clinical centers. All IRIS cases observed in the study were classified as paradoxical, tuberculosis-associated IRIS, described as a worsening of TB signs and symptoms starting after cART initiation during TB treatment, mainly presenting enlargement of lymph nodes and inflammatory signs, not explained by any other diseases or by an adverse effect of drug therapy (Robertson et al., 2006; Meintjes et al., 2008), as previously detailed by our group (Demitto et al., 2019). In general, the IRIS cases included in the present study were self-resolving, or, if necessary, the patients were treated with corticoid-based therapy, such as Prednisone.

Skin color was self-declared following the classification system used by the Brazilian Institute of Geography and Statistics (IBGE) (Instituto Brasileiro de Geografia e Estatística, 2013) (which is an entity linked to the Brazilian Federal Government that is responsible for the official collection of statistical, geographic, cartographic, geodetic, and environmental information in Brazil).

Genomic DNA extraction

DNA was extracted from whole blood using the QIAamp DNA Blood Mini Kit (Qiagen, Hilden, Nordrhein-Westfalen, Germany) according to the manufacturer's instructions. The DNA concentrations were determined using a Thermo Scientific NanoDrop 2000 (Thermo Fisher Scientific, Waltham, Massachusetts, USA), and the filtrates containing the isolated DNA were stored at -20°C until genomic analyses.

Single nucleotide polymorphism selection and genotyping

We selected 11 Single Nucleotide Polymorphism (SNPs) in six inflammasome genes by considering the relevance of each gene in the inflammasome pathway: CARD8 (rs2043211, rs6509365); AIM2 (rs2276405); IFI16 (rs1101996); CASP-1 (rs572687); IL-1β (rs1143634); and NLRP3 (rs10754558, rs1539019, rs4612666, rs3806268, and rs35829419). The Single Nucleotide Polymorphism (SNPs) were selected based on previous studies associating polymorphisms in inflammasome genes with HIV, tuberculosis, and HIV-TB (Pontillo et al., 2010; Pontillo et al., 2012; Pontillo et al., 2013). Single Nucleotide Polymorphism (SNP) genotyping was performed using commercially available TaqMan assays (Applied Biosystems/AB and Life Technologies) on the ABI7500 Real-Time platform (Applied Biosystems/AB and Life Technologies). Allelic discrimination was carried out employing Thermo Fisher Connect Software (Waltham, Massachusetts, EUA). The haplotype analyses were conducted by considering the most frequent haplotype of the NLRP3 (C-C-C-G-C haplotype) and CARD8 (AA) genes as the references. Detailed Single Nucleotide Polymorphism (SNP) information is provided in Table S1.

Inflammatory cytokine plasma levels

The plasma concentrations of the proinflammatory cytokines included in the study were measured at study entry (baseline) before anti-TB and cART therapies, as follows: IL-1β/IL-1F2 (DuoSet ELISA Kit, R & D Systems, #DY201); IL-18 (Human Instant ELISA Kit, Thermo Fisher, BMS267INST); and IL-6 and IL-33 (Human Mini ABTS ELISA Development Kit, PeproTech, Inc., Rocky Hill, NJ) according to the manufacturer's instructions. Standard curves were prepared by preparing serial dilutions of the aliquots that corresponded to the cytokine standards supplied by the manufacturers. Determination of the optical densities of samples and standards was performed using the BioTek ELx800TM absorbance microplate reader (BioTek® Instruments Inc., Vermont, USA) at wavelengths of either 405 or 450 nm, according to each protocol.

Statistical analyses

For the descriptions of the patient samples included in the study, according to the sociodemographic, clinical, and laboratory characteristics among the individuals of the four groups, nonparametric Kruskal–Wallis rank-sum tests were used for continuous numerical variables, while Fisher's exact tests were used for comparing the relative frequencies of the different levels of nominal/categorical variables. In the Single Nucleotide Polymorphism (SNP) analyses, the genotype frequencies were determined by direct count. The relative risks were described as adjusted odds ratios (aORs) with 95% CIs estimated through multiple unconditional logistic regression models. The log-transformed (base 10) least-squares mean differences of the plasma levels of cytokines that were measured by ELISA among the groups were estimated by fixed effects multiple linear regression models. The homozygous genotypes of the minor frequency allele (carriers) were compared with other genotypes (noncarriers) to observe better the differences caused by the variations. Adjustments to the confidence levels were made using Sidak's method, and P-value adjustments for multiple comparisons were made using Tukey's method whenever necessary. For both the cytokine serum levels and for the relative risk analysis, we included any clinical phenotypic marker that was associated with different outcomes as confounders in the modeling to eliminate any possible bias. All statistical analyses were performed using R version 4.1.3 (R Core Team, 2022).

Results

Sociodemographic, clinical, and laboratory characteristics

The sociodemographic, clinical, and laboratory characteristics of the 142 individuals included in the present study, which were categorized according to the presence or absence of TB, are listed in Table 1. Among the 88 TB-HIV coinfected individuals, 11 had paradoxical TB-HIV/IRIS. Most of the participants were males (73.9%). The overall proportions of individuals with white or brown skin color were equivalent (39.4% and 40.1%, respectively), which indicated that ethnicity was not dependent on group arrangement, which could influence the genetic analyses discussed here. Regarding educational levels, 43% of the individuals had lower secondary education, and 27.5% had an upper secondary education. No significant differences were observed among the groups (Table 1).

We further analyzed the sociodemographic, clinical, and laboratory characteristics according to the clinical TB presentations of the individuals included in this study [pulmonary (PTB) *vs.* extrapulmonary TB (EPTB)] and according to the occurrence or absence of TB in PLWH. As depicted in Tables S2 and S3, there were no statistically significant differences among the groups in either analysis.

The sociodemographic, clinical, and laboratory characteristics of TB-HIV coinfected individuals with and without IRIS are listed in Table S4. It is noteworthy that TB-HIV individuals with EPTB (ORadj=6.6; P=0.038) or CD8 ≤ 500 cells/mm3 (ORadj=12.32; P=0.010) values presented an increased risk for IRIS.

Alleles, genotypes, and haplotypes of inflammasome genes

The genotype frequencies of the 11 Single Nucleotide Polymorphism (SNPs) analyzed in the present study were in Hardy-Weinberg equilibrium among the groups (Table S1). An unconditional logistic multiple regression model that compared the genotypes, alleles, carriers, or haplotype frequencies of the 11 Single Nucleotide Polymorphism (SNPs) between the TB and without TB groups did not show any statistical significance (data not shown).

Among PLWH with and without TB, the unconditional logistic multiple regression model that compared the genotypes, alleles, carriers, or haplotype frequencies of the 11 Single Nucleotide Polymorphism (SNPs) showed an increased risk for TB onset only for individuals with the G/A genotype (ORadj=5.5; P=0.044) in the IL-1β rs1143634 polymorphism (Table 2). On the other hand, lower risk of TB onset among PLWH was associated with the CARD8 A-G haplotype (ORadj=0.17; P= 0.026) (Table 2). Similar analyses were also conducted according to the different clinical TB presentations (PTB and EPTB) regardless of HIV-1 coinfection (Table 2), and an increased risk for EPTB was associated with carrying the T/T genotype (ORadj=6.76; P=0.026) in the NLPR3 rs4612666 polymorphism or the NLRP3 C-C-T-G-C haplotype (ORadj=4.99; P= 0.017). On the other hand, protection against EPTB was associated with carrier C (ORadj=0.15; P=0.021) in

TABLE 1 Sociodemographic, clinical, and laboratory data for individuals included in the study categorized according to the presence or absence of TB.

Features	Overall N=142	All the groups		aOR[a] (95%CI)	*P*-value[b]
		With TB N=112	Without TB N=30		
Gender; n (%)					
Male	105 (73.9%)	86 (76.79%)	19 (63.33%)	Reference	Reference
Female	37 (26.1%)	26 (23.21%)	11 (36.67%)	0.53 (0.22-1.3)	0.166
SkinColor[c]; n (%)					
Brown	57 (40.1%)	41 (36.61%)	16 (53.33%)	Reference	Reference
Black	29 (20.4%)	25 (22.32%)	4 (13.33%)	2.45 (0.71-8.43)	0.313
White	56 (39.4%)	46 (41.07%)	10 (33.33%)	1.88 (0.74-4.78)	0.313
Education[d]; n (%)					
Bachelor	9 (6.3%)	6 (5.36%)	3 (10%)	1.11 (0.22-5.67)	1
Upper-secondary	39 (27.5%)	27 (24.11%)	12 (40%)	0.72 (0.28-1.85)	1
Lower-secondary	61 (43%)	46 (41.07%)	15 (50%)	Reference	Reference
Primary	26 (18.3%)	26 (23.21%)	0 (0%)	NC	NC
Unknown	7 (4.9%)	7 (6.25%)	0 (0%)	NC	NC
HIV status; n (%)					
Yes	108 (76.1%)	88 (78.57%)	20 (66.67%)	Reference	Reference
No	34 (24.9%)	24 (21.43%)	10 (33.33%)	1.74 (0.19-15.67)	0.621
CD4 count (cells/μL); n (%)					
≤ 200 cells/μL	87 (63%)	67 (62.04%)	20 (66.67%)	Reference	Reference
> 200 cells/μL	51 (37%)	41 (37.96%)	10 (33.33%)	11.37 (0.86-150.77)	0.065
CD8 count (cells/μL); n (%)					
≤ 500 cells/μL	60 (45.1%)	44 (42.72%)	16 (53.33%)	Reference	Reference
> 500 cells/μL	73 (54.9%)	59 (57.28%)	14 (46.67%)	1.42 (0.61-3.3)	0.418
CD4/CD8 ratio; n (%)					
≤ 1	106 (79.7%)	85 (82.52%)	21 (70%)	Reference	Reference
> 1	27 (20.3%)	18 (17.48%)	9 (30%)	0.31 (0.03-3.01)	0.311

[a]Odds ratios were adjusted by skin color, education, site of tuberculosis, HIV transmission route, and CD8 count. [b]P-values were calculated using the unconditional logistic regression model. Associations were considered significant with a value of P < 0.05. [c]Skin color categorization followed the classificatory system employed by the Brazilian Institute of Geography and Statistics (IBGE) (Instituto Brasileiro de Geografia e Estatística, 2013). [d]Classification, according to the International Standard Classification of Education (ISCED) maintained by the United Nations Educational, Scientific and Cultural Organization (UNESCO). N, number of individuals in each group; TB, tuberculosis; %, Frequencies; aOR, adjusted odds ratio; 95% CI, 95% confidence interval. NC, not calculated.

the NLPR3 rs4612666 polymorphism (Table 2). No significant associations were observed for other polymorphisms and outcomes.

TB-HIV/IRIS and inflammasome-related markers

By comparing the TB-HIV coinfected individuals with and without IRIS in relation to the allelic frequencies of the 11 Single Nucleotide Polymorphism (SNPs) analyzed in the present study, an increased risk for IRIS was associated with the C/T genotype (ORadj=61.06; P=0.026) and carrier-T (ORadj=61.06; P=0.026) in the AIM2 rs2276405 polymorphism. Nevertheless, a trend of increased risk for IRIS was also associated with bearing the T allele (ORadj= 1.49; P= 0.050) in the same polymorphism. Otherwise, lower risk IRIS onset was associated with the A/T genotype (ORadj=0.02; P=0.033) or carrier-T (ORadj=0.02; P=0.029) in the CARD8 rs2043211 polymorphism and with the CARD8 T-G haplotype (ORadj=0.07; P= 0.033) (Table 3). No significant associations were observed for the other polymorphisms.

Cytokines and inflammasome-related markers

By comparing the plasma cytokine levels (IL-1β, IL-6, IL-18, and IL-33) among the groups and outcomes, we observed that the plasma levels of IL-6 and IL-33 were higher among individuals with TB than those without TB (P <0.0001 for both comparisons) (Figure 1A). Similarly, higher levels of IL-6 and IL-33 were observed in PLWH with TB than in those without TB (P <0.0001, for both comparisons) (Figure 1B). No differences in the IL-1β and IL-18 levels were observed among

TABLE 2 Unconditional logistic multiple regression model of risk and protection factors for TB and for distinct TB clinical presentations according to selected inflammasome SNP genetic profiles.

Gene SNP (rs)	Genotypes, alleles and haplotypes	PLWH					Site of TB				
		With TB N=88	Without TB N=24	aOR[a]	95% CI	P-value[b]	PTB N=63	EPTB N=49	aOR[a]	95% CI	P-value[b]
IL-1β rs1143634	G/G	62 (70.45%)	17 (85%)	Ref			43 (68.25%)	35 (71.43%)	Ref		
	A/A	2 (2.27%)	1 (5%)	1.08	0.05-24.34	0.961	1 (1.59%)	1 (2.04%)	1.3	0.08-22.29	0.857
	G/A	24 (27.27%)	2 (10%)	5.5	1.04-29.02	**0.044**	19 (30.16%)	13 (26.53%)	0.64	0.26-1.61	0.346
	G	148 (84.09%)	36 (90%)	Ref		0.094	105 (83.33%)	83 (84.69%)			
	A	28 (15.91%)	4 (10%)	1.14	0.98-1.33		21 (16.67%)	15 (15.31%)	0.94	0.78-1.12	0.490
	Non-Carrier-G	2 (2.27%)	1 (5%)	Ref			1 (1.59%)	1 (2.04%)			
	Carrier-G	86 (97.73%)	19 (95%)	1.28	0.07-23.73	0.870	62 (98.41%)	48 (97.96%)	0.68	0.04-11.57	0.791
	Non-Carrier-A	62 (70.45%)	17 (85%)	Ref			43 (68.25%)	35 (71.43%)			
	Carrier-A	26 (29.55%)	3 (15%)	4.22	0.97-18.42	0.055	20 (31.75%)	14 (28.57%)	0.68	0.28-1.65	0.388
NLPR3 rs4612666	C/C	38 (45.24%)	6 (30%)	Ref			31 (51.67%)	19 (41.3%)	Ref		
	C/T	35 (41.67%)	12 (60%)	0.31	0.09-1.04	0.057	26 (43.33%)	18 (39.13%)	0.98	0.4-2.39	0.965
	T/T	11 (13.1%)	2 (10%)	0.63	0.1-3.94	0.618	3 (5%)	9 (19.57%)	6.76	1.26-36.23	**0.026**
	C	111 (66.07%)	24 (60%)	Ref			88 (73.33%)	56 (60.87%)	Ref		
	T	57 (33.93%)	16 (40%)	0.93	0.83-1.05	0.223	32 (26.67%)	36 (39.13%)	1.15	0.99-1.34	0.061
	Non-Carrier-C	11 (13.1%)	2 (10%)	Ref			3 (5%)	9 (19.57%)	Ref		
	Carrier-C	73 (86.9%)	18 (90%)	0.89	0.16-4.94	0.897	57 (95%)	37 (80.43%)	0.15	0.03-0.75	**0.021**
	Non-Carrier-T	38 (45.24%)	6 (30%)	Ref			31 (51.67%)	19 (41.3%)	Ref		
	Carrier-T	46 (54.76%)	14 (70%)	0.36	0.11-1.14	0.082	29 (48.33%)	27 (58.7%)	1.44	0.63-3.3	0.383
NLRP3 rs10754558 rs1539019 rs4612666 rs3806268 rs35829419	CCTGC	25 (14.88%)	9 (22.5%)	0.58	0.16-2.19	0.423	6 (5.26%)	15 (17.05%)	4.99	1.33-18.71	**0.017**
CARD8 rs2043211 rs6509365	AG	4 (2.27%)	4 (10%)	0.17	0.03-0.81	**0.026**	4 (3.17%)	2 (2.04%)	0.52	0.09-3.05	0.467

[a]Odds ratios were adjusted by skin color, education, site of tuberculosis, HIV transmission route, and CD8 count. [b]P-values were calculated using the unconditional logistic regression model. Associations were considered significant with a value of $P < 0.05$. N, number of individuals in each group; TB, tuberculosis; PLWH, people living with HIV; aOR, adjusted odds ratio; 95% CI, 95% confidence interval; Ref, Reference; PTB, Pulmonary TB; EPTB, Extrapulmonary TB, A, T, G, and C = each allele count, irrespective of the genotype. Carrier-A = total of genotypes with the A allele, Carrier-T = total of genotypes with T allele, Carrier-C = total of genotypes with the C allele, Carrier-G = total of genotypes with the G allele, Non-Carrier-A = total of genotypes without the A allele, Non-Carrier-T = total of genotypes without the T allele, Non-Carrier-C = total of genotypes without the C allele, Non-Carrier-G = total of genotypes without the G allele. Bold indicate statistically significant results.

the analyzed groups. Similar analyses were also conducted according to the different clinical TB presentations (PTB and EPTB), and no statistically significant differences were observed among the groups (Figure 1C). Moreover, analyses of the IL-1β, IL-6, IL-18, and IL-33 plasma levels between individuals with and without IRIS showed that the mean IL-33 plasma levels were slightly higher among individuals with IRIS than among those without IRIS (P=0.073), indicating a trend for associating IL-33

10.3389/fcimb.2022.962059

TABLE 3 Unconditional logistic multiple regression model of risk and protection factors for TB-HIV/IRIS among TB-HIV individuals.

GeneSNP (rs)	Genotypes, alleles and haplotypes	TB-HIV individuals		aOR[a] (CI95%)	*P*-value[b]
		Without IRIS (N =77)	With IRIS (N = 11)		
CARD8 rs2043211	A/A	43 (56.58%)	10 (90.91%)	Reference	
	A/T	25 (32.89%)	1 (9.09%)	0.02 (0-0.73)	**0.033**
	T/T	8 (10.53%)	0 (0%)	NC	NC
	A	111 (73.03%)	21 (95.45%)	Reference	
	T	41 (26.97%)	1 (4.55%)	0.9 (0.81-1)	0.060
	Non Carrier-A	8 (10.53%)	0 (0%)	Reference	
	Carrier-A	68 (89.47%)	11 (100%)	NC	NC
	Non Carrier-T	43 (56.58%)	10 (90.91%)	Reference	
	Carrier-T	33 (43.42%)	1 (9.09%)	0.02 (0-0.67)	**0.029**
CARD8 rs6509365	A/A	40 (51.95%)	9 (81.82%)	Reference	
	A/G	29 (37.66%)	2 (18.18%)	0.13 (0.01-1.21)	0.073
	G/G	8 (10.39%)	0 (0%)	NC	NC
	A	109 (70.78%)	20 (90.91%)	Reference	
	G	45 (29.22%)	2 (9.09%)	0.93 (0.84-1.03)	0.175
	Non Carrier-A	8 (10.39%)	0 (0%)	Reference	
	Carrier-A	69 (89.61%)	11 (100%)	NC	NC
	Non Carrier-G	40 (51.95%)	9 (81.82%)	Reference	
	Carrier-G	37 (48.05%)	2 (18.18%)	0.12 (0.01-1.08)	0.058
AIM2 rs2276405	C/C	72 (97.3%)	9 (90%)	Reference	
	C/T	2 (2.7%)	1 (10%)	61.06 (1.62-2294.92)	**0.026**
	C	146 (98.65%)	19 (95%)	Reference	
	T	2 (1.35%)	1 (5%)	1.49 (1-2.22)	**0.050**
	Non Carrier-C	74 (100%)	74 (100%)	Reference	
	Carrier-C	10 (100%)	10 (100%)	NC	NC
	Non Carrier-T	72 (97.3%)	9 (90%)	Reference	
	Carrier-T	2 (2.7%)	1 (10%)	61.06 (1.62-2294.92)	**0.026**
CARD8 rs2043211 rs6509365	TG	42 (27.27%)	1 (4.55%)	0.07 (0.01-0.81)	**0.033**

[a]Odds ratios were adjusted by skin color, education, site of tuberculosis, HIV transmission route, and CD8 count. [b]P-values were calculated using the unconditional logistic regression model. Associations were considered significant with a value of P < 0.05. N, number of individuals in each group; TB, tuberculosis; aOR, adjusted odds ratio; 95% CI, 95% confidence interval. A, T, G, and C = each allele count, irrespective of the genotype. Carrier-A = total of genotypes with the A allele, Carrier-T = total of genotypes with T allele, Carrier-C = total of genotypes with the C allele, Carrier-G = total of genotypes with the G allele, Non-Carrier-A = total of genotypes without the A allele, Non-Carrier-T = total of genotypes without the T allele, Non-Carrier-C = total of genotypes without the C allele, Non-Carrier-G = total of genotypes without the G allele. NC, not calcuated. Bold indicate statistically significant results.

plasma levels with TB-HIV/IRIS (Figure 1D). No statistical significance was observed for the plasma levels of the other cytokines (Figure 1D).

We next explored the relationships among the 11 Single Nucleotide Polymorphism (SNPs) and the plasma levels of the studied cytokines according to the carriers of the minor frequency allele (MFA) in the studied outcomes (with TB *vs.* without TB, PLWH with *vs.* without TB, PTB *vs.* EPTB, and with TB-HIV/IRIS *vs.* without IRIS) (Table 4). By comparing the carriers of the minor frequency allele in individuals with and without TB, CARD8 (rs2043211 and rs6509365), CASP-1 (rs572687), IFI16 (rs1101996), and NLRP3 (rs3806268, rs4612666, rs1539019, and rs10754558) had significant associations with the differences in IL-6 plasma levels; while IFI16 (rs1101996), and NLRP3 (rs3806268, rs1539019, and rs10754558) were significantly associated with differences in IL-33 plasma levels (Table 4). Among PLWH with and without TB, CARD8 (rs2043211 and rs6509365), CASP-1 (rs572687), IFI16 (rs1101996), IL-1β (rs1143634), and NLRP3 (rs3806268, rs4612666, rs1539019, and rs10754558) were significantly associated with differences in IL-6 plasma levels; while CARD8 (rs2043211 and rs6509365), IFI16 (rs1101996), and NLRP3 (rs3806268, rs4612666, rs1539019, and rs10754558) were significantly associated with differences in IL-33 plasma levels (Table 4). Among PTB and EPTB individuals, CARD8 (rs2043211 and rs6509365) was significantly associated with differences in IL-1β plasma levels (Table 4). Among individuals with and without IRIS, no statistically significant association was observed between the plasma cytokine levels and the minor frequency allele (Table S5).

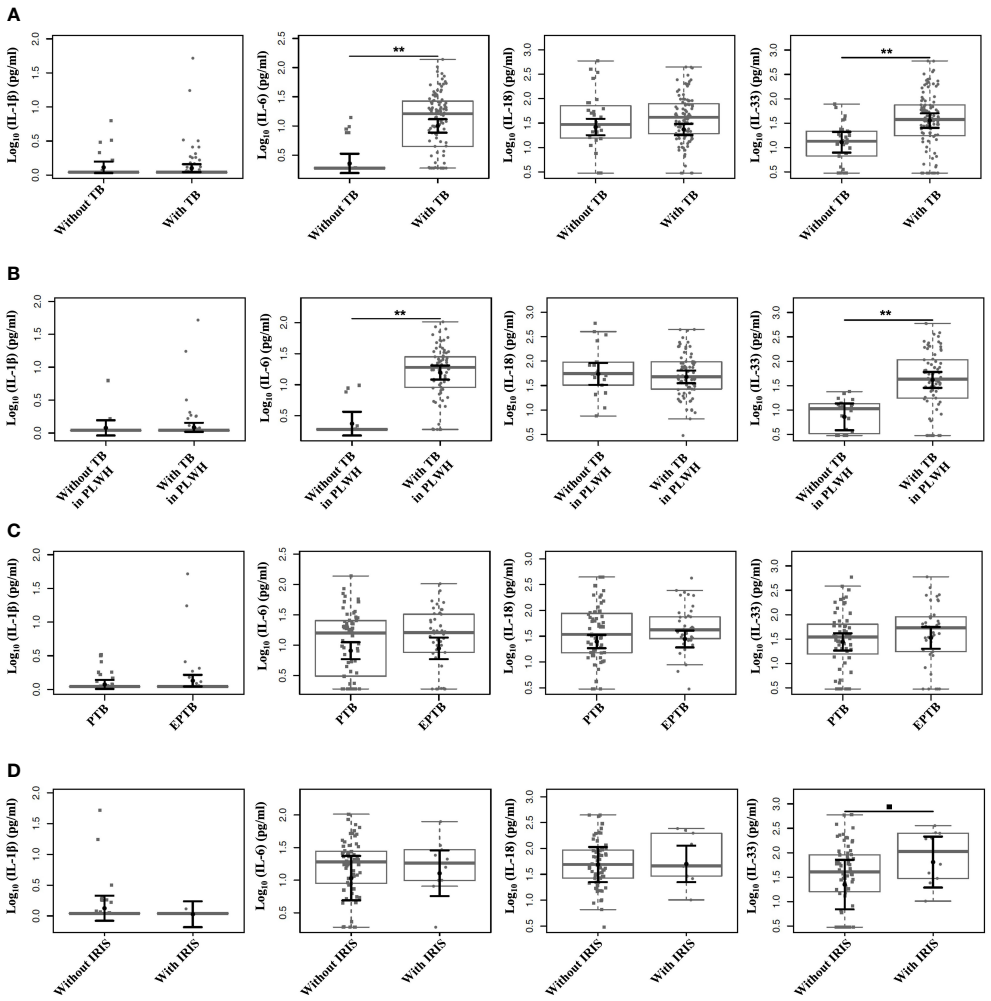

FIGURE 1
Comparison of plasma levels among the individuals included in the study categorized according to the outcomes. Plasma levels of IL-1β, IL-6, IL-18, and IL-33 measured by distinct ELISAs. **(A)** Comparison of plasma cytokine levels according to the presence or absence of TB. **(B)** Comparison of plasma cytokine levels according to the presence or absence of TB among PLWH. **(C)** Comparison of plasma cytokine levels according to different TB clinical presentations (PTB and EPTB). **(D)** Comparison of plasma cytokine levels according to the presence or absence of IRIS. Boxplots show the IQRs and sample medians (central solid gray line). Least-square means of log-transformed (base 10) levels of cytokines were pairwise compared among groups with T tests. Adjustments to the confidence levels were made by Sidak's method, and P value adjustments were made by multiple comparisons using Tukey's method. **P <0.0001; •P=0.073.

Discussion

Innate immunity and inflammation are biological mechanisms with important roles in susceptibility to or protection from HIV infection and/or TB-related outcomes (Salie et al., 2015; Ravimohan et al., 2018; Zhao et al., 2019). Aberrantly high inflammasome activation and its signaling in different cells and tissues lead to several inflammatory pathologies, including IRIS (Chang et al., 2014; Marais et al., 2017). TB-associated IRIS (TB-IRIS) incidence ranges from 4% to 54% in different populations (Bana et al., 2016). In the studies conducted by our group, the incidence of TB-HIV/IRIS was determined to be approximately 12% (Serra et al., 2007). The low incidence of TB-HIV/IRIS may be due to the introduction of antiretroviral therapy for newly diagnosed TB-HIV individuals in Brazil, who still had higher CD4 levels when at the time when they were recruited and included in this study. Beyond the very low CD4 counts (<100/mm3) and short time intervals between the initiation of anti-TB and antiretroviral therapies (Laureillard et al., 2013), the discrepancies in the IRIS frequencies could also be attributed to difficulties in clinical diagnosis (no specificity of symptoms) or differences in the genetic backgrounds among the populations included in the studies (Bourgarit et al., 2006; Wilkinson et al., 2015). Indeed, a previous study conducted by

10.3389/fcimb.2022.962059

TABLE 4 Plasma levels of cytokines according to the evaluated SNPs of the individuals included in the study.

Cytokines	Gene SNP (rs)	Carrier	Mean (CI95%)		P-value	Mean (CI95%)		P-value	Mean (CI95%)		P-value
			With TB	Without TB		With TB among HIV	Without TB among HIV		PTB	EPTB	
IL-1β	CARD8 rs2043211	A	0.142 (0.061 - 0.222)	0.202 (0.077 - 0.327)	0.842	0.151 (0.048 - 0.255)	0.129 (-0.063 - 0.321)	0.997	0.069 (-0.022 - 0.159)	0.319 (0.181 - 0.458)	**0.009**
	CARD8 rs6509365	A	0.139 (0.061 - 0.217)	0.165 (0.055 - 0.274)	0.981	0.141 (0.039 - 0.242)	0.102 (-0.046 - 0.251)	0.975	0.065 (-0.021 - 0.151)	0.301 (0.174 - 0.429)	**0.007**
	CASP-1 rs572687	G	0.055 (-0.039 - 0.149)	0.056 (-0.104 - 0.215)	1.000	0.039 (-0.082 - 0.159)	0.038 (-0.189 - 0.264)	1.000	0.025 (-0.114 - 0.163)	0.048 (-0.078 - 0.173)	0.994
	IFI16 rs1101996	C	0.083 (0.013 - 0.154)	0.081 (-0.032 - 0.194)	1.000	0.058 (-0.03 - 0.147)	-0.009 (-0.165 - 0.147)	0.864	0.06 (-0.025 - 0.145)	0.087 (-0.026 - 0.2)	0.977
	IL-1β rs1143634	G	0.1 (0.009 - 0.19)	0.042 (-0.125 - 0.208)	0.931	0.1 (-0.019 - 0.218)	0.058 (-0.235 - 0.352)	0.994	0.054 (-0.054 - 0.163)	0.176 (0.017 - 0.335)	0.573
	NLRP3 rs3806268	G	0.117 (0.044 - 0.191)	0.132 (0.003 - 0.26)	0.997	0.127 (0.039 - 0.214)	0.153 (-0.021 - 0.326)	0.993	0.052 (-0.039 - 0.143)	0.165 (0.059 - 0.271)	0.314
	NLRP3 rs35829419	C	0.048 (-0.135 - 0.232)	0.117 (-0.202 - 0.435)	0.982	0.06 (-0.238 - 0.357)	0.07 (-0.292 - 0.431)	1.000	0.032 (-0.201 - 0.264)	0.062 (-0.269 - 0.392)	0.999
	NLRP3 rs4612666	C	0.065 (-0.013 - 0.143)	0.091 (-0.016 - 0.198)	0.976	0.039 (-0.052 - 0.129)	0.047 (-0.091 - 0.186)	1.000	0.048 (-0.046 - 0.143)	0.053 (-0.064 - 0.17)	1.000
	NLRP3 rs1539019	C	0.092 (0.015 - 0.17)	0.068 (-0.062 - 0.197)	0.985	0.093 (0.001 - 0.185)	0.012 (-0.148 - 0.173)	0.798	0.073 (-0.029 - 0.174)	0.098 (-0.024 - 0.22)	0.987
	NLRP3 rs10754558	C	0.123 (0.054 - 0.193)	0.042 (-0.088 - 0.172)	0.652	0.109 (0.032 - 0.185)	0.039 (-0.118 - 0.197)	0.86	0.09 (-0.001 - 0.181)	0.158 (0.057 - 0.259)	0.684
IL-6	CARD8 rs2043211	A	0.953 (0.793 - 1.114)	0.353 (0.102 - 0.603)	**<0.001**	1.136 (0.966 - 1.307)	0.342 (0.024 - 0.659)	**<0.001**	0.84 (0.646 - 1.035)	1 (0.703 - 1.298)	0.775
	CARD8 rs6509365	A	0.899 (0.744 - 1.053)	0.385 (0.166 - 0.605)	**0.001**	1.071 (0.905 - 1.237)	0.45 (0.204 - 0.697)	**<0.001**	0.829 (0.641 - 1.018)	0.827 (0.555 - 1.1)	1.000
	CASP-1 rs572687	G	0.946 (0.756 - 1.135)	0.29 (-0.033 - 0.614)	**0.003**	1.15 (0.948 - 1.352)	0.289 (-0.094 - 0.671)	**0.001**	0.615 (0.329 - 0.901)	1.063 (0.803 - 1.322)	0.074
	IFI16 rs1101996	C	1.01 (0.869 - 1.15)	0.357 (0.133 - 0.581)	**<0.001**	1.185 (1.035 - 1.334)	0.354 (0.093 - 0.615)	**<0.001**	0.892 (0.715 - 1.069)	1.023 (0.788 - 1.258)	0.778
	IL-1β rs1143634	G	1.003 (0.827 - 1.178)	0.528 (0.197 - 0.858)	0.067	1.202 (1.012 - 1.392)	0.49 (-0.002 - 0.982)	**0.042**	0.978 (0.757 - 1.199)	0.867 (0.551 - 1.182)	0.934
	NLRP3 rs3806268	G	0.917 (0.774 - 1.061)	0.319 (0.073 - 0.565)	**<0.001**	1.095 (0.954 - 1.236)	0.391 (0.118 - 0.663)	**<0.001**	0.754 (0.571 - 0.938)	0.932 (0.72 - 1.145)	0.516
	NLRP3 rs35829419	C	0.726 (0.36 - 1.091)	0.155 (-0.478 - 0.789)	0.406	0.931 (0.434 - 1.429)	0.339 (-0.264 - 0.941)	0.432	0.578 (0.093 - 1.064)	0.857 (0.169 - 1.546)	0.916
	NLRP3 rs4612666	C	1.01 (0.855 - 1.166)	0.282 (0.07 - 0.494)	**<0.001**	1.226 (1.073 - 1.378)	0.386 (0.155 - 0.617)	**<0.001**	0.985 (0.789 - 1.182)	0.83 (0.591 - 1.069)	0.703
	NLRP3 rs1539019	C	0.913 (0.759 - 1.066)	0.317 (0.067 - 0.568)	**<0.001**	1.153 (1 - 1.307)	0.383 (0.12 - 0.646)	**<0.001**	0.838 (0.63 - 1.047)	0.86 (0.609 - 1.11)	0.999
	NLRP3 rs10754558	C	1.075 (0.939 - 1.211)	0.231 (-0.017 - 0.479)	**<0.001**	1.279 (1.156 - 1.402)	0.316 (0.072 - 0.56)	**<0.001**	1.03 (0.847 - 1.214)	0.987 (0.781 - 1.192)	0.985
IL-18	CARD8 rs2043211	A	1.363 (1.201 - 1.524)	1.333 (1.07 - 1.595)	0.997	1.591 (1.395 - 1.788)	1.684 (1.293 - 2.076)	0.975	1.329 (1.149 - 1.509)	1.588 (1.313 - 1.864)	0.345
	CARD8 rs6509365	A	1.31 (1.155 - 1.465)	1.417 (1.191 - 1.643)	0.857	1.516 (1.33 - 1.703)	1.773 (1.483 - 2.062)	0.467	1.28 (1.109 - 1.45)	1.523 (1.277 - 1.77)	0.303
	CASP-1 rs572687	G	1.333 (1.146 - 1.519)	1.43 (1.112 - 1.748)	0.947	1.69 (1.463 - 1.917)	1.667 (1.241 - 2.094)	1.000	1.303 (1.036 - 1.571)	1.458 (1.215 - 1.701)	0.801
	IFI16 rs1101996	C	1.361 (1.224 - 1.498)	1.413 (1.185 - 1.641)	0.976	1.695 (1.53 - 1.86)	1.636 (1.332 - 1.941)	0.986	1.418 (1.259 - 1.577)	1.381 (1.17 - 1.593)	0.991
	IL-1β rs1143634	G	1.548 (1.379 - 1.718)	1.354 (1.034 - 1.673)	0.716	1.826 (1.615 - 2.036)	1.668 (1.125 - 2.211)	0.95	1.617 (1.423 - 1.811)	1.522 (1.244 - 1.799)	0.939
		G			0.999		1.72 (1.365 - 2.076)	0.998			0.82

(Continued)

TABLE 4 Continued

Cytokines	Gene SNP (rs)	Carrier	Mean (CI95%)		P-value	Mean (CI95%)		P-value	Mean (CI95%)		P-value
			With TB	Without TB		With TB among HIV	Without TB among HIV		PTB	EPTB	
	NLRP3 rs3806268		1.353 (1.21 - 1.496)	1.336 (1.072 - 1.6)		1.684 (1.52 - 1.847)			1.36 (1.188 - 1.533)	1.466 (1.266 - 1.665)	
	NLRP3 rs35829419	C	1.301 (0.939 - 1.664)	1.37 (0.742 - 1.999)	0.998	1.338 (0.787 - 1.889)	1.77 (1.1 - 2.439)	0.751	1.497 (1.059 - 1.936)	1.014 (0.391 - 1.636)	0.6
	NLRP3 rs4612666	C	1.424 (1.273 - 1.576)	1.458 (1.243 - 1.674)	0.993	1.734 (1.565 - 1.903)	1.768 (1.493 - 2.042)	0.997	1.468 (1.289 - 1.648)	1.44 (1.222 - 1.657)	0.996
	NLRP3 rs1539019	C	1.345 (1.193 - 1.498)	1.39 (1.126 - 1.654)	0.989	1.611 (1.441 - 1.782)	1.725 (1.415 - 2.035)	0.91	1.345 (1.155 - 1.536)	1.459 (1.23 - 1.688)	0.846
	NLRP3 rs10754558	C	1.43 (1.294 - 1.565)	1.606 (1.341 - 1.871)	0.602	1.718 (1.577 - 1.859)	1.949 (1.642 - 2.257)	0.531	1.478 (1.308 - 1.648)	1.471 (1.281 - 1.662)	1.000
IL-33	CARD8 rs2043211	A	1.346 (1.142 - 1.55)	1.076 (0.757 - 1.394)	0.476	1.419 (1.172 - 1.665)	0.706 (0.248 - 1.164)	**0.038**	1.13 (0.896 - 1.365)	1.605 (1.246 - 1.964)	0.094
	CARD8 rs6509365	A	1.38 (1.184 - 1.577)	1.024 (0.745 - 1.303)	0.146	1.447 (1.208 - 1.685)	0.796 (0.441 - 1.151)	**0.018**	1.167 (0.941 - 1.393)	1.592 (1.265 - 1.919)	0.105
	CASP-1 rs572687	G	1.616 (1.372 - 1.861)	1.194 (0.777 - 1.61)	0.275	1.635 (1.346 - 1.925)	0.89 (0.344 - 1.437)	0.07	1.431 (1.057 - 1.805)	1.606 (1.267 - 1.946)	0.883
	IFI16 rs1101996	C	1.585 (1.406 - 1.764)	1.075 (0.789 - 1.361)	**0.008**	1.628 (1.415 - 1.84)	0.806 (0.436 - 1.176)	**0.001**	1.517 (1.294 - 1.74)	1.513 (1.217 - 1.808)	1.000
	IL-1β rs1143634	G	1.501 (1.274 - 1.728)	1.266 (0.838 - 1.694)	0.778	1.574 (1.302 - 1.847)	0.85 (0.143 - 1.556)	0.234	1.36 (1.08 - 1.641)	1.6 (1.199 - 2.001)	0.748
	NLRP3 rs3806268	G	1.544 (1.357 - 1.731)	1.035 (0.714 - 1.356)	**0.03**	1.608 (1.399 - 1.816)	0.863 (0.46 - 1.265)	**0.008**	1.35 (1.111 - 1.588)	1.583 (1.306 - 1.859)	0.51
	NLRP3 rs35829419	C	1.472 (0.995 - 1.95)	1.257 (0.429 - 2.085)	0.969	1.56 (0.844 - 2.276)	1.274 (0.406 - 2.141)	0.957	1.41 (0.786 - 2.034)	1.517 (0.632 - 2.403)	0.997
	NLRP3 rs4612666	C	1.514 (1.313 - 1.715)	1.097 (0.824 - 1.371)	0.051	1.576 (1.361 - 1.792)	0.969 (0.642 - 1.295)	**0.013**	1.393 (1.14 - 1.647)	1.475 (1.167 - 1.783)	0.971
	NLRP3 rs1539019	C	1.572 (1.372 - 1.772)	1.057 (0.731 - 1.383)	**0.022**	1.673 (1.454 - 1.892)	0.893 (0.517 - 1.268)	**0.002**	1.457 (1.19 - 1.724)	1.555 (1.235 - 1.875)	0.958
	NLRP3 rs10754558	C	1.662 (1.488 - 1.837)	0.96 (0.641 - 1.279)	**<0.001**	1.709 (1.528 - 1.889)	0.858 (0.5 - 1.216)	**<0.001**	1.602 (1.37 - 1.835)	1.572 (1.312 - 1.832)	0.997

P-values were calculated using the unconditional logistic regression model. Associations were considered significant with a value of $P < 0.05$. TB, tuberculosis; aOR, adjusted odds ratio; 95% CI, 95% confidence interval; PTB, Pulmonary TB; EPTB, Extrapulmonary TB. The AIM2 rs2276405 polymorphisms had insufficient observations and/or no way to calculate the standard error (all observations from one or more groups were equal to the lower detection limit of the assay) for the analyses between the groups with vs. without TB, with TB vs. without TB among HIV and PTB vs. EPTB. A, A allele; C, C allele; G, G allele. Bold indicate statistically significant results.

our group showed that the HLA-B*41 allele, KIR2DS2, and the combination of KIR/HLA-C pairs were associated with an increased risk of TB-HIV/IRIS onset (de Sá et al., 2020).

Here, we showed that the C/T genotype (ORadj=61.06; P=0.026) or carrier-T (ORadj=61.06; P=0.026) in the AIM2 rs2276405 polymorphism was associated with an increased risk of TB-HIV/IRIS in TB-HIV individuals, whereas lower risk IRIS onset was associated with the A/T genotype (ORadj=0.02; P=0.033) or carrier-T (ORadj=0.02; P=0.029) in the CARD8 rs2043211 polymorphism and with the CARD8 T-G haplotype (ORadj=0.07; P= 0.033).

Absent in melanoma 2 (AIM2) is a cytosolic sensor for double-stranded DNA (dsDNA) and tumor suppressor that is responsible for inflammasome activation and is involved in the host immune response to viruses and intracellular bacteria (Saiga et al., 2012). AIM2 binds to HIV dsDNA and may trigger acute inflammation and pyroptosis (Ekabe et al., 2021). Regarding the AIM2 rs2276405 polymorphism, to our knowledge, only one study showed a significant difference in the genotype frequencies of this Single Nucleotide Polymorphism (SNP) between individuals with and without TB in a Taiwanese population (Liu et al., 2020). In our study, no association between AIM2 polymorphisms and the occurrence of TB or its clinical presentations or inflammasome-related cytokines was observed.

CARD8 negatively regulates the expression of the NLRP3 inflammasome by inhibiting the oligomerization of this receptor in unstimulated cells (Tangi et al., 2012; Ito et al., 2014). The CARD8 gene rs2043211 polymorphism is an A to T transversion on the template strand (Ko et al., 2009). A Brazilian study found

an association between the CARD8 rs6509365 polymorphism and susceptibility to TB-HIV coinfection (Pontillo et al., 2013). This effect was stronger when this Single Nucleotide Polymorphism (SNP) was combined with the CARD8 rs2043211 polymorphism, supporting a novel association between the CARD8 gene and TB-HIV coinfection (Pontillo et al., 2013). However, in our study we did not observe any association of both CARD8 polymorphisms with TBHIV coinfection. However, when analyzing the CARD8 haplotypes a lower risk of TB onset among PLWH was observed. Moreover, a lower risk of IRIS associated with the CARD8 rs2043211 polymorphism and CARD8 haplotype was detected in our study. We also observed that carrying the MAF of both CARD8 polymorphisms was associated with increased levels of IL-6 in TB individuals compared to those without TB, IL-1β for those with EPTB clinical presentations, and IL-33 for TB-HIV cases.

Concerning the NLRP3 polymorphisms analyzed here, an increased risk for EPTB was associated with the TT genotype in the NLPR3 rs4612666 polymorphism or the C-C-T-G-C NLRP3 haplotype, whereas carrier-C in the NLRP3 rs4612666 polymorphism was associated with protection against EPTB. Increased levels of IL-6 or IL-33 and IL-18 or IL-33 were found in TB individuals both without and with HIV carrying the MFA of some selected NLRP3 polymorphisms. In addition, the G/A genotype in the IL-1β rs1143634 polymorphism was associated with TB risk among PLWH. Increased levels of IL-33 were found in TB individuals without and with HIV who were carrying the IL-1β rs1143634 MFA.

The NLPR3 rs4612666 polymorphism has already been associated with rheumatoid arthritis (Cheng et al., 2021) and cardiovascular diseases (Mahendra et al., 2021). The IL-1β rs1143634 polymorphism is associated with susceptibility to myocardial infarction (Fang et al., 2018), an aggressive phenotype of breast cancer (Wang and Yuan, [[NoYear]]), and is a predictive factor for a severe course of chronic periodontitis (Brodzikowska et al., 2019). To the best of our knowledge, this is the first study to report the association of these polymorphisms with the studied TB and TB-HIV outcomes. More studies are needed to confirm these findings.

It is evident that studying only one gene polymorphism is insufficient to explain the complexity of TB-HIV inflammatory outcomes. However, descriptions of genetic associations, even if at the Single Nucleotide Polymorphism (SNP) level, help understand the complex mechanisms that are involved in infectious diseases. It must be considered that other components of inflammasomes may regulate inflammation, in addition to other host genetic factors that are linked to TB-HIV immunopathogenesis. HLA and KIR alleles associations were previously described by our group (de Sá et al., 2020) and others, that should be considered in the search for genetic biomarkers of inflammatory diseases, including TB-HIV/IRIS. The importance of the selected inflammasome genes justifies the research conducted in the present study and the results obtained, which were generated using a suitable statistical approach, to adequately demonstrate the relationships among inflammasome-mediated innate immunity Single Nucleotide Polymorphism (SNPs) and TB-HIV/IRIS, as well as the occurrence of TB and its clinical presentations.

Several studies have related potential biomarkers to cytokine production as predictors of TB-HIV/IRIS onset. Tan et al. (2015) showed that individuals with TB-IRIS have higher levels of plasma IL-18 both in the pre-cART phase and during TB-HIV/IRIS (Tan et al., 2015). Similarly, Conesa-Botella et al. (2012) reported that in individuals without corticosteroid therapy, the levels of tumor necrosis factor (TNF), interferon-gamma (IFN-γ), and plasma levels of IL-6 and IL-18 were significantly higher in TB-HIV individuals with TB-IRIS than in those without IRIS at week two after starting cART. In contrast only the IFN-γ levels were higher in IRIS individuals at baseline (Conesa-Botella et al., 2012). In the present study, possibly due to the low number of subjects with TB-HIV/IRIS, no increase in the IL-1β and IL-18 cytokines, the typical inflammasome stimulation products, as well as IL-6 was detected for this group, but a trend toward increased IL-33 plasma levels was observed.

IL-6 is a known downstream target of IL-1β that is consistently higher in serum samples from individuals with NLRP3 inflammasome-mediated conditions (Brydges et al., [[NoYear]]; Tanaka et al., 2014). IL-6 is a proinflammatory cytokine with a pleiotropic effect on inflammation, immune response, and hematopoiesis (Tanaka et al., 2014). High levels of IL-6 have been described as a potential biomarker for TB and are associated with higher plasma viral loads and faster progression to AIDS in several studies (Boulware et al., 2011; Singh and Goyal, 2013; Joshi et al., 2015). In this study, IL-6 levels were higher in individuals with TB than those without TB and among PLWH with TB than those without TB.

Regarding IL-33, several studies report that this cytokine acts as an "alarm" that can be released upon tissue damage, stress, or infection, which acts as a danger signal for the immune system (Andreone et al., [[NoYear]]; Cayrol and Girard, [[NoYear]]; Neumann et al., 2018). In this study, the IL-33 levels were higher in individuals with TB than in those without TB and in PLWH with TB than those without TB. The role of this cytokine in HIV-1 infection and TB has already been described (Xuan et al., 2014; Wu et al., 2018), which shows potential therapeutic effects on established MTB infections, which might represent a novel therapy for PTB (Piñeros et al., 2017). Zhao et al., 2021 showed that the plasma IL-33 levels were significantly higher in individuals with PTB than in healthy individuals (Zhao et al., 2021).

As mentioned earlier, in addition to inflammasome stimulation and cytokine release in TB-HIV coinfection, these

processes can lead to extensive inflammation with cell damage and, consequently, overproduction of IL-33, which increases in those who progress to TB-HIV/IRIS, as suggested by our study. Therefore, additional studies are needed to investigate the roles of CARD8 and AIM2 gene variations in the modulation of inflammasome and cytokine secretion, mainly IL-33, in the context of TB-HIV/IRIS.

In conclusion, our study contributes to the generation of knowledge on the role of inflammasome Single Nucleotide Polymorphism (SNPs) and inflammatory cytokines in TB-HIV outcomes and the evolution toward TB-HIV/IRIS. Nevertheless, it is relevant to note that some limitations of the current study should be considered, mainly concerning the limited sample size and low frequency of HIV/TB-IRIS cases. Therefore, additional studies with larger populations are needed to understand better the importance and roles of inflammasome Single Nucleotide Polymorphism (SNPs) and inflammatory cytokines in TB-HIV/IRIS.

Data availability statement

The raw data supporting the conclusions of this article will be made available by the authors, without undue reservation.

Ethics statement

The studies involving human participants were reviewed and approved by IOC/FIOCRUZ (CAAE 51959215.5.0000.5248), INI/FIOCRUZ (CAAE 51959215.5.3002.5262), and HGNI (CAAE 51959215.5.3001.5254) Ethical Boards. The individuals/participants provided their written informed consent to participate in this study. The patients/participants provided their written informed consent to participate in this study.

Author contributions

NSá: conceptualization, methodology, validation, investigation, writing - original draft and visualization. NSo and MN-G: methodology, validation, and investigation. MR-A: software, formal analysis and resources, and writing - original draft. TS, JP, VR, CG-G, LdOP, and DS-A: resources and writing - review & editing. MM and ST: conceptualization, methodology, writing - original draft, and supervision. All authors read and approved the manuscript.

Funding

This work was supported by the Conselho Nacional de Desenvolvimento Científico e Tecnológico – CNPq (Grants numbers 404573/2012-6; 311345/2014-0; 435002/2018-0; 314064/2018-4), Fundação Carlos Chagas Filho de Amparo à Pesquisa do Estado do Rio de Janeiro- FAPERJ (Grant number E-26/010.001673/2019), and the France Recherche Nord & Sud Sida-HIV Hépatites - ANRS (Grant number ANRS12274). NBRS is recipient of INOVA FIOCRUZ/ Fundação Oswaldo Cruz postdoctoral fellowship. MGM is recipient of CNPQ (314064/2018-4) and FAPERJ (E-26/201.177/2021) research fellowships.

Acknowledgments

The authors are thankful to all individuals who agreed to participate in this study as volunteers and permitted the analysis of their biological material. We are in debt to Iury Amâncio Paiva and Jéssica Badolato Corrêa da Silva for technical support.

Conflict of interest

The authors declare that the research was conducted in the absence of any commercial or financial relationships that could be construed as a potential conflict of interest.

Publisher's note

All claims expressed in this article are solely those of the authors and do not necessarily represent those of their affiliated organizations, or those of the publisher, the editors and the reviewers. Any product that may be evaluated in this article, or claim that may be made by its manufacturer, is not guaranteed or endorsed by the publisher.

Supplementary material

The Supplementary Material for this article can be found online at: https://www.frontiersin.org/articles/10.3389/fcimb.2022.962059/full#supplementary-material

References

Andreone, S., Gambardella, A. R., Mancini, J., Loffredo, S., Marcella, S., La, S. V., et al. Anti-tumorigenic activities of IL-33: A mechanistic insight. *Front. Immunol.* 11, 571593. doi: 10.3389/fimmu.2020.571593

Antonelli, L. R. V., Mahnke, Y., Hodge, J. N., Porter, B. O., Barber, D. L., Dersimonian, R., et al. (2010). Elevated frequencies of highly activated CD4 T cells in HIV patients developing immune reconstitution inflammatory syndrome. *Blood* 116, 3818–3827. doi: 10.1182/blood-2010-05-285080

Bana, T. M., Lesosky, M., Pepper, D. J., van der Plas, H., Schutz, C., Goliath, R., et al. (2016). Prolonged tuberculosis-associated immune reconstitution

inflammatory syndrome: Characteristics and risk factors. *BMC Infect. Dis.* 16 (1), 1–12. doi: 10.1186/s12879-016-1850-2

Boulware, D. R., Hullsiek, K. H., Puronen, C. E., Rupert, A., Baker, J. V., French, M. A., et al. (2011). Higher levels of CRP, d-dimer, IL-6, and hyaluronic acid before initiation of antiretroviral therapy (ART) are associated with increased risk of AIDS or death. *J. Infect. Dis.* 203 (11), 1637–1646. doi: 10.1093/infdis/jir134

Bourgarit, A., Carcelain, G., Martinez, V., Lascoux, C., Delcey, V., Gicquel, B., et al. (2006). Explosion of tuberculin-specific Th1-responses induces immune restoration syndrome in tuberculosis and HIV co-infected patients. *AIDS* 20 (2), F1–F7. doi: 10.1097/01.aids.0000202648.18526.bf

Brodzikowska, A., Górska, R., and Kowalski, J. (2019). Interleukin-1 genotype in periodontitis. *Arch. Immunol. Ther. Exp. (Warsz)* 67 (6), 367. doi: 10.1007/s00005-019-00555-4

Cayrol, C., and Girard, J. P. (2018). Interleukin-33 (IL-33): A nuclear cytokine from the IL-1 family. *Immunol. Rev.* 281, 154–168. doi: 10.1111/imr.12619

Chang, C. C., Sheikh, V., Sereti, I., and French, M. A. (2014). Immune reconstitution disorders in patients with HIV infection: from pathogenesis to prevention and treatment. *Curr. HIV/AIDS Rep.* 11 (3), 223–232. doi: 10.1007/s11904-014-0213-0

Cheng, L., Liang, X., Qian, L., Luo, C., and Li, D. (2021). NLRP3 gene polymorphisms and expression in rheumatoid arthritis. *Exp. Ther. Med.* 22 (4):1100. doi: 10.3892/etm.2021.10544

Conesa-Botella, A., Meintjes, G., Coussens, A. K., van der Plas, H., Goliath, R., Schutz, C., et al. (2012). Corticosteroid therapy, vitamin d status, and inflammatory cytokine profile in the HIV-tuberculosis immune reconstitution inflammatory syndrome. *Clin. Infect. Dis.* 55 (7), 1004–1011. doi: 10.1093/cid/cis577

da Silva, T. P., Giacoia-Gripp, C. B. W., Schmaltz, C. A., Sant' Anna, F. M., Rolla, V., and Morgado, M. G. (2013). T Cell activation and cytokine profile of tuberculosis and HIV-positive individuals during antituberculous treatment and efavirenz-based regimens. *PloS One* 8 (6), 4–11. doi: 10.1371/journal.pone.0066095

da Silva, T. P., Giacoia-Gripp, C. B. W., Schmaltz, C. A., Sant'Anna, F. M., Saad, M. H., de Matos, J. A., et al. (2017). Risk factors for increased immune reconstitution in response to mycobacterium tuberculosis antigens in tuberculosis HIV-infected, antiretroviral-naïve patients. *BMC Infect. Dis.* 17 (1), 1–10. doi: 10.1186/s12879-017-2700-6.

De Lima, D. S., Ogusku, M. M., Dos Santos, M. P., De Melo Silva, C. M., De Almeida, V. A., Antunes, I. A., et al. (2016). Alleles of HLA-DRB1∗04 associated with pulmonary tuberculosis in Amazon Brazilian population. *PloS One* 11 (2), 1–13. doi: 10.1371/journal.pone.0147543

Demitto, F. O., Schmaltz, C. A. S., Sant'Anna, F. M., Arriaga, M. B., Andrade, B. B., and Rolla, V. C. (2019). Predictors of early mortality and effectiveness of antiretroviral therapy in TB-HIV patients from Brazil. *PloS One* 14 (6), e0217014. doi: 10.1371/journal.pone.0217014

de Sá, N. B. R., Ribeiro-Alves, M., da Silva, T. P., Pilotto, J. H., Rolla, V. C., Giacoia-Gripp, C. B. W., et al. (2020). Clinical and genetic markers associated with tuberculosis, HIV-1 infection, and TB/HIV-immune reconstitution inflammatory syndrome outcomes. *BMC Infect. Dis.* 20 (1), 59. doi: 10.1186/s12879-020-4786-5

Ekabe, C. J., Clinton, N. A., Kehbila, J., and Franck, N. C. (2021). The role of inflammasome activation in early HIV infection. *J. Immunol. Res.* 2021:1487287. doi: 10.1155/2021/1487287

Fang, Y., Xie, H., and Lin, Z. (2018). Association between IL-1β+3954C/T polymorphism and myocardial infarction risk: A meta-analysis. *Med. (Baltimore)* 97 (30):e11645. doi: 10.1097/MD.0000000000011645

Fellay, J., Ge, D., Shianna, K. V., Colombo, S., Ledergerber, B., Cirulli, E. T., et al. (2009). Common genetic variation and the control of HIV-1 in humans. *PloS Genet.* 5 (12), e1000791. doi: 10.1371/journal.pgen.1000791

French, M. A., Price, P., and Stone, S. F. (2004). Immune restoration disease after antiretroviral therapy. *AIDS.* 18, 1615–1627. doi: 10.1097/01.aids.0000131375.21070.06

Giacoia-Gripp, C. B. W., Cazote A da, S., da Silva, T. P., Sant'Anna, F. M., Schmaltz, C. A. S., Brum T de, S., et al. (2019). Changes in the NK cell repertoire related to initiation of TB treatment and onset of immune reconstitution inflammatory syndrome in TB/HIV Co-infected patients in Rio de Janeiro, Brazil–ANRS 12274. *Front. Immunol.* 10. doi: 10.3389/fimmu.2019.01800

Instituto Brasileiro de Geografia e Estatística (2013). Características étnico - raciais da população: classificação e identidades. estudos e análises: informação demográfica e socioeconômica 83–99.

Ito, S., Hara, Y., and Kubota, T. (2014). CARD8 is a negative regulator for NLRP3 inflammasome, but mutant NLRP3 in cryopyrin-associated periodic syndromes escapes the restriction. *Arthritis Res. Ther.* 16 (1):R52. doi: 10.1186/ar4483

Joshi, L., Ponnana, M., Sivangala, R., Chelluri, L. K., Nallari, P., Penmetsa, S., et al. (2015). Evaluation of TNF-α, IL-10 and IL-6 cytokine production and their correlation with genotype variants amongst tuberculosis patients and their household contacts. *PloS One* 10 (9), e0137727. doi: 10.1371/journal.pone.0137727. Subbian S.

Ko, D. C., Shukla, K. P., Fong, C., Wasnick, M., Brittnacher, M. J., Wurfel, M. M., et al. (2009). A genome-wide *In vitro* bacterial-infection screen reveals human variation in the host response associated with inflammatory disease. *Am. J. Hum. Genet.* 85 (2), 214–227. doi: 10.1016/j.ajhg.2009.07.012

Kulkarni, S., Martin, M. P., and Carrington, M. (2008). The yin and yang of HLA and KIR in human disease. *Semin. Immunol.* 20, 343–352. doi: 10.1016/j.smim.2008.06.003

Lai, R. P. J., Meintjes, G., Wilkinson, K. A., Graham, C. M., Marais, S., van der Plas, H., et al. (2015). HIV-Tuberculosis-associated immune reconstitution inflammatory syndrome is characterized by toll-like receptor and inflammasome signalling. *Nat. Commun.* 6, 8451. doi: 10.1038/ncomms9451

Laureillard, D., Marcy, O., Madec, Y., Chea, S., Chan, S., Borand, L., et al. (2013). Paradoxical tuberculosis-associated immune reconstitution inflammatory syndrome after early initiation of antiretroviral therapy in a randomized clinical trial. *AIDS* 27 (16), 2577–2586. doi: 10.1097/01.aids.0000432456.14099.c7

Levy, J. A. (2009). HIV Pathogenesis: 25 years of progress and persistent challenges. *AIDS* 23 (2), 147–160. doi: 10.1097/QAD.0b013e3283217f9f

Liu, C. W., Lin, C. J., Hu, H. C., Liu, H. J., Chiu, Y. C., Lee, S. W., et al. (2020). The association of inflammasome and TLR2 gene polymorphisms with susceptibility to tuberculosis in the han Taiwanese population. *Sci. Rep.* 10 (1):10184. doi: 10.1038/s41598-020-67299-6

Luetkemeyer, A. F., Kendall, M. A., Nyirenda, M., Wu, X., Ive, P., Benson, C. A., et al. (2014). Tuberculosis immune reconstitution inflammatory syndrome in A5221 STRIDE: timing, severity, and implications for HIV-TB programs. *J. Acquir. Immune Defic. Syndr.* 65 (4), 423–428. doi: 10.1097/QAI.0000000000000030

Mahendra, J., Rao, A. N., Mahendra, L., Fageeh, H. N., Fageeh, H. I., Balaji, T. M., et al. (2021). Genetic polymorphisms of nlrp3 (Rs4612666) and card8 (rs2043211) in periodontitis and cardiovascular diseases. *Biol. (Basel)* 10 (7):592. doi: 10.3390/biology10070592

Man, S. M., and Kanneganti, T.-D. (2015). Regulation of inflammasome activation. *Immunol. Rev.* 265 (1), 6–21. doi: 10.1111/imr.12296

Marais, S., Lai, R. P. J., Wilkinson, K. A., Meintjes, G., and Wilkinson, R. J. (2017). Inflammasome activation underlying central nervous system deterioration in HIV-associated tuberculosis 1), 677–689. doi: 10.1093/infdis/jiw561

Martin, M. P., and Carrington, M. (2013). Immunogenetics of HIV disease. *Immunol. Rev.* 254 (1), 245–264. doi: 10.1111/imr.12071

McGeough, MD, Pena, CA, Mueller, JL, Pociask, DA, Broderick, L, Hoffman HM, , et al. (2012). Cutting edge: IL-6 is a marker of inflammation with no direct role in inflammasome-mediated mouse models. *J. Immunol.* 189 (6), 2707–2711. doi: 10.4049/jimmunol.1101737

Meintjes, G., Lawn, S. D., Scano, F., Maartens, G., French, M. A., Worodria, W., et al. (2008). Tuberculosis-associated immune reconstitution inflammatory syndrome: case definitions for use in resource-limited settings. *Lancet Infect. Dis.* 8 (8), 516–523. doi: 10.1016/S1473-3099(08)70184-1

Müller, M., Wandel, S., Colebunders, R., Attia, S., Furrer, H., and Egger, M. (2010). Immune reconstitution inflammatory syndrome in patients starting antiretroviral therapy for HIV infection: a systematic review and meta-analysis. *Lancet Infect. Dis.* 10 (4), 251–261. doi: 10.1016/S1473-3099(10)70026-8

Naranbhai, V., and Carrington, M. (2017). Host genetic variation and HIV disease: from mapping to mechanism. *Immunogenetics* 69 (8–9), 489–498. doi: 10.1007/s00251-017-1000-z

Narendran, G., Kavitha, D., Karunaianantham, R., Gil-Santana, L., Almeida-Junior, J. L., Reddy, S. D., et al. (2016). Role of LTA4H polymorphism in tuberculosis-associated immune reconstitution inflammatory syndrome occurrence and clinical severity in patients infected with HIV. *PloS One* 11 (9):2732, 1–11. doi: 10.1371/journal.pone.0163298

Neumann, K., Schiller, B., and Tiegs, G. (2018). NLRP3 inflammasome and IL-33: Novel players in sterile liver inflammation. *Int. J. Mol. Sci.* 19 (9), 2732. doi: 10.3390/ijms19092732

Piñeros, A. R., Campos, L. W., Fonseca, D. M., Bertolini, T. B., Gembre, A. F., Prado, R. Q., et al. (2017). M2 macrophages or IL-33 treatment attenuate ongoing mycobacterium tuberculosis infection. *Sci. Rep.* 7:41240. doi: 10.1038/srep41240.

Pontillo, A., Brandão, L a, Guimarães, R. L., Segat, L., Athanasakis, E., and Crovella, S. (2010). A 3'UTR Single Nucleotide Polymorphism (SNP) in NLRP3 gene is associated with susceptibility to HIV-1 infection. *J. Acquir. Immune Defic. Syndr.* 54 (3), 236–240. doi: 10.1097/QAI.0b013e3181dd17d4

Pontillo, A., Carvalho, M. S., Kamada, A. J., Moura, R., Schindler, H. C., Duarte, A. J. S., et al. (2013). Susceptibility to mycobacterium tuberculosis infection in HIV-positive patients is associated with CARD8 genetic variant. *J. Acquir. Immune Defic. Syndr.* 63 (2), 147–151. doi: 10.1097/QAI.0b013e31828f93bb

Pontillo, A., Oshiro, T. M., Girardelli, M., Kamada, A. J., Crovella, S., and Duarte, A. J. S. (2012). Polymorphisms in inflammasome ' genes and susceptibility to HIV-1 infection. *BASIC Transl. Sci.* 59 (2), 121–125. doi: 10.1097/QAI.0b013e3182392ebe

Rathinam, V. A. K., and Fitzgerald, K. A. (2016). Inflammasome complexes: Emerging mechanisms and effector functions. *Cell* 165 (4), 792–800. doi: 10.1016/j.cell.2016.03.046

Ravimohan, S., Maenetje, P., Auld, S. C., Ncube, I., Mlotshwa, M., Chase, W., et al. (2020). A common nlrc4 gene variant associates with inflammation and pulmonary function in human immunodeficiency virus and tuberculosis. *Clin. Infect. Dis.* 71 (4), 924–932. doi: 10.1093/cid/ciz898

Ravimohan, S., Nfanyana, K., Tamuhla, N., Tiemessen, C. T., Weissman, D., and Bisson, G. P. (2018). Common variation in NLRP3 is associated with early death and elevated inflammasome biomarkers among advanced HIV/TB Co-infected patients in Botswana. *Open Forum Infect. Dis.* 5 (5):ofy075. doi: 10.1093/ofid/ofy075/4967683

Robertson, J., Meier, M., Wall, J., Ying, J., and Fichtenbaum, C. J. (2006). Immune reconstitution syndrome in HIV: validating a case definition and identifying clinical predictors in persons initiating antiretroviral therapy. *Clin. Infect. Dis.* 42 (11), 1639–1646. doi: 10.1086/503903

Saiga, H., Kitada, S., Shimada, Y., Kamiyama, N., Okuyama, M., Makino, M., et al. (2012). Critical role of AIM2 in mycobacterium tuberculosis infection. *Int. Immunol.* 24 (10), 637–644. doi: 10.1093/intimm/dxs062

Salie, M., Daya, M., Möller, M., and Hoal, E. G. (2015). Activating KIRs alter susceptibility to pulmonary tuberculosis in a south African population. *Tuberculosis.* 95 (6), 817–821. doi: 10.1016/j.tube.2015.09.003

Seaby, E. G., Wright, V. J., and Levin, M. (2016). Genome-wide association studies in infectious diseases. *Pediatr. Infect. Dis. J.* 35 (7), 802–804. doi: 10.1097/INF.0000000000001183

Serra, F. C., Hadad, D., Orofino, R. L., Marinho, F., Lourenço, C., Morgado, M., et al. (2007). Immune reconstitution syndrome in patients treated for HIV and tuberculosis in Rio de Janeiro. *Braz. J. Infect. Dis.* 11 (5), 462–465. doi: 10.1590/S1413-86702007000500004

Shelburne, S. A., Visnegarwala, F., Darcourt, J., Graviss, E. A., Giordano, T. P., White, A. C., et al. (2005). Incidence and risk factors for immune reconstitution inflammatory syndrome during highly active antiretroviral therapy. *AIDS* 19 (4), 399–406. doi: 10.1097/01.aids.0000161769.06158.8a

Singh, P. P., and Goyal, A. (2013). Interleukin-6: A potent biomarker of mycobacterial infection. *Springerplus.* 2 (1):686. doi: 10.1186/2193-1801-2-686

Tadokera, R., Meintjes, G., Skolimowska, K. H., Wilkinson, K. A., Matthews, K., Seldon, R., et al. (2011). Hypercytokinaemia accompanies HIV-tuberculosis immune reconstitution inflammatory syndrome. *Eur. Respir. J.* 37 (5), 1248–1259. doi: 10.1183/09031936.00091010

Tanaka, T., Narazaki, M., and Kishimoto, T. (2014). IL-6 in inflammation, immunity, and disease. *Cold Spring Harb. Perspect. Biol.* 6 (10), a016295. doi: 10.1101/cshperspect.a016295

Tangi, T. N., Elmabsout, A. A., Bengtsson, T., Sirsjö, A., and Franśen, K. (2012). Role of NLRP3 and CARD8 in the regulation of TNF-α induced IL-1β release in vascular smooth muscle cells. *Int. J. Mol. Med.* 30 (3), 697–702. doi: 10.3892/ijmm.2012.1026

Tan, H. Y., Yong, Y. K., Andrade, B. B., Shankar, E. M., Ponnampalavanar, S., Omar, S. F. S., et al. (2015). Plasma interleukin-18 levels are a biomarker of innate immune responses that predict and characterize tuberculosis-associated immune reconstitution inflammatory syndrome. *AIDS.* 29 (4):421-31. doi: 10.1097/QAD.0000000000000557

Tan, H. Y., Yong, Y. K., Shankar, E. M., Paukovics, G., Ellegård, R., Larsson, M., et al. (2016). Aberrant inflammasome activation characterizes tuberculosis-associated immune reconstitution inflammatory syndrome. *J. Immunol.* 196 (10), 4052–4063. doi: 10.4049/jimmunol.1502203

Tibúrcio, R., Barreto-Duarte, B., Naredren, G., Queiroz, A. T. L., Anbalagan, S., Nayak, K., et al. (2021). Dynamics of T-lymphocyte activation related to paradoxical tuberculosis-associated immune reconstitution inflammatory syndrome in persons with advanced HIV. *Front. Immunol.* 12, 4214. doi: 10.3389/fimmu.2021.757843

Tsiara, C. G., Nikolopoulos, G. K., Dimou, N. L., Pantavou, K. G., Bagos, P. G., Mensah, B., et al. (2018). Interleukin gene polymorphisms and susceptibility to HIV-1 infection: a meta-analysis. *J. Genet.* 97 (1), 235–251. doi: 10.1007/s12041-018-0907-y

Wang, B., and Yuan, F. (2022). The association between interleukin-1β gene polymorphisms and the risk of breast cancer: a systematic review and meta-analysis. *Arch. Med. Sci.* 18 (1), 1. doi: 10.5114/aoms/99839

Wilkinson, K. A., Walker, N. F., Meintjes, G., Deffur, A., Nicol, M. P., Skolimowska, K. H., et al. (2015). Cytotoxic mediators in paradoxical HIV–tuberculosis immune reconstitution inflammatory syndrome. *J. Immunol.* 194 (4), 1748–1754. doi: 10.4049/jimmunol.1402105

World Health Organization (2020) *Global tuberculosis report 2020*. Available at: https://www.who.int/publications/i/item/9789240013131.

Wu, X., Li, Y., Song, C.-B., Chen, Y.-L., Fu, Y.-J., Jiang, Y.-J., et al. (2018). Increased expression of sST2 in early HIV infected patients attenuated the IL-33 induced T cell responses. *Front. Immunol.* 9. doi: 10.3389/fimmu.2018.02850/full

Wu, Y., Tian, Z., and Wei, H. (2017). Developmental and functional control of natural killer cells by cytokines. *Front. Immunol.* 8. Frontiers Media S.A. doi: 10.3389/fimmu.2017.00930

Xuan, W. X., Zhang, J. C., Zhou, Q., Yang, W. B., and Ma, L. J. (2014). IL-33 levels differentiate tuberculous pleurisy from malignant pleural effusions. *Oncol. Lett.* 8 (1), 449–453. doi: 10.3892/ol.2014.2109

Zhao, J., Tang, W., Yao, J., Chen, Q., Xu, Q., and Wu, S. (2019). The role of killer immunoglobulin-like receptor genes in susceptibility to HIV-1 infection and disease progression: A meta-analysis. *AIDS Res. Hum. Retroviruses* 35 (10), 948–959. doi: 10.1089/aid.2019.0172

Zhao, Y., Zhang, J., Xue, B., Zhang, F., Xu, Q., Ma, H., et al. (2021). Serum levels of inhibitory costimulatory molecules and correlationswith levels of innate immune cytokines in patients with pulmonarytuberculosis. *J. Int. Med. Res.* 49 (8):3000605211036832. doi: 10.1177/03000605211036832

frontiers | Frontiers in Cellular and Infection Microbiology

TYPE Original Research
PUBLISHED 12 October 2022
DOI 10.3389/fcimb.2022.953443

OPEN ACCESS

EDITED BY
Divakar Sharma,
University of Delhi, India

REVIEWED BY
Mariza Gonçalves Morgado,
Oswaldo Cruz Foundation (Fiocruz), Brazil
Abolfazl Fateh,
Pasteur Institute of Iran (PII), Iran

*CORRESPONDENCE
Sarman Singh
sarman_singh@yahoo.com;
sarman.singh@gmail.com

SPECIALTY SECTION
This article was submitted to Clinical Microbiology, a section of the journal Frontiers in Cellular and Infection Microbiology

RECEIVED 26 May 2022
ACCEPTED 30 August 2022
PUBLISHED 12 October 2022

CITATION
Singh J, Singh N, Suresh G, Srivastava R, Aggarwal U, Behera D, Munisamy M, Malhotra AG and Singh S (2022) A comparative analysis of molecular genotypes of *Mycobacterium tuberculosis* isolates from HIV-positive and HIV-negative patients. *Front. Cell. Infect. Microbiol.* 12:953443. doi: 10.3389/fcimb.2022.953443

A comparative analysis of molecular genotypes of *Mycobacterium tuberculosis* isolates from HIV-positive and HIV-negative patients

Jitendra Singh[1,2], Niti Singh[3], Gayatri Suresh[3], Rahul Srivastava[3], Upasna Aggarwal[3], Digamber Behera[3,4], Murali Munisamy[2], Anvita Gupta Malhotra[5] and Sarman Singh[1,5,6]*

[1]Division of Clinical Microbiology and Molecular Medicine, All India Institute of Medical Sciences, New Delhi, India, [2]Translational Medicine Centre, All India Institute of Medical Sciences, Bhopal, India, [3]Department of Microbiology, National Institute of Tuberculosis and Respiratory Diseases (NITRD), New Delhi, India, [4]Department of Pulmonary Medicine, PGIMER, Chandigarh, India, [5]Department of Microbiology, All India Institute of Medical Sciences, Bhopal, India, [6]Medical Science and Engineering Research Centre, Indian Institute of Science Education and Research, Bhopal, India

Setting: Tuberculosis Research Laboratory, Division of Clinical Microbiology and Molecular Medicine, Department of Laboratory Medicine, All India Institute of Medical Sciences, and the National Institute of Tuberculosis and Respiratory Diseases (NITRD), both situated in New Delhi.

Objectives: We aimed to identify the distribution of various genotypes of *M. tuberculosis* among HIV-positive and HIV-negative patients suspected of having Tuberculosis, seen at the National Institute of Tuberculosis and Respiratory Diseases, New Delhi, which is a tertiary care dedicated TB hospital.

Patients and methods: Genotyping by Spoligotyping and 24 loci MIRU-VNTR was performed and analyzed using SITVITWEB and MIRU-VNTRplus. Drug susceptibility patterns were also analyzed.

Results: A total of 503 subjects who were PTB/EPTB suspected were recruited and 287 were culture positive. Among them, 276 had growth of *Mycobacterium tuberculosis* (MTB) and in 11 patients non-tuberculous mycobacteria (NTM) were grown. The isolation rate of NTM was predominantly from HIV positive [10 of 130 (7.6%)] patients. Of the total isolates of MTB, 156 (56.5%) were from HIV negative patients and 120 (43.5%) were from HIV positive patients. All 276 *M. tuberculosis* isolates were genotyped and tested for drug susceptibility patterns. The CAS genotype was most predominant [153 (55.4%)], followed by Beijing lineage [44 (15.9%)], East African India [25 (9.1%)] and others [54 (19.6%)]. Beijing genotype was

significantly more common in HIV positive patients (22.5%) than in HIV negative patients (10.9%). In MIRU-VNTR analysis, clustering was found to be more frequent in CAS strains irrespective of HIV status. In the HIV positive group, spoligotyping could differentiate various genotypes in 90% of isolates and MIRU-VNTR analysis in 84.2% of isolates. The clustering of various MTB strains was more associated with drug resistance.

Conclusion: The Beijing lineage was predominant in HIV-TB coinfected cases, even though the Central Asian Strain (CAS) was overall more predominant in the region.

KEYWORDS

spoligotyping, genotypes, HIV, *Mycobacterium tuberculosis*, molecular epidemiology

Introduction

Tuberculosis (TB) and Human immunodeficiency virus (HIV) infections are lethal chronic infections and are among the leading causes of mortality globally. In 2019, an estimated 1.2 million TB deaths occurred among HIV-negative people and 208,000 deaths amongst HIV-positive people (Global tuberculosis report 2020). As per a WHO 2020 report, 69% of notified TB patients had documented HIV test results, as compared to 64% in 2018. The burden of HIV-associated TB is the highest in the WHO African region, where 86% of TB patients had a documented HIV test result. Globally, 88% of the TB-HIV co-infected patients were on antiretroviral therapy (ART), while this proportion was 95% in India (WHO, 2016).

Although both TB and HIV are deadly by themselves, they have an additive pathogenic influence when they come together, thereby making the HIV-TB co-infection a "double trouble" for society (Munawwar and Singh, 2012). Coordinated pathogenesis of HIV and *Mycobacterium tuberculosis* poses a major medical challenge as HIV provides an enormous opportunity for *M. tuberculosis* to multiply rapidly within the intracellular setting, and *M. tuberculosis* provides a favorable environment for HIV to replicate unhindered *via* TB-associated protein malnutrition and increased depletion or non-activation of T lymphocytes (Friedland et al., 2007; Munawwar and Singh, 2012).

Molecular genotyping reveals the different levels of genetic polymorphisms of *M. tuberculosis* and is applicable in monitoring disease transmission, detecting outbreaks, and confirming laboratory cross-contaminations and clonal spread of dominant clones. Under certain circumstances, it is used to distinguish between members of the *M. tuberculosis* complex that have critical clinical importance (Allix-Béguec et al., 2010). Due to its clonal structure (Sreevatsan et al., 1997), the comparative genotype analysis of MTCs from different human populations can give unique insights into the dissemination dynamics and evolutionary genetics of this pathogen; therefore, spoligotyping has been used to understand the emerging problem of multidrug-resistant (MDR) TB and the virulence of certain epidemic strains of *M. tuberculosis* (for example; the Beijing strain), as well as to better understand the epidemiology of TB and TB-HIV co-infection (Cadmus et al., 2011).

Spoligotyping is based on polymorphism in the direct repeat (DR) locus and is used as a primary genotyping method in combination with molecular typing methods based on variable number tandem repeats (VNTRs) of the 24 loci DNA elements known as mycobacterial interspersed repetitive units (MIRU) (Supply et al., 2006). MIRU-VNTR in combination with spoligotyping has become a striking alternative to the traditional IS6110-RFLP fingerprinting method, with maximum discriminatory power (Pitondo-Silva et al., 2013).

Information on the genotypes of *M. tuberculosis* isolated from India, in comparison with those obtained globally, are important for understanding the global spread and phylogeographical specificity of the predominant circulating clones of tubercle bacilli. In addition, *M. tuberculosis* molecular genotyping data obtained from India so far have not addressed the issue of HIV-TB co-infected patients, a subpopulation involved in the spread of the disease in Asia in general and India in particular (Gutierrez et al., 2006; Sharma et al., 2008; Thomas et al., 2011; Vadwai et al., 2012; Singh et al., 2015). We have previously analyzed the molecular genotypes of

Abbreviation: TB, Tuberculosis; PTB, Pulmonary Tuberculosis; EPTB, Extrapulmonary Tuberculosis; HIV, Human Immunodeficiency Virus; MIRU-VNTR, Mycobacterial Interspersed Repetitive Unite - Variable Number Tandem Repeat; DST-SIRE, Drug Susceptibility Testing for Streptomycin (STR), Isoniazid (INH), Rifampin (RIF), and Ethambutol (EMB); CAS, Central Asian; EAI, East-African-Indian.

M. tuberculosis among extrapulmonary and pulmonary tuberculosis patients irrespective of their HIV status (Sankar et al., 2013; Singh et al., 2015). Here, we aimed to investigate the spoligotyping and 24 loci MIRU-VNTR based population structure of *M. tuberculosis* clinical isolates from HIV negative and MTB positive patients and HIV-TB co-infected patients, and to compare the patterns obtained with those available in the SIT-VIT web database of the Pasteur Institute of Guadeloupe (Demay et al., 2012).

Materials and methods

Patient inclusion

This study was performed at the Tuberculosis Research Laboratory, Division of Clinical Microbiology and Molecular Medicines, All India Institute of Medical Sciences (AIIMS), New Delhi. The total duration of the study was three years from April 2012 to March 2015. All the patients were recruited at the National Institute of Tuberculosis and Respiratory Diseases (NITRD), New Delhi. As a standard protocol in India, all TB suspected cases are tested for HIV as per the standard guidelines issued by the National AIDS Control Organization and WHO. The inclusion criteria were all HIV-positive patients suspected of concomitant tuberculosis infection and clinically suspected patients with pulmonary tuberculosis (PTB) and/or extra-pulmonary tuberculosis (EPTB). Informed consent was obtained from all the recruited cases. However, we excluded patients taking anti-tuberculous treatment (ATT) for more than two weeks at the time of recruitment, patients under immune-suppressive treatment, and pregnant female patients. This study was approved by the Institutional Ethics Committees of the All India Institute of Medical Sciences, and the National Institute of Tuberculosis and Respiratory Diseases, New Delhi.

Sample processing and identification

The clinical samples were transported on a daily basis to the Clinical Microbiology Laboratory at the All India Institute of Medical Sciences, New Delhi, where these were inoculated into BACTEC MGIT^{TM} 960 as described earlier (Sankar et al., 2013). Flashed positive cultures were confirmed as *M. tuberculosis* by species specific *multiplex* PCR (m-PCR), which amplifies *hsp65*, *esat6*, and *its* regions of the mycobacterial genome (Sankar et al., 2013).

Genotyping

DNA from the cultures was isolated as previously described (Sankar et al., 2013). After checking the quality of the DNA, spoligotyping was performed using a commercially available kit (Mapmygenome India Limited) as per the manufacturer's instructions (Thomas et al., 2011; Vadwai et al., 2012; Singh et al., 2015). Twenty-four loci MIRU-VNTR was performed by PCR amplification of individual loci using specific primers, as described previously (Supply et al., 2006).

Drug susceptibility test

The susceptibility pattern to Isoniazid (INH), Rifampicin (RIF), Streptomycin (SM), and Ethambutol (EMB) was determined using the BACTEC MGIT^{TM} 960 (Becton-Dickinson, Sparks, USA) following the manufacturer's instructions, as described earlier (Singh et al., 2015).

Data analysis

Genetic data analysis was performed using standard methods as described earlier (Hanekom et al., 2008; Narayanan et al., 2008), wherein spoligotypes were identified and analyzed as character types. The obtained spoligotyping patterns were compared with those available in the SITVIT_WEB database (http://www.pasteur-guadeloupe.fr:8081/SITVIT2). The Hunter-Gaston discriminatory index (HGDI) was used as a numerical index for MIRU-VNTR discriminatory power (Hunter and Gaston, 1988). The allelic diversity of the loci was identified as highly discriminant if the HGI was >0.6, moderately discriminant if the HGI was between 0.3 and 0.6, and poorly discriminant if the HGI was less than 0.3.

Differences among the lineages of the isolates and drug susceptibility patterns were analyzed by the chi-squared test and Fisher's exact test as appropriate using STATA 9.0. The adjusted odds ratio (OR) and 95 percent confidence interval (CI) were calculated. Statistical significance was defined as a p value of 0.05 or less.

Results

Patient population and *M. tuberculosis* isolates

A total of 503 subjects who were suspected to have PTB and/or EPTB, were recruited from the Antiretroviral Therapy (ART) center and OPDs and wards of NITRD, New Delhi. Most of the patients were residents of Delhi (n=215, 74.9%), and the rest were from neighboring states in India, including Haryana (29, 10.1%), Uttar Pradesh (27, 9.4%), and Bihar (16, 5.6%), as these patients had visited the NITRD, New Delhi for their diagnosis and treatment (Table 1).

These 503 patients were divided into two groups based on their HIV status. In the HIV/AIDS positive group, there were

249 of 503 (49.5%) patients who had HIV-TB coinfection, either PTB and/or EPTB. Their mean age was 35.6 ± 11.8 years. Of these, 130 (52.2%) subjects were mycobacterial culture positive and their mean age was 36.6 ± 12.5 years. In the HIV-negative group, we had 254 of 503 (50.5%) patients who had PTB and or EPTB. Their mean age was 32.8 ± 13.8 years. Of these patients, 156 (61.4%) were found to be mycobacterial culture positive with a mean age of 33.0 ± 14.0 years. This difference was statistically insignificant. Most patients were in the age group of 19-45 years with a *p*-value <0.001.

Of the 249 HIV seropositive patients, 220 (88.4%) were suspected of PTB and 29 (11.6%) were EPTB cases, while in 254 were HIV seronegative patients, 244 (96.1%) were PTB suspected, and the remaining 10 (3.9%) were EPTB suspected cases. Thus the prevalence of EPTB in HIV positive and HIV-negative was statistically highly significant (Table 1).

Overall, 287 patients were culture positive patients, of them 203 (70.7%) were male and 84 (29.3%) female. We found that male preponderance was common in both HIV-negative (62.2%) as well as in HIV-positive (80.9%) patients. However, this male preponderance was significantly (p <0.001) more in HIV-positive cases. All mycobacterial cultures were subjected to m-PCR to differentiate MTB and non-tuberculous mycobacteria (NTM). Samples from 11 (3.8%) patients were found to be NTM (all HIV positive) and the remaining 276 were MTB and subjected to genotyping studies (Table 2). Only one HIV-negative patient had NTM while in 10 HIV-positive patients (7.6%) NTM were isolated.

TABLE 1 Demographic details of the patients, drug resistance patterns, and phylogenetic lineages of the MTB isolates.

Characteristics	Total N(%)	HIV negative	HIV positive	OR* (95%CI)	p-value
Gender					
Female	84 (29.3)	59 (37.8)	25 (19.1)	1	<0.001
Male	203 (70.7)	97 (62.2)	106 (80.9)	2.6 (1.5-4.4)	
Age group					
<18	30 (10.5)	26 (16.7)	4 (3.1)	1	
19-45	194 (67.6)	95 (60.9)	99 (75.6)	6.8 (2.3-20.1)	<0.001
≥46	63 (21.9)	35 (22.4)	28 (21.3)	5.2 (1.6-16.7)	<0.006
State of Residence					
New Delhi	215 (74.9)	111 (73.1)	101 (77.1)	1	
Uttar Pradesh	27 (9.4)	22 (14.1)	5 (3.8)	0.3 (0.1-0.7)	<0.008
Haryana	29 (10.1)	10 (6.4)	19 (14.5)	2.1 (0.9-4.8)	<0.05
Bihar	16 (5.6)	10 (6.4)	6 (4.6)	0.6 (0.2-1.9)	<0.46
Qualifications					
Illiterate	44 (37.9)	22 (45.8)	22 (32.3)	1	
<10	24 (20.1)	3 (6.3)	21 (30.1)	7 (1.8-26.9)	<0.005
10^{th} pass	27 (23.3)	13 (27.1)	14 (20.6)	1.1 (0.4-2.8)	<0.88
Graduate and above	21 (18.1)	10 (20.8)	11 (16.2)	1.1 (0.4-3.1)	<0.858
Profession					
Housewife	21 (21.9)	17 (30.4)	4 (10.0)	1	
Unemployed	21 (21.9)	11 (19.6)	10 (25.0)	3.8 (0.9-15.4)	<0.056
Others	54 (56.2)	28 (50.0)	26 (65.0)	3.9 (1.1-13.3)	<0.027
Marital Status					
Married	202 (70.4)	116 (74.4)	86 (65.7)	1	
Unmarried	63 (22.0)	40 (25.7)	23 (17.5)	0.8 (0.4-1.4)	<0.001
Others**	22 (7.6)	-	22 (16.8)	-	
P/H/ATT*					
No	208 (72.5)	116 (74.4)	92 (70.2)		<0.435
Yes	79 (27.5)	40(25.6)	39 (29.8)		
DST Patterns*					
SIRE Sensitive	206 (74.6)	130 (83.3)	76 (63.3)		<0.001
MDR	46 (16.7)	16(10.3)	30 (25.0)		
Others (Mono, Dual, Poly)	24 (8.7)	10 (6.4)	14 (11.7)		
Lineages					
Beijing	44 (15.9)	17 (10.9)	27 (22.5)		<0.024
CAS	153 (55.4)	97 (62.2)	56 (46.7)		
EAI	25 (9.1)	12 (7.7)	13 (10.8)		
Others (Manu, LAM, T, U, X, Cameroon)	54 (19.6)	30 (19.2)	24 (20.0)		

*OR, Odds Ratio; P/H/ATT, Past History of Anti-Tuberculous Treatment; DST, Drug Susceptibility Testing; SIRE Sensitive, Sensitive for all four drugs (Streptomycin, Isoniazid, Rifampin, and Ethambutol); MDR, Multiple Drug Resistance.
** Others= widows/widowers, divorced or transgender.

TABLE 2 Lineage distribution in pulmonary and extrapulmonary tuberculosis.

Total Subjects: 503					
MGIT Culture Positive: 287					
Confirmed as *M. tuberculosis* by species specific *multiplex PCR and subjected to genotyping:* 276					
HIV Status		**Positive (n=120)**		**Negative (n=156)**	
TB Type		**PTB**	**EPTB**	**PTB**	**EPTB**
Total		109	11	154	2
Lineages	CAS	51	5	97	0
	LAM	6	0	0	0
	BEIJING	25	2	17	0
	T	7	0	18	1
	U	7	0	0	0
	EAI	10	3	12	0
	Cameroon	1	0	1	1
	MANU	0	1	8	0
	X	2	0	0	0
	M.africanum	0	0	1	0

The socio-economic and educational data revealed that in the HIV positive group, most of the patients were literate but not matriculate. Patients in the HIV-TB group were likely to be unemployed or have their own small businesses. Of the patients, 202 (70.4%) were married while 63 (22.0%) were unmarried. The remaining 22 (7.65) were widows/widowers, divorcees, or transgender.

A history (6 months or more) of taking anti-tuberculous treatment (ATT) showed that 208 out of 287 (72.5%) of all the mycobacterial culture positive patients had a previous history of ATT. The probability of having a past history of tuberculosis was similar irrespective of HIV status. (Table 1).

Before drug susceptibility testing and genotyping, all the culture isolates were checked by in-house multiplex PCR for species identification. Out of 287 isolates, 276 (96.2%) were identified as MTB, and the remaining 11 (3.8%) were identified as NTM. Ten (90.9%) NTM were isolated from HIV-positive patients and one (9.1%) from a HIV-negative patient.

Among 276 MTB isolates, 206 (74.6%) were sensitive to first line drugs and 46 (16.7%) were MDR. The remaining 24 (8.7%) were mono and dual resistant. Of the HIV-negative patients, 130 (83.3%) were SIRE sensitive while in HIV-positive cases, 76 (63.3%) were sensitive to first line drugs. Of the HIV-negative patients, 16 (10.3%) MDR cases were observed, while 30 (25.0%) MDR cases were observed in HIV-positive patients. The p-value was <0.001 (Table 1).

Of the 276 culture positive MTB isolates, 120 were HIV-positive and 156 were HIV-negative. The lineage distribution of these populations in pulmonary and extrapulmonary tuberculosis infection is illustrated in Table 2.

The molecular characterization of the 276 MTB isolates revealed that the Central Asian Strain (CAS) genotype was found to be most predominant [153 (55.4%)], followed by Beijing lineage [44 (15.9%)], East African Indian [25 (9.1%)], and other lineages [54 (19.6%)]. In HIV-negative patients, the CAS genotype was predominant (62.2%) followed by Beijing (10.9%), EAI (7.7%), and others (19.25%). The distribution of various genotypes in HIV-positive patients was not significantly different and CAS genotypes remained predominant (Tables 1, 2).

Based on the spoligotyping pattern and 24 loci MIRU-VNTR analysis, an Un-weighted pair group method with arithmetic mean (UPGMA) phylogenetic tree was generated (Figures 1A, B) using MIRU-VNTR Plus online tool. Accordingly, in HIV-negative patients, a total of 19 STs comprising 140 (89.7%) isolates were identified while the remaining 16 (10.3%) isolates had unique/unidentified ST patterns. The lineages and corresponding spoligotype patterns of 156 isolates are shown in Supplementary Table 1. Of the 19 different STs observed, ST26 of CAS1_DEL had a maximum of 51.3% strains, followed by ST1 of Beijing with 10.9%, ST25 of CAS1_DEL with 3.2%, ST22 with 0.6%, ST53 of T1 with 7.7%, EAI3_IND with 4.5% and the remaining belonged to other STs. While in the 120 HIV-positive patients, the CAS family consisted of six STs (Supplementary Table 2). Among the STs of the CAS family, 37.5% of strains belonged to ST26, 3.3% each belonged to ST289 and ST1343, while 0.8% belonged to ST25 and ST2419 each.

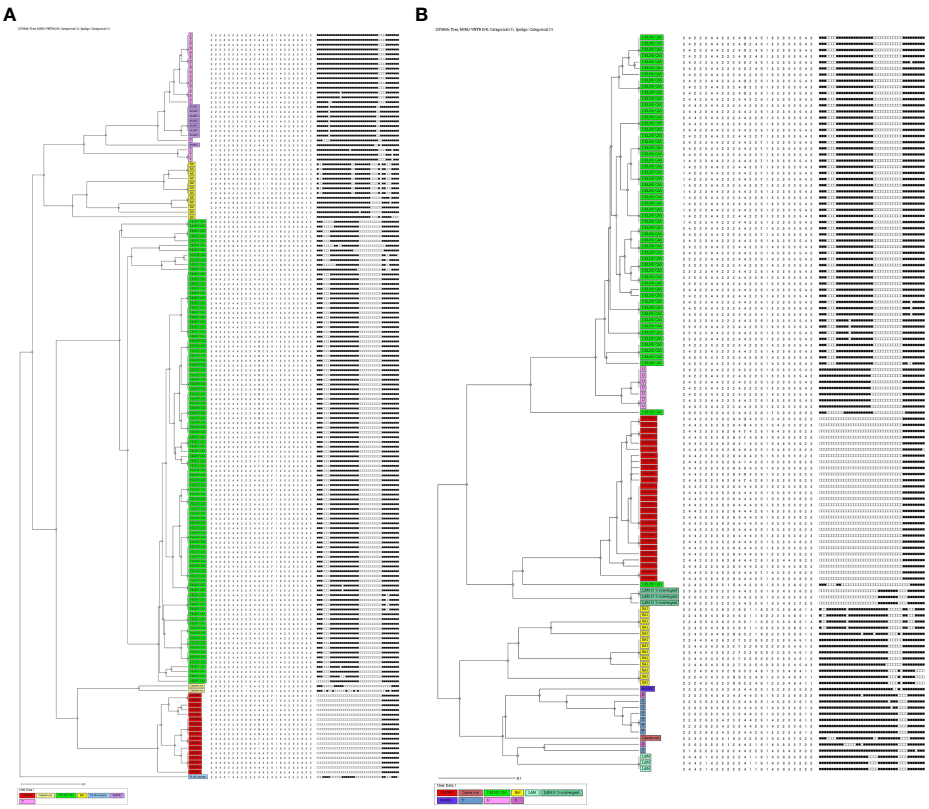

FIGURE 1
(A) UPGMA-dendrogram representing MIRU-VNTR and spoligotype patterns of 156 isolates from HIV-negative cases. **(B)** UPGMA-dendrogram representing MIRU-VNTR and spoligotype patterns of 120 isolates from HIV Positive cases.

In the EAI lineage, a total of 3 different STs were identified comprising 8 isolates of EAI, in which ST458 was found in 4 (3.3%) isolates followed by ST138 in 3 (2.5%) and ST1970 in 1 (0.8%) isolate. The single most dominant ST of the Beijing family was ST1 in 27 (22.5%) strains. Whereas other strains belonged to less predominant STs (Supplementary Table 2).

The distribution of the lineages in HIV positive and HIV negative patients were analyzed using the chi-square test which showed a significant (p=0.00816) difference in lineage distribution that was observed in both the study population (Table 3).

The combination of different epidemiological and phylogeographical techniques is important for better interpretation of molecular results. When the clustering rate by spoligotyping was determined, we found that Beijing was the most (100%) clustered lineage followed by CAS with 96.7% (89/92) in HIV-negative and 94.6% (53/56) in HIV-positive patients. The EAI lineage showed 87.5% clustering in HIV-negative while in HIV-positive patients it showed a 75% clustering rate. In HIV-negative cases, Manu was predominant with an 87.5% (7/8) clustering rate, followed by T lineage with 88.9% (16/18).

MIRU-VNTR revealed that 90.7% (88/97) and 96.4% (54/56) isolates of the largest cluster belonged to the CAS family in HIV-negative and HIV-positive patients respectively. In Beijing lineage, the clustering rate was 70.6% in HIV-negative and 63% in HIV-positive cases which was much lower than spoligotyping. Using MIRU-VNTR we identified 131 different genotypes in 34 clusters and 25 orphan isolates with a clustering rate of 84% in HIV negative cases, whereas in HIV positive cases 101 various genotypes were recognized in 28 clusters with an 84.2% clustering rate (Table 4).

In HIV-negative cases, the largest and smallest cluster comprised 80 and 2 isolates respectively by spoligotyping. However, in HIV-positive cases, the largest cluster consisted of 45 isolates, while the smallest cluster had 3 isolates. When orphan strains were checked by both methods in all lineages, we found 6.4% (10/156) of orphan strains by spoligotyping in HIV-negative cases, while using MIRU-VNTR, the rate was 16% (25/156). In HIV-positive cases, spoligotyping showed 10% (12/120) isolates as an orphan while MIRU-VNTR revealed 15.8% (19/120) (Table 5). We did not find any significant difference with regard to the demographic background of the patients as most of them were

TABLE 3 Distribution of TB lineages in HIV positive and HIV negative population.

HIV status	TB-Lineages						P value
	CAS	EAI	Beijing	MANU	T	Cameroon	
Negative	97	12	17	8	19	2	0.00816
Positive	56	13	27	1	7	1	

(Chi Square=15.576, df=5, p<0.05).

from North India only (Table 6). The results of 24 -loci MIRU-VNTRs analysis showed that loci QUB-26, Mtub21, ETR-c, and MIRU-26 were highly discriminant in MTB isolates from HIV-negative as well as HIV-positive cases (Figures 2A, B).

The minimum Spanning Tree (MST) analysis was done by using MIRU-VNTRplus. The various SITs amongst MTB isolates from HIV-negative patients (Figure 2A) and HIV-positive patients (Figure 2B) showed predominant SITs and

TABLE 4 Distribution and clustering patterns of various lineages of *M. tuberculosis* in HIV seronegative and HIV seropositive patients.

Lineage	HIV status	Method of typing	No. of isolates	No. of clusters (size)	No. of clustered strains (%)	No. of orphan strains (%)	No. of unique strains
CAS	**HIV Neg**	Spoligotyping	92	4 (2-80)	89 (96.7)	3 (3.3)	0
		MIRU-VNTR	97	21 (2-8)	88 (90.7)	9 (9.3)	0
	HIV Pos	Spoligotyping	56	3 (4-45)	53 (94.6)	3 (5.4)	0
		MIRU-VNTR	56	15 (2-6)	54 (96.4)	2 (3.6)	0
EAI	**HIV Neg**	Spoligotyping	8	1 (7)	7 (87.5)	1 (12.5)	0
		MIRU-VNTR	12	3 (2-3)	8 (66.7)	4 (33.3)	0
	HIV Pos	Spoligotyping	4	1 (3)	3 (75)	1 (25)	0
		MIRU-VNTR	13	3 (3-4)	10 (76.9)	3 (23.1)	0
Beijing	**HIV Neg**	Spoligotyping	17	1 (17)	17 (100)	0	0
		MIRU-VNTR	17	4 (2-4)	12 (70.6)	5 (29.4)	0
	HIV Pos	Spoligotyping	27	1 (27)	27 (100)	0	0
		MIRU-VNTR	27	5 (2-8)	17 (63)	10 (37)	0
Cameroon	**HIV Neg**	Spoligotyping	0	0	0	0	0
		MIRU-VNTR	2	0	0	2 (100)	0
LAM	**HIV Pos**	Spoligotyping	6	2 (3)	6 (100)	0	0
		MIRU-VNTR	6	2 (2-3)	5 (83.3)	1 (16.7)	0
MANU	**HIV Neg**	Spoligotyping	8	1 (7)	7 (87.5)	1 (12.5)	0
		MIRU-VNTR	8	1 (7)	7 (87.5)	1 (12.5)	0
	HIV Pos	Spoligotyping	1	0	0	1 (100)	0
		MIRU-VNTR	1	0	0	1 (100)	0
T	**HIV Neg**	Spoligotyping	18	3 (2-12)	16 (88.9)	2 (11.1)	0
		MIRU-VNTR	19	5 (2-5)	16 (84.2)	3 (15.8)	0
	HIV Pos	Spoligotyping	7	4 (4)	4 (57.1)	3 (42.9)	0
		MIRU-VNTR	7	2 (2-3)	5 (71.4)	2 (28.6)	0
X	**HIV Pos**	Spoligotyping	2	0	0	2 (100)	0
		MIRU-VNTR	2	0	0	2 (100)	0
U	**HIV Pos**	Spoligotyping	7	1 (7)	7 (100)	0	0
		MIRU-VNTR	7	2 (2-4)	6 (85.7)	1 (14.3)	0
M. africanum	**HIV Neg**	Spoligotyping	0	0	0	0	0
		MIRU-VNTR	1	0	0	1 (100)	0
UK	**HIV Neg**	Spoligotyping	13	1 (2)	2 (15.4)	3 (23.1)	8 (61.5)
		MIRU-VNTR	0	0	0	0	0
	HIV Pos	Spoligotyping	10	1 (4)	4 (40)	2 (20)	4 (40)
		MIRU-VNTR	0	0	0	0	0
Total	**HIV Neg**	Spoligotyping	156	11 (2-80)	138 (88.5)	10 (6.4)	8 (5.1)
		MIRU-VNTR	156	34 (2-8)	131 (84)	25 (16)	0
	HIV Pos	Spoligotyping	120	11 (3-45)	108 (90)	12 (10)	0
		MIRU-VNTR	120	28 (2-8)	101 (84.2)	19 (15.8)	0

TABLE 5 Overall clustering patterns of MTB isolates by both the molecular techniques in HIV-negative and HIV-positive patients.

Genotyping methods and type of patients	No. of isolates	No. of clusters (size)	No. of clustered strains (%)	No. of orphan strains (%)	No. of unique strains (%)
Spoligotyping					
HIV Negative	156	11 (2-80)	138 (88.5)	10 (6.4)	8 (5.0)
HIV Positive	120	11 (3-45)	108 (90.0)	12 (10.0)	–
MIRU-VNTR					
HIV Negative	156	34 (2-8)	131 (84.0)	25 (37)	0
HIV Positive	120	28 (2-8)	101 (84.2)	19 (15.8)	0

TABLE 6 Co-relation of various demographical and other factors between Clustered and Unique MTB strains.

Characteristics	Total N (%)	Genotyping patterns		OR (95%CI)	p-value
		Unique	Clustered		
Gender					
Female	84 (30.4)	10 (30.3)	74 (30.5)	1	
Male	192 (69.6)	23 (69.7)	169 (69.5)	0.9 (0.5-2.1)	0.986
Age group					
<18	29 (10.5)	3 (9.1)	26 (10.6)	1	
19-45	187 (67.6)	25 (75.7)	187 (67.7)	0.7 (0.2-2.7)	0.653
≥46	60 (21.7)	5 (15.2)	60 (21.7)	1.2 (0.3-5.7)	0.756
HIV Status					
HIV Negative	156 (56.5)	14 (42.4)	142 (58.4)	1	
HIV Positive	120 (43.5)	19 (57.6)	101 (41.6)	0.5 (0.3-1.1)	0.085
State of Residence					
New Delhi	206 (74.6)	22 (66.7)	184 (75.7)	1	
Uttar Pradesh	26 (9.4)	3 (9.1)	23 (9.4)	0.9 (0.3-3.3)	0.894
Haryana	28 (10.1)	6 (18.1)	28 (10.1)	0.4 (0.2-1.1)	0.108
Bihar	16 (5.8)	2 (6.1)	16 (5.8)	0.8 (0.2-3.9)	0.821
Qualifications					
Illiterate	44 (40.0)	5 (38.5)	39 (40.2)	1	
<10	21 (19.1)	2 (15.4)	19 (19.6)	1.2 (0.2-6.9)	0.823
10^{th} pass	27 (24.5)	4 (30.8)	23 (23.7)	0.7 (0.2-3.0)	0.672
Graduate and above	18 (16.4)	2 (15.3)	16 (16.5)	1.0 (0.2-5.8)	0.977
Profession					
Housewife	21 (23.1)	4 (26.7)	17 (22.4)	1	
Unemployed	21 (23.1)	6 (40.0)	15 (19.7)	0.6 (0.1-2.5)	0.471
Others	49 (53.9)	5 (33.3)	44 (57.9)	2.1 (0.5-8.6)	0.318
Marital Status					
Married	196 (71.0)	18 (54.5)	178 (73.3)	1	
Unmarried	63 (22.8)	13 (39.4)	50 (20.6)	0.4 (0.2-0.8)	<0.01
Others	17 (6.2)	2 (6.1)	15 (6.1)	0.8 (0.2-3.6)	0.727
P/H/ATT					
No	58 (39.2)	10 (50.0)	48 (37.5)	1	
Yes	90 (60.8)	10 (50.0)	80 (62.5)	1.7 (0.6-4.3)	0.290
DST Patterns					
SIRE Sensitive	206 (74.6)	24 (72.7)	182 (74.9)	1	
MDR	46 (16.7)	5 (15.2)	41 (16.9)	1.1 (0.4-3.0)	0.881
Others (Mono, dual etc)	24 (8.7)	4 (12.1)	20 (8.2)	0.6 (0.2-2.1)	0.480
Lineages					
Beijing	44 (15.9)	9 (27.3)	35 (14.4)	1	
CAS	153 (55.4)	6 (18.2)	147 (60.5)	6.2 (2.1-18.9)	<0.001
EAI	25 (9.1)	5 (15.2)	20 (8.2)	1.0 (0.3-3.5)	0.964
Others (Manu, LAM, T, U, X, Cameroon)	54 (19.6)	13 (39.4)	41 (16.9)	0.8 (0.3-2.1)	0.670

the evolutionary relationship between the lineages and their SITs.

Discussion

This study describes the genetic diversity in *M. tuberculosis* isolated from HIV-TB co-infected and HIV uninfected TB cases. Most of our patient population was from the North Indian states of Delhi's national capital region, Haryana and Uttar Pradesh. Therefore, the incidence and prevalence rates of HIV and TB were in line with other studies. However, in our study, we compared the drug resistance pattern and genotypes side-by-side isolated from these two patient groups under a controlled single laboratory study.

As reported in various other studies, we found that CAS was the predominant genotype followed by Beijing and EAI (Devi et al., 2015; Singh et al., 2015; Singh et al., 2021). Interestingly, the same pattern was seen in our patient populations irrespective of their HIV status. This could be explained based on the circulation of these genotypes in the environment and the ethnic make-up of North Indian patients (Sankar et al., 2013). In our earlier studies, we also found similar patterns in various genotypes (Sankar et al., 2013; Singh et al., 2015). Similar results were also found in the southern part of India (Narayanan et al., 2008). However, in this present study, the Beijing genotype was more prevalent in HIV seropositive patients rather than HIV-negative patients (Table 1). Similar results were also reported in a study conducted on HIV-positive patients with TB meningitis (Caws et al., 2006). Narayanan et al. (Narayanan et al., 2008) and Gupta et al. (2014) also reported Beijing genotype only in HIV-infected patients and not in HIV-uninfected patients. *et al*Veigas et al. (Viegas et al., 2013) suggested that the association of Beijing strain with HIV seropositive status could be due to the combination of the increased virulence of the strain, and higher susceptibility of HIV positive patients. However, a study from Western Maharashtra, India found no association between HIV status and spoligotypes (Chatterjee et al., 2010).

Generally, the prevalence of different genotypes of MTB is dependent on the geographical location and the ethnicities of the population, as reported in our previous studies (Sankar et al., 2013; Singh et al., 2015). In the present study, Beijing genotypes were also significantly more common in HIV-positive patients and CAS lineage was more common in HIV-negative cases, which could be explained by the fact that CAS lineage is the most common lineage circulating in northern parts of India (Sankar et al., 2013), and the same pattern was seen in this study. A population-based investigation for 20 years in rural Malawi reported ST129 (EAI5) to be the most common lineage associated with HIV status (Glynn et al., 2010). A study from Ethiopia found that in HIV-positive subjects, the T family was the most predominant (38.5%) (Mihret et al., 2012). This also suggests that the frequency of various lineages depends more on geographical locations rather than HIV status.

Anti-TB drug resistance can develop after acquiring the infection (secondary), but it can also be a baseline (primary) when the person is infected with drug-resistant strains of *M. tuberculosis*. In the present study, we observed an overall drug resistance (resistance to any drug) in 25.4% and MDR in 16.7% isolates (Table 1). A higher rate of MDR was found in isolates from HIV-positive patients as compared to isolates from HIV-negative patients. This may be attributed to the previous history of TB in a higher number of patients from the HIV-positive group, as well as the lower socio-economic status of these patients. Saldanha et al. (2019) also reported a high prevalence of MDR-TB in HIV-positive patients and associated this with the treatment of previous TB infection with sub-optimal anti-TB regimens. Similarly, Sethi et al. (2013) reported that TB was more prevalent in patients from lower socioeconomic backgrounds and that there was a higher number of MDR-MTB (27.3%) in HIV seropositive subjects compared to HIV seronegative subjects (15.4%). A prior study carried out by Isaakidis et al. (2014) also confirmed the very high burden of DR-TB in HIV-positive patients (38%) at an ART center in Mumbai. In the current study, most of our patients were from Delhi and its adjoining states. Our findings may not necessarily represent the entire country, as the socio-economic conditions of patients, HIV prevalence, and medical practices differ significantly from region to region. Clustering is often used to group strains with similar genotypic traits. On the analysis of clustering amongst the various phylogenetic lineages, we found clustering in 88.8% and 86.6% HIV-uninfected and HIV-infected patient groups. This reflects the high transmission rate within these population groups (Odhiambo et al., 1999). In addition to sub-lineage analysis, we also observed that CAS1_DEL (ST26) and Beijing (ST1) clades were predominant in both the study populations with no significant difference. These findings are in line with previous publications (Singh et al., 2004; Arora et al., 2009; Sankar et al., 2013; Singh et al., 2015).

Nutrition and timely medical care are important determinants of disease outcome. In India, even though TB is more prevalent in male patients and a poor disease outcome is more likely in females due to various socio-economic factors (Singh et al., 2012) and the finding of our study were on similar lines.

There was no significant difference in the prevalence of clustered or unique isolates among different age groups. The percentage of clustered isolates based on 24 loci MIRU-VNTR was, however, higher among married patients. This could be due to better opportunities for the circulation of these strains in the families, though it may an overestimation (García de Viedma et al., 2011). We found a higher percentage of clustered isolates of CAS lineage which showed a significantly higher clustering rate than other lineages. This may be because CAS is more prevalent in North India and most of the isolates from both groups are from

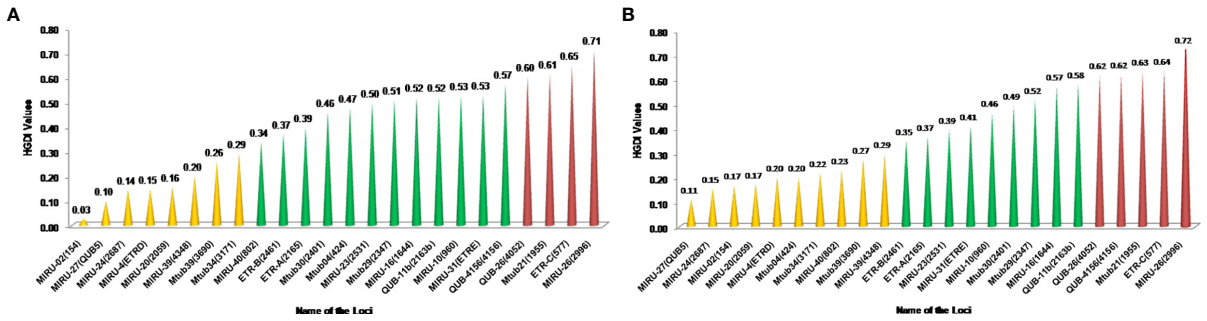

FIGURE 2
(A) Minimum spanning trees of MTC isolates from HIV-negative patients typed with both spoligotyping and MIRU-VNTR. Each circle represents a genotype. The distance between circles represents how closely related the different genotypes are to each other. MST connects each genotype based on the degree of changes required to go from one allele to another. The configuration of the tree is represented by branches *i.e.* continuous versus dotted lines and circles representing each pattern. The length of the branches denotes the distance between patterns whereas the intricacy of the lines indicates the number of spacers altered between two patterns. The thicker lines represent one change while thinner ones indicate 2 or 3. The size of the circle is comparable to the total number of MTB isolates in this study. The color of the circles represents the phylogenetic lineage to which the specific pattern belongs. Beijing patterns are circled in red. Patterns colored in green indicate Delhi/CAS strains. EAI strains are depicted in yellow. **(B)** Minimum spanning trees of MTC isolates from HIV-positive patients typed with both spoligotyping and MIRU-VNTR. Each circle represents a genotype. The distance between circles represents how closely related the different genotypes are to each other (detailed description as mentioned in Figure 3A).

north India (Arora et al., 2009; Singh et al., 2015). We also observed unique isolates with lineages like Manu, LAM, T, U X, and Cameroon, demonstrating an assortment of strains and newly emerging strains in these patients, and that this trend should be considered seriously by the program managers.

As per our findings in the HIV-negative group as well as in those in the HIV-positive group, MIRU26, ETRC, Mtub21, QUB4156, and QUB26 were highly discriminating, but MIRU2, MIRU24, MIRU20, and ETRD were feebly discriminating (Figures 3A, B). Earlier we also found that

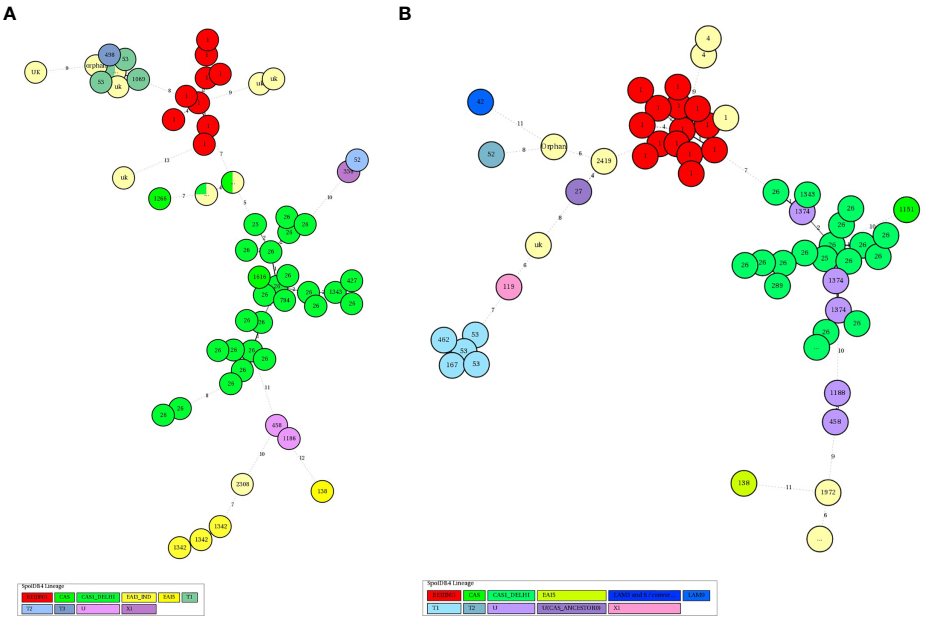

FIGURE 3
(A) The Hunter-Gaston discriminatory index of MIRU-VNTR alleles of TB isolates from HIV-Negative patients MIRU: Mycobacterial Interspersed Repetitive Units, VNTR, Variable Number Tandem Repeats; HGDI, Hunter-Gaston Diversity index. The allelic diversity of the loci was classified as highly discriminant [Hunter-Gaston Index **(HGI)** >0.6], moderately discriminant (HGI ≥0.3 to ≤0.6), and poorly discriminant (HGI < 0.3). **(B)** The Hunter-Gaston discriminatory index of MIRU-VNTR alleles of TB isolates from HIV- TB co-infected patients.

QUB4156, QUB26, and MIRU26 were highly discriminating and MIRU2, MIRU4 or ETRD and MIRU24 were poorly discriminating (Sankar et al., 2013).

It might be expected that some lineages and clones of MTB are more prevalent or have severe disease outcomes in HIV-positive patients. However, in the present study, we found that though all clones could be isolated from HIV-positive patients, the incidence of the Beijing genotype was more frequent in this group of patients. It is important to note that in North India, even though the CAS lineage is more prevalent, in HIV-infected patients CAS lineage had a low incidence compared to Beijing lineage. We are not able to explain fully why the EPTB in the HIV-infected patients in our study was not as common as that reported by others (Yang et al., 1995; Giri et al., 2013), but it was significantly more common (11.6%) than in HIV-negative patients (3.9%). This could be because our patient recruiting center is a dedicated TB hospital and EPTB cases are more commonly referred to other general care hospitals for want of wider scope for surgical and medical management.

Conclusions

The present study provides important molecular genotypic data of *M. tuberculosis* isolates from HIV-negative and HIV-positive patients of Northern India. Central Asian lineage despite being the most predominant isolate circulating in the study area and both HIV-positive and HIV-negative TB cases, the Beijing genotype showed a statistically significant high incidence rate in HIV-TB cases. However, the clustering rate of predominant genotypes was similar in both HIV-positive and HIV-negative TB cases, which shows the high transmissibility of these genotypes in the community. Probability of having extrapulmonary tuberculosis and isolation of non-tuberculous mycobacterial were also significantly more in HIV-infected patients.

Data availability statement

The original contributions presented in the study are included in the article/Supplementary Material. Further inquiries can be directed to the corresponding author.

Ethics statement

The studies involving human participants were reviewed and approved by Institutional Ethical Committee, All India Institute of Medical Sciences, New Delhi - 110029. Written informed consent to participate in this study was provided by the participants' legal guardian/next of kin.

Author contributions

SS, NS, DB, and UA designed the study. JS, NS, RS, and GS collected clinical samples and patient clinical information. JS performed genotyping analysis. JS, RS, and GS performed the experiments. SS and JS analysed data. JS, NS, and SS wrote the manuscript. Final modifications in manuscript done by MM and AM. SS arranged for financial support. All authors contributed to the article and approved the submitted version.

Funding

The study received financial support from Indian Council of Medical Research (ICMR), New Delhi (ICMR) Sanction Order Number: 5/8/5/15/10-ECD-I) and publication support from Indo-U.S. Science and Technology Forum (IUSSTF) (Award Letter No. IUSSTF/USISTEF/8th Call/HI-051/2017/2018-19).

Acknowledgments

We are thankful to all the patients who cooperated in this study. We are also grateful to Indian Council of Medical Research (ICMR), New Delhi (ICMR Sanction Order Number: 5/8/5/15/10-ECD-I) and Indo-U.S. Science and Technology Forum (IUSSTF) (Award Letter No. IUSSTF/USISTEF/8th Call/HI-051/2017/2018-19) for financial support.

Conflict of interest

The authors declare that the research was conducted in the absence of any commercial or financial relationships that could be construed as a potential conflict of interest.

Publisher's note

Supplementary material

The Supplementary Material for this article can be found online at: https://www.frontiersin.org/articles/10.3389/fcimb.2022.953443/full#supplementarymaterial

References

Allix-Béguec, C., Fauville-Dufaux, M., Stoffels, K., Ommeslag, D., Walravens, K., Saegerman, C., et al. (2010). Importance of identifying mycobacterium bovis as a causative agent of human tuberculosis. *Eur. Respir. J.* 35 (3), 692–694. doi: 10.1183/09031936.00137309

Arora, J., Singh, U. B., Suresh, N., Rana, T., Porwal, C., Kaushik, A., et al. (2009). Characterization of predominant mycobacterium tuberculosis strains from different subpopulations of India. *Infect. Genet. Evol.* 9 (5), 832–839. doi: 10.1016/j.meegid.2009.05.008

Global tuberculosis report. (2020) Geneva: World Health Organization 2020 Licence: CC BY-NC-SA 3.0 IGO. Available at: https://www.who.int/publications-detail-redirect/9789240013131"https://www.who.int/ https://www.who.int/publications-detail-redirect/9789240013131"publications-detail-redirect/9789240013131.

Cadmus, S., Hill, V., van, S. D., and Rastogi, N. (2011). Spoligotype profile of mycobacterium tuberculosis complex strains from HIV-positive and -negative patients in Nigeria: a comparative analysis. *J. Clin. Microbiol.* 49 (1), 220–226. doi: 10.1128/JCM.01241-10

Caws, M., Thwaites, G., Stepniewska, K., Lan, N. T. N., Duyen, N. T. H., Phuong, N. T., et al. (2006). Beijing Genotype of mycobacterium tuberculosis is significantly associated with human immunodeficiency virus infection and multidrug resistance in cases of tuberculous meningitis. *J. Clin. Microbiol.* 44 (11), 3934–3939. doi: 10.1128/JCM.01181-06

Chatterjee, A., D'Souza, D., Vira, T., Bamne, A., Ambe, G. T., Nicol, M. P., et al. (2010). Strains of mycobacterium tuberculosis from western maharashtra, India, exhibit a high degree of diversity and strain-specific associations with drug resistance, cavitary disease, and treatment failure. *J. Clin. Microbiol.* 48 (10), 3593–3599. doi: 10.1128/JCM.00430-10

Demay, C., Liens, B., Burguière, T., Hill, V., Couvin, D., Millet, J., et al. (2012). SITVITWEB–a publicly available international multimarker database for studying mycobacterium tuberculosis genetic diversity and molecular epidemiology. *Infect. Genet. Evol.* 12 (4), 755–766. doi: 10.1016/j.meegid.2012.02.004

Devi, K. R., Bhutia, R., Bhowmick, S., Mukherjee, K., Mahanta, J., and Narain, K. (2015). Genetic diversity of mycobacterium tuberculosis isolates from Assam, India: Dominance of Beijing family and discovery of two new clades related to CAS1_Delhi and EAI family based on spoligotyping and MIRU-VNTR typing. *Mokrousov I editor. PloS One* 10 (12), e0145860. doi: 10.1371/journal.pone.0145860

Friedland, G., Churchyard, G. J., and Nardell, E. (2007). Tuberculosis and HIV coinfection: current state of knowledge and research priorities. *J. Infect. Dis.* 196 Suppl 1, S1–S3. doi: 10.1086/518667

García de Viedma, D., Mokrousov, I., and Rastogi, N. (2011). Innovations in the molecular epidemiology of tuberculosis. *Enferm Infecc Microbiol. Clin.* 29 Suppl 1, 8–13. doi: 10.1016/s0213-005x(11)70012-x

Giri, P. A., Deshpande, J. D., and Phalke, D. B. (2013). Prevalence of pulmonary tuberculosis among HIV positive patients attending antiretroviral therapy clinic. *N Am. J. Med. Sci.* 5 (6), 367–370. doi: 10.4103/1947-2714.114169

Glynn, J. R., Alghamdi, S., Mallard, K., McNerney, R., Ndlovu, R., Munthali, L., et al. (2010). Changes in mycobacterium tuberculosis genotype families over 20 years in a population-based study in northern Malawi. *PloS One* 175 (8), e12259. doi: 10.1371/journal.pone.0012259

Gupta, A., Kulkarni, S., Rastogi, N., and Anupurba, S. (2014). A study of mycobacterium tuberculosis genotypic diversity & drug resistance mutations in varanasi, north India. *Indian J. Med. Res.* 139 (6), 892–902.

Gutierrez, M. C., Ahmed, N., Willery, E., Narayanan, S., Hasnain, S. E., Chauhan, D. S., et al. (2006). Predominance of ancestral lineages of mycobacterium tuberculosis in India. *Emerging Infect. Dis.* 12 (9), 1367–1374. doi: 10.3201/eid1209.050017

Hanekom, M., van der Spuy, G. D., Gey van Pittius, N. C., McEvoy, C. R. E., Hoek, K. G. P., Ndabambi, S. L., et al. (2008). Discordance between mycobacterial interspersed repetitive-unit-variable-number tandem-repeat typing and IS6110 restriction fragment length polymorphism genotyping for analysis of mycobacterium tuberculosis Beijing strains in a setting of high incidence of tuberculosis. *J. Clin. Microbiol.* 46 (10), 3338–3345. doi: 10.1128/JCM.00770-08

Hunter, P. R., and Gaston, M. A. (1988). Numerical index of the discriminatory ability of typing systems: an application of simpson's index of diversity. *J. Clin. Microbiol.* 26 (11), 2465–2466. doi: 10.1128/jcm.26.11.2465-2466.1988

Isaakidis, P., Das, M., Kumar, A. M. V., Peskett, C., Khetarpal, M., Bamne, A., et al. (2014). Alarming levels of drug-resistant tuberculosis in HIV-infected patients in metropolitan Mumbai, India. *PloS One* 9 (10), e110461. doi: 10.1371/journal.pone.0110461

Mihret, A., Bekele, Y., Loxton, A. G., Jordan, A. M., Yamuah, L., Aseffa, A., et al. (2012). Diversity of mycobacterium tuberculosis isolates from new pulmonary tuberculosis cases in Addis Ababa, Ethiopia. *Tuberc Res. Treat.* 2012, 892079. doi: 10.1155/2012/892079

Munawwar, A., and Singh, S. (2012). AIDS associated tuberculosis: a catastrophic collision to evade the host immune system. *Tuberculosis (Edinb).* 92 (5), 384–387. doi: 10.1016/j.tube.2012.05.006

Narayanan, S., Gagneux, S., Hari, L., Tsolaki, A. G., Rajasekhar, S., Narayanan, P. R., et al. (2008). Genomic interrogation of ancestral mycobacterium tuberculosis from south India. *Infect. Genet. Evol.* 8 (4), 474–483. doi: 10.1016/j.meegid.2007.09.007

Odhiambo, J. A., Borgdorff, M. W., Kiambih, F. M., Kibuga, D. K., Kwamanga, D. O., Ng'ang'a, L., et al. (1999). Tuberculosis and the HIV epidemic: increasing annual risk of tuberculous infection in Kenya, 1986-1996. *Am. J. Public Health* 89 (7), 1078–1082. doi: 10.2105/AJPH.89.7.1078

Pitondo-Silva, A., Santos, A. C. B., Jolley, K. A., Leite, C. Q. F., and Darini AL da, C. (2013). Comparison of three molecular typing methods to assess genetic diversity for mycobacterium tuberculosis. *J. Microbiol. Methods* 93 (1), 42–48. doi: 10.1016/j.mimet.2013.01.020

Saldanha, N., Runwal, K., Ghanekar, C., Gaikwad, S., Sane, S., and Pujari, S. (2019). High prevalence of multi drug resistant tuberculosis in people living with HIV in Western India. *BMC Infect. Dis.* 819, 391. doi: 10.1186/s12879-019-4042-z

Sankar, M. M., Singh, J., Angelin Diana, S. C., and Singh, S. (2013). Molecular characterization of mycobacterium tuberculosis isolates from north Indian patients with extrapulmonary. *Tuberculosis.* 93 (1), 75–83. doi: 10.1016/j.tube.2012.10.005

Sethi, S., Mewara, A., Dhatwalia, S. K., Singh, H., Yadav, R., Singh, K., et al. (2013). Prevalence of multidrug resistance in mycobacterium tuberculosis isolates from HIV seropositive and seronegative patients with pulmonary tuberculosis in north India. *BMC Infect. Dis.* 13 (1), 137. doi: 10.1186/1471-2334-13-137

Sharma, P., Chauhan, D. S., Upadhyay, P., Faujdar, J., Lavania, M., Sachan, S., et al. (2008). Molecular typing of mycobacterium tuberculosis isolates from a rural area of kanpur by spoligotyping and mycobacterial interspersed repetitive units (MIRUs) typing. *Infect. Genet. Evol.* 8 (5), 621–626. doi: 10.1016/j.meegid.2008.05.002

Singh, J., Sankar, M. M., Kumar, P., Couvin, D., Rastogi, N., Singh, S., et al. (2015). Genetic diversity and drug susceptibility profile of mycobacterium tuberculosis isolated from different regions of India. *J. Infect.* 71 (2), 207–219. doi: 10.1016/j.jinf.2015.04.028

Singh, S., Singh, J., Kumar, S., Gopinath, K., Balooni, V., Singh, N., et al. (2012). Poor performance of serological tests in the diagnosis of pulmonary tuberculosis: Evidence from a contact tracing field study. *Pai M editor. PloS One* 7 (7), e40213. doi: 10.1371/journal.pone.0040213

Singh, A. V., Singh, S., Yadav, A., Kushwah, S., Yadav, R., Sai, D. K., et al. (2021). Genetic variability in multidrug-resistant mycobacterium tuberculosis isolates from patients with pulmonary tuberculosis in north India. *BMC Microbiol.* 21 (1), 123. doi: 10.1186/s12866-021-02174-6

Singh, U. B., Suresh, N., Bhanu, N. V., Arora, J., Pant, H., Sinha, S., et al. (2004). Predominant tuberculosis spoligotypes, Delhi, India. *Emerging Infect. Dis.* 10 (6), 1138–1142. doi: 10.3201/eid1006.030575

Sreevatsan, S., Pan, X., Stockbauer, K. E., Connell, N. D., Kreiswirth, B. N., Whittam, T. S., et al. (1997). Restricted structural gene polymorphism in the mycobacterium tuberculosis complex indicates evolutionarily recent global dissemination. *Proc. Natl. Acad. Sci. U.S.A.* 94 (18), 9869–9874. doi: 10.1073/pnas.94.18.9869

Supply, P., Allix, C., Lesjean, S., Cardoso-Oelemann, M., Rüsch-Gerdes, S., Willery, E., et al. (2006). Proposal for standardization of optimized mycobacterial interspersed repetitive unit-variable-number tandem repeat typing of mycobacterium tuberculosis. *J. Clin. Microbiol.* 44 (12), 4498–4510. doi: 10.1128/JCM.01392-06

Thomas, S. K., Iravatham, C. C., Moni, B. H., Kumar, A., Archana, B. V., Majid, M., et al. (2011). Modern and ancestral genotypes of mycobacterium tuberculosis from andhra pradesh, India. *PloS One* 6 (11), e27584. doi: 10.1371/journal.pone.0027584

Vadwai, V., Shetty, A., Supply, P., and Rodrigues, C. (2012). Evaluation of 24-locus MIRU-VNTR in extrapulmonary specimens: study from a tertiary centre in Mumbai. *Tuberculosis (Edinb).* 92 (3), 264–272. doi: 10.1016/j.tube.2012.01.002

Viegas, S. O., Machado, A., Groenheit, R., Ghebremichael, S., Pennhag, A., Gudo, P. S., et al. (2013). Mycobacterium tuberculosis Beijing genotype is associated with HIV infection in Mozambique. *PloS One* 8 (8), e71999. doi: 10.1371/journal.pone.0071999

WHO (2016) *Global tuberculosis report*. Available at: http://apps.who.int/medicinedocs/en/d/Js23098en/.

Yang, Z. H., Mtoni, I., Chonde, M., Mwasekaga, M., Fuursted, K., Askgård, D. S., et al. (1995). DNA Fingerprinting and phenotyping of mycobacterium tuberculosis isolates from human immunodeficiency virus (HIV)-seropositive and HIV-seronegative patients in Tanzania. *J. Clin. Microbiol.* 33 (5), 1064–1069. doi: 10.1128/jcm.33.5.1064-1069.1995

frontiers | Frontiers in Cellular and Infection Microbiology

TYPE Original Research
PUBLISHED 02 December 2022
DOI 10.3389/fcimb.2022.1079184

OPEN ACCESS

EDITED BY
Amit Singh,
All India Institute of Medical Sciences, India

REVIEWED BY
Carolina Mehaffy,
Colorado State University, United States
Mariza Gonçalves Morgado,
Oswaldo Cruz Foundation (Fiocruz), Brazil

*CORRESPONDENCE
Qingshan Cai
caiqs66@163.com
Chao Song
chao.song@simceredx.com

†These authors have contributed equally to this work and share first authorship

SPECIALTY SECTION
This article was submitted to Clinical Microbiology, a section of the journal Frontiers in Cellular and Infection Microbiology

RECEIVED 25 October 2022
ACCEPTED 14 November 2022
PUBLISHED 02 December 2022

CITATION
Li B, Zhu C, Sun L, Dong H, Sun Y, Cao S, Zhen L, Qi Q, Zhang Q, Mo T, Wang H, Qiu M, Song C and Cai Q (2022) Performance evaluation and clinical validation of optimized nucleotide MALDI-TOF-MS for mycobacterial identification. *Front. Cell. Infect. Microbiol.* 12:1079184. doi: 10.3389/fcimb.2022.1079184

Performance evaluation and clinical validation of optimized nucleotide MALDI-TOF-MS for mycobacterial identification

Baiying Li[1†], Chi Zhu[2†], Lifang Sun[1], Hang Dong[2], Yaping Sun[1], Shangzhi Cao[2], Libo Zhen[1], Qi Qi[1], Quanquan Zhang[2], Ting Mo[1], Huijie Wang[1], Meihua Qiu[1], Chao Song[2*] and Qingshan Cai[1*]

[1]Department of Tuberculosis, Affiliated Hangzhou Chest Hospital, Zhejiang University School of Medicine, Hangzhou, China, [2]State Key Laboratory of Translational Medicine and Innovative Drug Development, Jiangsu Simcere Diagnostics Co., Ltd., Nanjing, China

Objective: To evaluate the performance and validate the diagnostic value of a nucleotide matrix-assisted laser desorption time-of-flight mass spectrometry (MALDI-TOF-MS) with the analysis process optimized in identification of mycobacterium species.

Methods: The optimized analysis process was used for mycobacterial identification in the nucleic MALDI-TOF-MS. 108 samples were used for assessing the performance of nucleic MALDI-TOF-MS, including 25 reference standards, 37 clinical isolates, 37 BALF, and 9 plasmids. The BALF of 38 patients suspected of pulmonary mycobacterial infection was collected for validation. Clinical etiological diagnosis was used as the gold standard to evaluate the diagnostic value of nucleotide MALDI-TOF-MS.

Results: The sensitivity, specificity, and accuracy of the nucleotide MALDI-TOF-MS in mycobacterial identification were 96.91%, 100% and 97.22%, respectively, and the limit of detection for mycobacterium tuberculosis (MTB) was 50 bacteria/mL. Among 38 patients suspected of pulmonary mycobacterial infection, 33 were diagnosed with pulmonary tuberculosis infection, and 5 with non-mycobacterial infection. In clinical validation, the positive rates of MALDI-TOF-MS, Xpert MTB/RIF, culture and AFS in BALF of patients diagnosed with tuberculosis infection were 72.7%, 63.6%, 54.5% and 27.3%, respectively. The sensitivity/specificity of MALDI-TOF-MS, Xpert, culture and AFS in diagnosing MTB were 72.7%/100%, 63.6%/100%, 54.5%/100%, 27.3%/100%, with the areas under the curve of 0.864, 0.818, 0.773, and 0.636, respectively.

Conclusion: Optimized nucleotide MALDI-TOF-MS has satisfactory sensitivity, specificity and low LOD in the identification of mycobacteria, which may serve as a potential assay for mycobacterial identification.

KEYWORDS

nucleotide MALDI-TOF-MS, mycobacterium, tuberculosis, NTM, diagnostic efficiency

1 Introduction

Tuberculosis (TB) has long been considered one of the world's leading causes of death. In 2020, 59% of the global TB cases were confirmed by bacteriological tests. So far, however, about 4.1 million TB patients worldwide have not been diagnosed or reported, and World Health Organization (WHO) modelling projections suggest that the number of TB patients and deaths could be even higher in 2021 and 2022 (Jeremiah et al., 2022). Non-tuberculous mycobacterium (NTM) refers to a general category of mycobacterium except mycobacterium tuberculosis (MTB) complex and mycobacterium leprae. In recent years, there has been an increasing trend of NTM infection. NTM can be temporarily, intermittently or long-term colonization in the lungs of the human body without causing disease, which results in considerable difficulties in deciding which patients to treat and when to treat. In addition, diseases caused by NTM have various characteristics, antimicrobial resistance spectrum, and treatment schemes. Identification of NTM species can help clinical diagnosis and treatment of NTM. Therefore, research and development of innovative technologies for MTB/NTM diagnosis is imminent.

Traditionally, identification of MTB depends on isolates and culture in liquid or solid medium in biosafety level 2/3 laboratory, which has a long culture period and low positive rate. Advances in high-throughput sequencing and bioinformatics technologies have led to a rapid increase in the application of metagenomics in pathogenic detection (Wilson et al., 2014; Simner et al., 2018; Armstrong et al., 2019; Blauwkamp et al., 2019; Ye et al., 2019). The newly revised Chinese health industry standard "Tuberculosis Diagnosis WS 288-2017" has added to the results of molecular biology in the confirmed diagnosis of TB, indicating that molecular biology technology will play an increasingly important role in the diagnosis and treatment of TB. The currently available molecular biological methods for rapid detection of MTB include Gene Chip (Wu et al., 2018), targeted NGS (tNGS) (Kambli et al., 2021), Xpert MTB/RIF (Xpert) (Bunsow et al., 2014), Loop-mediated isothermal amplification (LAMP) (Detjen et al., 2015), PCR (Shen et al., 2020), and more. Although these techniques can be used to detect clinical specimens directly, there are also some limitations, such as only detection of drug resistance genotypes but not bacterial identification and verification, simultaneous bacterial identification and resistance to a certain drug, identification of MTB but not NTM, time-consuming and costly. Nucleic MALDI-TOF-MS detection integrates the high sensitivity of PCR technology, high throughput of chip technology, and high precision of MALDI-TOF-MS. One reaction system can achieve multiple gene amplifications used to analyze single nucleotide polymorphisms, gene mutations, DNA methylation and copy number identification (Kang et al., 2018). The chip can be used in batches, with good expansibility. Single hole can realize 10-40 retesting, processing up to 3000 samples per day. In addition, manual operation is less than 30 minutes, the test results can be issued within 8 h at the earliest. Because the detection does not require the fluorescent probe, the overall cost of detection is low. In general, the detection efficiency and throughput of this technique are much higher than that of fluorescence quantitative PCR, and the detection cycle is much lower than that of the first- and second-generation sequencing (≥18 h) (Trembizki et al., 2014; Kriegsmann et al., 2015), so it has a broad application prospect in clinical practice.

There are many reports on the identification of mycobacteria based on protein MALDI-TOF-MS (Body et al., 2018; Luo et al., 2018; Rodriguez-Temporal et al., 2018; Rodriguez-Temporal et al., 2020; Fernández-Esgueva et al., 2021). However, the application of nucleotide MALDI-TOF-MS technology in the identification of mycobacterium is rarely reported. The aim of this study was to evaluate the performance of nucleotide MALDI-TOF-MS in mycobacterial identification and its real-world application.

2 Materials and methods

2.1 Study design and sample source

Reference standards, clinical isolates, bronchoalveolar lavage fluid (BALF), and plasmids were all included in performance

evaluation. qPCR and next-generation metagenomic sequencing (mNGS) were used to identify the species in BALF for MALDI-TOF-MS validation. The validation results were used as the gold standard to evaluate the performance of nucleotide MALDI-TOF-MS. The limit of detection (LOD) of nucleotide MALDI-TOF-MS was evaluated according to the national reference standards for PCR-based detection of MTB from National Institutes for Food and Drug Control (China). The LOD was determined by the lowest detected reference (S1-S4) repeated five times. S1, S2, S3 and S4 were single-cell suspensions of MTB (CMCC 93009), and the corresponding concentrations were 1×10^3 bacteria/mL, 2×10^2 bacteria/mL, 1×10^2 bacteria/mL, 50 bacteria/mL and 25 bacteria/mL, respectively.

The BALF of patients suspected of pulmonary mycobacterial infection in the Department of Tuberculosis, Affiliated Hangzhou Chest Hospital was collected prior to antituberculosis therapy and submitted for nucleotide MALDI-TOF-MS, along with acid-fast staining (AFS) (Wang et al., 2018), culture (Wang et al., 2018), Xpert MTB/RIF (Bunsow et al., 2014) and other experiments. These results of diagnostic methods were all obtained from the medical records of patients in the clinical service. Clinical etiological diagnosis was used as the gold standard to evaluate the diagnostic value of nucleotide MALDI-TOF-MS.

2.2 mNGS detection

A micro-sample genomic DNA extraction kit (DP316, Tiangen) was used to extract the nucleic acid. NEBNext Ultra II DNA Library Prep Kit (New England Biolabs Inc.) was used to construct Illumina sequencing libraries and Nextseq 550 DX (75 bp single-end reads; Illumina) was used for sequencing. An alignment tool (Burrows-Wheeler Alignment) was used to map to a human reference genome (GRCh38) to exclude human sequence data. The remaining sequencing data were aligned to NCBI nt database by SNAP. The specific detection method of mNGS can be referred to our previous report (Zhang et al., 2022).

2.3 Nucleotide MALDI-TOF-MS detection

Through the nucleotide MALDI-TOF-MS detection, various mycobacterial species including MTBC and 23 kinds of NTM can be identified. Details were shown in Table 1.

2.3.1 DNA extraction

The samples were extracted according to the instructions of MagPure DNA Kit. 40 μL proteinase K mixed with 0.5 mL samples and 50 μL buffer SDS into a 2 mL homogenate tub. After inverted mixing, the homogenizer was shaken for 2 minutes, and then incubated at 60°C for 10 min and centrifuged at 10 000 x g for 3 min. 500 μL of digestive solution was transferred to a new deep-well plate. The corresponding program was implemented after each deep-well plate was placed correctly in the corresponding position of the instrument. The DNA obtained was stored at -20°C after running the extraction procedure on the MagPure automatic extractor.

2.3.2 PCR reaction

The PCR reaction consisted of 1 μL10×PCR buffer with 25 mM $MgCl_2$, 0.8 μL 25 mM $MgCl_2$, 0.1 μL UNG (heat labile), 0.2 μL dUTP/dNTP Mix, 0.4 μL PCR enzyme, and 1 μL DNA template. During operation, the DNA was diluted to 10 ng/μL, 6.5 uL DNA was added to the PCR system. The PCR reaction

TABLE 1 The identification catalog of mycobacterial species.

NO.	Mycobacterial species	NO	Mycobacterial species
1	MTBC	13	M. scrofulaceum
2	M. kansasii	14	M. marinum
3	M. abscessus	15	M. gastri
4	M. chelonae	16	M. intracellulare
5	M.celatum	17	M. simiae
6	M. shimoidei	18	M. terrae
7	M. smegmatis	19	M. peregrinum
8	M. avium complex	20	M. gordonae
9	M. fortuitum	21	M. genavense
10	M. asiaticum	22	M. septicum
11	M. ulcerans	23	M. chimaera
12	M. xenopi	24	M. massiliense

MTBC, Mycobacterium tuberculosis complex.

was performed as follows: 25°C for 5 minutes, 95°C for 2 minutes, 45 cycles at 95°C for 30 seconds, at 56°C for 30 seconds, at 72°C for 60 seconds and final extension at 72°C for 5 minutes.

2.3.3 SAP reaction

SAP mix was prepared into a final volume of 4 μL (3.06 μL RNase-free water, 0.34 μL SAP buffer and 0.60 μL SAP enzyme), then added to the PCR and incubated for 40 minutes at 37°C, finally ended with 5 minutes of inactivation at 85°C.

2.3.4 Extension reaction

A 4.0 μL iPLEX extension reaction containing 1.24 μL RNase-free water, 0.40 μL iPLEX buffer plus (10×), 0.40 μL iPLEX termination mix, 0.08 μL iPLEX pro enzyme and 1.88 μL iPLEX pus extend primer mix were added to each well. The extension reaction was performed in the following steps: denaturation at 95°C for 30 seconds, followed by 40 cycles of 94°C for 5 seconds, five rounds of annealing at 52°C for 5 seconds, and extension at 80°C for 5 seconds, then final extension at 72°C for 3 minutes. The information of genes and primers designed for TB detection is shown in Table 2.

2.3.5 Sample desalting

10 μL of water was added to each well of the reaction plate, and the automatic desalting procedure was performed using the MASSARRAY® instrument.

2.3.6 Mass spectrometry analysis

Mass spectrometry data of the samples were obtained by MassARRAY® Typer, and bioinformatics was analyzed using the self-developed bioinformatics pipeline based on PYTHON 3. The positive samples were determined by calculating the extension rate of the assay site. The assay with an extension rate greater than the set threshold would be judged as positive, while that near the threshold would be in the grey area of analysis. The sites located in the gray area were manually interpreted and analyzed.

2.4 Statistical analysis

SPSS 22.0 statistical software was used for data analysis, and Graphpad Prism 8 and R were used for plotting. Non-normally distributed data were expressed as the median [first quartile (Q1), third quartile (Q3)], and non-parametric Mann-Whitney U test was used for comparison between groups. The counting data were expressed as the number of cases (percentage) [n (%)], and the data between groups were compared by chi-square test or Fisher's exact test. 2×2 contingency tables and receiver operating characteristic (ROC) curves were used to evaluate the diagnostic efficacy. A two-tailed value of $p<0.05$ represented significant differences.

TABLE 2 TB primer sequence and single base extension primer.

Target gene	Primer	Primer sequence(5'-3')	Amplified products (bp)	Single nucleotide extension	Relative molecular mass of extension primer	Extension base	Relative molecular mass of extension product	Gene reference sequence
IS1081	IS1081_F	ACGTTGGATGCGTGAGTACCGATCATAT	90	TTGGGCAACAACTGA	4602	A	4929.1	CCTGCTGCACTCCATCTACgaccagccgacgccga[A/G]tcagttgttgcccaATATGATCGGGTACTCGACG
	IS1081_R	ACGTTGGATGCTGCTGCACTCCATCTACGA						
IS6110	IS6110_F	ACGTTGGATGTCCAGCGCCGCTTCGGACCA	131	GACCTCACCTATGTGTC	5122.3	G	5409.5	CCTGCGAGCGTAGGCGTCGGtgacaaaggccacgtaggcgaaccctgcccaggt[A/G]gacacataggtgaggtctgctacccacagccggttaggtgctggtggtCCGAAGCGGCGCTGGACGAG
	IS6110_R	ACGTTGGATGCGTAGGCGTCGGTGACAAA						

F, forward primer; R, reverse primer.

3 Results

3.1 Sample selection and characteristics

A total of 108 samples were used for performance evaluation, containing 25 national reference standards, 37 clinical isolates, 37 verified BALF, and 9 plasmids, which covered 24 types of mycobacteria and other non-mycobacteria. From March to June 2022, a total of 40 clinical samples (BALF) were collected from patients with suspected pulmonary mycobacterial infection in the Department of Tuberculosis, Affiliated Hangzhou Chest Hospital for clinical validation. The sample data of metagenomic validation results are in Supplementary Table 1. Two samples were excluded due to missing clinical information. The selection diagram of samples for performance evaluation and clinical validation is shown in Figure 1.

Among 38 samples eligible for clinical validation, there were 22 males and 16 females, with the median age of 36 years. 34.2% of patients had pulmonary shadow by physical examination, and 44.7% experienced cough. Both lung lobes were involved in 68.4% of patients (Table 3). 86.8% were eventually diagnosed with pulmonary TB infection, among whom 1 case was diagnosed with a mixed infection of MTB and *mycobacterium cheloniae.*

3.2 Performance evaluation

105 of the 108 results of nucleotide MALDI-TOF-MS was consistent with reference samples. The remaining 3 cases of *M. abs* were negative in BALF samples. The positive results of MALDI-TOF-MS detection are shown in Supplementary Table 2. The sensitivity, specificity and accuracy of nucleotide MALDI-TOF-MS in the identification of mycobacterial species were 96.91%, 100% and 97.22%, respectively, with the area under the curve of 0.99 (Figure 2), and 1×10^3 bacteria/mL, 2×10^2 bacteria/mL, 1×10^2 bacteria/mL, 50 bacteria/mL could be detected stably. Notably, the result was negative when the concentration of MTB was diluted to 25 bacteria/mL. The LOD of MALDI-TOF-MS for MTB was 50 bacteria/mL.

3.3 MTB detected by multiple methods

The specific detection results of AFS, culture, Xpert, and MALDI-TOF-MS in BALF of 33 patients diagnosed with TB and 5 patients with non-TB infection were shown in Figure 3A. The positive rates of MALDI-TOF-MS, Xpert, culture and AFS in BALF of patients diagnosed with TB infection were 72.7%, 63.6%, 54.5% and 27.3%, respectively (Figure 3B).

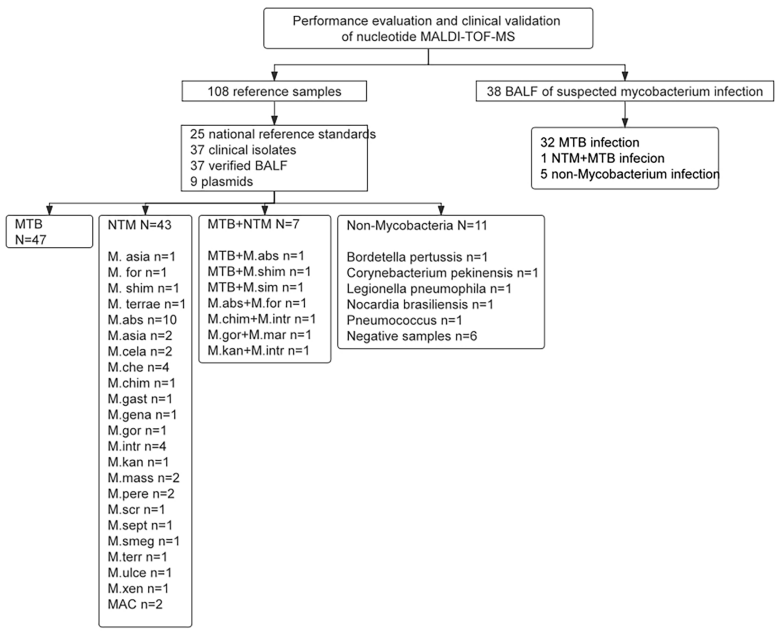

FIGURE 1
The selection diagram of samples for performance evaluation and clinical validation. MTB, Mycobacterium tuberculosis; NTM, Nontuberculous mycobacteria; MAC, Mycobacterium avium complex.

TABLE 3 Characteristics of 38 patients used for clinical validation.

Characteristics	Data
Age, years, median (Q1, Q3)	36 (26,64)
Gender, male, n (%)	22 (57.9)
Pulmonary shadow discovered by physical examination	13 (34.2)
Underlying disease, n (%)	
Hypertension	3 (7.9)
Diabetes	5 (13.2)
Renal insufficiency	2 (5.3)
Comorbidities, n (%)	
Cough	17 (44.7)
Chest distress and (or) chest pain	6 (15.8)
Fever	6 (15.8)
Discharged diagnosis, n (%)	
Pulmonary tuberculosis infection	33 (86.8)
Pulmonary infection (Non-TB/NTM)	5 (13.2)
Pulmonary lobe involvement, n (%)	
Both lung lobe	26 (68.4)
Right superior lobe	4 (10.5)
Left superior lobe	6 (15.8)
Right lobe	2 (5.3)

TB, Tuberculosis; NTM, Nontuberculous mycobacteria.

3.4 Clinical validation of MALDI-TOF-MS in diagnosing MTB

As shown in Figure 4A, the sensitivity/specificity of MALDI-TOF-MS, Xpert, culture and AFS in the diagnosis of MTB was 72.7%/100%, 63.6%/100%, 54.5%/100%, 27.3%/100%, respectively. The corresponding areas under the curve were 0.864, 0.818, 0.773, and 0.636, successively (Figure 4B). These findings further verified the superior performance of MALDI-TOF-MS in the diagnosis of MTB.

4 Discussion

The diagnostic value of nucleotide MALDI-TOF-MS for mycobacterial identification based on reference samples or clinical BALF samples from suspected pulmonary mycobacterial infection patients was promising. The high sensitivity, specificity and low LOD of nucleotide MALDI-TOF-MS in mycobacterial detection will greatly improve the positive rate of diagnosis and treatment of TB patients.

There have been studies reporting protein MALDI-TOF MS for the identification of NTM isolates has a concordance rate of 94% with the reference method (Rodríguez-Sánchez et al., 2015; Body et al., 2018). Through optimization of sample inactivation and protein extraction, the accuracy of MALDI-TOF MS in mycobacterial identification was improved to 93.9% (Luo et al., 2018). Absolutely, optimized protein extraction protocol can greatly improve the detection rate (Rodriguez-Temporal et al., 2018). Nucleotide MALDI-TOF MS allows DNA extraction directly from specimens instead of the protein extraction from isolates, which cost a period time to obtain isolates by culture for clinical application. In this study, the concordance rate of the optimized nucleic MALDI-TOF MS for MTB and NTM identification was 97.22 %. A systematic review of 25 studies on Xpert and LAMP for the diagnosis of pulmonary TB using culture as the reference method showed the pooled sensitivity and

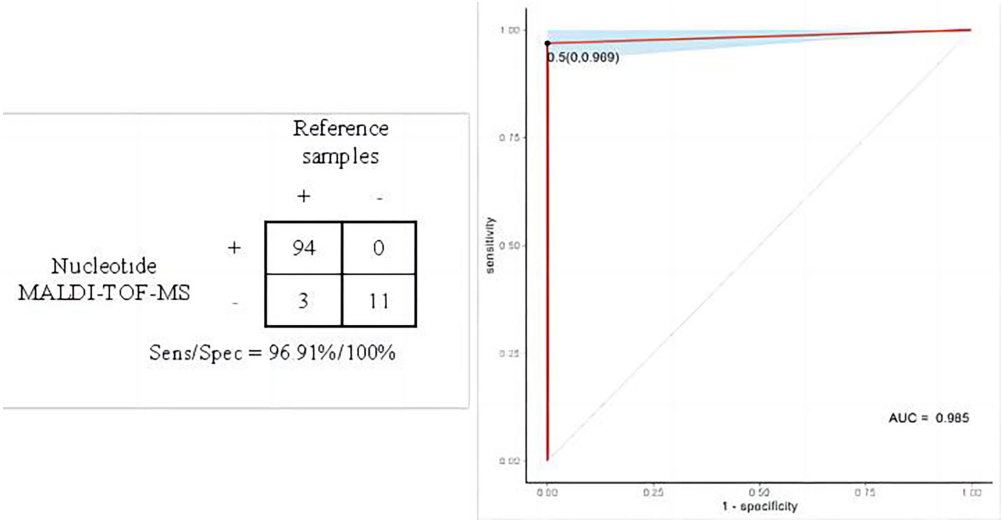

FIGURE 2
Performance evaluation of nucleotide MALDI-TOF-MS in the identification of mycobacterial species.

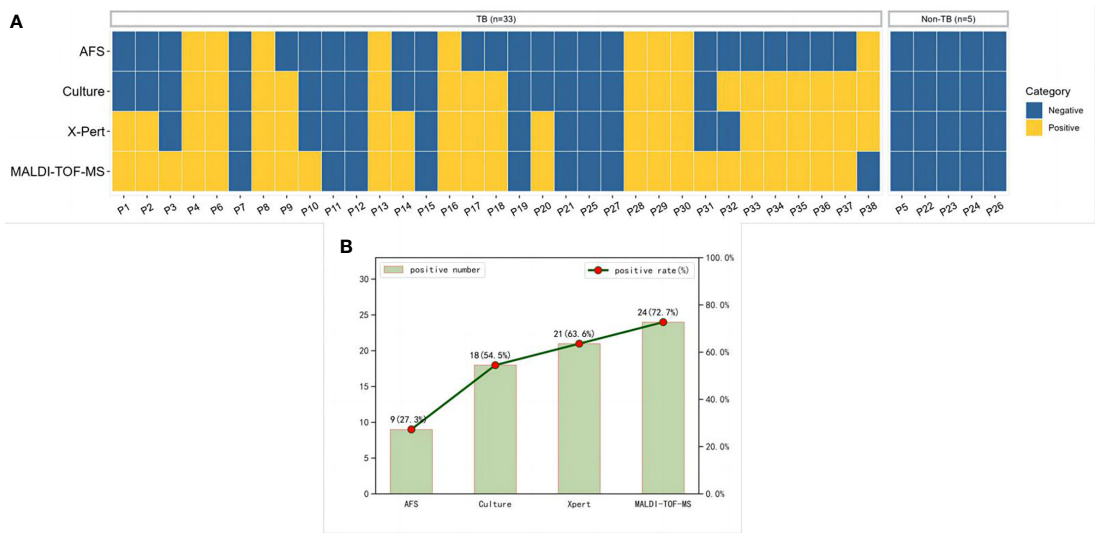

FIGURE 3
MTB results detected by multiple methods. **(A)** A heatmap depicting the identification of MTB in BALF samples by different methods. **(B)** Positive rates of each method in patients diagnosed with pulmonary tuberculosis. MTB, Mycobacterium tuberculosis; BALF, Bronchoalveolar lavage fluid.

specificity were 89% and 98%, 93% and 94%, respectively (Yan et al., 2016). In 2013, WHO revised the diagnostic criteria for TB, recommending that the positive detection results of Xpert and LAMP-TB technology should be regarded as positive bacteriological tests, which could be used as the basis for the diagnosis of pathogen-positive TB (Sha, 2021). In this study, we found that the performance characteristics of nucleic MALDI-TOF MS and Xpert were similar or even better, with sensitivity and specificity of 72.7% and 100%, 63.6% and 100%, respectively, suggesting the nucleic MALDI-TOF MS may be a potential assay for mycobacterial identification.

?>According to the WHO Global Tuberculosis Report, the global positive rate of pathogens was 58% in 2020 (Ren et al., 2020). In clinical validation, 18 out of 33 (54.5%) patients who were clinically diagnosed with TB were positive with etiological method. Combined with molecular biological methods, 24/33 (72.7%) cases of TB were found to have etiological basis. Unfortunately, there were still 8 cases clinically diagnosed with TB infection but negative for the four methods we used. In this study, the molecular methods including Xpert and MALDI-TOF MS improved the diagnostic efficiency of confirmed TB cases to 6/33 (18.2%). The positive rates of MALDI-TOF-MS, Xpert, culture and AFS in BALF of patients diagnosed with TB infection were 72.7%, 63.6%, 54.5%, and 27.3%, respectively, similar to 54.6%, 50.4%, 32% of Xpert, culture and AFS in patients with suspected pulmonary mycobacterial infection (Shen et al., 2020). In clinical validation, we found that nucleotide MALDI-TOF-MS showed the largest AUC in detecting MTB compared with other methods, indicating a superior performance of nucleotide MALDI-TOF-MS in the diagnosis of MTB. The nucleotide MALDI-TOF-MS has been used for identification, typing, and drug-resistance detection of pathogens, with the advantages of shorter turn-around time, higher throughput, and lower cost than traditional phenotypic drug susceptibility test (Trembizki et al., 2014). Through the self-built mass spectrometry analysis platform, the automated analysis of batch results can be carried out, greatly improving the speed of test reporting. In terms of mycobacterial identification, the nucleotide MALDI-TOF-MS with the analysis process optimized in this study improved the accuracy to 97.22%.Wu et al. applied nucleic MALDI-TOF-MS to evaluate TB drug resistance, and found that nucleotide MALDI-TOF-MS could be a promising tool for rapid detection of MTB drugs (Wu et al., 2022). TB drug resistance is an important research issue that needs to be addressed today. In the future, we will further explore the correlation between clinical phenotypic outcomes and molecular genotypes.

Our study has some limitations. First, the sample size used for clinical validation was small, leading to fewer patients in the negative group when assessing specificity. Second, we did not analyze the detection of gene resistance against TB by MALDI-TOF MS. Third, we only analyzed the value of MALDI-TOF MS in the detection of mycobacteria in BALF samples, but not other sample types, such as sputum, tissue, cerebrospinal fluid, pleural effusion, etc., which limited the establishment of evidence-based medicine for the diagnostic value of MALDI-TOF MS in

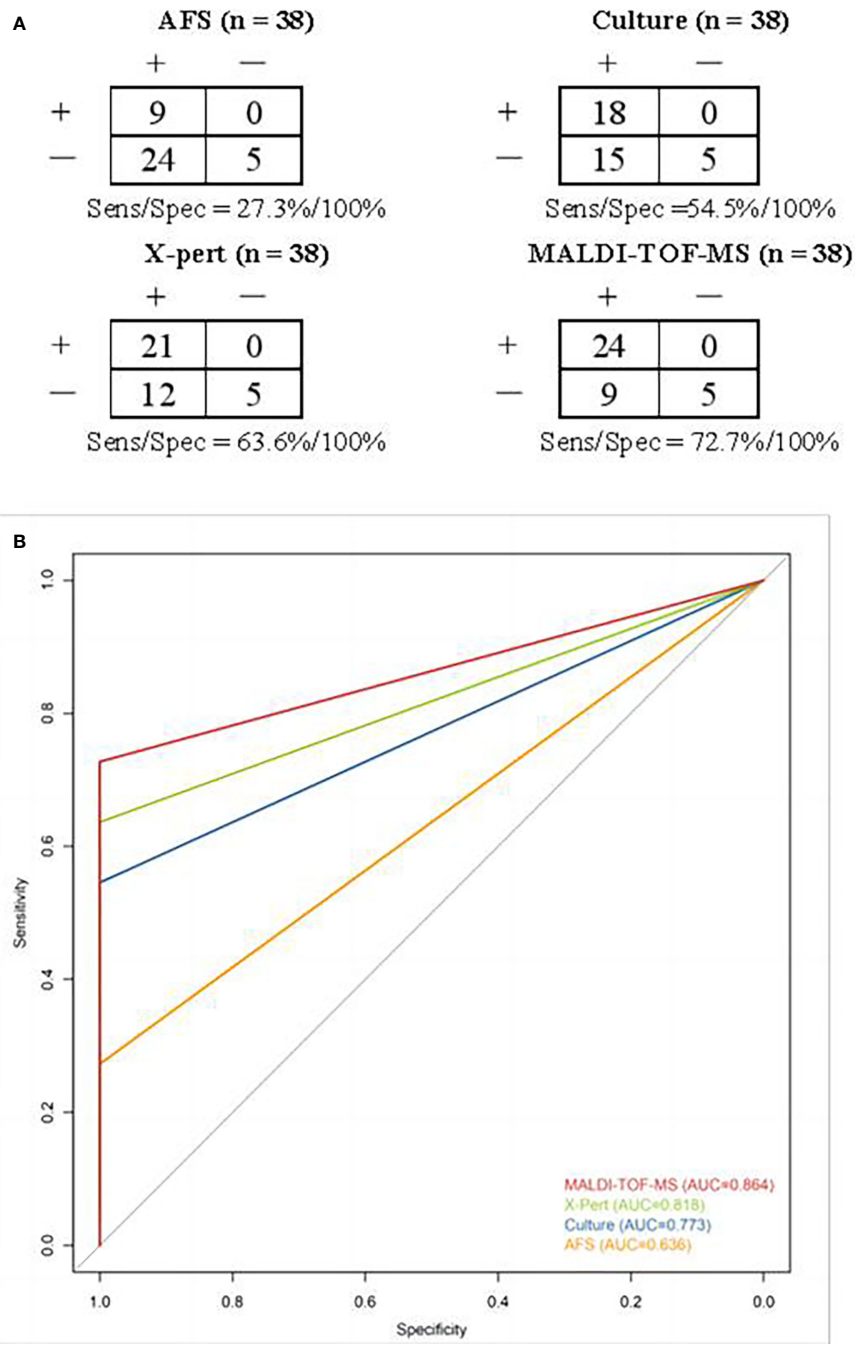

FIGURE 4
(A) Contingency tables for different methods in detecting MTB. Clinical discharge diagnosis was used as a reference method. **(B)** ROC curves and areas under the curve of different methods in diagnosing MTB. ROC, Receiver operator characteristics; MTB, Mycobacterium tuberculosis.

extrapulmonary TB. Additionally, due to the low incidence of NTM disease, there were not enough specimens containing NTM for analysis when the clinical validation samples were included. In the future, we will enroll large samples to evaluate the specificity of nucleic MALDI-TOF MS and investigate the difference between the drug resistance genotypes by MALDI-TOF MS and phenotypes.

In summary, optimized nucleotide MALDI-TOF-MS has satisfactory sensitivity, specificity and low LOD in the

identification of mycobacteria, which may serve as a potential assay for mycobacterial identification.

Data availability statement

The original contributions presented in the study are included in the article/Supplementary Material. Further inquiries can be directed to the corresponding authors.

Ethics statement

The studies involving human participants were reviewed and approved by medical committee of Affiliated Hangzhou Chest Hospital, Zhejiang University School of Medicine (No.2022-75). The patients/participants provided their written informed consent to participate in this study.

Author contributions

BL, CZ participated in writing the manuscript; LS, HD, YS conducted the study design; SC, QZ built the detection platform and optimize the process; LZ, QQ, TM, HW, MQ provided clinical information and case data; CS, QC were in charge of the whole research project. All authors contributed to the article and approved the submitted version.

Funding

This work was supported by project of Zhejiang Provincial Health Commission (NO.2023KY968).

Acknowledgments

We thank Furong Du for polishing the article, Jing Liu, Mengji Yu for analysis of results, Hongli Zhou for image optimization from Nanjing Simcere Diagnostics Co., Ltd.

Conflict of interest

Authors CZ, HD, SC, QZ, and CS were employed by Jiangsu Simcere Diagnostics Co., Ltd.

The remaining authors declare that the research was conducted in the absence of any commercial or financial relationships that could be construed as a potential conflict of interest.

Publisher's note

Supplementary material

The Supplementary Material for this article can be found online at: https://www.frontiersin.org/articles/10.3389/fcimb.2022.1079184/full#supplementary-material

References

Armstrong, G. L., MacCannell, D. R., Taylor, J., Carleton, H. A., Neuhaus, E. B., Bradbury, R. S., et al. (2019). Pathogen genomics in public health. *N Engl. J. Med.* 381 (26), 2569–2580. doi: 10.1056/NEJMsr1813907

Blauwkamp, T. A., Thair, S., Rosen, M. J., Blair, L., Lindner, M. S., Vilfan, I. D., et al. (2019). Analytical and clinical validation of a microbial cell-free DNA sequencing test for infectious disease. *Nat. Microbiol.* 4 (4), 663–674. doi: 10.1038/s41564-018-0349-6

Body, B. A., Beard, M. A., Slechta, E. S., Hanson, K. E., Barker, A. P., Babady, N. E., et al. (2018). Evaluation of the vitek MS v3.0 matrix-assisted laser desorption ionization-time of flight mass spectrometry system for identification of mycobacterium and nocardia species. *J. Clin. Microbiol.* 56 (6), e00237–e00218. doi: 10.1128/JCM.00237-18

Bunsow, E., Ruiz-Serrano, M. J., Roa, P. L., Kestler, M., Viedma, D. G., Bouza, E., et al. (2014). Evaluation of GeneXpert MTB/RIF for the detection of mycobacterium tuberculosis and resistance to rifampin in clinical specimens. *J. Infection* 68 (4), 338–343. doi: 10.1016/j.jinf.2013.11.012

Detjen, A. K., DiNardo, A. R., Leyden, J., Steingart, K. R., Menzies, D., Schiller, I., et al. (2015). Xpert MTB/RIF assay for the diagnosis of pulmonary tuberculosis in children: a systematic review and meta-analysis. *Lancet Respir. Med.* 3, 451–461. doi: 10.1016/S2213-2600(15)00095-8

Fernández-Esgueva, M., Fernández-Simon, R., Monforte-Cirac, M. L., López-Calleja, A. I., Fortuño, B., Viñuelas-Bayon, J., et al. (2021). (Bruker daltonics) for identification of mycobacterium species isolated directly from liquid medium. *Enferm Infecc Microbiol. Clin. (Engl Ed).* 39 (5), 241–243. doi: 10.1016/j.eimc.2020.05.011

Jeremiah, C., Petersen, E., Nantanda, R., Mungai, B. N., Migliori, G. B., Amanullah, F., et al. (2022). The WHO global tuberculosis 2021 report - not so good news and turning the tide back to end TB. *Int. J. Infect. Dis.* 20, S1201–9712 (22)00149-7. doi: 10.1016/j.ijid.2022.03.011

Kambli, P., Ajbani, K., Kazi, M., Sadani, M., Naik, S., Shetty, A., et al. (2021). Targeted next generation sequencing directly from sputum for comprehensive genetic information on drug resistant mycobacterium tuberculosis. *Tuberculosis* 127, 102051. doi: 10.1016/j.tube.2021.102051

Kang, X., Chen, C., Liu, X., Zhang, H., Cao, F., Chen, Y., et al. (2018). China Expert consensus group on nucleic acid mass spectrometry application. Chinese expert consensus on application of nucleic acid mass spectrometry. *Natl. Med. J. China* 98 (12), 895–900.

Kriegsmann, M., Arens, N., Endris, V., Weichert, W., and Kriegsmann, J. (2015). Detection of KRAS, NRAD and BRAF by mass spectrometry: A sensitive, reliable, fast and cost-effective technique. *Diagn. Pathol.* 10, 132. doi: 10.1186/s13000-015-0364-3

Luo, L., Cao, W., Chen, W., Zhang, R., Jing, L., Chen, H., et al. (2018). Evaluation of the VITEK MS knowledge base version 3.0 for the identification of clinically relevant mycobacterium species. *Emerg. Microbes Infect.* 7 (1), 114. doi: 10.1038/s41426-018-0120-3

Ren, T. T., Lu, X. Z., Deng, D. F., Fu, L., and Zhang, P. (2020). WHO global tuberculosis report: Global and China key data analysis. *Emerging Infect. Dis. electronic J.* 5 (4), 280 284. doi: 10.19871/j.carolcarrollnkiXFCRBZZ.2020.04.015

Rodríguez-Sánchez, B., Ruiz-Serrano, M. J., Marín, M., López Roa, P., RodríguezCréixems, M., and Bouza, E. (2015). Evaluation of matrix-assisted laser desorption ionization–time of flflight mass spectrometry for identifification of nontuberculous mycobacteria from clinical isolates. *J. Clin. Microbiol.* 53, 2737–2740. doi: 10.1128/JCM.01380-15

Rodriguez-Temporal, D., Perez-Risco, D., Struzka, E. A., Mas, M., and Alcaide, F. (2018). Evaluation of two protein extraction protocols based on freezing and mechanical disruption for identifying nontuberculous mycobacteria by matrix-assisted laser desorption ionization-time of flight mass spectrometry from liquid and solid cultures. *J. Clin. Microbiol.* 56 (4), e01548–e01517. doi: 10.1128/JCM.01548-17

Rodriguez-Temporal, D., Rodríguez-Sánchez, B., and Alcaide, F. (2020). Evaluation of MALDI biotyper interpretation criteria for accurate identification of nontuberculous mycobacteria. *J. Clin. Microbiol.* 58 (10), e01103–e01120. doi: 10.1128/JCM.01103-20

Sha, W. (2021). Standardize the rational use of molecular biological detection technology for early and accurate diagnosis of tuberculosis. *Chin. J. Antituberc.* 43 (10), 983–986. doi: 10.3969/j.issn.1000-6621.2021.10.001.

Shen, Y., Fang, L., Xu, X., Ye, B., and Yu, G. (2020). CapitalBio mycobacterium real-time polymerase chain reaction detection test: rapid diagnosis of mycobacterium tuberculosis and nontuberculous mycobacterial infection, international journal of infectious diseases. *Int. J. Infect. Dis.* 98:1–5. doi: 10.1016/j.ijid.2020.06.042

Simner, P. J., Miller, H. B., Breitwieser, F. P., Pinilla Monsalve, G., Pardo, C. A., Salzberg, S. L., et al. (2018). Development and optimization of metagenomic next-generation sequencing methods for cerebrospinal fluid diagnostics. *J. Clin. Microbiol.* 56 (9), e00472-18. doi: 10.1128/JCM.00472-18

Trembizki, E., Smith, H., Lahra, M. M., Chen, M., Donovan, B., Fairley, C. K., et al. (2014). High-throughput informative single nucleotide polymorphism-based typing of neisse- ria gonorrhoeae using the sequenom MassARRAY iPLEX platform. *J. Antimicrob. Chemother.* 69 (6), 1526–1532. doi: 10.1093/jac/dkt544

Wang, L., Chen, S., Zhou, L., Zhao, Y., Gao, M., Chu, N., et al. (2018). Diagnosis of tuberculosis WS 288-2017. *Chin. J. Infection Control* 17 (7), 642–652. doi: 10.3969/j.issn.1671-9638.2018.07.019

Wilson, M. R., Naccache, S. N., Samayoa, E., Biagtan, M., Bashir, H., Yu, G., et al. (2014). Actionable diagnosis of neuroleptospirosis by next-generation sequencing. *N Engl. J. Med.* 370 (25), 2408–2417. doi: 10.1056/NEJMoa1401268

Wu, W., Cheng, P., Lyu, J., Zhang, Z., and Xu, J. (2018). Tag array gene chip rapid diagnosis anti-tuberculosis drug resistance in pulmonary tuberculosis-a feasibility study, tuberculosis. *Tuberculosis* 110, 96–103. doi: 10.1016/j.tube.2018.03.010

Wu, X., Tan, G., Yang, J., Guo, Y., Huang, C., Sha, W., et al. (2022). Prediction of mycobacterium tuberculosis drug resistance by nucleotide MALDI-TOF-MS. *Int. J. Infect. Dis.* 121, 47–54. doi: 10.1016/j.ijid.2022.04.061

Yan, L., Xiao, H., and Zhang, Q. (2016). Systematic review: Comparison of xpert MTB/RIF, LAMP and SAT methods for the diagnosis of pulmonary tuberculosis. *Tuberculosis* 96, 75–86. doi: 10.1016/j.tube.2015.11.005

Ye, S. H., Siddle, K. J., Park, D. J., and Sabeti, P. C. (2019). Benchmarking metagenomics tools for taxonomic classifification. *Cell* 178 (4), 779–794.

Zhang, J., Gao, L., Zhu, C., Jin, J., Song, C., Dong, H., et al. (2022). Clinical value of metagenomic next-generation sequencing by illumina and nanopore for the detection of pathogens in bronchoalveolar lavage flfluid in suspected community-acquired pneumonia patients. *Front. Cell. Infect. Microbiol.* 12. doi: 10.3389/fcimb.2022.1021320

frontiers | Frontiers in Cellular and Infection Microbiology

TYPE Original Research
PUBLISHED 22 March 2023
DOI 10.3389/fcimb.2023.1154939

OPEN ACCESS

EDITED BY
Amit Singh,
Central University of Punjab, India

REVIEWED BY
Parul Singh,
All India Institute of Medical Sciences Gorakhpur, India
Guoliang Zhang,
Shenzhen Third People's Hospital, China

*CORRESPONDENCE
Xiao-Yong Fan
xyfan008@fudan.edu.cn
Hui Zhang
Zhang.hui@zs-hospital.sh.cn

†These authors have contributed equally to this work

SPECIALTY SECTION
This article was submitted to Clinical Microbiology, a section of the journal Frontiers in Cellular and Infection Microbiology

RECEIVED 31 January 2023
ACCEPTED 07 March 2023
PUBLISHED 22 March 2023

CITATION
Xu J-C, Shi X, Ma X, Gu W-f, Fang Z-x, Zhang H and Fan X-Y (2023) Diagnosis of extrapulmonary tuberculosis by ultrasound-guided biopsy: A retrospective comparison study. *Front. Cell. Infect. Microbiol.* 13:1154939. doi: 10.3389/fcimb.2023.1154939

Diagnosis of extrapulmonary tuberculosis by ultrasound-guided biopsy: A retrospective comparison study

Jin-Chuan Xu[1†], Xia Shi[1†], Xin Ma[1†], Wen-fei Gu[1,2], Zhi-xiong Fang[3], Hui Zhang[1*] and Xiao-Yong Fan[1,2*]

[1]Shanghai Public Health Clinical Center, Fudan University, Shanghai, China, [2]School of Laboratory Medicine and Life Science, Wenzhou Medical University, Wenzhou, China, [3]Department of Infectious Diseases and Public Health, Central Hospital of Xiangtan, Xiangtan, China

Objective: To compare the diagnostic performance of laboratory assays on the ultrasound-guided core needle biopsy samples for diagnosis of extra-pulmonary tuberculosis (EPTB) in HIV-positive and HIV-negative patients.

Methods: A total of 217 patients suspected to have EPTB underwent lesion biopsy from 2017 to 2020. Results of laboratory tests on the biopsy and non-biopsy samples were collected with clinical data for retrospective analysis of test utility. The calculated diagnostic accuracy of the tests was stratified according to the specimen types and HIV status.

Results: The cohort contained 118 patients with a final positive diagnosis of extrapulmonary tuberculosis (EPTB group, 54.4%) and 99 finally diagnosed as without TB (non-EPTB group, 45.6%). The risk factor for EPTB was HIV co-infection (OR 2.22, 95% CI 1.17-4.28, p = 0.014). In biopsy samples, GeneXpert (Xpert) showed higher sensitivity (96.6% [91.6-98.7], p < 0.0001) than culture (56.1% [47.0-64.9]). Regardless of HIV status, Xpert had the highest sensitivity (>95%) and specificity (nearly 100%) of any methods. In non-biopsy samples, only T-SPOT.*TB* (T-SPOT) showed higher sensitivity than culture (90.9% [62.3-99.5] *vs* 35.3% [17.3-58.7], p = 0.0037). Furthermore, the sensitivities of Xpert were lower in non-biopsy samples (60.0% [23.1-92.9], p = 0.022) than in biopsy samples (100% [86.7-100]). Even in smear-negative biopsy samples, Xpert still had higher sensitivity than culture and retained high specificity (100% [95.7-100]).

Conclusion: Superior performance of Xpert in diagnosing EPTB was observed regardless of HIV status and specimen types. Nevertheless, the biopsy samples still substantially facilitated the accurate diagnosis of extrapulmonary tuberculosis.

KEYWORDS

extrapulmonary tuberculosis (EPTB), diagnosis, biopsy, Xpert, human immunodeficiency virus (HIV)

1 Introduction

Tuberculosis (TB) is a communicable disease caused by the mycobacterium tuberculosis complex (MTBC). Globally, an estimated 10.6 million people (range, 9.9-11.0 million) fell ill with TB in 2021, an increase of 4.5% from 10.1 million (95% UI: 9.5-10.7 million) in 2020; and about 1.6 million died from TB in the same year, up from a best estimate of 1.5 million in 2020 (WHO, 2022).

Extrapulmonary tuberculosis (EPTB) refers to TB occurring in parts of the body other than the lungs (e.g., lymph nodes, meninges, abdomen, pleura, genitourinary tract, skin, joints, and bones) (Golden and Vikram, 2005). As per the Global TB Report 2020, EPTB constituted 16% of the 7.5 million notified TB cases in 2019, ranging from 8% in the Western Pacific Region to 24% in the Eastern Mediterranean Region (WHO, 2020). In China, EPTB accounted for approximately 24% of TB cases, with a maximum of 33% in the western region (Li et al., 2022). In the context of WHO's End TB Strategy, timely diagnosis and treatment of EPTB is a challenge we have to face.

The main risk factors associated with EPTB vary widely and include human immunodeficiency virus (HIV) co-infection, female sex, age (young children or over 65 years of age), and diabetes (Shivakoti et al., 2017; Ohene et al., 2019; Pang et al., 2019; Banta et al., 2020). Due to the absence of typical TB symptoms, EPTB is often misdiagnosed as other diseases, such as cancers (Xiang et al., 2021) and inflammatory diseases (Aisenberg et al., 2005; Jain, 2011). Laboratory diagnosis plays a decisive role in the diagnosis of EPTB. However, studies comparing various laboratory assays based on biopsy samples are limited, probably because biopsy samples are not readily available (Norbis et al., 2014; Park and Kon, 2021).

This study analyzed the records from laboratory investigations of specimens from suspected extrapulmonary tuberculosis patients in an infectious disease hospital from 2017 to 2020 to compare the accuracy of different methods of laboratory diagnosis.

2 Methods

2.1 Study population and specimens

This study was conducted in Shanghai Public Health Clinical Center, one of the designated National Tuberculosis Hospitals in China. Patients with suspected EPTB (WHO, 2021a) who had undergone biopsy between July 01 2017 and September 30 2020 were enrolled. The inclusion criteria were patients with lymph node enlargement and typical symptoms of TB (fever, wasting, night sweats, etc.), or a positive PPD/TSPOT.TB test, or suspicion of TB on imaging, and willing to receive puncture procedures. The exclusion criteria were the patient refusing the biopsy or patients with contraindications to puncture, such as coagulation dysfunction. The biopsy samples were collected by an ultrasound-guided core needle biopsy. For the non-biopsy samples, we collected data from the hospital's Laboratory Examination Control System by matching the patient's ID and the exact test date. Demographic information (sex, age, HIV status, and diagnosis) and anatomical locations of EPTB were recorded upon enrollment. The results of pathological and microbiological tests were included.

2.2 Clinical definition and classification

The culture (combined with the MPB64 test) and Xpert results were used as a microbiological reference standard. Patients were eventually classified into the EPTB group (culture (4 cases), Xpert (54 cases), or culture-Xpert (60 cases) positive) and non-EPTB group [culture and Xpert negative (99 cases)].

2.3 Laboratory methods

Biopsy samples were collected by ultrasound-guided biopsy in the Ultrasound Intervention Department and sent to the Laboratory and Pathology Departments for diagnostic tests and histological examinations. Non-biopsy samples were collected and tested routinely in the Laboratory Department. An optimized sample pre-treatment process was used to concentrate mycobacteria in the specimens and thus improve the accuracy of the assays (Rickman and Moyer, 1980; Peterson et al., 1999). Briefly, Large-volume liquid specimens were first centrifuged at 3000-3800g for 15 min, the supernatant was discarded and digested with 2-4% NaOH for 15-20 min. Solid samples were digested directly with 2-4% NaOH. After digestion, the samples were neutralized with sterile PBS, then centrifuged at 3000-3800g for 15 min and the supernatant was discarded. The digested samples were mixed with 0.1-1mL of PBS and used for subsequent assays. Routine tests included culture (BACTEC MGIT 960 rapid culture method), smear (Auramine O staining kit, Zhuhai Baso Biotechnology Co.), and Xpert (Gene X-Pert MTB/RIF, Cepheid, USA). T-SPOT.TB (Oxford Immunotec Ltd, UK), was carried out using kits based upon the hospital's programmatic laboratory procedures. Species identification was carried out with an MPB64 monoclonal antibody assay (Hangzhou Genesis Biodetection & Biocontrol Co., Ltd, Hangzhou, China) based on positive cultures. Next-generation sequencing is done by Shanghai Simple Gene Medical Laboratory (Kindstar Globalgene Technology, Inc. Shanghai, China) when required.

The pathological tissues were fixed with 4.0% formaldehyde, routinely dehydrated and paraffin-embedded, and serially sectioned at a thickness of 4 μm. HE stain and acid-fast stain (Zhuhai Baso Biotechnology Co. Zhuhai, China) were performed in sections for routine microscopic diagnosis. EPTB positive was identified when there was typical epithelioid granuloma formation, caseation, and positive acid-fast staining.

2.4 Statistical analysis

We used R studio version 4.0.0 to process the data and GraphPad Prism version 8.0 for all analyses. The baseline table was performed using the R-based tableone package (version 0.13.2). The χ^2 test (including McNemar's test) was used to calculate

differences in diagnostic accuracy metrics; the Mann-Whitney U test was used to calculate differences in non-parametric data; the two-sample proportion test (Chi-square test) was used to compare, for example, sensitivity across two groups.

3 Results

In this study, we enrolled 217 cases of suspected EPTB, including 118 (54.4%) cases that had been confirmed as EPTB patients and 99 (45.6%) cases that had been finally diagnosed as non-EPTB patients (Figure 1). The locations of the biopsy were the neck (134 cases), axillary (25 cases), musculoskeletal (14 cases), abdominal (13 cases), chest (9 cases), supraclavicular (9 cases), limb (6 cases), testicular or epididymal (5 cases), fossailiaca (1 case) and face (1 case). In addition, data from 53 non-biopsy samples (mostly sputum) were retrieved based on patient ID and sampling date. As shown in Figure 2, culture, smear, Xpert, Hematoxylin-eosin staining (HE), and Acid Fast Bacteria (AFB) Stain were performed on biopsy samples. For non-biopsy samples, culture, Xpert, and TSPOT assays were done.

Males were more likely to have EPTB than females (OR 1.89, 95%CI 1.10-3.29, $p = 0.021$). Using patients < 25 years of age as a control group, we found that patients exhibited an increased risk of extrapulmonary TB with increasing age (OR 1.16, 95% CI 0.60-2.25 for patients 25-44 years of age; OR 1.30, 95% CI 0.58-2.93 for patients 45-64 years of age; OR 2.05, 95% CI 0.76-5.76 for patients > 65 years of age). As expected, HIV-positive patients were more frequently affected by EPTB than HIV-negative ones (OR 2.22, 95% CI 1.17-4.28, $p = 0.014$). However, the lump diameter, pus volume, and length of patients' biopsy samples were not related to the likelihood of a positive diagnosis of EPTB (Table 1).

Firstly, we compared the diagnostic accuracy of conventional assays with 217 biopsy samples (Table 2). In biopsy samples, the sensitivity, specificity, positive predictive value (PPV), and negative predictive value (NPV) of the culture were56.1% [47.0-64.9], 96.9% [91.3-99.2], 95.5% [87.6-98.8] and 57.2% [32.6-72.6], respectively. Notably, Xpert had higher sensitivity (96.6% [91.6-98.7] vs 56.1% [47.0-64.9]; $p < 0.0001$), specificity (100% [95.8-100] vs 96.9% [91.3-99.2]; $p = 0.096$, and PPV (100% [96.7-100] vs 95.5% [87.6-98.8]; $p = 0.023$), and NPV (95.7% [89.4-98.3] vs 57.2% [32.6-72.6]; $p < 0.0001$) when compared with culture (Table 2). The histological assays (HE and AFB) had a better sensitivity performance (HE 92.4% [85.7-96.1], $p < 0.0001$; AFB 81.7% [73.2-88.0], $p < 0.0001$) and NPV (HE 88.6% [79.0-94.1], $p = 0.0003$; AFB 76.8% [66.6-84.6], $p = 0.07$) than culture, but poorer performance in specificity (HE 71.3% [61.0-79.7], $p < 0.0001$; AFB 73.3% [63.1-81.5], $p < 0.0001$), and PPV (HE 79.5% [71.5-85.7], $p = 0.003$; AFB 78.7% [70.1-85.4], $p = 0.0024$), consistent with a previous report (sensitivity: 95.6%, specificity: 64.6%, PPV: 74.1%, NPV: 93.2%) (Bennani et al., 2019). Unexpectedly, the sensitivity and NPV of the smear were slightly higher than that of the culture, but the difference was not significant (Table 2).

By HIV status, culture had greater sensitivity (70.0% [48.1-85.5] vs 53.2% [43.2-63.0], $p = 0.17$) and NPV (82.9% [67.3-91.9] vs 59.6% [50.3-68.4], $p = 0.012$) in HIV-positive patients than HIV-negative ones. Both specificity (93.6% [79.3-98.9] vs 98.5% [91.9-99.9], $p = 0.50$) and PPV (87.5% [64.0-97.8] vs 98.0% [89.7-99.9], $p = 0.28$) of culture were lower in HIV-positive patients than in HIV-negative patients. Similar trends were observed for the smear and histological methods, but the specificity (HE: 54.2% [35.1-72.1] vs 77.8% [66.1-86.3], $p = 0.056$; AFB: 53.9% [35.5-71.2] vs 81.7% [70.1-89.4], $p = 0.016$) and PPV (smear: 83.3% [60.8-94.2] vs 98.4% [91.5-99.9], $p = 0.033$; HE: 62.1% [44.0-77.3] vs 85.0% [76.3-90.8],

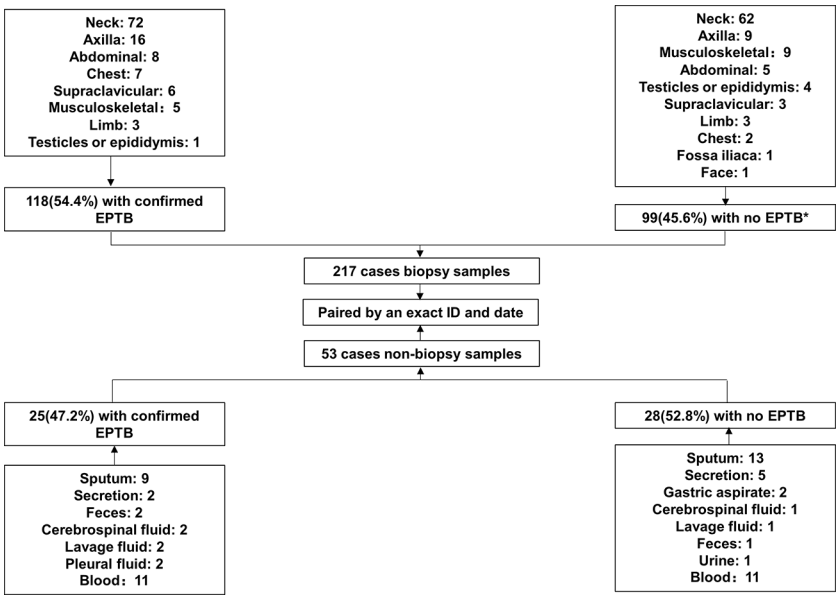

FIGURE 1
Study profile.* 26 cases of lymphadenitis, 2 cases of NTM infection, 3 cases of BCG infection, 8 cases of tumor, 4 cases of *Penicillium marneffei* infection, 3 cases of *Staphylococcus aureus* infection, and 53 cases of other non-TB diseases.

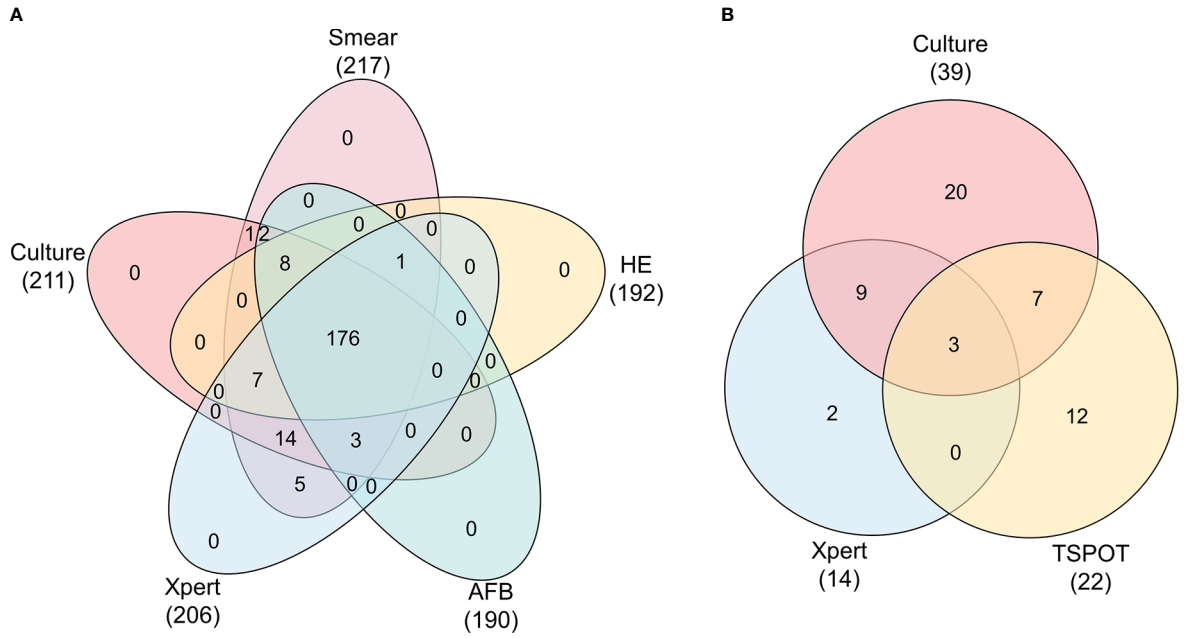

FIGURE 2
Venn diagram showing the relationship between tests of biopsy and non-biopsy samples. Data are shown stratified according to: **(A)** Veen diagram of culture, smear, HE, AFB, Xpert tests in biopsy samples, **(B)** Veen diagram of culture, Xpert, TSPOT tests in non-biopsy samples.

p = 0.016; AFB: 58.6% [40.7-74.5] vs 86.1% [76.8-92.0], p = 0.0047) of the assays for HIV-positive patients were significantly lower than for HIV-negative patients, because HIV-positive patients were more likely to be infected by non-tuberculous mycobacteria (NTM) (Álvaro-Meca et al., 2015) (3.8% in this study). Remarkably, Xpert had the highest sensitivity, specificity, PPV, and NPV values of all assays and did not differ significantly between HIV-positive and negative patients (Figure 3; Supplementary Table S1).

In 53 non-biopsy samples (Table 3), TSPOT had higher sensitivity than culture (90.9% [62.3-99.5] vs 35.3% [17.3-58.7], p = 0.0037), but lower specificity (63.6% [35.4-84.8] vs 100% [85.1-100], p = 0.0026). The sensitivity and specificity of Xpert and culture did not differ significantly, most likely due to the small sample size (Table 3). We also compared the performance of different assays between biopsy samples and non-biopsy samples. The Xpert showed higher sensitivity (100% [86.7-100] vs 60.0% [23.1-92.9], p = 0.022) and NPV (100% [86.2-100] vs 81.8% [52.3-96.8], p = 0.032) in biopsy samples than in non-biopsy samples, but not higher specificity or PPV. The same trend was observed for culture, but not significantly (Figure 4; Supplementary Table S2).

TABLE 1 Demographic and clinical characteristics of the studied patients*.

Characteristic	Level	Overall	EPTB	Non-EPTB	OR	*P* Ratio
		217	118	99		
Gender (%)	Female	102 (47.0)	64 (54.2)	38 (38.4)	Ref.	Ref.
	Male	115 (53.0)	54 (45.8)	61 (61.6)	**1.89 [1.10;3.29]**	**0.021**
Age (%)	< 25	61 (28.1)	36 (30.5)	25 (25.3)	Ref.	Ref.
	25-44	94 (43.3)	52 (44.1)	42 (42.4)	1.16 [0.60;2.25]	0.655
	45-64	40 (18.4)	21 (17.8)	19 (19.2)	1.30 [0.58;2.93]	0.527
	> 65	22 (10.1)	9 (7.6)	13 (13.1)	2.05 [0.76;5.76]	0.156
HIV (%)	Negative	166 (76.5)	98 (83.1)	68 (68.7)	Ref.	Ref.
	Positive	51 (23.5)	20 (16.9)	31 (31.3)	**2.22 [1.17;4.28]**	**0.014**
LD (median [IQR])		28.0 [21.0, 41.7]	30.0 [23.0, 42.0]	25.0 [20.0, 40.0]	0.98 [0.96;1.01]	0.179
PV (median [IQR])		0.0 [0.0, 1.5]	0.0 [0.0, 2.75]	0.0 [0.0, 0.5]	1.01 [0.99;1.02]	0.607
SL (median [IQR])		20.0 [10.0, 30.0]	20.0 [10.0, 30.0]	20.0 [11.0, 25.0]	1.0 [0.99;1.01]	0.798

*LD, Lump diameter (mm); PV, Pus volume (ml); SL, Sample length (mm); Ref, Reference variable in categorical variables; OR, Odds ratio.
Bold means the P value is less than 0.05, with a statistical difference.

TABLE 2 Diagnostic utility of culture, smear, Xpert, HE, and AFB in the examination of biopsy samples.

Test and (*p*)	Sensitivity	Specificity	PPV	NPV
Culture	64/114 (56.1; 47.0-64.9)	94/97 (96.9; 91.3-99.2)	64/67 (95.5; 87.6-98.8)	94/144 (57.2; 32.6-72.6)
Smear	77/118 (65.3; 56.3-73.2)	95/99 (96.0; 90.1-98.4)	77/81 (95.1; 88.0-98.1)	95/136 (69.9; 61.7-76.9)
Smear vs Culture (*p*)	0.16	0.72	0.90	0.41
Xpert	114/118 (96.6; 91.6-98.7)	88/88 (100; 95.8-100)	114/114 (100; 96.7-100)	88/92 (95.7; 89.4-98.3)
Xpert vs Culture (*p*)	**< 0.0001**	0.096	**0.023**	**< 0.0001**
HE	97/105 (92.4; 85.7-96.1)	62/87 (71.3; 61.0-79.7)	97/122 (79.5; 71.5-85.7)	62/70 (88.6; 79.0-94.1)
HE vs Culture (*p*)	**< 0.0001**	**< 0.0001**	**0.0030**	**0.0003**
AFB	85/104 (81.7; 73.2-88.0)	63/86 (73.3; 63.1-81.5)	85/108 (78.7; 70.1-85.4)	63/82 (76.8; 66.6-84.6)
AFB vs Culture (*p*)	**< 0.0001**	**< 0.0001**	**0.0024**	0.070

Shown are the fraction of positive results, n/N and % with 95% CI in parentheses, with p-values where appropriate. NPV, negative predictive value; PPV, positive predictive value.
Bold means the P value is less than 0.05, with a statistical difference.

In smear-negative biopsy samples (Table 4), the Xpert had significantly higher sensitivity (92.7% [80.6-97.5] vs 45.0% [30.7-60.2], $p < 0.0001$) and NPV (96.6% [90.5-99.1] vs 80.9% [72.7-87.0], $p = 0.0007$) than culture, and comparable specificity and PPV to culture. The sensitivity (86.5% [72.0-94.1] vs 45.0% [30.7-60.2], $p = 0.0001$) and NPV (92.5% [83.7-96.8] vs 80.9% [72.7-87.0], $p = 0.033$) of HE were also higher than culture, while the specificity (HE: 73.8% [63.5-82.0] vs 100% [96.0-100], $p < 0.0001$; AFB: 75.9% [65.7-83.8] vs 100% [96.0-100], $p < 0.0001$) and PPV (HE: 59.3% [46.0-71.3] vs 100% [82.4-100], $p = 0.0012$; AFB: 52.4% [37.7-66.6] vs 100% [82.4-100], $p = 0.0003$) of histological methods were lower than culture (Table 4).

4 Discussion

In this retrospective analysis, we used biopsy samples and non-biopsy samples from patients with presumptive EPTB to determine

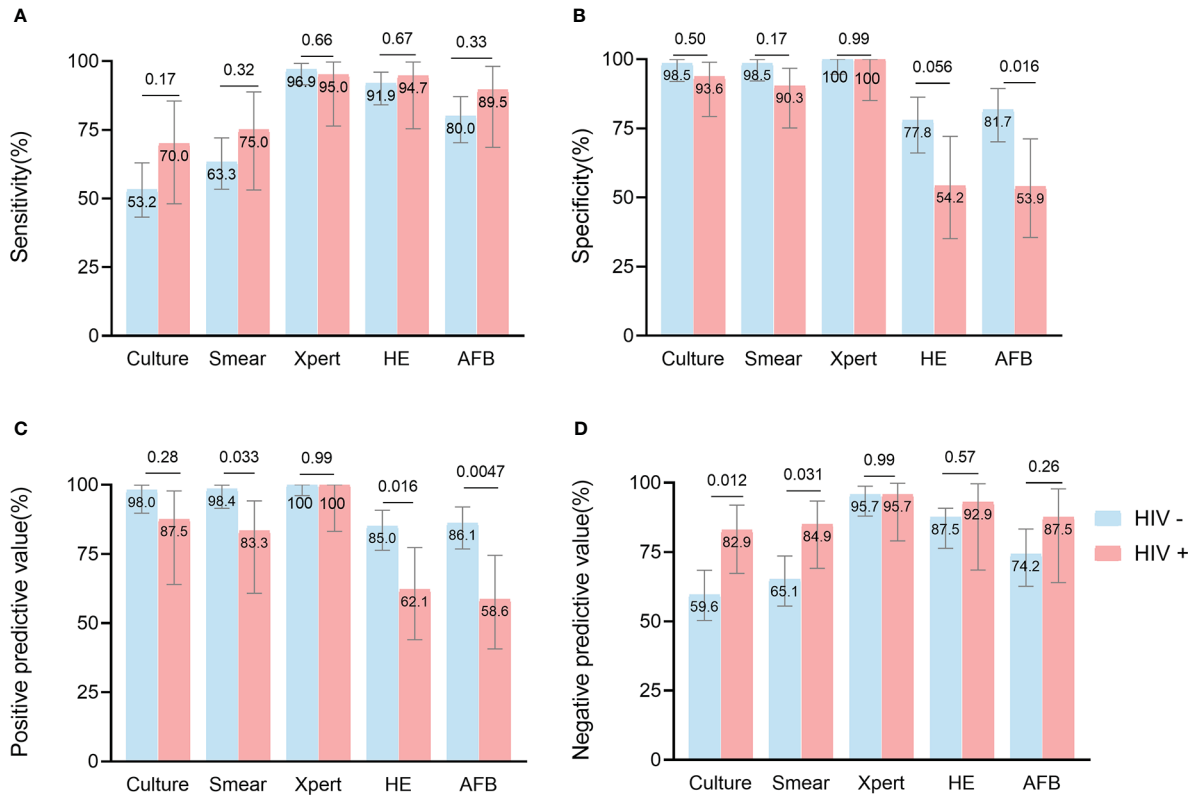

FIGURE 3
Head-to-head comparison of test accuracy in biopsy samples, by HIV status. Data are shown stratified according to: **(A)** sensitivity, **(B)** specificity, **(C)** positive predictive value, **(D)** negative predictive value.

TABLE 3 The diagnostic accuracy of culture, smear, Xpert, PCR, and TSPOT in non-biopsy samples.

Test and (*p*)	Sensitivity	Specificity	PPV	NPV
Culture	6/17 (35.3; 17.3-58.7)	22/22 (100; 85.1-100)	6/6 (100; 61.0-100)	22/33 (66.7; 49.6-80.3)
Xpert	3/5 (60.0; 23.1-92.9)	9/9 (100; 70.1-100)	3/3 (100; 43.9-100)	9/11 (81.8; 52.3-96.8)
Xpert vs Culture (*p*)	0.32	> 0.99	> 0.99	0.34
TSPOT	10/11 (90.9; 62.3-99.5)	7/11 (63.6; 35.4-84.8)	10/14 (71.4; 45.4-88.3)	7/8 (87.5; 52.9-99.4)
TSPOT vs Culture (*p*)	**0.0037**	**0.0026**	0.14	0.25

Shown are the numbers of positive results, n/N and % with 95% CI in parentheses, with p-values where appropriate. NPV, negative predictive value; PPV, positive predictive value. Bold means the P value is less than 0.05, with a statistical difference.

the diagnostic accuracy, sensitivity, and specificity of the assays. Our key finding was that Xpert performed better than other laboratory assays regardless of the HIV status of the patients or the types of specimens. Overall, the biopsy samples provided more realistic pictures of the patient's conditions and a more accurate diagnosis of EPTB than non-biopsy samples.

From the demographic aspects, several studies have reported similar findings that HIV co-infection and age (> 65 years old) contribute to EPTB infection (Lakoh et al., 2020; Winter et al., 2020; Barreto-Duarte et al., 2021), consistent with our results. However, we found that males were more likely to have EPTB than females (OR 1.89, 95%CI 1.10-3.29, p = 0.021), which was not consistent with some previous studies (Peto et al., 2009; Pang et al., 2019). This may be attributed to a higher proportion of HIV-positive men than women (34.8% vs 10.8%, p < 0.0001; Supplementary Table S3), although the relationship between gender and EPTB is controversial in current studies (Liu et al., 2020; Barreto-Duarte et al., 2021).

Culture is the gold standard for TB diagnosis, but culture cannot distinguish between MTB, BCG, and NTM, and its specificity is compromised (96.9% [91.3-99.2] in this study) when used in populations susceptible to NTM disease (e.g. HIV-positive patients) (Álvaro-Meca et al., 2015). Unexpectedly, the sensitivity (%65.3 [56.3-73.2] vs 56.1% [47.0-64.9], p = 0.16) of the smear was slightly higher than that of the culture. Compared to direct smears, centrifugally concentrated specimens can increase the sensitivity of the smear by 10-30%(Perera and Arachchi, 1999; Peterson et al., 1999), and the Auramine O staining used in this study had a higher sensitivity (66-85.9% vs 30-60%) than Ziehl-Neelsen staining (Marais et al., 2008;

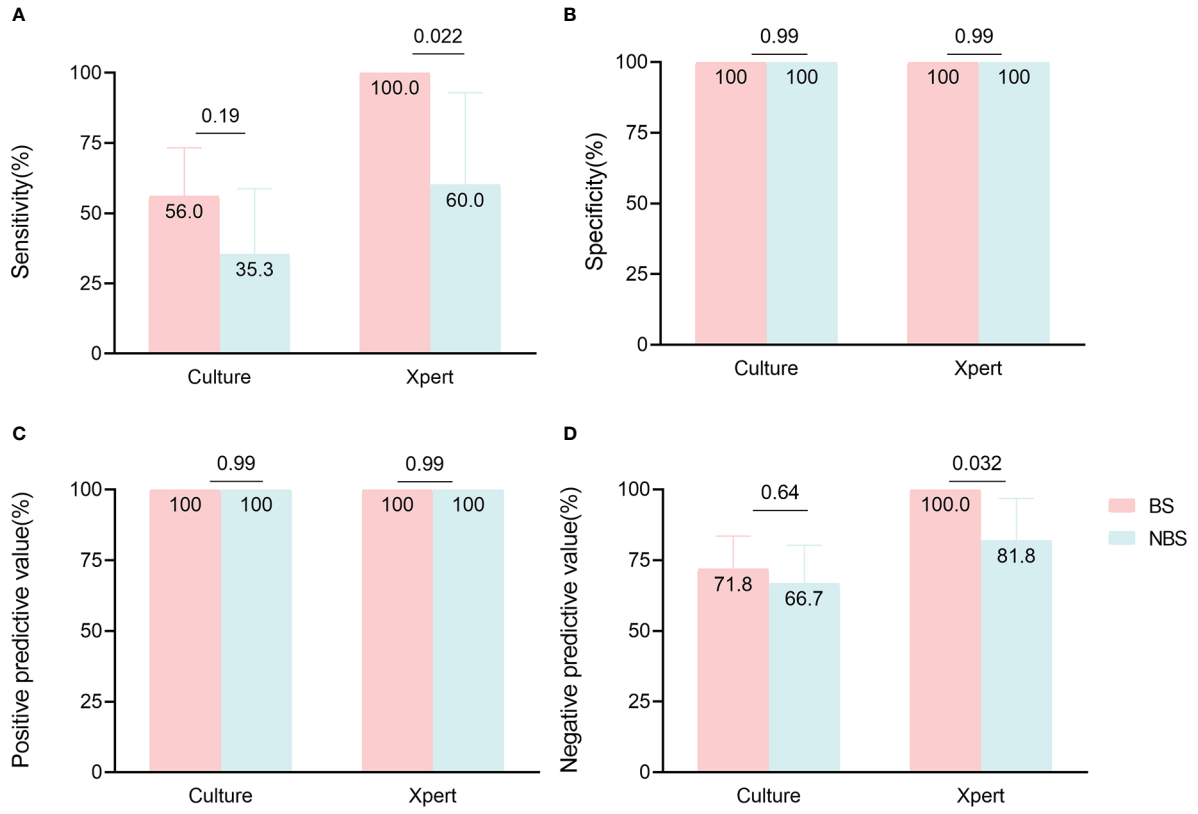

FIGURE 4
Comparison of culture and Xpert accuracy in paired biopsy samples (BS) and non-biopsy samples (NBS). Data are shown stratified according to **(A)** sensitivity, **(B)** specificity, **(C)** positive predictive value, **(D)** negative predictive value.

TABLE 4 Culture, Xpert, HE, and AFB diagnostic accuracy in smear-negative biopsy samples.

Test and (*p*)	Sensitivity	Specificity	PPV	NPV
Culture	18/40 (45.0; 30.7-60.2)	93/93 (100; 96.0-100)	18/18 (100; 82.4-100)	93/115 (80.9; 72.7-87.0)
Xpert	38/41 (92.7; 80.6-97.5)	85/85 (100; 95.7-100)	38/38 (100; 90.8-100)	85/88 (96.6; 90.5-99.1)
Xpert vs Culture (*p*)	**< 0.0001**	> 0.99	> 0.99	**0.0007**
HE	32/37 (86.5; 72.0-94.1)	62/84 (73.8; 63.5-82.0)	32/54 (59.3; 46.0-71.3)	62/67 (92.5; 83.7-96.8)
HE vs Culture (*p*)	**0.0001**	**< 0.0001**	**0.0012**	**0.033**
AFB	22/37 (59.5; 43.5-73.7)	63/83 (75.9; 65.7-83.8)	22/42 (52.4; 37.7-66.6)	63/78 (80.8; 70.7-88.0)
AFB vs Culture (*p*)	**0.20**	**< 0.0001**	**0.0003**	0.98

Shown are the numbers of positive results, n/N and % with 95% CI in parentheses, with p-values where appropriate. NPV, negative predictive value; PPV, positive predictive value.
Bold means the P value is less than 0.05, with a statistical difference.

Laifangbam et al., 2009; Hooja et al., 2011; Runa et al., 2011; Assefa et al., 2021; Gulati et al., 2021), but the NaOH used to digest the specimens may have reduced the viability of mycobacteria or even killed mycobacteria (Mtafya et al., 2019; Stephenson et al., 2021). Auramine O staining is not able to distinguish between dead or live bacteria, but culture only detects viable bacteria, thus NaOH used in sample pre-treatment may result in lower sensitivity of culture than smear. Obtaining appropriate specimens for histological examinations was recommended for a patient with suspected EPTB (Hopewell et al., 2006; Migliori et al., 2018). In general, histopathology is highly sensitive (86%-95% reported; HE: 92.4% [85.7-96.1] and AFB: 81.7% [73.2-88.0] in this study), but not very specific (64%-92% reported; HE: 71.3% [61.0-79.7] and AFB: 73.3% [63.1-81.5] in this study), for the diagnosis of tuberculosis (Bennani et al., 2019; Shen et al., 2022; Tahseen et al., 2022).

Xpert was recommended by the World Health Organization as a rapid initial diagnostic test for tuberculosis (WHO, 2021b). For the diagnosis of EPTB, Xpert showed different performance in various types of samples (Scott et al., 2014; Kohli et al., 2021), with excellent performance in lymph node tissue and aspirates (sensitivity: 80-100%; specificity:90-100%) (Ablanedo-Terrazas et al., 2014; Scott et al., 2014; Tadesse et al., 2019), as demonstrated in this study (sensitivity: 96.6%[91.6-98.7]; specificity:100%[95.8-100]). HIV-positive patients are more likely to have comorbidities such as tumors (Lerner et al., 2020), and opportunistic infections (fungal infections, NTM infections, etc.) (Limper et al., 2017), and this may affect the specificity of detection of MTB (decreased specificity in this study: culture 5%; smear 8%; HE 23%; AFB 27%). However, Xpert maintained high sensitivity (>95%) and specificity (nearly 100%) in both HIV-positive and -negative patients, consistent with previous reports (sensitivity: >80%; specificity: 97-99%) (Horne et al., 2019; Tomaz et al., 2021). Finally, we evaluated the performance of different assays in smear-negative samples, and Xpert still had higher sensitivity (92.7% [80.6-97.5]) and specificity (100% [95.7-100]) compared to culture. This was slightly higher than the reported sensitivity (70-85%) (Bankar et al., 2018; Rakotoarivelo et al., 2018; Horne et al., 2019), perhaps due to the different choice of the reference standard (culture and Xpert were used in this study).

We found little statistical difference in the sensitivity, specificity, and predictive values of the non-biopsy samples-based Xpert compared to culture, mainly due to the small sample size. However, in agreement with previous studies, TSPOT showed a high sensitivity (70-100%) compared to culture and Xpert (Zhou et al., 2015; Li et al., 2020), predicting that TSPOT can be used as a powerful screening method for EPTB (Antel et al., 2020). Furthermore, the culture and Xpert performed better with biopsy samples than with non-biopsy samples, suggesting that biopsy is important for the accurate diagnosis of EPTB.

There are several limitations to this study. The smaller sample size of non-biopsy samples may affect the methodological comparison between non-biopsy samples and biopsy samples. The small number of samples assayed by various methods in non-biopsy samples was not conducive to evaluating the diagnostic accuracy of the method, for instance, the sensitivity of Xpert may be underestimated. In addition, we did not exclude patients with both pulmonary and extrapulmonary TB (42 cases), which may affect the comparison of assays between biopsy and non-biopsy samples.

In summary, our study compared the diagnostic accuracy of commonly used EPTB diagnostic methods across HIV status and sample types, highlighting the superiority of Xpert in different clinical settings and the critical contribution of biopsy samples in the diagnosis of EPTB. Further clinical studies evaluating the performance of the different laboratory assays in extrapulmonary samples and HIV populations are warranted to help clinicians choose the best diagnostic methods when faced with various dilemmas.

Data availability statement

The original contributions presented in the study are included in the article/Supplementary Material. Further inquiries can be directed to the corresponding authors.

Ethics statement

The studies involving human participants were reviewed and approved by Ethics Committee of Shanghai Public Health Clinical Center (2019-S030-02). Written informed consent to participate in this study was provided by the participants' legal guardian/next of kin.

Author contributions

Project concept conceived (X-YF and HZ), experiments performed (J-CX and W-FG), sampling (XM and XS), data analysis (J-CX, XM, W-FG, X-YF, and HZ), and paper writing (J-CX and X-YF). All authors contributed to the article and approved the submitted version.

Funding

This study was supported by the National Key Research and Development Program of China (2022YFC2302900, 2021YFC2301503), National Natural and Science Foundation of China (82171815, 82171739), Shanghai Municipal Health Bureau (2022XD060) and Shanghai Science and Technology Commission (20Y11903400, 18411970800).

Acknowledgments

We are thankful to Dr. Douglas B. Lowrie for his critical reading and improvement on this work.

Conflict of interest

The authors declare that the research was conducted in the absence of any commercial or financial relationships that could be construed as a potential conflict of interest.

Publisher's note

Supplementary material

The Supplementary Material for this article can be found online at: https://www.frontiersin.org/articles/10.3389/fcimb.2023.1154939/full#supplementary-material

References

Ablanedo-Terrazas, Y., Alvarado-de la Barrera, C., Hernández-Juan, R., Ruiz-Cruz, M., and Reyes-Terán, G. (2014). Xpert MTB/RIF for diagnosis of tuberculous cervical lymphadenitis in HIV-infected patients. *Laryngoscope* 124 (6), 1382–1385. doi: 10.1002/lary.24478

Aisenberg, G. M., Jacobson, K., Chemaly, R. F., Rolston, K. V., Raad, I. I., and Safdar, A. (2005). Extrapulmonary tuberculosis active infection misdiagnosed as cancer: Mycobacterium tuberculosis disease in patients at a comprehensive cancer center, (2001-2005). *Cancer* 104 (12), 2882–2887. doi: 10.1002/cncr.21541

Álvaro-Meca, A., Rodríguez-Gijón, L., Díaz, A., Gil, Á., and Resino, S. (2015). Trends in nontuberculous mycobacterial disease in hospitalized subjects in Spain, (1997-2010) according to HIV infection. *HIV Med.* 16 (8), 485–493. doi: 10.1111/hiv.12251

Antel, K., Oosthuizen, J., Malherbe, F., Louw, V. J., Nicol, M. P., Maartens, G., et al. (2020). Diagnostic accuracy of the xpert MTB/Rif ultra for tuberculosis adenitis. *BMC Infect. Dis.* 20 (1), 33. doi: 10.1186/s12879-019-4749-x

Assefa, G., Desta, K., Araya, S., Girma, S., Mihret, A., Hailu, T., et al. (2021). Diagnostic efficacy of light-emitting diode (LED) fluorescence based microscope for the diagnosis of tuberculous lymphadenitis. *PloS One* 16 (7), e0255146. doi: 10.1371/journal.pone.0255146

Bankar, S., Set, R., Sharma, D., Shah, D., and Shastri, J. (2018). Diagnostic accuracy of xpert MTB/RIF assay in extrapulmonary tuberculosis. *Indian J. Med. Microbiol.* 36 (3), 357–363. doi: 10.4103/ijmm.IJMM_18_173

Banta, J. E., Ani, C., Bvute, K. M., Lloren, J. I. C., and Darnell, T. A. (2020). Pulmonary vs. extra-pulmonary tuberculosis hospitalizations in the US [1998-2014]. *J. Infect. Public Health* 13 (1), 131–139. doi: 10.1016/j.jiph.2019.07.001

Barreto-Duarte, B., Araújo-Pereira, M., Nogueira, B. M. F., Sobral, L., Rodrigues, M. M. S., Queiroz, A. T. L., et al. (2021). Tuberculosis burden and determinants of treatment outcomes according to age in Brazil: A nationwide study of 896,314 cases reported between 2010 and 2019. *Front. Med.* 8. doi: 10.3389/fmed.2021.706689

Bennani, K., Khattabi, A., Akrim, M., Mahtar, M., Benmansour, N., Essakalli Hossyni, L., et al. (2019). Evaluation of the yield of histopathology in the diagnosis of lymph node tuberculosis in Morocco 2017: Cross-sectional study. *JMIR Public Health Surveill* 5 (4), e14252. doi: 10.2196/14252

Golden, M. P., and Vikram, H. R. (2005). Extrapulmonary tuberculosis: An overview. *Am. Fam Physician* 72 (9), 1761–1768.

Gulati, H. K., Mawlong, M., Agarwal, A., and Ranee, K. R. (2021). Comparative evaluation of clinical, cytological and microbiological profile in abdominal vs. cervical lymph nodal tuberculosis with special emphasis on utility of auramine-O staining. *J. Cytol* 38 (4), 191–197. doi: 10.4103/joc.Joc_61_20

Hooja, S., Pal, N., Malhotra, B., Goyal, S., Kumar, V., and Vyas, L. (2011). Comparison of ziehl neelsen & auramine O staining methods on direct and concentrated smears in clinical specimens. *Indian J. Tuberc* 58 (2), 72–76.

Hopewell, P. C., Pai, M., Maher, D., Uplekar, M., and Raviglione, M. C. (2006). International standards for tuberculosis care. *Lancet Infect. Dis.* 6 (11), 710–725. doi: 10.1016/s1473-3099(06)70628-4

Horne, D. J., Kohli, M., Zifodya, J. S., Schiller, I., Dendukuri, N., Tollefson, D., et al. (2019). Xpert MTB/RIF and xpert MTB/RIF ultra for pulmonary tuberculosis and rifampicin resistance in adults. *Cochrane Database Syst. Rev.* 6 (6), Cd009593. doi: 10.1002/14651858.CD009593.pub4

Jain, A. (2011). Extra pulmonary tuberculosis: a diagnostic dilemma. *Indian J. Clin. Biochem.* 26 (3), 269–273. doi: 10.1007/s12291-010-0104-0

Kohli, M., Schiller, I., Dendukuri, N., Yao, M., Dheda, K., Denkinger, C. M., et al. (2021). Xpert MTB/RIF ultra and xpert MTB/RIF assays for extrapulmonary tuberculosis and rifampicin resistance in adults. *Cochrane Database Syst. Rev.* 1 (1), Cd012768. doi: 10.1002/14651858.CD012768.pub3

Laifangbam, S., Singh, H. L., Singh, N. B., Devi, K. M., and Singh, N. T. (2009). A comparative study of fluorescent microscopy with ziehl-neelsen staining and culture for the diagnosis of pulmonary tuberculosis. *Kathmandu Univ Med. J.* 7 (27), 226–230. doi: 10.3126/kumj.v7i3.2728

Lakoh, S., Jiba, D. F., Adekanmbi, O., Poveda, E., Sahr, F., Deen, G. F., et al. (2020). Diagnosis and treatment outcomes of adult tuberculosis in an urban setting with high HIV prevalence in Sierra Leone: A retrospective study. *Int. J. Infect. Dis.* 96, 112–118. doi: 10.1016/j.ijid.2020.04.038

Lerner, A. M., Eisinger, R. W., and Fauci, A. S. (2020). Comorbidities in persons with HIV: The lingering challenge. *Jama* 323 (1), 19–20. doi: 10.1001/jama.2019.19775

Li, S., Lin, L., Zhang, F., Zhao, C., Meng, H., and Wang, H. (2020). A retrospective study on xpert MTB/RIF for detection of tuberculosis in a teaching hospital in China. *BMC Infect. Dis.* 20 (1), 362. doi: 10.1186/s12879-020-05004-8

Li, T., Yan, X., Du, X., Huang, F., Wang, N., Ni, N., et al. (2022). Extrapulmonary tuberculosis in China: A national survey. *Int. J. Infect. Dis.* 128, 69–77. doi: 10.1016/j.ijid.2022.12.005

Limper, A. H., Adenis, A., Le, T., and Harrison, T. S. (2017). Fungal infections in HIV/AIDS. *Lancet Infect. Dis.* 17 (11), e334–e343. doi: 10.1016/s1473-3099(17)30303-1

Liu, Y., Jiang, Z., Chen, H., Jing, H., Cao, X., Coia, J. E., et al. (2020). Description of demographic and clinical characteristics of extrapulmonary tuberculosis in Shandong, China. *Hippokratia* 24 (1), 27–32.

Marais, B. J., Brittle, W., Painczyk, K., Hesseling, A. C., Beyers, N., Wasserman, E., et al. (2008). Use of light-emitting diode fluorescence microscopy to detect acid-fast bacilli in sputum. *Clin. Infect. Dis.* 47 (2), 203–207. doi: 10.1086/589248

Migliori, G. B., Sotgiu, G., Rosales-Klintz, S., Centis, R., D'Ambrosio, L., Abubakar, I., et al. (2018). ERS/ECDC statement: European union standards for tuberculosis care 2017 update. *Eur. Respir. J.* 51 (5), 1702678. doi: 10.1183/13993003.02678-2017

Mtafya, B., Sabiiti, W., Sabi, I., John, J., Sichone, E., Ntinginya, N. E., et al. (2019). Molecular bacterial load assay concurs with culture on NaOH-induced loss of mycobacterium tuberculosis viability. *J. Clin. Microbiol.* 57 (7), e01992-18. doi: 10.1128/jcm.01992-18

Norbis, L., Alagna, R., Tortoli, E., Codecasa, L. R., Migliori, G. B., and Cirillo, D. M. (2014). Challenges and perspectives in the diagnosis of extrapulmonary tuberculosis. *Expert Rev. Anti Infect. Ther.* 12 (5), 633–647. doi: 10.1586/14787210.2014.899900

Ohene, S. A., Bakker, M. I., Ojo, J., Toonstra, A., Awudi, D., and Klatser, P. (2019). Extra-pulmonary tuberculosis: A retrospective study of patients in Accra, Ghana. *PloS One* 14 (1), e0209650. doi: 10.1371/journal.pone.0209650

Pang, Y., An, J., Shu, W., Huo, F., Chu, N., Gao, M., et al. (2019). Epidemiology of extrapulmonary tuberculosis among inpatients, China 2008-2017. *Emerg. Infect. Dis.* 25 (3), 457–464. doi: 10.3201/eid2503.180572

Park, M., and Kon, O. M. (2021). Use of xpert MTB/RIF and xpert ultra in extrapulmonary tuberculosis. *Expert Rev. Anti Infect. Ther.* 19 (1), 65–77. doi: 10.1080/14787210.2020.1810565

Perera, J., and Arachchi, D. M. (1999). The optimum relative centrifugal force and centrifugation time for improved sensitivity of smear and culture for detection of mycobacterium tuberculosis from sputum. *Trans. R Soc. Trop. Med. Hyg* 93 (4), 405–409. doi: 10.1016/s0035-9203(99)90135-9

Peterson, E. M., Nakasone, A., Platon-DeLeon, J. M., Jang, Y., de la Maza, L. M., and Desmond, E. (1999). Comparison of direct and concentrated acid-fast smears to identify specimens culture positive for mycobacterium spp. *J. Clin. Microbiol.* 37 (11), 3564–3568. doi: 10.1128/jcm.37.11.3564-3568.1999

Peto, H. M., Pratt, R. H., Harrington, T. A., LoBue, P. A., and Armstrong, L. R. (2009). Epidemiology of extrapulmonary tuberculosis in the united states 1993-2006. *Clin. Infect. Dis.* 49 (9), 1350–1357. doi: 10.1086/605559

Rakotoarivelo, R., Ambrosioni, J., Rasolofo, V., Raberahona, M., Rakotosamimanana, N., Andrianasolo, R., et al. (2018). Evaluation of the xpert MTB/RIF assay for the diagnosis of smear-negative pulmonary and extrapulmonary tuberculosis in Madagascar. *Int. J. Infect. Dis.* 69, 20–25. doi: 10.1016/j.ijid.2018.01.017

Rickman, T. W., and Moyer, N. P. (1980). Increased sensitivity of acid-fast smears. *J. Clin. Microbiol.* 11 (6), 618–620. doi: 10.1128/jcm.11.6.618-620.1980

Runa, F., Yasmin, M., Hoq, M. M., Begum, J., Rahman, A. S., and Ahsan, C. R. (2011). Molecular versus conventional methods: Clinical evaluation of different methods for the diagnosis of tuberculosis in Bangladesh. *J. Microbiol. Immunol. Infect.* 44 (2), 101–105. doi: 10.1016/j.jmii.2010.05.001

Scott, L. E., Beylis, N., Nicol, M., Nkuna, G., Molapo, S., Berrie, L., et al. (2014). Diagnostic accuracy of xpert MTB/RIF for extrapulmonary tuberculosis specimens: establishing a laboratory testing algorithm for south Africa. *J. Clin. Microbiol.* 52 (6), 1818–1823. doi: 10.1128/jcm.03553-13

Shen, Y., Fang, L., Ye, B., Xu, X., Yu, G., and Zhou, L. (2022). The role of core needle biopsy pathology combined with molecular tests in the diagnosis of lymph node tuberculosis. *Infect. Drug Resist.* 15, 335–345. doi: 10.2147/idr.S350570

Shivakoti, R., Sharma, D., Mamoon, G., and Pham, K. (2017). Association of HIV infection with extrapulmonary tuberculosis: A systematic review. *Infection* 45 (1), 11–21. doi: 10.1007/s15010-016-0960-5

Stephenson, D., Perry, A., Nelson, A., Robb, A. E., Thomas, M. F., Bourke, S. J., et al. (2021). Decontamination strategies used for AFB culture significantly reduce the viability of mycobacterium abscessus complex in sputum samples from patients with cystic fibrosis. *Microorganisms* 9 (8), 1597. doi: 10.3390/microorganisms9081597

Tadesse, M., Abebe, G., Bekele, A., Bezabih, M., Yilma, D., Apers, L., et al. (2019). Xpert MTB/RIF assay for the diagnosis of extrapulmonary tuberculosis: a diagnostic evaluation study. *Clin. Microbiol. Infect.* 25 (8), 1000–1005. doi: 10.1016/j.cmi.2018.12.018

Tahseen, S., Ambreen, A., Ishtiaq, S., Khanzada, F. M., Safdar, N., Sviland, L., et al. (2022). The value of histological examination in the diagnosis of tuberculous lymphadenitis in the era of rapid molecular diagnosis. *Sci. Rep.* 12 (1), 8949. doi: 10.1038/s41598-022-12660-0

Tomaz, A. P. O., Raboni, S. M., Kussen, G. M. B., da Silva Nogueira, K., Lopes Ribeiro, C. E., and Costa, L. M. D. (2021). The xpert® MTB/RIF diagnostic test for pulmonary and extrapulmonary tuberculosis in immunocompetent and immunocompromised patients: Benefits and experiences over 2 years in different clinical contexts. *PloS One* 16 (3), e0247185. doi: 10.1371/journal.pone.0247185

Winter, J. R., Smith, C. J., Davidson, J. A., Lalor, M. K., Delpech, V., Abubakar, I., et al. (2020). The impact of HIV infection on tuberculosis transmission in a country with low tuberculosis incidence: a national retrospective study using molecular epidemiology. *BMC Med.* 18 (1), 385. doi: 10.1186/s12916-020-01849-7

WHO (2020). *Global tuberculosis report 2020*. Geneva, Switzerland. Available at: http://www.who.int/tb/publications/global_report/en/

WHO. (2021a). *WHO consolidated guidelines on tuberculosis. Module 2: Screening - systematic screening for tuberculosis disease*. Geneva, Switzerland. Available at: https://www.who.int/publications/i/item/9789240022614

WHO (2021b). *WHO consolidated guidelines on tuberculosis: module 3: diagnosis: rapid diagnostics for tuberculosis detection*. Geneva, Switzerland. Available at: https://www.who.int/publications/i/item/9789240029415

WHO (2022). *Global tuberculosis report 2022*. Geneva, Switzerland. Available at: http://www.who.int/tb/publications/global_report/en/

Xiang, Y., Huang, C., He, Y., and Zhang, Q. (2021). Cancer or tuberculosis: A comprehensive review of the clinical and imaging features in diagnosis of the confusing mass. *Front. Oncol.* 11. doi: 10.3389/fonc.2021.644150

Zhou, X. X., Liu, Y. L., Zhai, K., Shi, H. Z., and Tong, Z. H. (2015). Body fluid interferon-γ release assay for diagnosis of extrapulmonary tuberculosis in adults: A systematic review and meta-analysis. *Sci. Rep.* 5, 15284. doi: 10.1038/srep15284

frontiers | Frontiers in Cellular and Infection Microbiology

TYPE Original Research
PUBLISHED 24 March 2023
DOI 10.3389/fcimb.2023.1150632

OPEN ACCESS

EDITED BY
Amit Singh,
Central University of Punjab, India

REVIEWED BY
Changwu Wu,
Leipzig University, Germany
Liyan Mao,
Huazhong University of Science and Technology, China
Anand Kumar Maurya,
All India Institute of Medical Sciences, Bhopal, India

*CORRESPONDENCE
Qile Gao
gaoql@csu.edu.cn

SPECIALTY SECTION
This article was submitted to Clinical Microbiology, a section of the journal Frontiers in Cellular and Infection Microbiology

RECEIVED 24 January 2023
ACCEPTED 14 March 2023
PUBLISHED 24 March 2023

CITATION
Hu X, Zhang G, Zhang H, Tang M, Liu S, Tang B, Xu D, Zhang C and Gao Q (2023) A predictive model for early clinical diagnosis of spinal tuberculosis based on conventional laboratory indices: A multicenter real-world study. *Front. Cell. Infect. Microbiol.* 13:1150632. doi: 10.3389/fcimb.2023.1150632

A predictive model for early clinical diagnosis of spinal tuberculosis based on conventional laboratory indices: A multicenter real-world study

Xiaojiang Hu[1,2], Guang Zhang[1,2], Hongqi Zhang[1,2], Mingxing Tang[1,2], Shaohua Liu[1,2], Bo Tang[1,2], Dongcheng Xu[1,2], Chengran Zhang[1,2] and Qile Gao[1,2]*

[1]Department of Spine Surgery and Orthopaedics, Xiangya Hospital, Central South University, Changsha, China, [2]National Clinical Research Center for Geriatric Disorders, Xiangya Hospital, Central South University, Changsha, China

Background: Early diagnosis of spinal tuberculosis (STB) remains challenging. The aim of this study was to develop a predictive model for the early diagnosis of STB based on conventional laboratory indicators.

Method: The clinical data of patients with suspected STB in four hospitals were included, and variables were screened by Lasso regression. Eighty-five percent of the cases in the dataset were randomly selected as the training set, and the other 15% were selected as the validation set. The diagnostic prediction model was established by logistic regression in the training set, and the nomogram was drawn. The diagnostic performance of the model was verified in the validation set.

Result: A total of 206 patients were included in the study, including 105 patients with STB and 101 patients with NSTB. Twelve variables were screened by Lasso regression and modeled by logistic regression, and seven variables (TB.antibody, IGRAs, RBC, Mono%, RDW, AST, BUN) were finally included in the model. AUC of 0.9468 and 0.9188 in the training and validation cohort, respectively.

Conclusion: In this study, we developed a prediction model for the early diagnosis of STB which consisted of seven routine laboratory indicators.

KEYWORDS

spinal tuberculosis, early diagnosis, nomogram, predictive model, conventional laboratory indices

1 Introduction

Tuberculosis (TB) is a chronic infectious disease caused by infection with Mycobacterium tuberculosis, and it is the oldest infectious disease that has been identified in humans (Scorrano et al., 2022). According to the latest Global TB Report published by the World Health Organization in 2021, in 2020, an estimated 10 million people worldwide had tuberculosis. This included 5.6 million men, 3.3 million women, and 1.1 million children. In 2020, an estimated 1.5 million people died from TB, making it the second highest infectious disease killer after novel coronavirus pneumonia (World Health Organization, 2021).

Spinal tuberculosis (STB) is an extrapulmonary manifestation of tuberculosis that occurs as a secondary infection caused by Mycobacterium tuberculosis in the spinal vertebrae and adnexal tissues. STB accounts for approximately 2% of all tuberculosis cases and 50% of all osteoarticular tuberculosis cases. Worldwide, the annual incidence of spinal tuberculosis exceeds 100,000 (Khanna and Sabharwal, 2019a). STB can cause bone destruction, collapse, and fracture of the vertebral body, which can compress the spinal cord and cause paraplegia in approximately 10%-30% of affected patients (Hristea et al., 2008). The devastating and disabling effects of STB cannot be ignored, and early diagnosis of STB is essential to reduce the incidence of postoperative complications in patients. The gold standard for the diagnosis of spinal tuberculosis involves invasive tests such as surgical needle biopsy puncture to obtain a specimen of the lesion; diagnosis is then determined by using techniques such as Mycobacterium tuberculosis culture and Xpert, but this often occurs late in the patient's hospitalization (Held et al., 2014; Beltran et al., 2022). If the patient receives an accurate diagnosis early in the course of the disease, the spine surgeon can recommend early treatment with anti-tuberculosis drugs, thereby improving the patient's prognosis (Li et al., 2020).

However, early diagnosis in patients with spinal tuberculosis has been difficult, and cases are frequently missed or misdiagnosed (Mann et al., 2021). Patients with spinal tuberculosis typically lack early clinical symptoms; it is also difficult to distinguish STB from diseases such as septic spondylitis and spinal tumors, which have similar imaging manifestations as spinal tuberculosis, including bone destruction (Liu et al., 2021; Rule et al., 2021). Moreover, routine laboratory tests of inflammatory markers such as blood sedimentation, white blood cell count, and C-reactive protein are not specific for the diagnosis of tuberculosis, and these markers are also elevated in septic spondylitis (Liu et al., 2022). Interferon gamma release assays (IGRAs) have shown better diagnostic efficacy, as confirmed by our previously published study (Hu et al., 2022). However, we also observed that IGRAs alone do not meet the clinical need for diagnostic accuracy in spinal tuberculosis. Additionally, IGRAs cannot distinguish between active and latent tuberculosis and show no correlation with the duration of disease, limiting its use in the diagnosis of spinal tuberculosis (Hamada et al., 2021).

In our present study, we collected routine laboratory serology upon admission of patients with spinal tuberculosis, screened variables by lasso regression, built a model by logistic regression, and drew a nomogram for the early diagnosis of spinal tuberculosis based on a model used for patients in a multicenter retrospective study.

2 Method

2.1 Inclusion and exclusion criteria, and diagnosis criteria

This study included 206 patients with suspected spinal tuberculosis who were admitted to the Xiangya Hospital of Central South University, Xiangya Boai Hospital, Changsha First Hospital, and Hunan Chest Hospital from January 2016 to October 2022. The data of the included patients were taken from the first routine serological examination at the time of patient admission for treatment. The inclusion criteria were as follows: 1. CT and MRI reports of patients included in the study showed that patients had suspected spinal tuberculosis, including irregular lytic lesions or bone destruction that affect the vertebral body, endplate, or adjacent margin of the intervertebral disc, featuring fragmentary destruction, osteolytic destruction, and local destruction with sclerotic margins. Intervertebral disc destruction or decreased disc height, calcification or bone fragment formation accompanied by abscesses, vertebral collapse or posterior convex deformity, as well as soft tissue involvement and large paravertebral abscesses (Khanna and Sabharwal, 2019b); 2. Patients had complete clinical examination data. The exclusion criteria were as follows: 1. concomitant autoimmune diseases or HIV; 2. infections in multiple sites; and 3. patients with severe systemic chronic underlying diseases.

Patients included in this study were diagnosed with spinal tuberculosis if they met one of the following criteria (Pai et al., 2016): 1. positive culture for Mycobacterium tuberculosis from surgical needle biopsy; 2. positive molecular tests for Mycobacterium tuberculosis (including Xpert and mNGS); 3. relevant pathologic histologic features (at least one of the following features: caseous necrosis, positive acid-fast staining, and granulomatous inflammation) Meanwhile, anti-tuberculosis treatment of patients is effective.

Patients were classified into the NSTB group based on the following criteria: 1. microbiological evidence that the infection was caused by other bacteria, fungi or viruses; 2. pathological histological diagnosis of other lesions of the spine (including septicemia and tumors).

Ethical Approval: Institutional Review Board approval was obtained (IRB#: 201303232). This study was approved by the Ethics Committee of Xiangya Hospital Central South University, and written informed consent was obtained from all patients.

2.2 Routine laboratory test data collection

We collected the following routine laboratory test data at the time of admission for the study population: tubercle bacillus antibody (TB.antibody), interferon-γ release assays (IGRAs), white blood cell

(WBC), red blood cell (RBC), hemoglobin (HGB), platelet (PLT), neutrophil (Neut), lymphocyte (lymph), eosinophil (EO), basophil (BASO), monocyte (Mono), neutrophil % (Neut%), lymphocyte % (Lymph%), basophil % (BASO%), eosinophil% (Eo%), monocyte % (Mono%), red blood cell distribution width (RDW), platelet volume (PCT), mean platelet volume (MPV), total protein (TP), albumin (A), globulin (G), albumin/globulin (AG), alanine aminotransferase (ALT), aspartate aminotransferase (AST), blood urea nitrogen (BUN), creatinine (Cr), triglyceride (TG), cholesterol (Chol), high-density lipoprotein (HDL), low-density lipoprotein (LDL), glucose (BS), prothrombin time (PT), activated partial thromboplatin time (APTT), international normalized ratio (INR), D dimer (DD), erythrocyte sedimentation rate (ESR), C-reactive protein (CRP).

2.3 Statistical analysis

All statistical analyses and graphing were based on R version 4.2.2. The "CBCgrps" (Zhang et al., 2017) package was used to draw baseline tables in which categorical variables were analyzed for differences in distribution between the two groups using chi-square tests (or Fisher's exact probability method). Continuous data that conformed to a normal distribution are described as the mean (± standard deviation) and analyzed for differences between two groups using t tests, and data that did not conform to a normal distribution are described as the median (percentile), and differences between the two groups were analyzed using rank sum tests. The data that did not conform to the normal distribution are described as the median (percentile), and the differences between the two groups were analyzed using the rank sum test. The results of the comparison between the groups are expressed using p values. Heatmaps of correlations between variables were calculated and plotted using the "corrplot" package. The selection of variables was based on Lasso regression, and the continuous variables entered into the Lasso regression were standardized using the min-max transformation method. Lasso regression was performed by the "glmnet" package (nfolds were set to 20). The number of variables within one standard error was selected as the optimal number of variables. Eighty-five percent of the cases were randomly selected as the training set, and the rest of the cases were included in the validation set for the internal validation of the model. The "Rms" package was used to build the logistic regression model. The variables included in the logistic regression were selected based on the Lasso regression screening results, and variables lacking significance in the logistic model were excluded to refine the model. The calibration curves of the prediction model were plotted by the "caret" package. The column line plots were plotted using the "regplot" package, and the ROC curves were calculated and plotted using the "pROC" and "ggplot2" packages.

3 Result

3.1 Characteristics of the patient

A total of 206 patients with suspected spinal tuberculosis were enrolled according to the inclusion and exclusion criteria established for the study. We diagnosed 105 cases as spinal tuberculosis and 101 cases as non-STB according to the diagnostic criteria. The characteristics of the patients, routine laboratory data, and the results of statistical comparisons of these indicators between the STB and NSTB groups are presented in Table 1. There were no significant differences between the two groups in terms of age and sex. Detailed information on the underlying diseases included in the patients' medical history is provided in Table 2. The NSTB group comprised 45 cases of pyogenic spinal infection, 20 cases of spinal brucellosis, 12 cases of spinal tumors, 18 cases of other non-specific infections, 4 cases of spinal fungal infections, and 2 cases of spinal viral infections (Supplementary Figure 1).

3.2 The performance of individual indicators in conventional laboratory tests for discriminating between STB and NSTB

The results of the univariate analyses for STB patients and NSTB patients are presented in Table 1. We observed significant differences between the two groups in TB.antibody, RBC, mono%, lymph, and IGRAs ($p < 0.001$). In addition, the BS, Lymph%, A, BUN, AG, ALT, TG, and HGB were significantly different between the two groups ($p < 0.05$). We plotted ROC curves by using these univariate indicators (Figure 1A) and presented the results of their AUCs in a Lollipop Chart (Figure 1B). In the univariate analysis, we observed that only IGRAs had a high diagnostic validity with an AUC over 0.80, while the other indicators had a low univariate diagnostic validity, none of which exceeded 0.7.

3.3 Screening of variables by Lasso regression

We observed a strong correlation between some of the variables in our dataset (Figure 2A). To minimize the effect of covariance between weighted variables for each indicator in the linear model, we used Lasso regression to screen 40 variables (Figures 2B, C), and we identified12 indicators that could be used for subsequent predictive model fitting, including TB.antibody, IGRAs, WBC, RBC, Lymph%, Mono%, RDW, A, AST, BUN, TG, and PT.

3.4 Establishment of a predictive model for early diagnosis of STB and nomogram

We attempted to build logistic diagnostic models in the training set using twelve variables (TB.antibody, IGRAs, WBC, RBC, Lymph %, Mono%, RDW, A, AST, BUN, TG, PT) screened by Lasso regression, and we excluded variables that were not significant in the logistic regression model. We finally included seven variables, including TB.antibody, IGRAs, RBC, Mono%, RDW, AST, and BUN. We rebuilt the logistic regression model with these seven variables and drew a nomogram based on the logistic regression model that could be used in clinical practice (Figure 3).

10.3389/fcimb.2023.1150632

TABLE 1 Univariate analysis of patients and variables for included cases.

Variables	Total (n = 206)	NSTB (n = 101)	STB (n = 105)	p value
sex, n (%)				0.92
female	88 (43)	44 (44)	44 (42)	
male	118 (57)	57 (56)	61 (58)	
age, years	54.5 (46, 63)	56 (49, 63)	53 (44, 63)	0.47
TB.antibody, n (%)				< 0.001
negative	176 (85)	98 (97)	78 (74)	
positive	30 (15)	3 (3)	27 (26)	
IGRAs, n (%)				< 0.001
negative	77 (37)	72 (71)	5 (5)	
positive	129 (63)	29 (29)	100 (95)	
WBC, 10^9/L	6 (4.7, 7.68)	6.2 (4.8, 7.8)	5.8 (4.3, 7.5)	0.068
RBC, 10^12/L	4.11 ± 0.58	3.93 ± 0.55	4.27 ± 0.56	< 0.001
HGB, g/L	120.19 ± 16.12	117.94 ± 16.16	122.36 ± 15.85	0.049
PLT, 10^9/L	235 (184.25, 296.5)	231 (180, 293)	237 (189, 305)	0.721
Neut, 10^9/L	3.7 (2.8, 5.2)	3.8 (2.7, 5.1)	3.6 (2.9, 5.4)	0.682
lymph, 10^9/L	1.3 (1, 1.8)	1.5 (1.2, 2)	1.2 (0.9, 1.6)	< 0.001
EO, 10^9/L	0.1 (0.1, 0.2)	0.1 (0.1, 0.2)	0.1 (0.1, 0.2)	0.912
BASO, 10^9/L	0 (0, 0.03)	0 (0, 0.03)	0 (0, 0.03)	0.106
Mono, 10^9/L	0.5 (0.4, 0.7)	0.5 (0.4, 0.6)	0.6 (0.4, 0.7)	0.109
Neut%, %	65.75 (57.73, 71.6)	65.7 (55.7, 70.8)	65.8 (60.5, 72.1)	0.205
Lymph%, %	21.8 (16.95, 28)	22.9 (18.3, 31.3)	20.8 (15.9, 26.3)	0.012
BASO%, %	0.5 (0.4, 0.7)	0.5 (0.3, 0.6)	0.5 (0.4, 0.7)	0.233
Eo%, %	1.9 (1.1, 3.2)	1.8 (1.1, 3.1)	2 (1.1, 3.4)	0.519
Mono%, %	8.95 (7.23, 10.4)	8.4 (6.7, 9.6)	9.4 (8.1, 11.2)	< 0.001
RDW, %	14.05 (13.1, 14.8)	13.8 (13.2, 14.8)	14.1 (13.1, 14.8)	0.548
PCT, 10^9/L	0.2 (0.17, 0.25)	0.19 (0.17, 0.25)	0.2 (0.17, 0.25)	0.324
MPV, fL	8.46 (7.67, 9.26)	8.35 (7.65, 9.23)	8.69 (7.78, 9.32)	0.347
TP, g/L	70.1 (65.32, 73.7)	70.1 (65.1, 73.7)	70.1 (65.8, 73.7)	0.738
A, g/L	36.8 ± 4.44	36.03 ± 4.98	37.54 ± 3.72	0.015
G, g/L	32.45 (29, 37.27)	33.3 (28.9, 38.3)	31.6 (29.1, 35.8)	0.236
AG	1.1 (0.92, 1.3)	1.1 (0.9, 1.3)	1.2 (1, 1.4)	0.036
ALT, U/L	17.7 (11.9, 27.02)	19.3 (13.4, 33.4)	16.6 (11.1, 23.7)	0.041
AST, U/L	21.85 (16.8, 28.45)	23.1 (16.8, 28.7)	21 (16.8, 26.6)	0.359
BUN, mmol/L	4.68 (3.7, 6.04)	5.15 (3.81, 6.89)	4.59 (3.53, 5.58)	0.024
Cr, umol/L	71.55 (62, 84)	71.9 (62, 86.6)	71.1 (62, 81.2)	0.251
TG, mmol/L	1.23 (0.92, 1.65)	1.3 (0.95, 1.72)	1.17 (0.88, 1.5)	0.045
Chol, mmol/L	4.44 (3.63, 5.07)	4.58 (3.68, 5.14)	4.3 (3.61, 4.9)	0.294
HDL, mmol/L	1.02 (0.84, 1.21)	1.02 (0.84, 1.23)	1.04 (0.87, 1.15)	0.876
LDL, mmol/L	2.74 (2.28, 3.19)	2.79 (2.26, 3.31)	2.69 (2.3, 3.18)	0.447

(Continued)

TABLE 1 Continued

Variables	Total (n = 206)	NSTB (n = 101)	STB (n = 105)	p value
BS, mmol/L	5.16 (4.74, 5.68)	5.27 (4.95, 5.89)	5.04 (4.71, 5.49)	0.002
PT, s	12.6 (11.72, 13.6)	12.4 (11.5, 13.4)	12.8 (12, 13.7)	0.052
APTT, s	31.35 (28.15, 35.4)	30.2 (27.3, 35)	32 (29.3, 35.5)	0.105
INR	1.03 (0.95, 1.09)	1.02 (0.94, 1.07)	1.03 (0.96, 1.09)	0.312
D_dimer, mg/L	0.27 (0.16, 0.46)	0.28 (0.18, 0.51)	0.26 (0.15, 0.42)	0.213
ESR, mm/h	70 (39, 101.75)	75 (41, 104)	66 (38, 94)	0.256
CRP, mg/L	15.58 (6, 41.47)	15.9 (5.71, 42.4)	12.6 (6.28, 37.8)	0.782

Continuous variables are expressed as mean ± standard deviation or median (25th percentile, 75th percentile).

TABLE 2 The clinical characteristics of recruited patients.

	STB (n = 105)	NSTB (n = 101)	P value
Diabetes, n (%)	9 (9)	14 (14)	0.325
Hypohepatia, n (%)	4 (4)	7 (7)	0.493
Renal Insufficiency, n (%)	1 (1)	6 (6)	0.061
Cancer, n (%)	2 (2)	12 (12)	0.01
pulmonary tuberculosis, n (%)	30 (29)	0 (0)	< 0.001

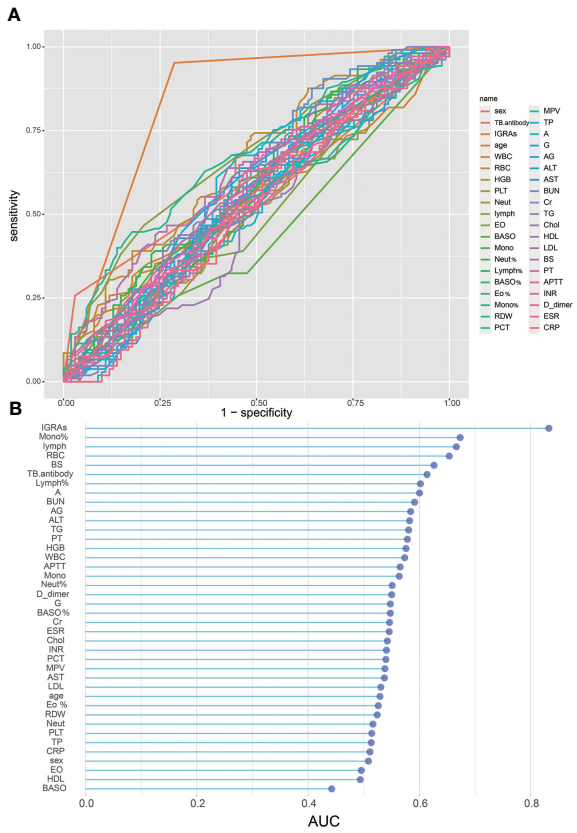

FIGURE 1
Single variable on STB diagnostic capability: **(A)**, ROC curve of single variable on STB diagnosis; **(B)**, AUC of single variables for STB diagnosis.

10.3389/fcimb.2023.1150632

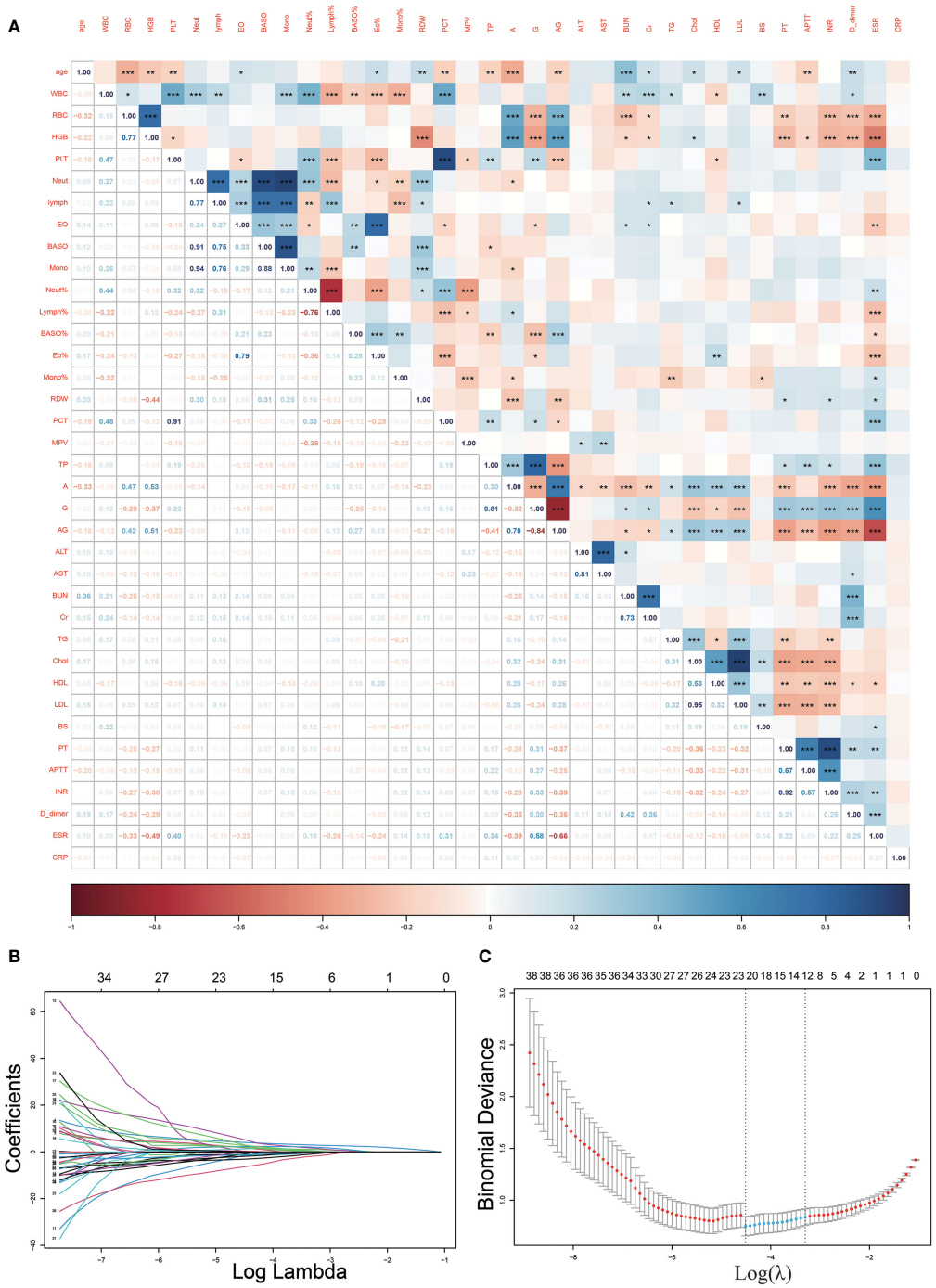

FIGURE 2
Heat map of correlations between variables and Lasso regression screening variables. **(A)**, The heat map of correlations between continuous variables demonstrates the existence of covariance between many variables (*p<0.05, **p<0.01; ***p<0.001); **(B, C)**, Lasso regression filtered out 12 variables from the 40.

3.5 Evaluation of a predictive model for early diagnosis of STB

We first plotted the calibration curve of the model in the training set (Figure 4A). We observed the model has a good fit based on the calibration curve. In addition, we plotted the ROC curve of the model for the training cohort, and its AUC was 0.9468 (Figure 4B). Since the model was fitted based on the training cohort, we used an additional validation set to further evaluate the predictive performance of the model. After plotting the ROC curve of the prediction model in the validation cohort, we found that the AUC of the prediction model was 0.9188 (Figure 4C).

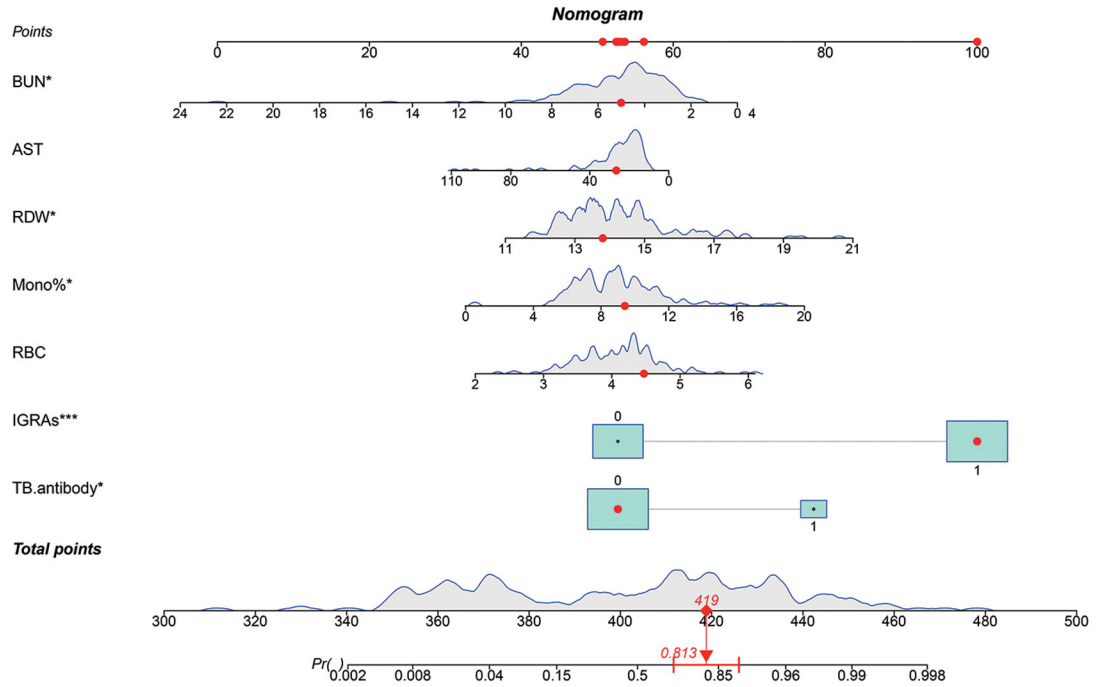

FIGURE 3
A predictive nomogram model for the early diagnosis of spinal tuberculosis. The red dots in the figure demonstrate the usage of the nomogram. A patient's information was projected on the nomogram, and this patient had a final score of 419, corresponding to a probability of 0.813 (>0.5), so we judged this patient to have a final diagnosis of spinal tuberculosis (STB). The patient's final diagnosis was consistent with our prediction.

4 Discussion

Early diagnosis of spinal tuberculosis plays an important role in reducing complications and speeding up the recovery of patients (Chen et al., 2016). Early diagnosis of STB can guide physicians to use anti-tuberculosis drugs more effectively. Currently, the early diagnosis of STB before surgery relies on imaging and IGRAs. It is difficult to distinguish STB from septic spinal infections and some spinal tumors, which also manifest as bone destruction (Liu et al., 2021). IGRAs have been shown to be highly sensitive for the diagnosis of spinal tuberculosis (Hu et al., 2022) However, IGRAs have a low specificity for the diagnosis of STB due to their inability to differentiate between active and latent TB. Spine surgeons lack a tool that can be used for early differential diagnosis of spinal tuberculosis, leading to missed and misdiagnosed cases of spinal tuberculosis. Underdiagnosis of spinal tuberculosis delays the initiation of antituberculosis treatment in patients with spinal tuberculosis, preventing the early initiation and regular administration of antituberculosis treatment, whereas misdiagnosis of spinal tuberculosis results in patients with NSTB taking large amounts of antituberculosis drugs that are unnecessary (Dunn and Ben Husien, 2018). Antituberculosis drugs have considerable adverse effects, including hepatotoxicity, allergic reactions, peripheral neuritis, optic nerve damage, and hearing loss (Xu et al., 2017). In addition, the misuse of antituberculosis treatment may lead to the emergence of drug-resistant TB, which has been defined by the World Health Organization as a public health crisis; the incidence of drug-resistant TB has continued to increase in recent years, making the prevention of drug-resistant TB an urgent priority (World Health Organization,).

In this study, we enrolled patients with suspected spinal tuberculosis from three hospitals. After removing data containing missing values and excluding patients that did not meet the inclusion and diagnostic criteria, a total of 206 eligible patients with suspected spinal tuberculosis were included for analysis. The final diagnosis was determined by postoperative pathogenic microbiology or pathology, and a total of 105 STB cases and 101 NSTB cases were identified. There were no significant differences in age or sex between patients in the STB and NSTB groups. Further univariate analysis of the results of 38 routine laboratory tests in STB patients and NSTB patients demonstrated that there were statistically significant differences between the two groups in TB.antibody, IGRAs, RBC, mono%, lymph, Lymph%, A, AG, BUN, BS, ALT, TG, and HGB ($p < 0.05$). Nevertheless, by plotting the ROC curves and calculating the AUC, we found that, except for IGRAs, which had good performance in the diagnosis of STB (AUC = 0.8326), other variables did not play a significant role in the diagnosis of STB (AUC < 0.7). An increasing number of studies have shown that one indicator alone is often unable to lead to a valid and accurate diagnosis, and the use of multiple indicators is more widely applicable. To meet practical clinical needs and minimize test costs, combining multiple routine laboratory tests to improve the early diagnostic efficacy of spinal tuberculosis can be applied for patients with spinal tuberculosis in underserved and remote areas.

Thirty-eight routine laboratory test variables and 2 other variables, including the age and sex of the patients, were included

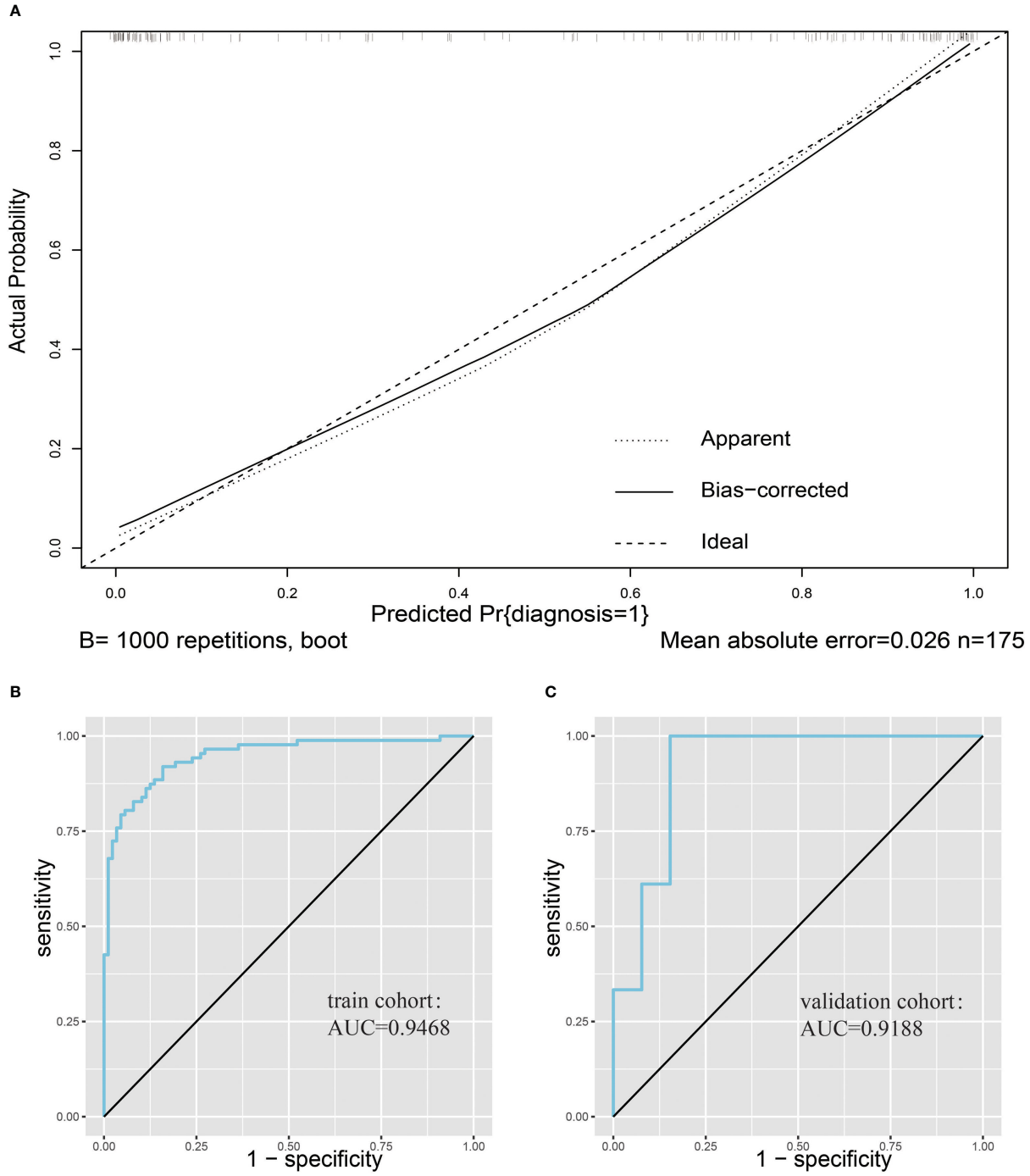

FIGURE 4
Evaluation of nomogram clinical prediction models. **(A)**, Calibration curve of the model. **(B)**, ROC curve of the model for the training cohort, and its AUC was 0.9468. **(C)**, ROC curve of the model for the validation cohort, and its AUC was 0.9188.

in this study. The variables selected are generally available at most hospitals to ensure practical application of the predictive model. Correlation analysis identified a high correlation between many of the variables, and this could be observed on the correlation heatmap. The problem of multicollinearity among the characteristics could not be resolved in the stepwise regression local optimum estimation of logistic regression (Bayman and Dexter, 2021). Therefore, we used Lasso regression, a regularization method widely used for model improvement and variable selection, for variable selection to optimize our model (Ternès et al., 2016). When multicollinearity existed in the original variables, Lasso regression could effectively screen the variables with multicollinearity (Fernández-Delgado et al., 2019). Using Lasso regression, we identified 12 variables that could be used for inclusion in the subsequent model.

Logistic regression was used to construct a predictive model for spinal tuberculosis. Twelve variables identified by Lasso regression were included in the logistic regression equation, and variables that were not significant in the logistic regression model were eliminated. Finally, seven variables were retained, including TB.antibody, IGRAs, RBC, Mono%, RDW, AST, and BUN were retained, and the model was refitted with these variables. Column line plots were drawn for better applicability to clinical practice. To evaluate the predictive model, we plotted calibration curves and ROC curves in a validation cohort different from the training cohort. The calibration curves showed a good fit, and the prediction model achieved an AUC value of 0.9188 in the validation cohort. The final model had good diagnostic validity. Based on our findings, increased levels of RBC, RDW, and mono% in patients could indicate a greater likelihood of STB diagnosis, whereas elevated BUN and AST levels may suggest a higher probability of NSTB diagnosis. In previously published studies, elevated RDW and mono% were commonly observed in patients with TB (Baynes et al., 1986). Patients with chronic TB infection often suffer from malnutrition, resulting in the development of anemia (Cobelens and Kerkhoff, 2021). However, in our study, the differential diagnosis of STB was often made in patients with other septic spinal infections and spinal tumors, who also had a poor nutritional status. This resulted in elevated levels of BUN and AST in both diseases, making it difficult to distinguish between them. Further studies are needed to better understand the distinction between these diseases.

In published studies, we noted that Liyi Chen et al. (2022) also attempted early diagnosis of spinal tuberculosis by drawing columnar maps, but they included fewer variables and lacked specific indicators for the diagnosis of spinal tuberculosis (IGRAs, TB antibody), and they did not develop strict inclusion and diagnostic criteria. A prospective study published in 2022 also diagnosed STB by combining multiple indicators, but we observed that this study included diagnostic indicators such as Xpert, acid-fast staining, and other indicators that occur late in the patient's hospitalization (Qi et al., 2022); therefore, this study did not focus on the early diagnosis of STB. In addition, a recent study focused on a deep learning model for early diagnosis of spinal tuberculosis using imaging data analysis to determine the early diagnosis of spinal tuberculosis (Li et al., 2022), whereas our study focused on routine laboratory findings. In a follow-up study, we plan to combine both imaging data and routine laboratory findings to further optimize the early diagnosis prediction model of spinal tuberculosis through imaging histology and machine learning.

To enhance the generalizability of our model, we incorporated two distinct methods for IGRAs, namely QuantiFERON-TB Gold In-Tube and T-SPOT(®).TB, both of which share a similar underlying principle. Moreover, previous studies have highlighted the potential utility of the TBAg/PHA ratio as a means of improving diagnostic accuracy in tuberculosis (Wang et al., 2016; Luo et al., 2020), with particular promise demonstrated in the diagnosis of extrapulmonary disease (Wang et al., 2019). Although we were unable to include this variable in the current analysis, we eagerly anticipate the opportunity to assess the diagnostic efficacy of the TBAg/PHA ratio in T-SPOT(®).TB for spinal tuberculosis in a larger cohort of patients.

This study was a retrospective study, and due to missing data, we excluded some cases and other factors, such as calcitoninogen and body mass index, that might have been meaningful. We intend to conduct further prospective studies informed by our present results which will include complete clinical data and patient imaging data to further improve the early diagnosis of spinal tuberculosis.

5 Conclusion

In this study, we developed a nomogram to predict the occurrence of spinal tuberculosis for early diagnosis. Our model contained seven conventional laboratory indicators, including TB.antibody, IGRAs, RBC, Mono%, RDW, AST, and BUN. We hope to use this model to improve the early diagnosis of STB, especially in hospitals in poor and remote areas where testing is limited.

Data availability statement

The raw data supporting the conclusions of this article will be made available by the authors, without undue reservation.

Ethics statement

The studies involving human participants were reviewed and approved by the Ethics Committee of Xiangya Hospital Central South University. The patients/participants provided their written informed consent to participate in this study.

Author contributions

XH and QG designed research, performed research, analyzed data, and wrote the paper. HZ, MT and SL developed the idea for the study. GZ, BT and DX collected the data. All authors contributed to the article and approved the submitted version.

Funding

This work was supported by National Natural Science Foundation of China(serial number: 82072460, 82170901); Natural Science Foundation of Hunan Province(serial number: 2020JJ4892, 2020JJ4908)

Acknowledgments

I would like to thank all the surgeons in the Department of Spine Surgery at Xiangya Hospital of Central South University for their help and guidance.

Conflict of interest

The authors declare that the research was conducted in the absence of any commercial or financial relationships that could be construed as a potential conflict of interest.

Publisher's note

All claims expressed in this article are solely those of the authors and do not necessarily represent those of their affiliated organizations, or those of the publisher, the editors and the reviewers. Any product that may be evaluated in this article, or claim that may be made by its manufacturer, is not guaranteed or endorsed by the publisher.

Supplementary material

The Supplementary Material for this article can be found online at: https://www.frontiersin.org/articles/10.3389/fcimb.2023.1150632/full#supplementary-material

References

Bayman, E. O., and Dexter, F. (2021). Multicollinearity in logistic regression models. *Anesth. Analgesia.* 133 (2), 362–365. doi: 10.1213/ane.0000000000005593

Baynes, R. D., Flax, H., Bothwell, T. H., Bezwoda, W. R., Atkinson, P., and Mendelow, B. (1986). Red blood cell distribution width in the anemia secondary to tuberculosis. *Am. J. Clin. Pathol.* 85 (2), 226–229. doi: 10.1093/ajcp/85.2.226

Beltran, C. G. G., Venter, R., Mann, T. N., Davis, J. H., Kana, B. D., and Walzl, G. (2022). Culture filtrate supplementation can be used to improve mycobacterium tuberculosis culture positivity for spinal tuberculosis diagnosis. *Front. Cell. Infection Microbiol.* 12. doi: 10.3389/fcimb.2022.1065893

Chen, C. H., Chen, Y. M., Lee, C. W., Chang, Y. J., Cheng, C. Y., and Hung, J. K. (2016). Early diagnosis of spinal tuberculosis. *J. Formosan Med. Assoc. = Taiwan yi zhi.* 115 (10), 825–836. doi: 10.1016/j.jfma.2016.07.001

Chen, L., Liu, C., Liang, T., Ye, Z., Huang, S., Chen, J., et al. (2022). Mechanism of COVID-19-Related proteins in spinal tuberculosis: Immune dysregulation. *Front. Immunol.* 13. doi: 10.3389/fimmu.2022.882651

Cobelens, F., and Kerkhoff, A. D. (2021). Tuberculosis and anemia-cause or effect? *Environ. Health Prev. Med.* 26 (1), 93. doi: 10.1186/s12199-021-01013-4

Dunn, R. N., and Ben Husien, M. (2018). Spinal tuberculosis: review of current management. *Bone Joint J.* 100-b (4), 425–431. doi: 10.1302/0301-620x.100b4.Bjj-2017-1040.R1

Fernández-Delgado, M., Sirsat, M. S., Cernadas, E., Alawadi, S., Barro, S., and Febrero-Bande, M. (2019). An extensive experimental survey of regression methods. *Neural Networks Off. J. Int. Neural Network Society.* 111, 11–34. doi: 10.1016/j.neunet.2018.12.010

Hamada, Y., Cirillo, D. M., Matteelli, A., Penn-Nicholson, A., Rangaka, M. X., and Ruhwald, M. (2021). Tests for tuberculosis infection: landscape analysis. *Eur. Respir. J.* 58 (5), 2100167. doi: 10.1183/13993003.00167-2021

Held, M., Laubscher, M., Zar, H. J., and Dunn, R. N. (2014). GeneXpert polymerase chain reaction for spinal tuberculosis: an accurate and rapid diagnostic test. *Bone Joint J.* 96-b (10), 1366–1369. doi: 10.1302/0301-620x.96b10.34048

Hristea, A., Constantinescu, R. V., Exergian, F., Arama, V., Besleaga, M., and Tanasescu, R. (2008). Paraplegia due to non-osseous spinal tuberculosis: report of three cases and review of the literature. *Int. J. Infect. Dis. IJID Off. Publ. Int. Soc. Infect. Diseases.* 12 (4), 425–429. doi: 10.1016/j.ijid.2007.12.004

Hu, X., Zhang, H., Li, Y., Zhang, G., Tang, B., Xu, D., et al. (2022). Analysis of the diagnostic efficacy of the QuantiFERON-TB gold in-tube assay for preoperative differential diagnosis of spinal tuberculosis. *Front. Cell. Infection Microbiol.* 12. doi: 10.3389/fcimb.2022.983579

Khanna, K., and Sabharwal, S. (2019a). Spinal tuberculosis: A comprehensive review for the modern spine surgeon. *Spine J. Off. J. North Am. Spine Society.* 19 (11), 1858–1870. doi: 10.1016/j.spinee.2019.05.002

Khanna, K., and Sabharwal, S. (2019b). Spinal tuberculosis: a comprehensive review for the modern spine surgeon. *Spine J.* 19 (11), 1858–1870. doi: 10.1016/j.spinee.2019.05.002

Li, Y., Dong, W., Lan, T., Fan, J., Qin, S., and Guo, A. (2020). Distribution of linezolid in tuberculosis lesions in patients with spinal multidrug-resistant tuberculosis. *Antimicrobial Agents Chemotherapy.* 64 (7), e00450–20. doi: 10.1128/aac.00450-20

Li, Z., Wu, F., Hong, F., Gai, X., Cao, W., Zhang, Z., et al. (2022). Computer-aided diagnosis of spinal tuberculosis from CT images based on deep learning with multimodal feature fusion. *Front. Microbiol.* 13. doi: 10.3389/fmicb.2022.823324

Liu, H., Li, Y., Yi, J., Zhou, W., Zhao, S., and Yin, G. (2022). Neutrophil-lymphocyte ratio as a potential marker for differential diagnosis between spinal tuberculosis and pyogenic spinal infection. *J. Orthopaedic Surg. Res.* 17 (1), 357. doi: 10.1186/s13018-022-03250-x

Liu, X., Zheng, M., Sun, J., and Cui, X. (2021). A diagnostic model for differentiating tuberculous spondylitis from pyogenic spondylitis on computed tomography images. *Eur. Radiology.* 31 (10), 7626–7636. doi: 10.1007/s00330-021-07812-1

Luo, Y., Tang, G., Lin, Q., Mao, L., Xue, Y., Yuan, X., et al. (2020). Combination of mean spot sizes of ESAT-6 spot-forming cells and modified tuberculosis-specific antigen/phytohemagglutinin ratio of T-SPOT.TB assay in distinguishing between active tuberculosis and latent tuberculosis infection. *J. Infect.* 81 (1), 81–89. doi: 10.1016/j.jinf.2020.04.038

Mann, T. N., Davis, J. H., Walzl, G., Beltran, C. G., du Toit, J., Lamberts, R. P., et al. (2021). Candidate biomarkers to distinguish spinal tuberculosis from mechanical back pain in a tuberculosis endemic setting. *Front. Immunol.* 12. doi: 10.3389/fimmu.2021.768040

Pai, M., Behr, M., Dowdy, D., Dheda, K, Divangahi, M, Boehme, CC, et al. (2016). Tuberculosis. *Nat. Rev. Dis. Primers* 2, 16076. doi: 10.1038/nrdp.2016.76

Qi, Y., Liu, Z., Liu, X., Fang, Z., Liu, Y., and Li, F. (2022). Tuberculosis-specific Antigen/Phytohemagglutinin ratio combined with GeneXpert MTB/RIF for early diagnosis of spinal tuberculosis: A prospective cohort study. *Front. Cell. Infection Microbiol.* 12. doi: 10.3389/fcimb.2022.781315

Rule, R., Mitton, B., Govender, N. P., Hoffmann, D., and Said, M. (2021). Spinal epidural abscess caused by aspergillus spp masquerading as spinal tuberculosis in a person with HIV. *Lancet Infect. Diseases.* 21 (11), e356–ee62. doi: 10.1016/s1473-3099(20)30979-8

Scorrano, G., Viva, S., Pinotti, T., Fabbri, P. F., Rickards, O., and Macciardi, F. (2022). Bioarchaeological and palaeogenomic portrait of two pompeians that died during the eruption of Vesuvius in 79 AD. *Sci. Rep.* 12 (1), 6468. doi: 10.1038/s41598-022-10899-1

Ternès, N., Rotolo, F., and Michiels, S. (2016). Empirical extensions of the lasso penalty to reduce the false discovery rate in high-dimensional cox regression models. *Stat Med.* 35 (15), 2561–2573. doi: 10.1002/sim.6927

Wang, F., Hou, H. Y., Wu, S. J., Zhu, Q., Huang, M., Yin, B., et al. (2016). Using the TBAg/PHA ratio in the T-SPOT(®).TB assay to distinguish TB disease from LTBI in an endemic area. *Int. J. Tuberc Lung Dis.* 20 (4), 487–493. doi: 10.5588/ijtld.15.0756

Wang, T., Tan, Y. J., Wu, S. J., Huang, M., Yin, B. T., Huang, J., et al. (2019). [The ratio of tuberculosis-specific antigen to phytohemagglutinin in T-SPOT assay in the diagnosis of active tuberculosis]. *Zhonghua Jie He He Hu Xi Za Zhi.* 42 (4), 262–267. doi: 10.3760/cma.j.issn.1001-0939.2019.04.003

World Health Organization *Global tuberculosis report 2021*. Available at: https://www.who.int/news-room/fact-sheets/detail/tuberculosis (Accessed 13 December 2022).

Xu, Y., Wu, J., Liao, S., and Sun, Z. (2017). Treating tuberculosis with high doses of anti-TB drugs: Mechanisms and outcomes. *Ann. Clin. Microbiol. Antimicrobials.* 16 (1), 67. doi: 10.1186/s12941-017-0239-4

Zhang, Z., Gayle, A. A., Wang, J., Zhang, H., and Cardinal-Fernández, P. (2017). Comparing baseline characteristics between groups: an introduction to the CBCgrps package. *Ann. Trans. Med.* 5 (24), 484. doi: 10.21037/atm.2017.09.39

frontiers | Frontiers in Cellular and Infection Microbiology

TYPE Original Research
PUBLISHED 02 June 2023
DOI 10.3389/fcimb.2023.1152665

OPEN ACCESS

EDITED BY
Amit Singh,
Central University of Punjab, India

REVIEWED BY
Norman Nausch,
Deutsche Gesellschaft für Internationale Zusammenarbeit, Germany
Jitendra Singh,
All India Institute of Medical Sciences, Bhopal, India

*CORRESPONDENCE
Liping Pan
panliping2006@163.com
Jianyun Wang
wjyno.1@163.com
Yanzheng Song
yanzhengsong@163.com

†These authors have contributed equally to this work

RECEIVED 28 January 2023
ACCEPTED 22 May 2023
PUBLISHED 02 June 2023

CITATION
Tang Y, Yu Y, Wang Q, Wen Z, Song R, Li Y, Zhou Y, Ma R, Jia H, Bai S, Abdulsalam H, Du B, Sun Q, Xing A, Pan L, Wang J and Song Y (2023) Evaluation of the *IP-10* mRNA release assay for diagnosis of TB in HIV-infected individuals.
Front. Cell. Infect. Microbiol. 13:1152665.
doi: 10.3389/fcimb.2023.1152665

Evaluation of the *IP-10* mRNA release assay for diagnosis of TB in HIV-infected individuals

Yang Tang[1†], Yanhua Yu[2†], Quan Wang[3†], Zilu Wen[4], Ruixue Song[5], Yu Li[2], Yingquan Zhou[6], Ruiying Ma[3], Hongyan Jia[5], Shaoli Bai[6], Harimulati Abdulsalam[7], Boping Du[5], Qi Sun[5], Aiying Xing[5], Liping Pan[5*], Jianyun Wang[8*] and Yanzheng Song[9*]

[1]Department of Infection and Immunity, Shanghai Public Health Clinical Center, Fudan University, Shanghai, China, [2]Department of Clinical Laboratory, Beijing Youan Hospital, Capital Medical University, Beijing, China, [3]Department of Clinical Laboratory, The Eighth Affiliated Hospital, Xinjiang Medical University, Urumqi, China, [4]Department of Scientific Research, Shanghai Public Health Clinical Center, Fudan University, Shanghai, China, [5]Beijing Chest Hospital, Capital Medical University, Beijing Key Laboratory for Drug Resistant Tuberculosis Research, Beijing Tuberculosis and Thoracic Tumor Research Institute, Beijing, China, [6]Department of Infectious Diseases, Gansu Provincial Infectious Disease Hospital, Lanzhou, China, [7]Department of Infectious Diseases, The Eighth Affiliated Hospital, Xinjiang Medical University, Urumqi, China, [8]Department of Geriatric Medicine, Gansu Province Hospital Rehabilitation Center, Lanzhou, China, [9]Department of Thoracic Surgery, Shanghai Public Health Clinical Center, Fudan University, Shanghai, China

HIV-infected individuals are susceptible to *Mycobacterium tuberculosis* (*M.tb*) infection and are at high risk of developing active tuberculosis (TB). Interferon-gamma release assays (IGRAs) are auxiliary tools in the diagnosis of TB. However, the performance of IGRAs in HIV-infected individuals is suboptimal, which limits clinical application. Interferon-inducible protein 10 (IP-10) is an alternative biomarker for identifying *M.tb* infection due to its high expression after stimulation with *M.tb* antigens. However, whether *IP-10* mRNA constitutes a target for the diagnosis of TB in HIV-infected individuals is unknown. Thus, we prospectively enrolled HIV-infected patients with suspected active TB from five hospitals between May 2021 and May 2022, and performed the IGRA test (QFT-GIT) alongside the *IP-10* mRNA release assay on peripheral blood. Of the 216 participants, 152 TB patients and 48 non-TB patients with a conclusive diagnosis were included in the final analysis. The number of indeterminate results of *IP-10* mRNA release assay (13/200, 6.5%) was significantly lower than that of the QFT-GIT test (42/200, 21.0%) (P = 0.000026). *IP-10* mRNA release assay had a sensitivity of 65.3% (95%CI 55.9% – 73.8%) and a specificity of 74.2% (95%CI 55.4% – 88.1%), respectively; while the QFT-GIT test had a sensitivity of 43.2% (95%CI 34.1% – 52.7%) and a specificity of 87.1% (95%CI 70.2% – 96.4%), respectively. The sensitivity of the *IP-10* mRNA release assay was significantly higher than that of QFT-GIT test (P = 0.00062), while no significant difference was detected between the specificities of these two tests (P = 0.198). The *IP-10* mRNA release assay showed a lower dependence on $CD4^+$ T cells than that of QFT-GIT test. This was evidenced by the fact that the QFT-GIT test had a higher number of indeterminate results and a lower sensitivity when the $CD4^+$ T cells counts were decreased ($P < 0.05$), while no significant difference in the number of indeterminate results and sensitivity were observed for the *IP-10* mRNA release assay among HIV-infected individuals with varied $CD4^+$T cells counts

($P > 0.05$). Therefore, our study suggested that *M.tb* specific *IP-10* mRNA is a better biomarker for diagnosis of TB in HIV-infected individuals.

KEYWORDS

tuberculosis, M.TB infection, HIV co-infection, IP-10, mRNA, IGRA

Introduction

Tuberculosis (TB) is an infectious disease caused by *Mycobacterium tuberculosis* (*M.tb*) and seriously threatens human health, with an estimated 10.6 million new cases and 1.6 million deaths occurring worldwide in 2021 (WHO, 2022). However, only 63% of patients with TB were bacteriologically-confirmed. Furthermore, the diagnosis of TB is particularly difficult among HIV co-infected individuals (Scott et al., 2017; MacLean et al., 2019). Although interferon-gamma release assays (IGRAs) have been considered as a useful method for diagnosis of *M.tb* infection and an auxiliary method for diagnosis of active TB (Gao et al., 2015; Getahun et al., 2015), the sensitivity of IGRAs is reduced among immunocompromised individuals (Jung et al., 2012; Pan et al., 2015), including HIV-infected patients, which limits the clinical application of this methodology (Cattamanchi et al., 2011; Metcalfe et al., 2011; Santin et al., 2012). HIV-positive persons are particularly susceptible to *M.tb* infection, with an infection rate 2 –5 times higher than that of HIV-negative people (Mhango et al., 2021). Furthermore, the risk of developing active TB is 20 – 30 times higher for HIV and *M.tb* co-infection individuals than for those infected with *M.tb* alone. Consequently, the mortality of TB/HIV co-infected patients is also higher than that of patients with TB alone (Bell and Noursadeghi, 2018; Ignatius and Swindells, 2020). Furthermore, WHO has recommended to identify TB cases among high risk populations, such as HIV-infected individuals (WHO, 2023). Therefore, more sensitive and rapid test should be developed for the diagnosis of TB in HIV-infected individuals.

Many studies have identified an alternative biomarker for TB, namely the interferon-gamma induced protein 10 (IP-10) (Ruhwald et al., 2011; Kumar et al., 2021; Ortakoylu et al., 2022; Uzorka et al., 2022). IP-10 is expressed at a higher level than IFN-γ in the peripheral blood after exposure to *M.tb*-specific antigens (Lu et al., 2011; Ruhwald et al., 2012). Meta-analyses have shown that IP-10 detection has a sensitivity of 86% (95%CI = 80%–90%) and a specificity of 88% (95%CI = 82%–92%) in the diagnosis of active TB (Qiu et al., 2019b), and a sensitivity of 85% (95%CI = 80%–88%) and a specificity of 89% (95%CI = 84%–92%) in the diagnosis of *M.tb* infection, respectively (Qiu et al., 2019a). However, these studies have used IP-10 protein as the target, which is not detected unless the peripheral blood is stimulated overnight (18-20h) with *M.tb* antigens. This leads to the delayed reporting of diagnostic results. In contrast, the expression of *IP-10* mRNA can be up-regulated by about one hundred times within 2.5-8h of *M.tb*-specific antigen stimulation (Blauenfeldt et al., 2014). Although the sample sized was not large, recent study has showed that elevated *IP-10* at the mRNA level was also associated with pulmonary TB (Fisher et al., 2022). Thus, the development of novel diagnostic technologies, using *IP-10* mRNA as a target, may improve the speed and diagnostic sensitivity of TB testing. Such a methodology may also be more suitable for clinical use.

Our previous study has confirmed that the *IP-10* mRNA can be effectively used as a target for the diagnosis of *M.tb* infection in HIV-infected individuals, as evidenced by its higher sensitivity and lower indeterminate rate of the detection (Pan et al., 2021; Pan et al., 2022). However, whether it can be used as an auxiliary method for diagnosis of TB, should also be validated in a larger cohort. Herein, we prospectively enrolled suspected TB patients with HIV infection, and evaluated the performance of *M.tb*-specific IP-*10* mRNA release assay for TB diagnosis.

Materials and methods

Ethical approval

This study was performed in accordance with the guidelines of the Helsinki Declaration and was approved by the Ethics Committee of the Shanghai Public Health Clinical Center (Ethical approval number: 2020-S213-03). Written informed consents were obtained from each participant before blood collection.

Study design and participants

This multicenter, prospective study was performed across five hospitals in China, including the Shanghai Public Health Clinical Center (Eastern), the Beijing Chest Hospital (Eastern), the Beijing Youan Hospital (Eastern), the Gansu Provincial Infectious Disease Hospital (Western) and the Eighth Affiliated Hospital, Xinjiang Medical University (Western). According to the positive rate of *IP-10* mRNA release assay (92.9%) and IGRA (61.5%) among HIV-coinfected patients in our previous study (Pan et al., 2022), we performed sample size calculation and the final minimum sample size of TB/HIV co-infected patients was 143. Therefore, we prospectively and continuously recruited the suspected HIV/TB co-infected patients from the five participating hospitals and ended when the HIV/TB co-infected patients in case group was enough, between May 2021 and May 2022. The *IP-10* mRNA release assay and QuantiFERON-TB gold In-Tube (QFT-GIT) assay were then

performed in parallel using peripheral blood collected from each participant. The clinicians were blinded to the laboratory test results before the end of the clinical trial enrollment, while the laboratory technicians were blinded to the diagnosis of the patients throughout the study. Furthermore, the laboratory technicians who performed the *IP-10* mRNA release assay were unaware of QFT-GIT results, and vice versa.

Categorization of participants

The final diagnosis was based on clinical manifestations, biochemical examinations, and the histopathological, radiological, microbiological and nucleic acid amplification information. All participants were followed up for at least 6 months to monitor whether there were changes in their diagnosis. HIV infection was defined according to the national guidelines (AIDS and Hepatitis Group of Infectious Diseases et al., 2018). Patients were categorized as having: (1) Definite TB: patients who had a positive *M.tb* culture, or positive Xpert MTB/RIF, microscopy, or histology results. (2) Probable TB: patients who had clinical and radiological evidences of TB, and presented well response to anti-TB treatment, but lacked microbiological, histopathological or nucleic acid amplification evidence of *M.tb* infection. (3) Non-TB patients: patients who has no history of TB or previous known exposure with TB, and were initially suspected of having active TB, but ended up not having active TB, due to either an alternative diagnosis was made or clinical improvement occurred without recent anti-TB therapy.

Blood collection

A total of 10 mL of peripheral blood was collected in heparin-containing vacutainer tubes from each participant, and the *IP-10* mRNA release assay and QFT-GIT test were subsequently performed.

The *IP-10* mRNA release assay

The commercial *IP-10* mRNA release assay was performed according to the instructions of the manufacturer, using the following kits: the kit for blood incubation and RNA extraction (CLR001A48, InnowaveDx Co.,Ltd, Suzhou, China) and the kit for reverse transcription (RT) and qPCR testing (CLR002A48, InnowaveDx Co.,Ltd, Suzhou, China), Briefly, the blood was divided into 3 tubes (1.5mL per tube): (i) one tube was coated with *M.tb*-specific peptides (ESAT6, CFP-10 and PPE68); (ii) one tube was coated with phytohemagglutinins (PHA) as a positive control; (iii) one tube had no antigen coating and was used as a negative control (Nil). The tubes were then incubated immediately for 4–6h at 37°C and the RNA was automatically extracted from the incubated whole blood in a 100 μL volume. A total of 10 μL RNA and 10 μL RT solution (composed of buffer and the reverse transcriptase) were mixed and reverse transcribed to cDNA using the following conditions: 50°C for 20 min and 85°C for 2 min. RNA extraction and RT were performed using the automatic nucleic acid extraction and detection system Innovo-100 (InnowaveDx Co.,Ltd, Suzhou, China). All the commercial reagents and kits for RNA extraction and RT were compatible with the instrument used. A total of 10 μL cDNA was then mixed with 15 μL quantitative real-time PCR (qPCR) mix (including enzyme, buffer and probe). qPCR was performed on the ABI 7500 Real-time PCR System (Thermo Fisher Scientific, Waltham, MA, USA) using the following conditions: 50°C for 2 min, 95°C for 2 min, and then 40 cycles of 95°C for 10 s and 60°C for 30 s. The cycle threshold (CT) for the target gene (*IP-10*, Gene ID: 3627) and housekeeping gene (*CHMP2A*, Gene ID: 27243) detector was automatically determined. ΔCT (the CT value for the target gene minus the CT value for the housekeeping gene) was calculated and used to determine relative gene expression as previously described (Schmittgen and Livak, 2008). The relative amount of *IP-10* mRNA in each tube (with or without antigens) was calculated separately. The test results were classified as indeterminate, negative, or positive according to the previously published criteria (Pan et al., 2022). Briefly, the test result was positive if the relative amount of IP-10 mRNA (ΔCT) in *M.tb* antigen tube minus that in Nil control tube was ≤ -1.04; the test result was negative if the ΔCT value in *M.tb* antigen tube minus that in Nil control tube was > -1.04 and the ΔCT value in mitogen tube minus that in Nil control tube was ≤ -1.2; and 'indeterminate' was defined as that the ΔCT value in *M.tb* antigen tube minus that in Nil control tube was > -1.04 and the ΔCT value in mitogen tube minus that in Nil control tube was > -1.2.

The QFT-GIT test

The QFT-GIT test (QIAGEN, German) was performed in accordance with the manufacturer's instructions. Briefly, the peripheral blood was divided into 3 tubes (1mL per tube): (i) one tube coated with *M.tb*-specific peptides (ESAT-6, CFP-10 and TB 7.7); (ii) one tube coated with the mitogen as a positive control; (iii) one tube without antigen as a negative control (Nil). The tubes were shaken about 10 times to ensure that the blood properly mixed with entire content of the tube, and then they were incubated immediately for 16–24h at 37°C. After centrifugation at 3000 × g for 15 min, the plasma IFN-γ concentration was measured immediately by ELISA according to the instructions. The test results were classified as indeterminate, negative, or positive according to the previously published criteria (Wu et al., 2018).

Statistical analysis

Sample size calculation was performed using PASS software, version 11 (NCSS, LLC. Kaysville, Utah, USA), the parameters were set as follow: type I error (α) was 0.05, permissible error (1-β) was 0.08 and the positive rate of the tests was estimated as 61.5% as previous study (Pan et al., 2022). Data analysis was performed using SPSS for Windows, version 21 (SPSS, Inc). Categorical variables were compared by Pearson's Chi-square test or Fisher's exact test

(when any of the sample size in the 2×2 contingency table is less than 5), while continuous variables were compared by the Student's t-test (parametric test for analyzing the continuous variables with normal distribution) or Mann-Whitney U-test (Non-parametric test for analyzing the continuous variables without normal distribution), as appropriate. Receiver operating characteristic (ROC) curves were constructed to obtain the area under the curve (AUC) and evaluate the diagnostic value of each assay. The sensitivity and specificity of each test were also calculated to evaluate diagnostic performance. Concordance between the *IP-10* mRNA release assay and QFT-GIT assay was calculated using the Cohen's kappa test. The criterion for statistical significance was $P < 0.05$.

Results

Demographic characteristics of participants

A total of 216 suspected TB patients with HIV infection were prospectively enrolled from five hospitals in China (Figure 1). According to their final diagnosis and a further 6-months follow-up, 81 definite TB patients with HIV infection, 71 probable TB patients with HIV infection and 48 non-TB patients with HIV infection were included in the analysis. Other 16 patients were excluded, including 12 patients who had inconclusive diagnosis, 2 patients were enrolled twice and 2 patients who had invalid peripheral blood samples. No significant differences were detected in age ($P = 0.081$) and gender ($P = 0.056$) between the TB group and non-TB group. The peripheral blood $CD4^+$ T cell counts of the TB group was significantly higher than those of the non-TB group ($P = 0.001$). The detailed demographic and clinical characteristics of the participants are shown in Table 1.

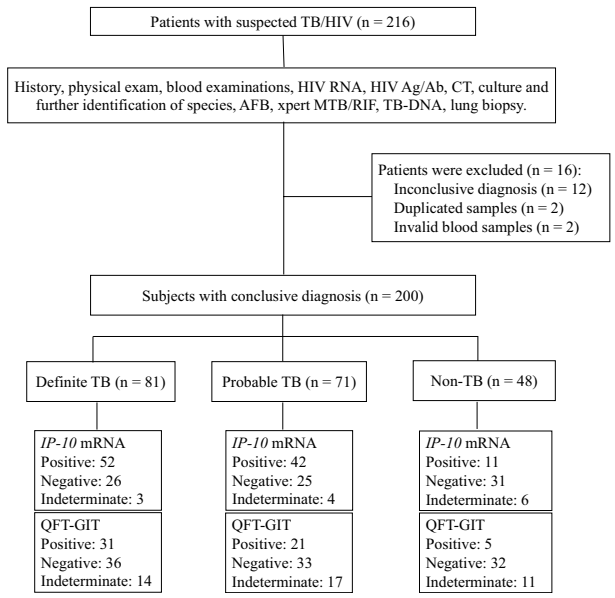

FIGURE 1
Flow chart of the study participants. Of the 216 patients with suspected TB/HIV co-infection, the following were eligible for inclusion in the final analysis: 81 were definite TB/HIV co-infected patients, 71 had probable TB/HIV co-infected patients and 48 were non-TB patients with HIV infection. TB, tuberculosis; HIV, human immunodeficiency virus; CT, computed tomography; AFB, acid-fast bacilli.

Indeterminate results of *IP-10* mRNA release assay and QFT-GIT test

Among the 200 suspected TB patients with HIV infection who were included in the final analysis, 13 patients (6.5%) had invalid results of *IP-10* mRNA release assay due to invalid ΔCT in the mitogen control tube (> -1.2), including 7 TB patients and 6 non-TB patients. Meanwhile, 42 patients (21.0%) had invalid results of QFT-GIT assay due to higher IFN-γ concentrations (> 8 IU/mL) in the Nil control tube (1 patient) or lower IFN-γ concentrations (< 0.5 IU/mL) in the positive control tube (41 patients), including 31 TB patients and 11 non-TB patients. The rate of indeterminate results of the *IP-10* mRNA release assay was significantly lower than that of QFT-GIT assay ($P = 0.000026$). Collectively, a total of 51 indeterminate results were obtained by the two assays. In addition, we found that patients with invalid results were significantly more likely to have $CD4^+$ T cell counts below 200 cells/μL (43/47, 91.5%) than patients with valid results (101/138, 73.2%), suggesting that lower $CD4^+$ T cell counts was a significant risk factor for indeterminate results ($P = 0.0091$).

The concordance between the *IP-10* mRNA release assay and the QFT-GIT test

The concordance between the *IP-10* mRNA release assay and QFT-GIT assay was also analyzed in the 149 participants who had both valid results of *IP-10* mRNA release assay and QFT-GIT assay (Table 2). Both the *IP-10* mRNA release assay and QFT-GIT assay were positive in 44 participants and negative in 53 participants, suggesting that *IP-10* mRNA release assay and QFT-GIT assay have a weak concordance (Kappa value = 0.33, $P < 0.001$). The overall concordance between the two assays was 65.1% (95%CI = 57.5% – 72.8%), the positive agreement was 61.0% (95%CI= 52.2% – 69.8%) and the negative agreement was 80.6% (95%CI 66.7% – 94.6%), respectively.

The diagnostic performance of the *IP-10* mRNA release assay versus QFT-GIT assay for TB

The diagnostic performances of the *IP-10* mRNA release assay and QFT-GIT assay were analyzed among 118 TB patients (66 definite TB patients and 52 probable TB patients) and 31 non-TB patients, who had valid results of *IP-10* mRNA release assay and valid QFT-GIT assay (Table 3). The expression levels of *M.tb*-specific *IP-10* mRNA in the TB patients were significantly higher

10.3389/fcimb.2023.1152665

TABLE 1 The demographic and clinical characteristics of the participants (n = 200).

	TB			Non-TB	*P*-values*
	Definite TB	Probable TB	Total TB		
Number of patients	81	71	152	48	
Age (years, range)	42 (22–72)	41 (18–79)	41 (18–29)	38 (18–63)	0.081
Gender					0.056
Male	74	67	141	48	
Female	7	4	11	0	
$CD4^+$ T cell counts[§]	91 (0–587)	104 (2–1141)	102 (1–1141)	40.5 (2–336)	0.001
M.tb culture					
Positive	29	0	29	0	
Negative	37	62	99	34	
Not done	15	9	24	14	
Smear microscopy					
Positive	28	0	28	0	
Negative	50	68	118	44	
Not done	3	3	6	4	
Xpert MTB/RIF					
Positive	60	0	60	0	
Negative	16	64	80	35	
Not done	5	7	12	13	
Histologic results					
Positive	3	0	3	0	
Negative	2	5	7	4	
Not done	76	66	142	44	
Pulmonary TB	69	53	122	–	
Extra-pulmonary TB	12	18	30	–	
Lymph nodes	3	5	8	–	
Meninges	4	4	8	–	
Pleura	2	5	7	–	
Intestine	2	1	3		
Skeleton	0	3	3	–	
Blooddissemination	1	0	1	–	
Cause of diseases					
Pneumocystis	–	–	–	16	
Cryptococcus	–	–	–	6	
NTM diseases	–	–	–	6	
Cytomegalovirus	–	–	–	5	
Pseudomonas aeruginosa				4	
Lymphoma	–	–	–	3	

(Continued)

TABLE 1 Continued

	TB			Non-TB	*P*-values*
	Definite TB	Probable TB	Total TB		
Aspergillus	–	–	–	3	
Candida albicans	–	–	–	2	
Streptococcus	–	–	–	1	
Rhodococcusequi				1	
Mucor				1	

NTM, non-tuberculous mycobacterial.
*Comparison between the total TB and non-TB group. The student's t-test was used for the age comparison between TB and non-TB group, Fisher's exact test was used for gender comparison between TB and non-TB group, and the Mann-Whitney U-test was used for the comparison of $CD4^+$ T cell counts between TB and non-TB group.
$^{\$}CD4^+$ T cell counts were missed among 11 TB patients and 4 non-TB patients.

TABLE 2 Analysis of the concordance between the *IP-10* mRNA release assay and the QFT-GIT assay.

		QFT-GIT		Agreement (95%CI)	Kappa value (95%CI)
		Positive	Negative		
IP-10 mRNA release assay	Positive	44	41	65.1 (57.5 – 72.8)	0.33 (0.19 – 0.46)
	Negative	11	53		

than those in the non-TB patients (Figure 2A). The ROC analysis showed that the AUC value for the *IP-10* mRNA release assay was 0.70 (95%CI =0.62 – 0.77), with a sensitivity of 65.3% (95%CI = 55.9% – 73.8%) and a specificity of 74.2% (95%CI = 55.4% – 88.1%). Meanwhile, the results of the QFT-GIT assay showed that the *M.tb*-specific IFN-γ concentrations were also significantly higher in the TB patients than those in the non-TB patients (Figure 2B). The ROC analysis showed that the AUC value for the QFT-GIT assay was 0.65 (95%CI = 0.57 – 0.72), with a sensitivity of 43.2% (95%CI = 34.1% – 52.7%) and a specificity of 87.1% (95%CI = 70.2% – 96.4), respectively. The sensitivity of the *IP-10* mRNA release assay was significantly higher than that of the QFT-GIT assay ($P = 0.00062$), while no significant difference was detected in the specificities between the *IP-10* mRNA release assay and the QFT-GIT assay ($P = 0.198$).

The diagnostic performance of the combination of *IP-10* mRNA release assay and QFT-GIT assay was also evaluated, and the positive result was assumed when either test was positive and a negative result was deemed when both tests were negative (Table 3). Based on this standard, the diagnostic sensitivity and specificity

TABLE 3 Diagnostic performance of the *IP-10* mRNA release assay and QFT-GIT assay for TB.

	TB (N =118)	Non-TB (n = 31)	Sensitivity% (95%CI)	Specificity% (95%CI)	NPV% (95%CI)	PPV% (95%CI)	LR+ (95% CI)	LR- (95% CI)
IP-10 mRNA release assay			65.3 (55.9–73.8)	74.2 (55.4–88.1)	35.9 (28.9–43.7)	90.6 (83.9–94.7)	2.53 (1.40–4.70)	0.47 (0.30–0.60)
Positive	77	8						
Negative	41	23						
QFT-GIT			43.2 (34.1–52.7)	87.1 (70.2–96.4)	28.7 (24.7–33.2)	92.7 (83.3–97.0)	3.35 (1.30–8.60)	0.65 (0.50–0.80)
Positive	51	4						
Negative	67	27						
IP-10 or QFT-GIT *			73.7 (64.8–81.4)	71.0 (52.0–85.8)	41.5 (32.7–50.8)	90.6 (84.7–94.4)	2.54 (1.40–4.40)	0.37 (0.30-0.50)
Positive	87	9						
Negative	31	22						

NPV, negative predictive value; PPV, positive predictive value; LR+, likelihood ratio for positive test; LR–, likelihood ratio for negative value.
*A result was considered positive when either test was positive, and a result was deemed negative when both tests were negative.

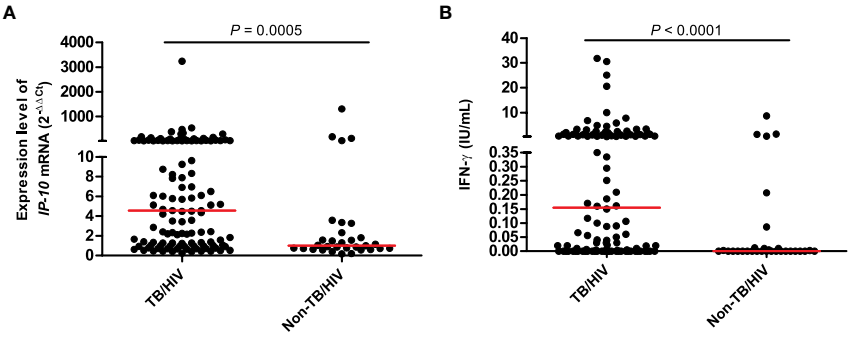

FIGURE 2
The expression level of *IP-10* mRNA in *IP-10 mRNA* release assay **(A)** and the released IFN-γ concentration in QFT-GIT assay **(B)**. TB/HIV group: n = 118; Non-TB/HIV group: n = 31; the Mann-Whitney U-test was used to perform the comparison of the expression level of *IP-10* mRNA between TB and non-TB group, as well as the comparison of IFN-γ concentration between TB and non-TB group.

were 73.7% (95%CI = 64.8%– 81.4%) and 71.0% (95%CI = 52.0%–85.8%), respectively. In comparison with the QFT-GIT assay alone, the combination of tests significantly increased the sensitivity of TB detection by 30.5%, although this was accompanied by a 16.1% decrease in the specificity. However, the highly improved sensitivity may be of great benefit for identifying of TB in HIV-infected individuals.

Subgroup analyses were also performed in definite TB group and probable TB group (Supplementary Table 1). The sensitivities of the *IP-10* mRNA release assay and the QFT-GIT assay in the definite TB group were 68.2% (95%CI = 55.6%– 79.1%)and 47.0% (95%CI = 34.6%– 59.7%), respectively. The sensitivities of the *IP-10* mRNA release assay and the QFT-GIT assay in the probable TB group were 61.5% (95%CI = 47.0%– 74.7%)and 38.5% (95%CI = 25.3%– 53.0%), respectively. Significant differences were detected in the sensitivity between the *IP-10* mRNA release assay and the QFT-GIT assay, in both definite TB group ($P = 0.0137$) and probable TB group ($P = 0.0186$). However, there is no significant differences in the sensitivity between definite TB group and probable TB group, either in the *IP-10* mRNA release assay ($P = 0.452$) or in the QFT-GIT assay ($P = 0.354$).

The impact of $CD4^+$ T cell exhaustion on the *IP-10* mRNA release assay and the QFT-GIT assay

Both the *IP-10* mRNA release assay and QFT-GIT assay function on the basis of the lymphocyte response to *M.tb*-specific antigens. Since $CD4^+$ T cells exhaustion commonly occurred in HIV-infected individuals, we analyzed whether $CD4^+$ T cell exhaustion could affect the outcomes of the two tests. The indeterminate results rate and positive result rate of the two tests were calculated for the HIV-infected individuals with different amount of $CD4^+$ T cell counts. As shown in Figure 3A, there was no significant difference in the indeterminate result rate between the *IP-10* mRNA release assay and the QFT-GIT assay among HIV-positive patients with $CD4^+$ T cell counts > 200 cells/μL. However, the indeterminate result rates of the *IP-10* mRNA release assay were significantly lower than those of the QFT-GIT assay among the patients with $CD4^+$ T cell counts < 200 cells/μL (≤ 100 cells/μL: $P = 0.0015$; 101-200 cells/μL: $P = 0.0029$). No significant difference in the indeterminate result rate of the *IP-10* mRNA release assay was detected between patients with different amount of $CD4^+$T cells ($P > 0.05$), suggesting that there was no significant impact of $CD4^+$T cells exhaustion on the results of the *IP-10* mRNA release assay. However, the indeterminate result rate of the QFT-GIT assay was significantly higher in patients with $CD4^+$ T cell counts < 200 cells/μL than those in patients with $CD4^+$ T cell counts > 200 cells/μL ($P= 0.012$), suggesting that $CD4^+$ T cells exhaustion had a significant impact on the performance of the QFT-GIT assay.

As shown in Figure 3B, the positive result rate of the *IP-10* mRNA release assay was significantly higher than that of the QFT-GIT assay among TB/HIV co-infected patients with $CD4^+$ T cell counts < 350 cells/μL (≤ 100 cells/μL: $P = 0.015$; 101-200 cells/μL: $P = 0.047$; 201-350cells/μL: $P = 0.027$). Furthermore, no significant difference in the positive result rate of the *IP-10* mRNA release assay was detected between TB/HIV co-infected patients with different amounts of $CD4^+$ T cells ($P > 0.05$), also indicating that there was no significant impact of $CD4^+$ T cells exhaustion on the performance of the *IP-10* mRNA release assay. Nevertheless, the positive result rate of the QFT-GIT assay was significantly higher in the TB/HIV co-infected patients with $CD4^+$ T cell counts > 350 cells/μL than those in the patients with $CD4^+$ T cell counts < 350 cells/μL (≤ 100 cells/μL *vs.*> 350 cells/μL: $P = 0.020$; 101-200 cells/μL *vs.*> 350 cells/μL: $P = 0.009$; 201-350 cells/μL *vs.*> 350 cells/μL: $P = 0.037$), indicating that $CD4^+$ T cells exhaustion had a significant impact on the outcome of the QFT-GIT assay.

Discussion

The identification of TB cases and the implementation of anti-TB treatment in high risk population, including HIV-infected individuals, have been recommended by the WHO (WHO, 2023). However, the utility of traditional immunological tests (e. g. tuberculin test and IGRAs) has been limited for auxiliary TB diagnosis in immunocompromised individuals (Cattamanchi

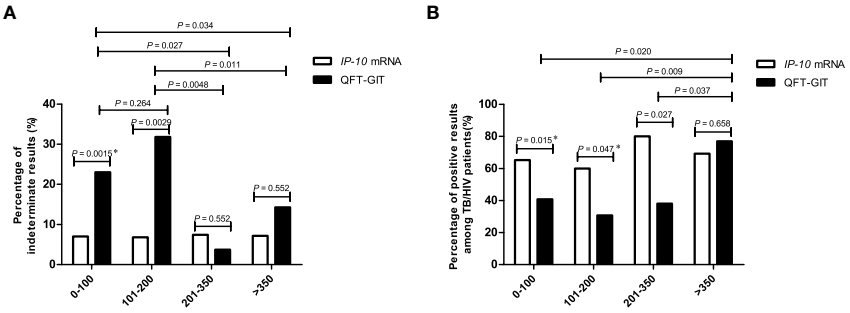

FIGURE 3
The percentages of indeterminate results and positive results of the *IP-10* mRNA release assay and the QFT-GIT assay in HIV-infected patients with different $CD4^+$ T-cell counts. **(A)** The percentages of indeterminate results obtained via each of the tests in the cohort of HIV-infected individuals enrolled in this study. The number of patients with different $CD4^+$ T cells were described as follow: ≤ 100/μL,n = 100; 101-200/μL, n = 44; 201-350/μL, n = 27; > 350/μL, n = 14. The $CD4^+$ T cell counts were missed in 15 patients. *Pearson's Chi-square test was used for comparison of the percentage of indeterminate results between *IP-10* mRNA release assay and QFT-GIT in the patients with $CD4^+$ T cells counts less than 100/μL. Other comparisons were performed using Fisher's exact test between patients with different $CD4^+$ T cells counts, or between *IP-10* mRNA release assay and QFT-GIT. **(B)** The percentages of positive results obtained by each of the tests among TB/HIV co-infected individuals. The number of TB/HIV co-infected patients with different $CD4^+$ T cells were described as follow: ≤ 100/μL, n = 49; 101-200/μL, n = 25; 201-350/μL, n = 20; > 350/μL, n = 13. The $CD4^+$ T cell counts were missed in 11 TB/HIV co-infected patients. *Pearson's Chi-square test was used for comparison of the percentage of positive results between *IP-10* mRNA release assay and QFT-GIT in the patients with $CD4^+$ T cells counts less than 100/μL, as well as in the patients with $CD4^+$ T cells counts range from 101/μL to 200/μL. Other comparisons were performed using Fisher's exact test between patients with different $CD4^+$ T cells counts, or between *IP-10* mRNA release assay and QFT-GIT.

et al., 2011). In this study, we used *IP-10* mRNA as a target due to its higher transient expression levels after stimulation with *M.tb*-specific antigens. We found that the *IP-10* mRNA release assay had a positive rate (65.3%) for the detection of TB in HIV co-infected individuals that was more than 20% higher than that of the conventional QFT-GIT assay. This result was consistent with previous studies that used the IP-10 protein as a target. Data from countries with a moderate or low TB burden suggested that when used as a target, the IP-10 protein yielded a higher positive rate (66.7%) of diagnosing *M. tb* infection than the IGRAs (52.4%) among HIV-infected persons. Furthermore, the outcome of the IP-10 protein detection test is not influenced by the reduction in $CD4^+$ T cell counts due to HIV-mediated exhaustion (Vanini et al., 2012). It was also reported that the IP-10 protein test had a higher positive rate (45.0% *vs.* 38.0%) and a lower indeterminate rate (5.0% *vs.* 9.0%) than the IGRAs test in HIV-infected individuals from a country with a higher TB burden (Kabeer et al., 2011). Another study has shown that IP-10 protein instead of IFN-γ yielded higher positive rate either after stimulation with commercial *M.tb* antigens in IGRA test (85.7% *vs.* 60.7%) or stimulation with in-house *M.tb* antigens (75.0% *vs.* 42.9%) (Goletti et al., 2010). Our results and these previous reports collectively indicated that either the IP-10 protein or its mRNA could improve the identification of TB among HIV-infected persons. We envisage that this strategy will help early screen of active TB in immuno-compromised individuals.

The higher positive rate of the *IP-10* mRNA release assay in TB/HIV co-infected individuals may be due to the higher expression level of *IP-10* mRNA after *M.tb* specific antigen stimulation. As a downstream amplification molecule of IFN-γ-mediated signaling, IP-10 is more highly expressed than IFN-γ (Tsuboi et al., 2011). On the other hand, IP-10 is not only released in response to IFN-γ stimulation, but is also induced by other cytokines, including IFN-α, IL-17 and IL-23 (Khader et al., 2007; Simmons et al., 2013). Furthermore, IP-10 is mainly released by monocytes, meaning that the impact of $CD4^+$ T cell exhaustion on the outcome of the *IP-10* mRNA release assay will be lower (Wu et al., 2017).

The specificity of the *IP-10* mRNA release assay was lower than that of QFT-GIT assay in non-TB patients, although the difference did not reach statistical significance. Since the study design involved the prospective enrollment of highly suspected TB patients with HIV infection, there were only 48 non-TB patients enrolled in the study. Of these non-TB patients, 31 had both valid results of the *IP-10* mRNA release assay and the QFT-GIT assay. The small size of the non-TB patients may lead to the enlarged difference between the specificities of these two tests. Our previous study found that there was no significant difference in specificity between the *IP-10* mRNA release assay and the IGRA assay among patients without HIV infection (Pan et al., 2022). Furthermore, Vanini et al. also reported that although IP-10 protein as a target yielded a slight higher positive result rate than that IFN-γ as a target in the non-TB patients with HIV infection, there were no significant differences between the use of IP-10 and IFN-γ as a target either in individuals with a higher risk of *M.tb* infection (IP-10 40.0%*vs.* IFN-γ 37.5%) or in individuals with a lower risk of *M.tb* infection (IP-10 12.9%*vs.* IFN-γ 4.8%) (Vanini et al., 2012). However, given that there is no gold standard test for latent *M.tb* infection, we cannot determine whether those patients with negative IGRA results but positive IP-10 results are *M.tb* infection or not. Therefore, we should also pay attention to the abovementioned patients and performed further exploration in a larger sample set. In addition, the positive results of these two tests in non-TB patients may be caused by the higher rate of latent TB infection (LTBI) in China. The previously estimated prevalence of LTBI in China was about 20.3% among persons older than 15 years, based on the results of the IGRA tests (Gao et al., 2015; Institute of Pathogen Biology, CAMS, et al., 2022). This value is consistent with the positive result rate in the non-TB patients in

our study. Since, like IGRAs, the *IP-10* mRNA release assay is also a method for the diagnosis of *M.tb* infection and auxiliary method for diagnosis of TB, some positive results within the non-TB patient group were also expected.

The *IP-10* mRNA release assay and the QFT-GIT assay both detect the host immune response to antigen stimulation. Due to the dysfunctional immune system of HIV-infected persons, some of the patients presented no response to the PHA positive control, which was the main reason for the indeterminate results. Our data also showed that a significantly higher number of patients with $CD4^+$ T cell counts below 200 cells/μL had invalid test results. Nevertheless, the indeterminate result rate of the *IP-10* mRNA release assay was significantly lower than that of the QFT-GIT assay, which may be caused by the different antigens used in the two tests. There may also be another reason for the stronger response to *M.tb*-specific antigens exhibited by the *IP-10* mRNA release assay; the higher expression level of the *IP-10* mRNA may lead to more positive results (and fewer indeterminate ones) even in the absence of a response to the PHA positive control.

In the present study, the concordance between the *IP-10* mRNA release assay and QFT-GIT assay was low. This may be due to the different targets (IP-10 *vs.* IFN-γ) and the different expression level (mRNA *vs*. protein) between the two tests. Furthermore, the *M.tb*-specific antigens were different between the two tests. The antigens in the QFT-GIT assay were ESAT-6, CFP-10 and TB7.7, while the antigens in the *IP-10* mRNA release assay were ESAT6, CFP-10 and PPE68. It is worth noting that the negative concordance rate between the two tests in non-TB patients was better than the positive concordance rate between the two tests in TB patients. This lower positive concordance rate mainly due to the lower sensitivity of the QFT-GIT test and represents a further significant difference between the two tests in HIV-infected individuals.

The results of the QFT-GIT test were influenced by $CD4^+$ T cells exhaustion, while those of the *IP-10* mRNA release assay were not. When the $CD4^+$ T cell counts were at a normal level (>350 cells/μL), there was no significant difference between the indeterminate rate or sensitivity of the *IP-10* mRNA release assay and the QFT-GIT assay. These results were consistent with our previous study involving non-HIV individuals (Pan et al., 2022). However, the indeterminate result rate of the QFT-GIT assay was higher and the sensitivity was lower when $CD4^+$ T cell counts decreased. This is likely because HIV infection impairs $CD4^+$ T cell proliferation and function (Day et al., 2017; Amelio et al., 2019) and leads to dysfunctional Th1 immune response, which reduces IFN-γ release. It is currently believed that the reduction in IFN-γ release due to the depletion of *M.tb*-specific Th1 cells during HIV infection is a typical mechanism by which the virus damages host defense against *M.tb* (Kalsdorf et al., 2009). The lesser impact of $CD4^+$ T cells exhaustion on the performance of the *IP-10* mRNA release assay indicates that the release of *IP-10* mRNA may not be completely dependent on $CD4^+$ T cells. Flow cytometry was used to shown that the expression of high levels of *IP-10* mRNA in HIV-infected individuals was mainly a feature of monocytes and myeloid dendritic cells (mDCs) (Rempel et al., 2010; Simmons et al., 2013). Although *IP-10* mRNA in T lymphocytes was also up-regulated after HIV infection, it gradually decreased following antiviral treatment initiation (Foley et al., 2005). Therefore, unlike the release kinetics of IFN-γ, *IP-10* mRNA release may not depend on T lymphocytes and thus is less affected by the depletion of $CD4^+$ T cells induced by HIV infection. Furthermore, these results also suggested that the combined use of the *IP-10* mRNA release assay and conventional IGRAs assay could identify more individuals with TB.

Apart from the better performance of *IP-10* mRNA release assay in HIV co-infected populations, previously we also found that the performance of *IP-10* mRNA release assay was similar with IGRA in patients without HIV co-infection, indicating the wider application of *IP-10* mRNA release assay in clinical practice (Pan et al., 2022). Furthermore, there are some other advantages. Firstly, The higher expression level of *IP-10* mRNA after *M.tb* antigen stimulation leads to higher sensitivity in diagnosis, and it is better to avoid the adverse effects of non-specific IP-10 release by other infections or background IP-10 release. Furthermore, the whole procedures of *IP-10* mRNA release assay are automatic and this will reduce the bias by manual operation. In addition, the detection linear range of the PCR technique is wider than that of ELISA test, and it does not rely on a standard curve to determine concentrations. Lastly, after covid-19 pandemic, the PCR technique is already an integrated tool in most TB laboratories and the cost is reduced due to the widely use in clinical practice, so the PCR platform used for diagnosis is reasonable. In the present study, we prospectively evaluate the diagnostic performance of the *IP-10* mRNA release assay in the diagnosis of TB in a cohort of HIV-infected individuals. However, our research has limitations. Firstly, it would have been beneficial to validate the inconsistencies between the *IP-10* mRNA release assay and QFT-GIT test results using a third method. However, the fact that the positive result rate of the *IP-10* mRNA release assay was significantly higher than that of the QFT-GIT assay in the group of patients with definite TB (who had microbiological evidence for *M.tb* infection) indirectly indicates the better performance of the *IP-10* mRNA release assay. Secondly, our study only prospectively enrolled patients from multiple centers within one year. This meant that the sample size was not large enough to evaluate of the performance of IP-10 for diagnosing TB in HIV-infected individuals, although it is larger than previous studies. Further validation in a larger sample set would yield more convincing evidence. Thirdly, we did not analyze the impact of the antiretroviral therapy on the performance of the two tests due to the limited sample size. In future, an in-depth analysis of diagnostic performance of *IP-10* mRNA release assay for TB in patients receiving different forms or duration of antiretroviral therapy will facilitate for reasonable utility of this novel test. Finally, this study was performed in adults. Whether the *IP-10* mRNA release assay performs better in immunocompromised children with suspected TB should be validated in future studies.

In conclusion, our study has evaluated side by side the performance of the two tests which are based on whole blood antigen stimulation, and confirmed that the *IP-10* mRNA release assay was superior at detecting TB in HIV-infected patients than the conventional QFT-GIT test. The higher sensitivity and lower indeterminate result rate of the *IP-10* mRNA release assay will

likely aid the early detection of TB in this higher risk population of immunocompromised individuals.

Data availability statement

The raw data supporting the conclusions of this article will be made available by the authors, without undue reservation.

Ethics statement

The studies involving human participants were reviewed and approved by the Ethics Committee of the Shanghai Public Health Clinical Center. The patients/participants provided their written informed consent to participate in this study.

Author contributions

YS, LP, JW, YY and QW designed the experiments. YT, RS, YL, YZ, RM, BP and QS conducted the experiments. YY, ZW, HA, HJ, SB and AX enrolled the subjects. LP and YT analyzed the data. LP wrote the paper. All authors contributed to the article and approved the submitted version.

Funding

This work was supported by grants from the Tongzhou Science and Technology Project (KJ2022CX042), National Natural Science Foundation (82172279), National Key Research and Development Program of China (2022YFA130350) and Tongzhou Yunhe Project (YH201807 and YH202001).

Acknowledgments

We thank the research nurses at the five hospitals for their work in recruitment of participants.

Conflict of interest

The authors declare that the research was conducted in the absence of any commercial or financial relationships that could be construed as a potential conflict of interest.

Publisher's note

Supplementary material

The Supplementary Material for this article can be found online at: https://www.frontiersin.org/articles/10.3389/fcimb.2023.1152665/full#supplementary-material

References

AIDS and Hepatitis Group of Infectious Diseases, Branch of Chinese Medical Association and Chinese Center for Disease Control and Prevention (2018). Guidelines for AIDS diagnosis and treatment in China. *Chin. J. Infect. Dis.* 36 (12), 705–724. doi: 10.3760/cma.j.issn.1000-6680.2018.12.001

Amelio, P., Portevin, D., Hella, J., Reither, K., Kamwela, L., Lweno, O., et al. (2019). HIV Infection functionally impairs mycobacterium tuberculosis-specific CD4 and CD8 T-cell responses. *J. Virol.* 93 (5), e01728-18. doi: 10.1128/JVI.01728-18

Bell, L. C. K., and Noursadeghi, M. (2018). Pathogenesis of HIV-1 and mycobacterium tuberculosis co-infection. *Nat. Rev. Microbiol.* 16 (2), 80–90. doi: 10.1038/nrmicro.2017.128

Blauenfeldt, T., Heyckendorf, J., Graff Jensen, S., Lange, C., Drabe, C., Hermansen, T. S., et al. (2014). Development of a one-step probe based molecular assay for rapid immunodiagnosis of infection with m. tuberculosis using dried blood spots. *PloS One* 9 (9), e105628. doi: 10.1371/journal.pone.0105628

Cattamanchi, A., Smith, R., Steingart, K. R., Metcalfe, J. Z., Date, A., Coleman, C., et al. (2011). Interferon-gamma release assays for the diagnosis of latent tuberculosis infection in HIV-infected individuals: a systematic review and meta-analysis. *J. Acquir. Immune Defic. Syndr.* 56 (3), 230–238. doi: 10.1097/QAI.0b013e31820b07ab

Day, C. L., Abrahams, D. A., Harris, L. D., van Rooyen, M., Stone, L., de Kock, M., et al. (2017). HIV-1 infection is associated with depletion and functional impairment of mycobacterium tuberculosis-specific CD4 T cells in individuals with latent tuberculosis infection. *J. Immunol.* 199 (6), 2069–2080. doi: 10.4049/jimmunol.1700558

Fisher, K. L., Moodley, D., Rajkumar-Bhugeloo, K., Baiyegunhi, O. O., Karim, F., Ndlovu, H., et al. (2022). Elevated IP-10 at the protein and gene level associates with pulmonary TB. *Front. Cell Infect. Microbiol.* 12, 908144. doi: 10.3389/fcimb.2022.908144

Foley, J. F., Yu, C. R., Solow, R., Yacobucci, M., Peden, K. W., and Farber, J. M. (2005). Roles for CXC chemokine ligands 10 and 11 in recruiting CD4+ T cells to HIV-1-infected monocyte-derived macrophages, dendritic cells, and lymph nodes. *J. Immunol.* 174 (8), 4892–4900. doi: 10.4049/jimmunol.174.8.4892

Gao, L., Lu, W., Bai, L., Wang, X., Xu, J., Catanzaro, A., et al. (2015). Latent tuberculosis infection in rural China: baseline results of a population-based, multicentre, prospective cohort study. *Lancet Infect. Dis.* 15 (3), 310–319. doi: 10.1016/S1473-3099(14)71085-0

Getahun, H., Matteelli, A., Chaisson, R. E., and Raviglione, M. (2015). Latent mycobacterium tuberculosis infection. *N Engl. J. Med.* 372 (22), 2127–2135. doi: 10.1056/NEJMra1405427

Goletti, D., Raja, A., Syed Ahamed Kabeer, B., Rodrigues, C., Sodha, A., Carrara, S., et al. (2010). Is IP-10 an accurate marker for detecting m. tuberculosis-specific response in HIV-infected persons? *PloS One* 5 (9), e12577. doi: 10.1371/journal.pone.0012577

Ignatius, E. H., and Swindells, S. (2020). Are we there yet? short-course regimens in TB and HIV: from prevention to treatment of latent to XDR TB. *Curr. HIV/AIDS Rep.* 17 (6), 589–600. doi: 10.1007/s11904-020-00529-8

Institute of Pathogen Biology, China Academy of Medical Sciences and Peking Union Medical College, China Center for Disease Control and Prevention, Union Medical Institute of Geographic Sciences and Natural Resources Research and Chinese Academy of Sciences (2022). Expert consensus on the estimation of the national burden on latent tuberculosis infection. *Chin. J. Antituberculosis* 44 (1), 4–8. doi: 10.19982/j.issn.1000-6621.20210662

Jung, J. Y., Lim, J. E., Lee, H. J., Kim, Y. M., Cho, S. N., Kim, S. K., et al. (2012). Questionable role of interferon-gamma assays for smear-negative pulmonary TB in

immunocompromised patients. *J. Infect.* 64 (2), 188–196. doi: 10.1016/j.jinf.2011.09.008

Kabeer, B. S., Sikhamani, R., and Raja, A. (2011). Comparison of interferon gamma-inducible protein-10 and interferon gamma-based QuantiFERON TB gold assays with tuberculin skin test in HIV-infected subjects. *Diagn. Microbiol. Infect. Dis.* 71 (3), 236–243. doi: 10.1016/j.diagmicrobio.2011.07.012

Kalsdorf, B., Scriba, T. J., Wood, K., Day, C. L., Dheda, K., Dawson, R., et al. (2009). HIV-1 infection impairs the bronchoalveolar T-cell response to mycobacteria. *Am. J. Respir. Crit. Care Med.* 180 (12), 1262–1270. doi: 10.1164/rccm.200907-1011OC

Khader, S. A., Bell, G. K., Pearl, J. E., Fountain, J. J., Rangel-Moreno, J., Cilley, G. E., et al. (2007). IL-23 and IL-17 in the establishment of protective pulmonary CD4+ T cell responses after vaccination and during mycobacterium tuberculosis challenge. *Nat. Immunol.* 8 (4), 369–377. doi: 10.1038/ni1449

Kumar, N. P., Hissar, S., Thiruvengadam, K., Banurekha, V. V., Suresh, N., Shankar, J., et al. (2021). Discovery and validation of a three-cytokine plasma signature as a biomarker for diagnosis of pediatric tuberculosis. *Front. Immunol.* 12, 653898. doi: 10.3389/fimmu.2021.653898

Lu, C., Wu, J., Wang, H., Wang, S., Diao, N., Wang, F., et al. (2011). Novel biomarkers distinguishing active tuberculosis from latent infection identified by gene expression profile of peripheral blood mononuclear cells. *PloS One* 6 (8), e24290. doi: 10.1371/journal.pone.0024290

MacLean, E., Saravu, K., and Pai, M. (2019). Diagnosing active tuberculosis in people living with HIV: an ongoing challenge. *Curr. Opin. HIV AIDS* 14 (1), 46–54. doi: 10.1097/COH.0000000000000512

Metcalfe, J. Z., Everett, C. K., Steingart, K. R., Cattamanchi, A., Huang, L., Hopewell, P. C., et al. (2011). Interferon-gamma release assays for active pulmonary tuberculosis diagnosis in adults in low- and middle-income countries: systematic review and meta-analysis. *J. Infect. Dis.* 204 Suppl 4, S1120–S1129. doi: 10.1093/infdis/jir410

Mhango, D. V., Mzinza, D. T., Jambo, K. C., and Mwandumba, H. C. (2021). New management approaches to tuberculosis in people living with HIV. *Curr. Opin. Infect. Dis.* 34 (1), 25–33. doi: 10.1097/QCO.0000000000000704

Ortakoylu, M. G., Bahadir, A., Iliaz, S., Soy Bugdayci, D., Uysal, M. A., Paker, N., et al. (2022). Interferon-inducible protein-10 as a marker to detect latent tuberculosis infection in patients with inflammatory rheumatic diseases. *J. Pers. Med.* 12 (7), 1027. doi: 10.3390/jpm12071027

Pan, L., Gao, M., Jia, H., Huang, M., Wei, R., Sun, Q., et al. (2021). Diagnostic performance of a novel mycobacterium tuberculosis specific T-cell based assay for tuberculosis. *Chin. J. Tuberculosis Respir. Dis.* 44 (5), 1–7. doi: 10.3760/cma.j.cn112147-20200821-00916

Pan, L., Huang, M., Jia, H., Deng, G., Chen, Y., Wei, R., et al. (2022). Diagnostic performance of a novel CXCL10 mRNA release assay for mycobacterium tuberculosis infection. *Front. Microbiol.* 13, 825413. doi: 10.3389/fmicb.2022.825413

Pan, L., Jia, H., Liu, F., Sun, H., Gao, M., Du, F., et al. (2015). Risk factors for false-negative T-SPOT.TB assay results in patients with pulmonary and extra-pulmonary TB. *J. Infect.* 70 (4), 367–380. doi: 10.1016/j.jinf.2014.12.018

Qiu, X., Tang, Y., Yue, Y., Zeng, Y., Li, W., Qu, Y., et al. (2019a). Accuracy of interferon-gamma-induced protein 10 for diagnosing latent tuberculosis infection: a systematic review and meta-analysis. *Clin. Microbiol. Infect.* 25 (6), 667–672. doi: 10.1016/j.cmi.2018.12.006

Qiu, X., Xiong, T., Su, X., Qu, Y., Ge, L., Yue, Y., et al. (2019b). Accumulate evidence for IP-10 in diagnosing pulmonary tuberculosis. *BMC Infect. Dis.* 19 (1), 924. doi: 10.1186/s12879-019-4466-5

Rempel, H., Sun, B., Calosing, C., Pillai, S. K., and Pulliam, L. (2010). Interferon-alpha drives monocyte gene expression in chronic unsuppressed HIV-1 infection. *AIDS* 24 (10), 1415–1423. doi: 10.1097/QAD.0b013e32833ac623

Ruhwald, M., Aabye, M. G., and Ravn, P. (2012). IP-10 release assays in the diagnosis of tuberculosis infection: current status and future directions. *Expert Rev. Mol. Diagn.* 12 (2), 175–187. doi: 10.1586/erm.11.97

Ruhwald, M., Dominguez, J., Latorre, I., Losi, M., Richeldi, L., Pasticci, M. B., et al. (2011). A multicentre evaluation of the accuracy and performance of IP-10 for the diagnosis of infection with m. tuberculosis. *Tuberculosis (Edinb)* 91 (3), 260–267. doi: 10.1016/j.tube.2011.01.001

Santin, M., Munoz, L., and Rigau, D. (2012). Interferon-gamma release assays for the diagnosis of tuberculosis and tuberculosis infection in HIV-infected adults: a systematic review and meta-analysis. *PloS One* 7 (3), e32482. doi: 10.1371/journal.pone.0032482

Schmittgen, T. D., and Livak, K. J. (2008). Analyzing real-time PCR data by the comparative C(T) method. *Nat. Protoc.* 3 (6), 1101–1108. doi: 10.1038/nprot.2008.73

Scott, L., da Silva, P., Boehme, C. C., Stevens, W., and Gilpin, C. M. (2017). Diagnosis of opportunistic infections: HIV co-infections - tuberculosis. *Curr. Opin. HIV AIDS* 12 (2), 129–138. doi: 10.1097/COH.0000000000000345

Simmons, R. P., Scully, E. P., Groden, E. E., Arnold, K. B., Chang, J. J., Lane, K., et al. (2013). HIV-1 infection induces strong production of IP-10 through TLR7/9-dependent pathways. *AIDS* 27 (16), 2505–2517. doi: 10.1097/01.aids.0000432455.06476.bc

Tsuboi, H., Wakamatsu, E., Iizuka, M., Nakamura, Y., Sugihara, M., Suzuki, T., et al. (2011). Importance of serine727 phosphorylated STAT1 in IFNgamma-induced signaling and apoptosis of human salivary gland cells. *Int. J. Rheum Dis.* 14 (1), 86–91. doi: 10.1111/j.1756-185X.2010.01575.x

Uzorka, J. W., Bakker, J. A., van Meijgaarden, K. E., Leyten, E. M. S., Delfos, N. M., Hetem, D. J., et al. (2022). Biomarkers to identify mycobacterium tuberculosis infection among borderline QuantiFERON results. *Eur. Respir. J.* 60 (2), 2102665. doi: 10.1183/13993003.02665-2021

Vanini, V., Petruccioli, E., Gioia, C., Cuzzi, G., Orchi, N., Rianda, A., et al. (2012). IP-10 is an additional marker for tuberculosis (TB) detection in HIV-infected persons in a low-TB endemic country. *J. Infect.* 65 (1), 49–59. doi: 10.1016/j.jinf.2012.03.017

World health organization (2022). *Global tuberculosis report 2021* (Geneva: World Health Organization).

World health organization (2023). *WHO standard: universal access to rapid tuberculosis diagnostics* (Geneva: World Health Organization).

Wu, U. I., Chuang, Y. C., Sheng, W. H., Sun, H. Y., Jhong, Y. T., Wang, J. Y., et al. (2018). Use of QuantiFERON-TB gold in-tube assay in screening for neutralizing anti-interferon-gamma autoantibodies in patients with disseminated nontuberculous mycobacterial infection. *Clin. Microbiol. Infect.* 24 (2), 159–165. doi: 10.1016/j.cmi.2017.06.029

Wu, X., Zhang, L. L., Yin, L. B., Fu, Y. J., Jiang, Y. J., Ding, H. B., et al. (2017). Deregulated MicroRNA-21 expression in monocytes from HIV-infected patients contributes to elevated IP-10 secretion in HIV infection. *Front. Immunol.* 8, 1122. doi: 10.3389/fimmu.2017.01122

frontiers | Frontiers in Immunology

TYPE Case Report
PUBLISHED 14 September 2023
DOI 10.3389/fimmu.2023.1249878

OPEN ACCESS

EDITED BY
Amit Singh,
Central University of Punjab, India

REVIEWED BY
Deepak Tripathi,
The University of Texas Health Science Center at Tyler, United States
Priyam Batra,
All India Institute of Medical Sciences, India
Ravi Ranjan Kumar,
Jawaharlal Nehru University, India

*CORRESPONDENCE
Xianming Zhang
zxm13078524367@163.com

†These authors have contributed equally to this work

RECEIVED 29 June 2023
ACCEPTED 25 August 2023
PUBLISHED 14 September 2023

CITATION
Weng T, Dong Y, Huang N, Zhao C, Zhang L, Cao S, Tang J, Zhang D and Zhang X (2023) Disseminated tuberculosis in a child during the COVID-19 pandemic: a case report and literature review. *Front. Immunol.* 14:1249878. doi: 10.3389/fimmu.2023.1249878

Disseminated tuberculosis in a child during the COVID-19 pandemic: a case report and literature review

Taoping Weng†, Yaqiong Dong†, Niwen Huang†, Chenqu Zhao, Lei Zhang, Shan Cao, Jing Tang, Danni Zhang and Xianming Zhang*

Department of Respiratory and Critical Care Medicine, The Affiliated Hospital of Guizhou Medical University, Guiyang, China

Background: Disseminated tuberculosis is an uncommon but devastating form of tuberculosis, possibly developing with the immune response of patients. COVID-19 infection may produce an immunosuppressive effect with possible implications for tuberculosis dissemination.

Case presentation: A 17-year-old female patient with a history of tuberculous pleurisy presented to the hospital with a high fever and life-threatening dyspnea after contracting a COVID-19 infection. Her condition deteriorated rapidly with grand mal epilepsy and acute gastrointestinal bleeding with a grossly depressed CD4 T-cell count, which was indicative of her profoundly immunosuppressed state. After identifying *Mycobacterium tuberculosis* in her cerebrospinal fluid and a subcutaneous abscess in her left lower back, she was diagnosed with disseminated tuberculosis involving both lungs, the central nervous system, the terminal ileum, the liver, bilateral adnexal tissue, and subcutaneous soft tissue in accordance with the chest and abdominal CT. Empirical treatment was initiated with dexamethasone (5 mg/day) and an anti-tuberculosis regimen of isoniazid, rifampicin, pyrazinamide, amikacin, and meropenem, which was replaced with faropenem after she left the hospital. The therapeutic effect was considered satisfied in the second month of follow-up.

Conclusion: To the best of our knowledge, we report the first case report of disseminated tuberculosis after COVID-19 infection. Tuberculosis may disseminate and progress during the COVID-19 pandemic, requiring more significant studies to provide better diagnosis and treatment options for the co-infection.

KEYWORDS

tuberculosis, disseminated tuberculosis, COVID-19, immunosuppression, treatment, case report

Introduction

Tuberculosis (TB) is an ancient communicable disease that is a major cause of ill health and one of the leading causes of death globally. There were approximately 10.6 million patients with TB in 2021, according to the Global Tuberculosis Report (1), with partial increases in 2021 due to the coronavirus (COVID-19) pandemic. This includes impacts on the provision of and access to essential TB services, the number of people diagnosed with TB and notified as TB cases through national disease surveillance systems, and the TB disease burden, including incidence and mortality. Furthermore, COVID-19 may lead to TB progression and fatal outcomes with the increased production of inflammation factors (2). Usually, the predilection sites of tuberculosis were the lungs, while over 15% of tuberculosis cases occur in the form of extrapulmonary infections that can affect any tissue in the body and are particularly difficult to diagnose and treat (3). Dissemination of *Mycobacterium tuberculosis* out of the lungs is thought to be more than just a rare event leading to extrapulmonary tuberculosis, but rather a prerequisite step that occurs during all infections, producing secondary lesions that can become latent or productive (4). COVID-19 may diminish the pool of *Mycobacterium tuberculosis*-specific memory T cell responses, with possible implications for TB disease progression (5) and dissemination. Here we report a case of the diagnosis and treatment of a child with disseminated tuberculosis during the epidemic period of COVID-19.

Case presentation

A 17-year-old girl presented to our hospital on 31 January 2023, with 2 days of intermittent fever, dyspnea, and a maximum temperature of 38.5°C after a surgical operation for a perianal abscess. She had a history of tuberculous pleurisy, which was diagnosed the previous year, and complained of regular anti-tuberculosis treatment for the whole year. At the time of presentation, she was still on the anti-tuberculosis regimen of isoniazid, rifampicin, pyrazinamide, ethambutol, moxifloxacin, and linezolid. Meanwhile, the girl was infected with COVID-19, which was diagnosed by real-time PCR in December 2022. She denied a history of immunodeficiency virus (HIV) infection and hepatitis B and C. On 29 January 2023, she received an operation of incision and drainage of a perianal abscess at another hospital, and then the young patient experienced fever with chills, distress, and dyspnea. She came to our hospital for further emergency treatment.

On admission, she complained of obvious dyspnea with a temperature of 37.8°C, a heart rate of 167 per minute, a respiratory rate of 59 per minute, a blood pressure of 132/92 mmHg, and an oxygen saturation in room air of 74%. She was admitted to our respiratory intensive care unit due to critical hypoxia. Physical examination revealed moist rales in both lungs, slight neck rigidity, a positive Kerning's sign, a positive Brudzinski's sign, a regional subcutaneous mass with fluctuation in the left lower back, and a perianal wound after the operation. No other abnormal signs were found. Her laboratory results showed elevated white blood cells (15.91 g/L, normal value 4.1–11 g/L) with a mainly increasing count of neutrophils (14.34 g/L, normal value 1.8–8.3 g/L), anemia with decreased hemoglobin (86 g/L, normal value 114–145g/L), elevated C-reactive protein (89.98 mg/L, normal value < 5 mg/L), elevated serum adenosine deaminase (24.1 U/L, normal value < 20 U/L), and decreased CD4-T-lymphocytes (234/uL, normal value 554–1109/uL). The results of HIV infection and hepatitis B and C tests were negative. Considering intermittent fever, sputum smears and sputum and blood cultures of bacteria and fungus were also negative. Her bedside chest radiograph showed diffuse infectious foci in both lungs with a slight bilateral pleural effusion (Figure 1).

Unexpectedly, this patient soon developed grand mal epilepsy with loss of consciousness, a fixed gaze, and rigidity. We immediately operated on the lumbar puncture to obtain a specimen of her cerebrospinal fluid (CSF) to identify the cause of the epilepsy after the seizure was controlled. Her CSF results showed elevated interleukin-6 (421.70 pg/mL) with normal levels of CSF routine, biochemistry, and adenosine deaminase. Meanwhile, the CSF culture of bacteria was negative. Considering the possibility of tuberculous meningitis, an acid-fast bacilli smear, GeneXpert MTB/RIF, and next-generation sequencing (NGS) of her CSF were detected. Her CSF acid-fast bacilli smear and GeneXpert MTB/RIF were all negative. Simultaneously, her cranial computed tomography (CT) scan showed no abnormalities. Remarkably, *Mycobacterium tuberculosis* was detected according to the results of NGS, with evidence of high sensitivity and specificity in the diagnosis of tuberculous meningitis (6, 7). Tuberculous meningitis was confirmed, which led to the young patient's epilepsy seizure. Combined with her tuberculous pleurisy history and the diffuse foci in both of her lungs, this girl was diagnosed with disseminated tuberculosis involving at least the lungs, pleura, and central system. Considering the girl had

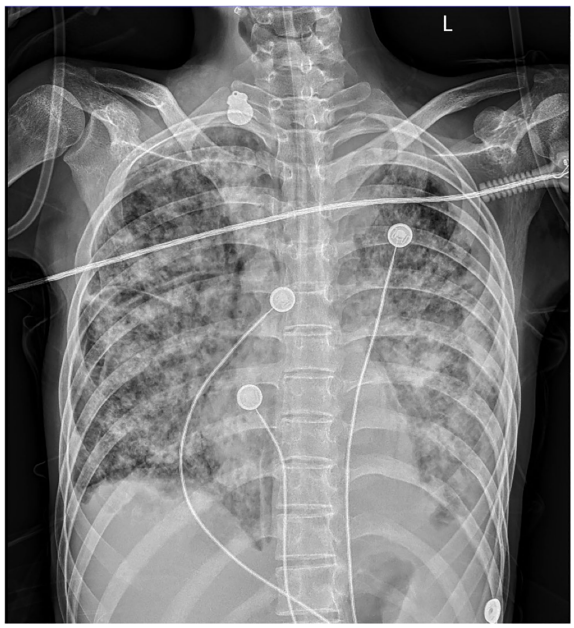

FIGURE 1
Bedside chest radiography. Diffuse infectious foci in both lungs with a slight bilateral pleural effusion.

moderate anemia, we stopped the linezolid with its main adverse effect of myelosuppression and continued the anti-tuberculosis regimen of isoniazid, rifampicin, pyrazinamide, and ethambutol, accompanied by the antibiotic piperacillin/tazobactam, to control pneumonia diagnosed on the bedside radiography. Meanwhile, thymalfasin (thymosin-alpha 1) was also used as an immune system enhancer for the treatment of the immunosuppressed patient with a grossly depressed CD4 T-cell count. The child's dyspnea subsided, her temperature sustained a normal level, and epilepsy never occurred again. The treatment seemed to be effective and the girl was transferred to the general ward of the respiratory department on 8 February 2023.

Nevertheless, the patient developed acute gastrointestinal bleeding with black tarry stool and severe anemia of 50g/L hemoglobin on the second day in the general ward, and the child complained of obvious left hypogastralgia. A physical examination showed unstable vital signs with a heart rate of 144 per minute, a respiratory rate of 25 per minute, a blood pressure of 98/52 mmHg, and a severe anemic appearance. Immediately, the patient was transferred to the intensive care unit again for monitoring and stabilization. Though persistent internal hemostatic treatment was carried out, there was still active gastrointestinal bleeding. Therefore, a gastroscopy and colonoscopy were performed. There was no active bleeding on the gastroscopy, while the colonoscopy revealed multiple hemorrhagic ulcers in the terminal ileum (Figure 2A), as well as ulcers in the rectum (Figure 2C) and anal fistula (Figure 2D). Argon plasma coagulation and hemoclip therapy (Figure 2B) were performed so that the gastrointestinal bleeding was resolved with a significant improvement. Since there was active bleeding in the terminal ileum, we did not get a biopsy of the lesions, which made it difficult to make a differential diagnosis between intestinal tuberculosis and Crohn's disease. We adjusted the treatment plan by adding the glucocorticoid (dexamethasone sodium phosphate, 5mg/day) for this girl with tuberculous meningitis, which was strongly recommended according to the World Health Organization (WHO) guidelines (8). In the meantime, the anti-tuberculosis regimen was regulated into isoniazid, rifampicin, pyrazinamide, amikacin (0.2g, I.V., q12 h), and meropenem (0.5g, I.V., q8 h), considering most bacteria and *Mycobacterium tuberculosis* were sensitive to the beta-lactam antibiotic, which was also recommended by the WHO guidelines for the treatment of drug-resistant tuberculosis (9).

The symptoms apparently subsided after our therapy and nursing care, and her vital signs were maintained at a normal level. Consequently, the patient was transferred to the general ward, where she could undergo chest and abdominal CT scans after the life-threatening stage. Her chest and abdominal CT showed multiple infectious foci and miliary nodules, considering

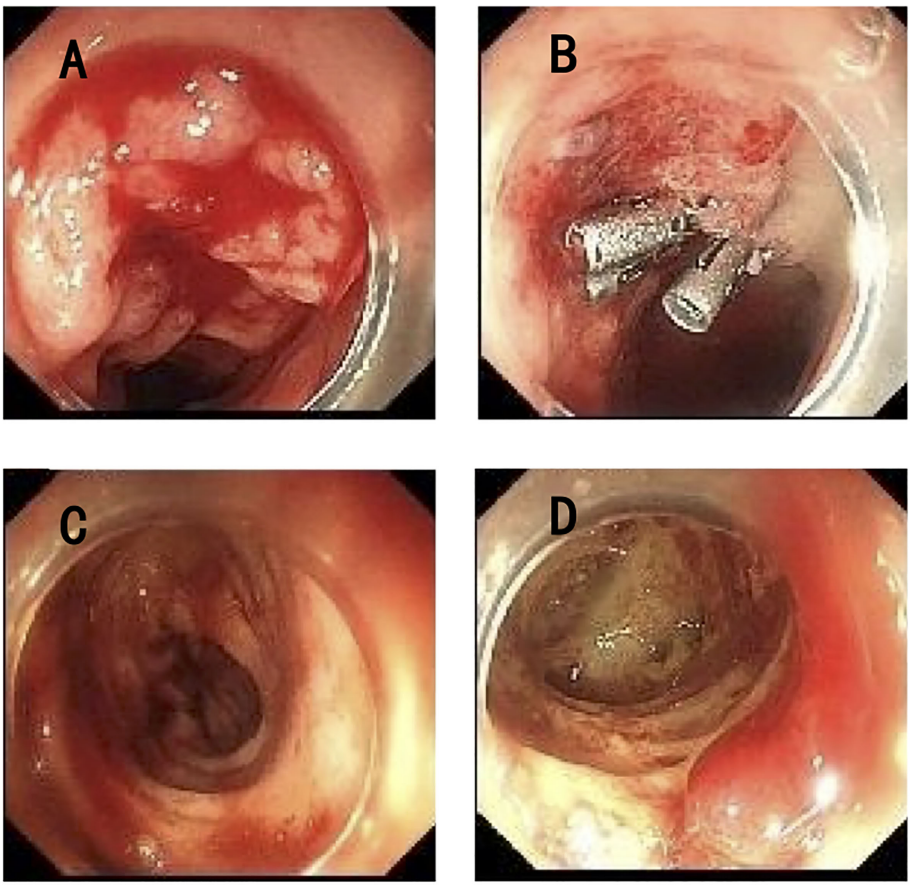

FIGURE 2
Endoscopy of the lower gastrointestinal tract. **(A)** Multiple ulcers with active bleeding in the terminal ileum. **(B)** Argon plasma coagulation and hemoclip therapy in the terminal ileum. **(C)** Multiple ulcers in the rectum. **(D)** Anal fistula.

tuberculosis and bacterial pneumonia, bilateral pleural effusion (Figures 3A–C), a low-density lesion in the left lobe of the liver, suspecting hepatic abscess, and slightly high-density and gas-accumulated lesions in bilateral adnexal and subcutaneous encapsulated effusion in the left lower back, considering tuberculosis cold abscess. We considered that the multiple lesions at the different sites originated from disseminated tuberculosis. The girl then underwent percutaneous puncture drainage of the subcutaneous encapsulated abscess, and her pus specimen acid-fast bacilli smear was positive, which established the diagnosis of disseminated tuberculosis. Thus, the girl continued the anti-tuberculosis regimen of isoniazid, rifampicin, pyrazinamide, amikacin, and meropenem, along with dexamethasone. The patient responded well to the treatment, with marked improvement in fever and lymphopenia (Figures 4A, B). She also suffered from a drug-induced liver injury, which interrupted the anti-tuberculosis therapy. After receiving liver function-protecting treatment containing bicyclol and ademetionine, her transaminase recovered to a normal level (Figures 4A, C). She underwent chest and abdominal CT on 6 March 2023, and, encouragingly, the multiple infection foci in both lungs and subcutaneous effusion in the left lower back were reduced (Figures 3a–c). The patient was discharged on 23 March 2023, continuing with an oral anti-tuberculosis regimen of isoniazid (0.3 g/day), rifampicin (0.45 g/day), pyrazinamide (1.0 g/day), and faropenem (0.2 g, T.i.d.). Constructive follow-up is still ongoing, with an obvious absorption of lesions on bilateral lungs in the second month (Figure 3i–iii), and we will adjust the anti-tuberculosis regimen based on the therapeutic efficacy and adverse effects of the patient.

Discussion and conclusion

Disseminated tuberculosis can cause systemic inflammatory response syndrome. Our report describes the case of a girl with tuberculous pleurisy under regular anti-tuberculosis therapy who developed disseminated tuberculosis involving both lungs, the central nervous system, the terminal ileum, the liver, bilateral adnexal tissue, and subcutaneous soft tissue after COVID-19 infection. The female patient's grossly depressed CD4 T-cell count was indicative of her profoundly immunosuppressed state, closely related to the extrapulmonary disseminated tuberculosis (10). SARS-Cov2 will probably continue to circulate (11), making the diagnosis and treatment of disseminated tuberculosis in patients with COVID-19 more important for clinicians.

Individuals infected with *Mycobacterium tuberculosis* may either have a latent tuberculosis infection or develop active tuberculosis disease. For active tuberculosis disease, a small subset of patients (19.3–39.3%) present with either primary extrapulmonary tuberculosis or concurrent pulmonary involvement (12). Pathogen-associated molecular pattern signaling, antigen presentation, and immune recognition may mediate latency induction and pathogen reactivation, which are also believed to be important in establishing the site of disease presentation and dissemination (13). Additionally, the recovery of the immune response profile of inflammatory cytokines was observed in children with pulmonary tuberculosis but not in those with extrapulmonary tuberculosis after 6 months of treatment, which suggested the host immune response following treatment is specific to the disease rather than due to the within-

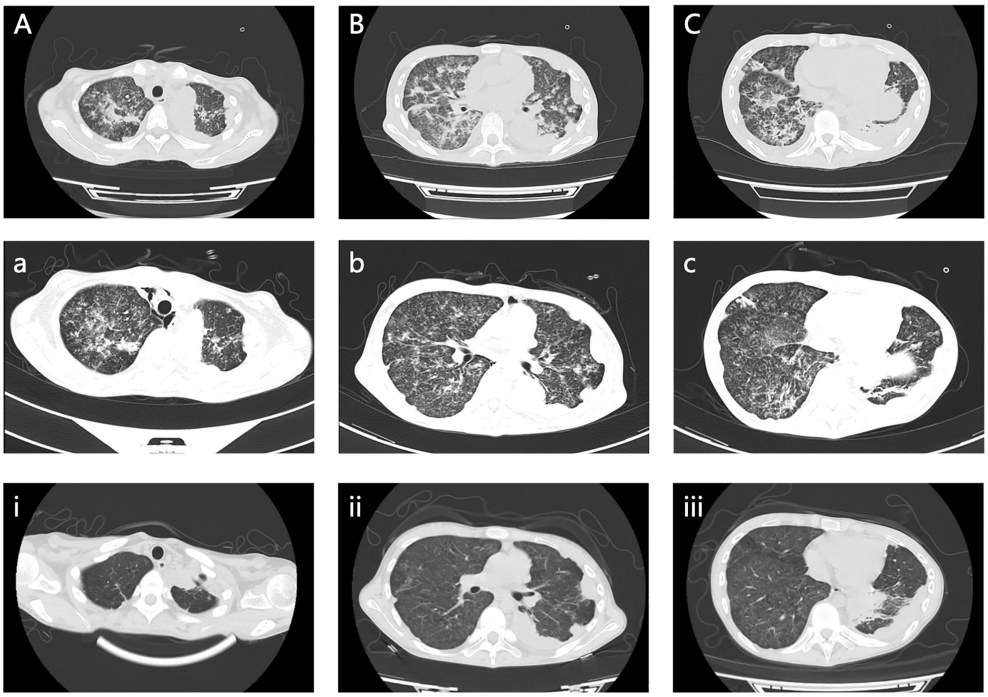

FIGURE 3
Chest and abdominal CT scan images. **(A–C)** Multiple infectious foci in both lungs and bilateral pleural effusion on 17 February 2023. **(a, b, c)** Multiple infection foci in both lungs were reduced on 6 March 2023. **(i, ii, iii)** Clearly decreased foci in both lungs on 28 April 2023.

10.3389/fimmu.2023.1249878

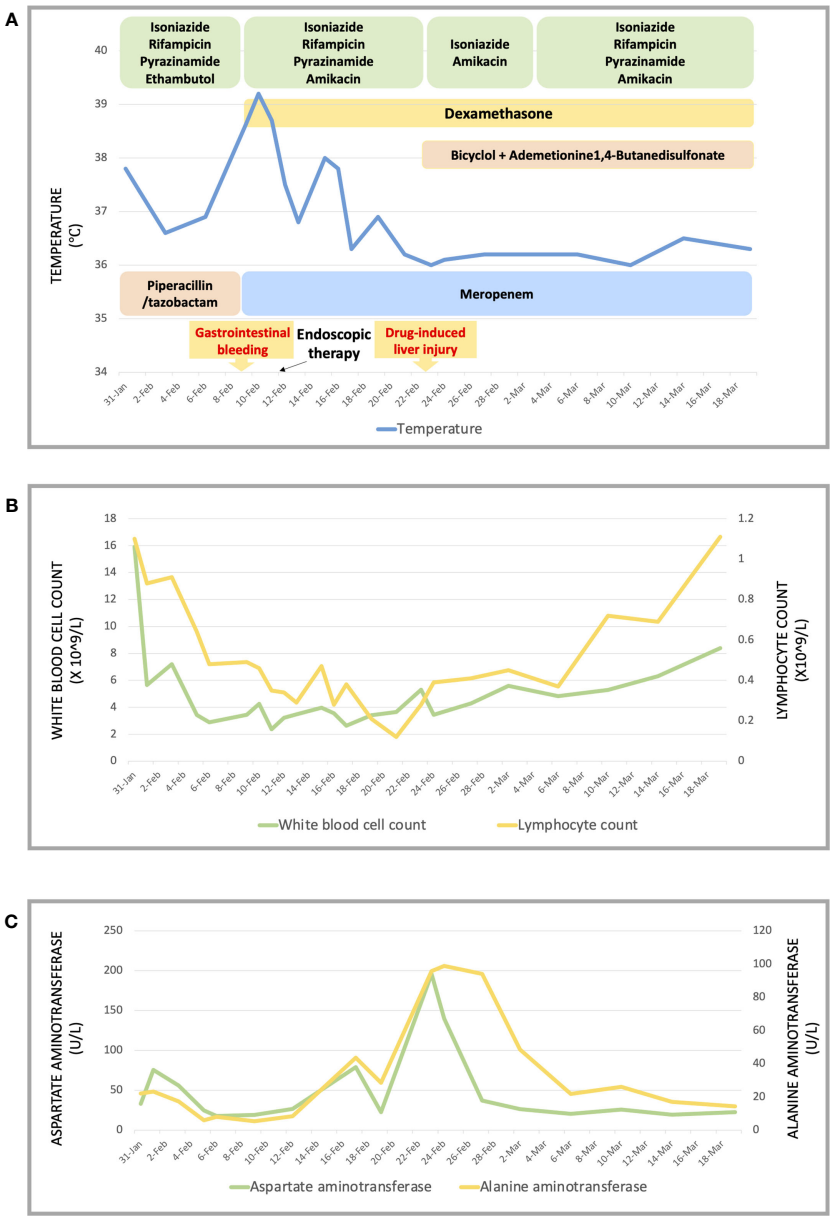

FIGURE 4
Treatment and observation during hospitalization. **(A)** Monitoring of body temperature and treatment. **(B)** Counting of white blood cells and lymphocytes. **(C)** Level of aspartate aminotransferase and alanine aminotransferase.

host defense and cannot explain why one individual develops pulmonary tuberculosis while another develops extrapulmonary tuberculosis (14). Our patient developed disseminated tuberculosis after COVID-19 infection, which may be associated with abnormal immune responses.

Little evidence is available about how the co-infection of SARS-Cov2 and *Mycobacterium tuberculosis* impairs the host's immune responses (15). Tuberculosis status may be associated with COVID-19 infection and exacerbation (16, 17), possibly because of the increased abundance of circulating myeloid subpopulations, which are also found in the lungs of patients with severe COVID-19 (18). Conversely, COVID-19 infection may play a role in active and latent tuberculosis. Increased IFN production and the type I and III IFN response signatures are significantly upregulated in COVID-19 (2), which may lead to tuberculosis progression and a fatal outcome. Moreover, many viruses, including SARS-CoV-2, cause a temporary immunosuppressive effect, which could lead to the reactivation and dissemination of *Mycobacterium tuberculosis* infection (19). A significant reduction in the frequency of *M. tuberculosis*-specific CD4 T-cells in patients with COVID-19 could affect the ability of the host to control latent or new *M. tuberculosis* infection (5, 20, 21). For our patient, other causes of immunosuppression were excluded, including chronic hepatitis B and C, HIV infection, primary immunodeficiency diseases, a depressed response to vaccination, and cancer. However, critical infection-induced immunosuppression (22) could not be differentiated without the result of *M. tuberculosis*-specific CD4 T-cells. Furthermore, longitudinal studies are required to investigate whether homeostatic reexpansion or peripheral redistribution of the

M. tuberculosis-specific memory T cell pool has an impact on tuberculosis clinical outcomes after COVID-19 recovery.

The optimal anti-tuberculosis regimen for drug-susceptible tuberculosis usually consists of well-known first-line drugs, including rifampicin, isoniazid, pyrazinamide, and ethambutol. A meropenem/faropenem-containing regimen was designed for our patient with disseminated tuberculosis, despite no evidence of drug resistance. *M. tuberculosis* possesses a class C beta-lactamase that can inactivate carbapenems (23), while meropenem was the most stable carbapenem in the presence of the chromosomally encoded *blaC* beta-lactamase (24), considered a potentially useful anti-tuberculosis drug and classified by the WHO as Group C for drug-resistant tuberculosis (9). Meanwhile, oral faropenem is stable against the *blaC* enzyme present in *M. tuberculosis*, which managed to successfully kill *M. tuberculosis* growth *in vitro* (25). The activity of carbapenems against mycobacteria has been extensively reported in the past several years (26), for instance, carbapenems can limit activity in a more physiologically hypoxic model emulating granuloma conditions (27). In particular, carbapenems occupy a significant niche in treating life-threatening infections (28). Our young patient received first-line drugs and fluoroquinolones for a whole year with a poor prognosis. Thereby, we made the meropenem/faropenem-containing regimen, which produced obvious therapeutic efficacy in the period of admission. Complementarily, ethambutol was not utilized considering the ocular toxicity, which may have generated confusion from the symptoms of epilepsy in this patient with tuberculous meningitis.

The process, from the initial symptoms of fever and dyspnea to the clinical diagnosis of disseminated tuberculosis, was tortuous but meaningful for us. Our young female patient is continuing the anti-tuberculosis therapy, and we will closely follow up on the effectiveness of her treatment and her prognosis.

To the best of our knowledge, ours is the first case report of disseminated tuberculosis after COVID-19 infection. Tuberculosis and other diseases may progress and develop with COVID-19 co-infection, yet studies related to tuberculosis and COVID-19 interaction are still limited. There is a need for more valuable research results to provide better diagnosis and treatment options for those patients.

Data availability statement

The original contributions presented in the study are included in the article/Supplementary Material. Further inquiries can be directed to the corresponding author.

Ethics statement

Written informed consent was obtained from the parents of the patient for the publication of this Case report and any accompanying images.

Author contributions

TW, YD, and NH collected clinical data and conducted the literature review. TW wrote the manuscript. CZ, LZ, SC, JT, and DZ generated and interpreted data. All authors contributed to the revision of the manuscript for important intellectual content, approved the final version, and agreed to be accountable for all aspects of the work.

Funding

This work was supported by the funding of the Doctor Start-up Fund of the Affiliated Hospital of Guizhou Medical University (NO: gyfybsky-2023-23).

Conflict of interest

The authors declare that the research was conducted in the absence of any commercial or financial relationships that could be construed as a potential conflict of interest.

Publisher's note

Supplementary material

The Supplementary Material for this article can be found online at: https://www.frontiersin.org/articles/10.3389/fimmu.2023.1249878/full#supplementary-material

References

1. WHO. *Global tuberculosis report 2022*. Geneva: World Health Organization (2022).

2. Acharya D, Liu G, Gack MU. Dysregulation of type I interferon responses in COVID-19. *Nat Rev Immunol* (2020) 20(7):397–8. doi: 10.1038/s41577-020-0346-x

3. Behr MA, Edelstein PH, Ramakrishnan L. Revisiting the timetable of tuberculosis. *BMJ* (2018) 362:k2738. doi: 10.1136/bmj.k2738

4. Moule MG, Cirillo JD. Mycobacterium tuberculosis dissemination plays a critical role in pathogenesis. *Front Cell Infect Microbiol* (2020) 10:65. doi: 10.3389/fcimb.2020.00065

5. Riou C, du Bruyn E, Stek C, Daroowala R, Goliath RT, Abrahams F, et al. Relationship of SARS-CoV-2–specific CD4 response to COVID-19 severity and impact

of HIV-1 and tuberculosis coinfection. *J Clin Invest* (2021) 131(12):e149125. doi: 10.1172/JCI149125

6. Yan L, Sun W, Lu Z, Fan L. Metagenomic Next-Generation Sequencing (mNGS) in cerebrospinal fluid for rapid diagnosis of Tuberculosis meningitis in HIV-negative population. *Int J Infect Dis* (2020) 96:270–5. doi: 10.1016/j.ijid.2020.04.048

7. Wilson MR, Sample HA, Zorn KC, Arevalo S, Yu G, Neuhaus J, et al. Clinical metagenomic sequencing for diagnosis of meningitis and encephalitis. *N Engl J Med* (2019) 380(24):2327–40. doi: 10.1056/NEJMoa1803396

8. WHO. *WHO operational handbook on tuberculosis Module 4: Treatment – drug-susceptible tuberculosis treatment*. Geneva: World Health Organization (2022).

9. WHO. *WHO consolidated guidelines on tuberculosis. Module 4: treatment - drug-resistant tuberculosis treatment, 2022 update*. Geneva: World Health Organization (2022).

10. Qian X, Nguyen DT, Lyu J, Albers AE, Bi X, Graviss EA. Risk factors for extrapulmonary dissemination of tuberculosis and associated mortality during treatment for extrapulmonary tuberculosis. *Emerg Microbes Infect* (2018) 7(1):102. doi: 10.1038/s41426-018-0106-1

11. Martín-Sánchez FJ, Martínez-Sellés M, Molero García JM, Moreno Guillén S, Rodríguez-Artalejo FJ, Ruiz-Galiana J, et al. Insights for COVID-19 in 2023. *Rev Esp Quimioter* (2023) 36(2):114–24. doi: 10.37201/req/122.2022

12. Sama JN, Chida N, Polan RM, Nuzzo J, Page K, Shah M. High proportion of extrapulmonary tuberculosis in a low prevalence setting: a retrospective cohort study. *Public Health* (2016) 138:101–7. doi: 10.1016/j.puhe.2016.03.033

13. Pai M, Behr MA, Dowdy D, Dheda K, Divangahi M, Boehme CC, et al. Tuberculosis. *Nat Rev Dis Primer* (2016) 2:16076. doi: 10.1038/nrdp.2016.76

14. Whittaker E, Nicol M, Zar HJ, Kampmann B. Regulatory T cells and pro-inflammatory responses predominate in children with tuberculosis. *Front Immunol* (2017) 8:448. doi: 10.3389/fimmu.2017.00448

15. Visca D, Ong CWM, Tiberi S, Centis R, D'Ambrosio L, Chen B, et al. Tuberculosis and COVID-19 interaction: A review of biological, clinical and public health effects. *Pulmonol* (2021) 27(2):151–65. doi: 10.1016/j.pulmoe.2020.12.012

16. Yasri S, Wiwanitkit V. Tuberculosis and novel Wuhan coronavirus infection: Pathological interrelationship. *Indian J Tuberc* (2020) 67(2):264. doi: 10.1016/j.ijtb.2020.02.004

17. Tamuzi JL, Ayele BT, Shumba CS, Adetokunboh OO, Uwimana-Nicol J, Haile ZT, et al. Implications of COVID-19 in high burden countries for HIV/TB: A systematic review of evidence. *BMC Infect Dis* (2020) 20(1):744. doi: 10.1186/s12879-020-05450-4

18. Sheerin D, Abhimanyu, Wang X, Johnson WE, Coussens A. Systematic evaluation of transcriptomic disease risk and diagnostic biomarker overlap between COVID-19 and tuberculosis: a patient-level meta-analysis. *MedRxiv Prepr Serv Health Sci* (2020) 26:2020.11.25.20236646. doi: 10.1101/2020.11.25.20236646

19. Singh A, Prasad R, Gupta A, Das K, Gupta N. Severe acute respiratory syndrome coronavirus-2 and pulmonary tuberculosis: convergence can be fatal. *Monaldi Arch Chest Dis Arch Monaldi Mal Torace* (2020) 90(3). doi: 10.4081/monaldi.2020.1368

20. Zhou R, To KK, Wong YC, Liu L, Zhou B, Li X, et al. Acute SARS-CoV-2 infection impairs dendritic cell and T cell responses. *Immunity* (2020) 53(4):864–877.e5. doi: 10.1016/j.immuni.2020.07.026

21. Toor SM, Saleh R, Sasidharan Nair V, Taha RZ, Elkord E. T-cell responses and therapies against SARS-CoV-2 infection. *Immunology* (2021) 162(1):30–43. doi: 10.1111/imm.13262

22. Zhang W, Fang X, Gao C, Song C, He Y, Zhou T, et al. MDSCs in sepsis-induced immunosuppression and its potential therapeutic targets. *Cytokine Growth Factor Rev* (2023) 69:90–103. doi: 10.1016/j.cytogfr.2022.07.007

23. Barnier JP, Saidjalolov S, Bouchet F, Mayer L, Edoo Z, Sayah I, et al. Modulation of the Specificity of Carbapenems and Diazabicyclooctanes for Selective Activity against Mycobacterium tuberculosis. *Antimicrob Agents Chemother* (2022) 66(9):e0235721. doi: 10.1128/aac.02357-21

24. England K, Boshoff HI, Arora K, Weiner D, Dayao E, Schimel D, et al. Meropenem-clavulanic acid shows activity against Mycobacterium tuberculosis in *vivo*. *Antimicrob Agents Chemother* (2012) 56(6):3384–7. doi: 10.1128/AAC.05690-11

25. Dhar N, Dubée V, Ballell L, Cuinet G, Hugonnet JE, Signorino-Gelo F, et al. Rapid cytolysis of Mycobacterium tuberculosis by faropenem, an orally bioavailable β-lactam antibiotic. *Antimicrob Agents Chemother* (2015) 59(2):1308–19. doi: 10.1128/AAC.03461-14

26. Sotgiu G, D'Ambrosio L, Centis R, Tiberi S, Esposito S, Dore S, et al. Carbapenems to treat multidrug and extensively drug-resistant tuberculosis: A systematic review. *Int J Mol Sci* (2016) 17(3):373. doi: 10.3390/ijms17030373

27. Solapure S, Dinesh N, Shandil R, Ramachandran V, Sharma S, Bhattacharjee D, et al. *In vitro* and in *vivo* efficacy of β-lactams against replicating and slowly growing/nonreplicating Mycobacterium tuberculosis. *Antimicrob Agents Chemother* (2013) 57(6):2506–10. doi: 10.1128/AAC.00023-13

28. Hoagland DT, Liu J, Lee RB, Lee RE. New agents for the treatment of drug-resistant Mycobacterium tuberculosis. *Adv Drug Delivery Rev* (2016) 102:55–72. doi: 10.1016/j.addr.2016.04.026

frontiers | Frontiers in Cellular and Infection Microbiology

TYPE Original Research
PUBLISHED 15 December 2023
DOI 10.3389/fcimb.2023.1280223

OPEN ACCESS

EDITED BY
Amit Singh,
Central University of Punjab, India

REVIEWED BY
Yu Gao,
Karolinska Institutet, Sweden
Pier Maria Fornasari,
Regenhealthsolutions, Italy

*CORRESPONDENCE
Zhen Wang
wangzhen@scu.edu.cn
Kefei Yuan
ykf13@163.com

†These authors have contributed equally to this work and share first authorship

RECEIVED 19 August 2023
ACCEPTED 07 November 2023
PUBLISHED 15 December 2023

CITATION
Huang T, He J, Zhou X, Pan H, He F, Du A, Yu B, Jiang N, Li X, Yuan K and Wang Z (2023) Discovering common pathogenetic processes between COVID-19 and tuberculosis by bioinformatics and system biology approach.
Front. Cell. Infect. Microbiol. 13:1280223.
doi: 10.3389/fcimb.2023.1280223

Discovering common pathogenetic processes between COVID-19 and tuberculosis by bioinformatics and system biology approach

Tengda Huang[1†], Jinyi He[1†], Xinyi Zhou[1], Hongyuan Pan[1], Fang He[2], Ao Du[1], Bingxuan Yu[1], Nan Jiang[1], Xiaoquan Li[1], Kefei Yuan[1*] and Zhen Wang[1*]

[1]Division of Liver Surgery, Department of General Surgery and Laboratory of Liver Surgery, and State Key Laboratory of Biotherapy, West China Hospital, Sichuan University, Chengdu, China, [2]Center of Infectious Diseases, West China Hospital, Sichuan University, Chengdu, China

Introduction: The coronavirus disease 2019 (COVID-19) pandemic, stemming from the severe acute respiratory syndrome coronavirus 2 (SARS-CoV-2), has persistently threatened the global health system. Meanwhile, tuberculosis (TB) caused by *Mycobacterium tuberculosis* (*M. tuberculosis*) still continues to be endemic in various regions of the world. There is a certain degree of similarity between the clinical features of COVID-19 and TB, but the underlying common pathogenetic processes between COVID-19 and TB are not well understood.

Methods: To elucidate the common pathogenetic processes between COVID-19 and TB, we implemented bioinformatics and systematic research to obtain shared pathways and molecular biomarkers. Here, the RNA-seq datasets (GSE196822 and GSE126614) are used to extract shared differentially expressed genes (DEGs) of COVID-19 and TB. The common DEGs were used to identify common pathways, hub genes, transcriptional regulatory networks, and potential drugs.

Results: A total of 96 common DEGs were selected for subsequent analyses. Functional enrichment analyses showed that viral genome replication and immune-related pathways collectively contributed to the development and progression of TB and COVID-19. Based on the protein-protein interaction (PPI) network analysis, we identified 10 hub genes, including IFI44L, ISG15, MX1, IFI44, OASL, RSAD2, GBP1, OAS1, IFI6, and HERC5. Subsequently, the transcription factor (TF)–gene interaction and microRNA (miRNA)–gene coregulatory network identified 61 TFs and 29 miRNAs. Notably, we identified 10 potential drugs to treat TB and COVID-19, namely suloctidil, prenylamine, acetohexamide, terfenadine, prochlorperazine, 3′-azido-3′-deoxythymidine, chlorophyllin, etoposide, clioquinol, and propofol.

Conclusion: This research provides novel strategies and valuable references for the treatment of tuberculosis and COVID-19.

KEYWORDS

SARS-CoV-2, tuberculosis, differentially expressed genes, protein-protein interaction (PPI), hub gene, drug molecule

Introduction

Coronavirus disease 2019 (COVID-19), resulting from severe acute respiratory syndrome coronavirus 2 (SARS-CoV-2), is an atypical respiratory disease (Pollard et al., 2020). According to the World Health Organization (WHO), as of January 2023, there have been more than 659 million confirmed cases and over 6.6 million deaths worldwide. The common symptoms of COVID-19 include fever, dyspnea, dizziness, upper airway congestion, dry cough, and sputum production (Jin et al., 2020). Additionally, vomiting, headaches, dizziness, loss of taste and smell, and diarrhea have also been reported (Shi et al., 2020; Spinato et al., 2020). The primary mode of SARS-CoV-2 transmission is through respiratory droplets released when an infected person sneezes or coughs, potentially infecting individuals in close proximity (Umakanthan et al., 2020). SARS-CoV-2 belongs to the β coronaviruses and is composed of four structural proteins: spike (S), nucleocapsid (N), membrane (M), and envelope (E) (Chan et al., 2020). The spike protein plays a critical role in binding to host cell receptors and facilitating the fusion of cellular and viral membranes. Angiotensin-converting enzyme 2 (ACE2) is a pivotal receptor for SARS-CoV-2's invasion of host cells and is abundantly present in the bladder, heart, lung, kidney, and ileum (Chen et al., 2020; Gheblawi et al., 2020; Zou et al., 2020). Certain preexisting conditions substantially elevate the risk of severe complications and mortality among COVID-19 patients (Huang et al., 2023b; Huang et al., 2023a; Song et al., 2023).

Tuberculosis (TB), caused by *Mycobacterium tuberculosis* (*M. tuberculosis*), is a grave infectious disease that poses a significant threat to global public health due to its high global mortality and morbidity rates (Behr et al., 2021). TB can affect individuals of all age groups and both sexes, with adult men constituting 56% of all TB cases (Chakaya et al., 2021). TB is a severe infectious pulmonary disorder, resulting in pulmonary consolidation, cavitary lesions, and bronchial wall thickening (Deshpande et al., 2020). Furthermore, COVID-19 patients with active pulmonary tuberculosis face a higher risk of mortality due to compromised lung immunity in comparison to patients without tuberculosis (Aggarwal et al., 2021). Additionally, individuals with severe COVID-19 are at greater risk of TB infection compared to those with milder cases (Gao et al., 2021). These studies illustrate that there is a strong interaction and association between TB and COVID-19.

As our understanding of these diseases has deepened, numerous similarities between TB and COVID-19 have been discovered in terms of pathogenesis, clinical symptoms, and sequelae. Within host cells, both *M. tuberculosis* and SARS-CoV-2 can induce proinflammatory cytokines, potentially leading to a cytokine storm if not properly regulated, and they share similar mechanisms for evading the immune system and host cell responses (Zhai et al., 2019; Ragab et al., 2020; Callaway, 2021). Notably, *M. tuberculosis* infection boosts the expression of ACE2, causing significantly severe multi-organ injury (Ziegler et al., 2020). Bacillus Calmette–Guérin (BCG), a weakened live vaccine against *M. tuberculosis*, is helpful in decreasing the proportion of incidence of SARS-CoV-2 IgG seroconversion and clinical symptoms in COVID-19 patients (Benn et al., 2013; Rivas et al., 2021).

Exploring the transcriptional profiles of TB and COVID-19 may provide new insights into the common pathogenesis of the two diseases. The TB datasets (GSE126614) and COVID-19 datasets (GSE196822) were obtained from the Gene Expression Omnibus (GEO) database. Then differentially expressed genes (DEGs) in TB and COVID-19 were filtrated, and their shared DEGs were identified to investigate their functions in these two diseases. In addition, we utilized the common DEGs to establish a protein–protein interaction (PPI) network chart and extracted the hub genes, which are used for the recognition of engaged transcription factors (TF), microRNAs (miRNA), and the prediction of potential drugs. The sequential workflow of the analysis is presented in Figure 1.

Methods

Data sources

To determine common pathogenetic processes among TB and COVID-19, we used RNA-seq datasets from the GEO database of the National Center for Biotechnology Information (NCBI, https://www.ncbi.nlm.nih.gov/geo/) (Barrett et al., 2013). The GEO accession number of the COVID-19 dataset was GSE196822, which was transcriptional profiling of the peripheral blood of 34 patients with COVID-19 and nine healthy individuals. The COVID-19 dataset was obtained through high-throughput sequencing on the Illumina Hiseq 4000 platform (*Homo sapiens*) for extracting RNA sequences (Huang et al., 2023a; Li et al., 2022). For the TB dataset, we utilized the GEO accession ID of GSE126614 (Del Rosario et al., 2022), which contains the transcriptomic profiles for peripheral blood mononuclear cells from 19 healthy controls and 20 patients with active TB infection. The TB dataset was

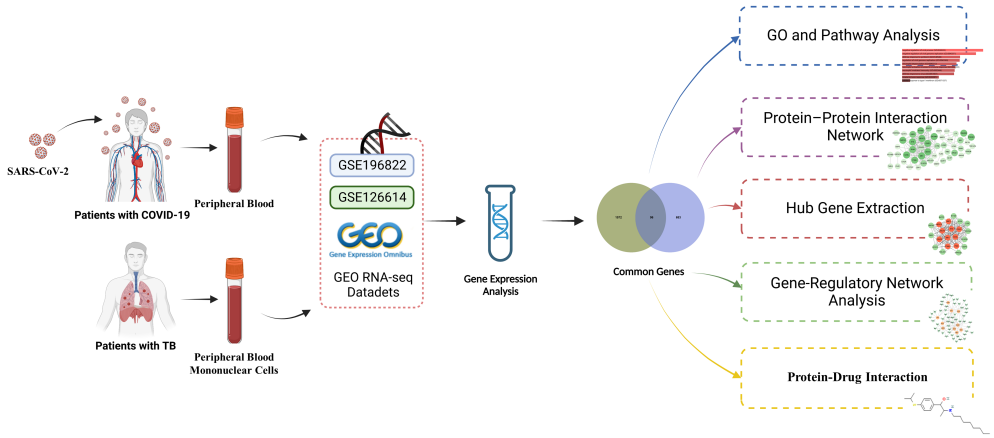

FIGURE 1
A schematic illustration of the overall general workflow of this study.

obtained through high-throughput sequencing on the Illumina HiSeq 2000 system (*Homo sapiens*). Supplementary Tables S1, S2 show the baseline characteristics of samples in COVID-19 and TB.

Identification of DEGs and common DEGs in COVID-19 and TB

A statistically significant difference between diverse test circumstances at the transcriptional level is generally accepted as the criterion for determining whether the genes are expressed differently (Kvam et al., 2012). The DEGs were detected from the expression read count values by the DEseq2 R package with a Benjamini–Hochberg correction to control the false discovery rate (FDR) (Love et al., 2014). The main role of the analysis is to acquire DEGs for the GSE196822 and GSE126614 datasets. The genes that comply with $|\log_2 \text{Fold Change}| > 1$ and FDR < 0.05 were viewed as significantly DEGs. The mutual DEGs of GSE196822 and GSE126614 were obtained by Jvenn (http://jvenn.toulouse.inra.fr/app/example.html), an online Venn analysis program (Bardou et al., 2014).

Gene ontology and pathway enrichment analysis

Gene enrichment analysis is a considerable systematic effort to illuminate and categorize shared biological knowledge (Subramanian et al., 2005). EnrichR (https://maayanlab.cloud/enrichr/) is a versatile web-based tool that was used to identify gene ontology functional enrichment (biological processes (BP), molecular function (MF), and cellular component (CC)) and signaling pathway enrichment to clarify potential biological mechanisms of common DEG (Kuleshov et al., 2016). Three databases (Bioplanet, Kyoto Encyclopedia of Genes and Genomes (KEGG), and WikiPathways) were used for pathway enrichment analysis.

PPI network analysis and hub gene extraction

STRING (version 11.5), a protein interaction database, was utilized to build the PPI network using common DEGs to describe the physical and functional relationship between COVID-19 and TB (Szklarczyk et al., 2019). The medium confidence score set in the analysis was 0.400 to conduct the PPI network. Cytoscape (version 3.9.1) was applied to visualize and process the PPI network (Smoot et al., 2011).

Hub gene extraction

The PPI network covers edges, nodes, and their links. In this network, the most prominent nodes are supposed to be hub genes. Cytohubba (http://apps.cytoscape.org/apps/cytohubba), a remarkable plug-in in Cytoscape, is used for analyzing nodes and the relationships between them in the PPI network (Ma et al., 2021). Applying the Maximal Clique Centrality (MCC) method of Cytohubba, we confirmed the top 10 genes within the PPI network as the hub genes.

Gene-regulatory network analysis

Transcription factors are proteins that can specifically identify the corresponding genes and control the transcription rate (Rustad et al., 2014). The gene–TF interaction network was conducted by NetworkAnalyst (http://www.networkanalyst.ca) (Zhou et al., 2019). The topologically credible TFs within the network that were inclined to bind to specific hub genes were from the JASPAR database. JASPAR is an open-access database that contains TF profiles from six taxonomic groups (Fornes et al., 2020). Moreover, miRNAs targeting gene interaction were used to identify miRNAs that have the potential to regulate the hub genes at the post-transcriptional level. MiRTarBase is one of the most known gene–miRNA interplay repositories (Huang et al., 2020). From the miRNA–gene interaction via NetworkAnalyst, we

retrieved the miRNAs that can interplay with hub genes concentrated on topological analysis from the miRTarBase database (v 8.0). In Cytoscape, the gene–TF and the gene–miRNA interaction networks were visualized.

Identification of candidate drugs

The identification of drug molecules is one of the most crucial parts of the research. Based on the hub genes of TB and COVID-19, the drug molecule was discovered using the Drug Signatures Database (DSigDB) via EnrichR. DSigDB is a data management repository for recognizing the chemical compounds of the medicine that correspond with the genes (Yoo et al., 2015). The drug function of EnrichR provides easy access to the DSigDB database.

Results

Identification of DEGs and shared DEGs between COVID-19 and TB

To investigate the common pathogenetic processes between COVID-19 and TB, we filtrated the DEGs from transcriptional datasets and identified the common DEGs that cause COVID-19 and TB. From the assessment of the COVID-19 dataset (GES196822), there are 1,668 DEGs, including 839 upregulated DEGs and 829 downregulated DEGs (Supplementary Table S3). Similarly, based on RNA-seq profiling of patients with TB (GSE126614), we identified 779 DEGs, where 470 DEGs were upregulated and 309 DEGs were downregulated (Supplementary Table S4). The summarized information on DEGs for COVID-19 and TB is listed in Table 1. Moreover, there are 96 shared DEGs identified from the COVID-19 and TB datasets by the accomplishment of the cross-comparison evaluation on Jvenn (Figure 2). These results reveal that the 96 common genes screened in this study mediated the regulation of COVID-19 and TB, suggesting that there are some mechanismal commonalities and common pathogenetic processes between COVID-19 and TB.

Analyses of gene ontology and pathway enrichment

To further understand the biological significance and the common signaling pathways of the dataset, we used the common DEGs to implement the GO enrichment approach and pathway enrichment method through EnrichR. For gene ontology analysis, the top 10 terms related to the biological process, molecular function, and cellular component categories are summarized in Table 2. The bar graph in Figure 3 indicates the comprehensive ontological analysis for each category. Notably, viral genome replication and immune-related pathways are significantly enriched, including negative regulation of viral process (GO:0048525), negative regulation of viral genome replication (GO:0045071), regulation of viral genome replication (GO:0045069), neutrophil activation involved in immune response (GO:0002283), neutrophil-mediated immunity (GO:0002446), defense response to viruses (GO:0051607), and innate immune response (GO:0045087).

To find the most significant pathways of the mutual DEGs, three global databases were utilized, including Bioplanet, KEGG, and WikiPathways. The identified top 10 pathways in the three databases are outlined in Table 3. Moreover, the pathway enrichment study is described in the bar graph in Figure 4. The Bioplanet enrichment analysis showed that the common DEGs are mainly involved in the regulation of immune-related pathways, including interferon signaling, interferon alpha/beta signaling, type II interferon signaling (interferon-gamma), interferon-gamma signaling pathway, immune system, antiviral mechanism by interferon-stimulated genes, and interleukin-2 signaling pathway. Furthermore, the KEGG analysis showed the shared DEGs may influence the progression of a variety of infectious diseases, including coronavirus disease, influenza A, measles, hepatitis C, and Epstein–Barr virus infection. Most important of all, the WikiPathways analysis revealed mutual DEGs significantly enriched in the immune response to tuberculosis (WP4197), type I interferon induction and signaling during SARS-CoV-2 infection (WP4868), and host–pathogen interaction of human coronaviruses—interferon induction (WP4880). These results strongly suggest that these mutual DEGs are involved in the occurrence and development of these two infectious diseases through viral genome replication and immune-related pathways.

Protein–protein interaction analysis and hub gene extraction

To identify the interplay and adhesion routes of common DEGs, we analyzed the PPI network constructed from STRING and visualized it in Cytoscape. Figure 5 demonstrates the PPI network of common DEGs, which consists of 176 edges and 49 nodes. As shown, the size and color depth of the circles indicated the degree of intercorrelation of the proteins, and the most prominent nodes are considered the hub genes. From the PPI network analysis utilizing the Cytohubba plugin, 10 hub genes were selected. Figure 6 shows the submodule network of hub-gene connections that consists of 22 nodes and 142 edges. These hub

TABLE 1 Overview of the datasets in this analysis.

Disease name	GEO accession	GEO platform	Total DEG count	Upmodulated DEG count	Downmodulated DEG count
COVID-19	GES196822	GPL20301	1,668	839	829
TB	GSE126614	GPL11154	779	470	309

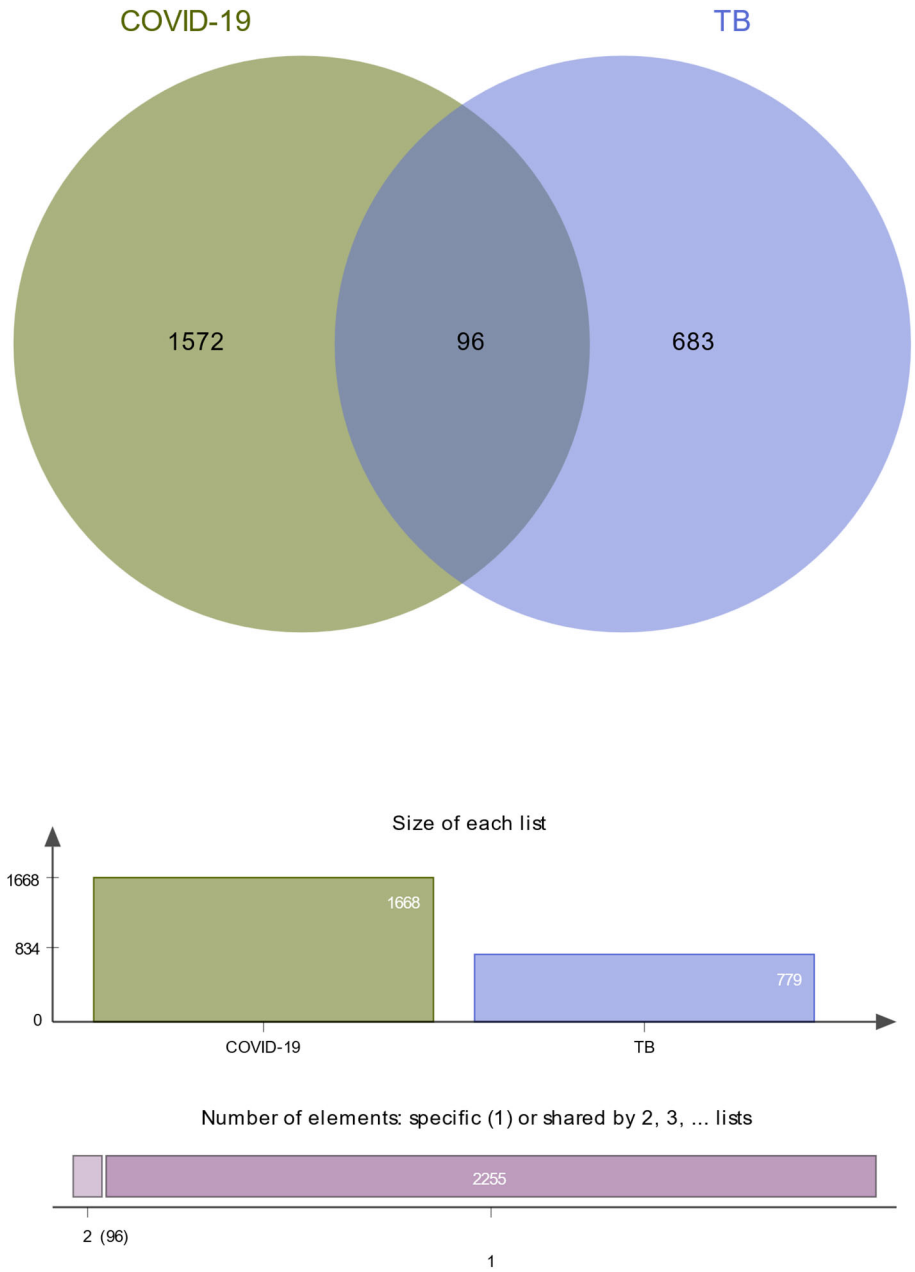

FIGURE 2
The study incorporates TB (GSE126614) and COVID-19 (GSE196822). The Venn diagram revealed 96 common DEGs for TB and COVID-19.

genes comprised IFI44L, ISG15, MX1, IFI44, OASL, RSAD2, GBP1, OAS1, IFI6, and HERC5, which could be potential biomarkers for common pathogenetic processes between COVID-19 and TB and may accelerate the development of novel therapeutic strategies.

Determination of regulatory networks at the transcriptional level

To investigate the transcriptional regulation of hub genes, a network-based technique was utilized to decipher the regulatory TFs and miRNAs. Figure 7 shows TF regulators interplay with the hub genes, which have 61 nodes and 99 edges. Moreover, Figure 8 depicts the interactions of miRNAs and hub genes, consisting of 29 nodes and 32 edges. From TF-gene and miRNA-gene interaction networks, 61 TFs such as GATA2, FOXC1, USF2, MEF2A, STAT1, SREBF1, POU2F2, and 29 miRNAs such as hsa-mir-26b-5p, hsa-mir-15b-3p, hsa-mir-146a-3p, hsa-mir-34b-3p, hsa-mir-1248, hsa-mir-4256, hsa-mir-3921, and hsa-mir-4653-5p, are discovered.

Identification of candidate drugs

The protein–drug interaction analyses may be useful in drug discovery (Al-Mustanjid et al., 2020). Protein–drug interaction is vital to understanding the function of proteins and discovering

10.3389/fcimb.2023.1280223

TABLE 2 Ontological analysis of common DEGs between TB and COVID-19.

Category	GO ID	Term	*p*-value	Genes
GO biological process	GO:0048525	Negative regulation of the viral process	2.96*E*−14	IFITM3; PARP10; PLSCR1; RSAD2; OAS1; MX1; EIF2AK2; ISG15; PML; OASL; LTF
	GO:0045071	Negative regulation of viral genome replication	8.07*E*−14	IFITM3; PARP10; PLSCR1; RSAD2; OAS1; MX1; EIF2AK2; ISG15; OASL; LTF
	GO:0140546	Defense response to symbiont	7.55*E*−13	IFITM3; ZBP1; PLSCR1; RSAD2; OAS1; MX1; IFI6; EIF2AK2; ISG15; RNASE2; IFI44L; OASL
	GO:0045069	Regulation of viral genome replication	7.94*E*−13	IFITM3; PARP10; PLSCR1; RSAD2; OAS1; MX1; EIF2AK2; ISG15; OASL; LTF
	GO:0043312	Neutrophil degranulation	1.25*E*−12	TNFAIP6; ANXA3; CRISP3; RNASE3; RETN; OLFM4; MMP8; RNASE2; VNN1; LCN2; OLR1; BPI; S100P; GYG1; CAMP; HSPA1B; CD177; LTF; SIGLEC5
	GO:0002283	Neutrophil activation is involved in the immune response	1.44*E*−12	TNFAIP6; ANXA3; CRISP3; RNASE3; RETN; OLFM4; MMP8; RNASE2; VNN1; LCN2; OLR1; BPI; S100P; GYG1; CAMP; HSPA1B; CD177; LTF; SIGLEC5
	GO:0002446	Neutrophil-mediated immunity	1.60*E*−12	TNFAIP6; ANXA3; CRISP3; RNASE3; RETN; OLFM4; MMP8; RNASE2; VNN1; LCN2; OLR1; BPI; S100P; GYG1; CAMP; HSPA1B; CD177; LTF; SIGLEC5
	GO:0051607	Defense response to virus	1.75*E*−12	IFITM3; ZBP1; PLSCR1; RSAD2; OAS1; MX1; IFI6; EIF2AK2; ISG15; RNASE2; IFI44L; OASL
	GO:0045087	Innate immune response	1.49*E*−11	IFITM3; CRISP3; MX1; IFI6; ISG15; RNASE3; RNASE2; PML; VNN1; OAS1; LCN2; BPI; APOL1; CAMP; LTF
	GO:0071357	Cellular response to type I interferon	8.44*E*−10	IFITM3; RSAD2; OAS1; MX1; IFI6; ISG15; IFI35; OASL
GO cellular component	GO:0042581	Specific granule	2.98*E*−10	ANXA3; CRISP3; LCN2; OLR1; BPI; RETN; OLFM4; MMP8; CAMP; CD177; LTF
	GO:0035580	Specific granule lumen	5.72*E*−10	CRISP3; LCN2; BPI; RETN; MMP8; OLFM4; CAMP; LTF
	GO:0034774	Secretory granule lumen	3.72*E*−09	CRISP3; RNASE3; RETN; OLFM4; MMP8; RNASE2; LCN2; SERPING1; BPI; S100P; GYG1; CAMP; LTF
	GO:0070820	Tertiary granule	9.47*E*−08	TNFAIP6; CRISP3; OLR1; OLFM4; MMP8; CAMP; CD177; LTF; SIGLEC5
	GO:1904724	Tertiary granule lumen	2.50*E*−07	TNFAIP6; CRISP3; MMP8; OLFM4; CAMP; LTF
	GO:0042582	Azurophil granule	1.03*E*−04	VNN1; BPI; RNASE3; RETN; OLFM4; RNASE2
	GO:0035578	Azurophil granule lumen	9.29*E*−04	BPI; RNASE3; RETN; RNASE2
	GO:0005775	Vacuolar lumen	1.08*E*−03	BPI; RNASE3; RETN; RNASE2; GYG1
	GO:0034364	High-density lipoprotein particle	3.70*E*−03	CETP; APOL1
	GO:0070821	Tertiary granule membrane	5.23*E*−03	OLR1; CD177; SIGLEC5
GO molecular function	GO:0003725	Double-stranded RNA binding	4.21*E*−04	ZBP1; OAS1; EIF2AK2; OASL
	GO:0046914	Transition metal ion binding	1.36*E*−03	RPH3A; MT2A; PLSCR1; LCN2; TIMM10; MMP8; GYG1; LTF
	GO:0004518	Nuclease activity	3.01*E*−03	PLSCR1; RNASE3; RNASE2
	GO:0070566	Adenylyltransferase activity	4.95*E*−03	OAS1; OASL

(Continued)

10.3389/fcimb.2023.1280223

TABLE 2 Continued

Category	GO ID	Term	*p*-value	Genes
	GO:0017111	Nucleoside-triphosphatase activity	1.10*E*−02	GBP6; MX1; RHOH; GBP1; HSPA1B
	GO:0003924	GTPase activity	2.03*E*−02	GBP6; MX1; RHOH; GBP1
	GO:0008270	Zinc ion binding	2.30*E*−02	RPH3A; MT2A; PLSCR1; TIMM10; MMP8
	GO:0030283	Testosterone dehydrogenase [NAD(P)] activity	2.38*E*−02	DHRS9
	GO:0048406	Nerve growth factor binding	2.38*E*−02	SORT1
	GO:0031721	Hemoglobin alpha binding	2.38*E*−02	HBD

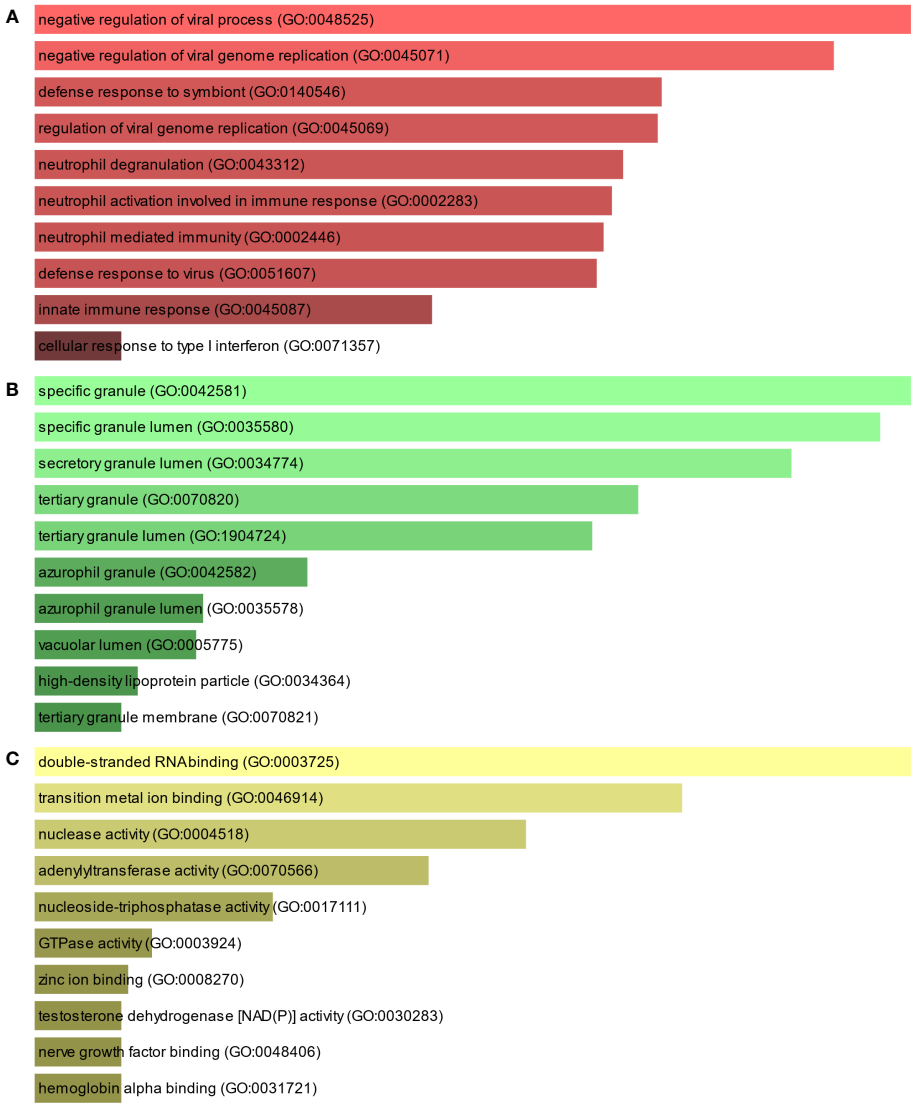

FIGURE 3
The bar chart of the GO assessment of the shared DEGs between TB and COVID-19. **(A)** Biological processes, **(B)** Cellular components, and **(C)** Molecular function.

10.3389/fcimb.2023.1280223

TABLE 3 Pathway enrichment analysis of common DEGs between TB and COVID-19.

Category	Pathways	*p*-value	Genes
Bioplanet	Interferon signaling	1.43*E*−12	IFITM3; GBP6; MX1; IFI6; EIF2AK2; ISG15; IFI35; PML; OASL; HERC5; MT2A; OAS1; GBP1
	Immune system signaling by interferons, interleukins, prolactin, and growth hormones	8.61*E*−10	IFITM3; GBP6; MX1; IFI6; EIF2AK2; ISG15; IFI35; PML; OASL; HERC5; MT2A; OAS1; GBP1
	Interferon alpha/beta signaling	2.34*E*−08	IFITM3; OAS1; MX1; IFI6; ISG15; IFI35; OASL
	Type II interferon signaling (interferon-gamma)	4.10*E*−06	OAS1; IFI6; EIF2AK2; ISG15; GBP1
	Interferon-gamma signaling pathway	7.26*E*−06	GBP6; MT2A; OAS1; GBP1; PML; OASL
	Immune system	2.02*E*−05	IFITM3; ZBP1; GBP6; MX1 IFI6; EIF2AK2; ISG15; IFI35; PML; OASL; HERC5; MT2A; OAS1; FBXO6; TLR5; GBP1
	Antiviral mechanism by interferon-stimulated genes	3.59*E*−04	HERC5; MX1; EIF2AK2; ISG15
	Oncostatin M	3.87*E*−03	MT2A; OAS1; ANXA3; LCN2; S100P; CAMP
	Interleukin-2 signaling pathway	7.43*E*−03	IFITM3; MT2A; SMARCD3; IL24; MX1; TBC1D8; IFI44; GBP1; IL18R1; LY6E
KEGG	Influenza A	1.44*E*−03	RSAD2; OAS1; MX1; EIF2AK2; PML
	Measles	4.53*E*−03	OAS1; MX1; EIF2AK2; HSPA1B
	Hepatitis C	6.94*E*−03	RSAD2; OAS1; MX1; EIF2AK2
	Cholesterol metabolism	2.41*E*−02	CETP; SORT1
	Coronavirus disease	2.56*E*−02	OAS1; MX1; EIF2AK2; ISG15
	Legionellosis	3.07*E*−02	TLR5; HSPA1B
	Inflammatory bowel disease	3.90*E*−02	TLR5; IL18R1
	Protein processing in the endoplasmic reticulum	4.93*E*−02	EIF2AK2; FBXO6; HSPA1B
	NOD-like receptor signaling pathway	5.66*E*−02	OAS1; GBP1; CAMP
	Epstein–Barr virus infection	7.34*E*−02	OAS1; EIF2AK2; ISG15
WikiPathways	Type II interferon signaling (IFNG) WP619	8.85*E*−07	OAS1; IFI6; EIF2AK2; ISG15; GBP1
	Immune response to tuberculosis WP4197	1.77*E*−04	OAS1; MX1; IFI35
	Nongenomic actions of 1,25-dihydroxyvitamin D3 WP4341	3.79*E*−04	RSAD2; ISG15; IFI44L; CAMP
	Type I interferon induction and signaling during SARS-CoV-2 infection WP4868	9.68*E*−03	OAS1; EIF2AK2
	Host–pathogen interaction of human coronaviruses-interferon induction WP4880	1.09*E*−02	OAS1; EIF2AK2
	Neural crest cell migration in cancer WP4565	1.81*E*−02	SORT1; MMP8
	Male infertility WP4673	3.33*E*−02	EPSTI1; BRCA2; LTF
	p53 transcriptional gene network WP4963	4.12*E*−02	ISG15; PML
	IL-18 signaling pathway WP4754	4.21*E*−02	CETP; NRN1; MMP8; IL18R1
	Composition of lipid particles WP3601	4.24*E*−02	CETP

advancing drugs. Ten possible drug molecules were predicted using EnrichR based on transcriptome characteristics from the DSigDB database, including suloctidil, prenylamine, acetohexamide, terfenadine, prochlorperazine, 3′-azido-3′-deoxythymidine, chlorophyllin, etoposide, clioquinol, and propofol. The 10 potential medications are extracted in accordance with their *p*-value. Table 4 depicts the potential drugs in the DSigDB database for hub genes. These potential drugs are recommended for the hub genes, a common compound used to treat two diseases.

Discussion

Due to the high incidence and mortality of TB and COVID-19, the main target organ of both is the lung. More importantly, some research recently indicated that there is a strong association

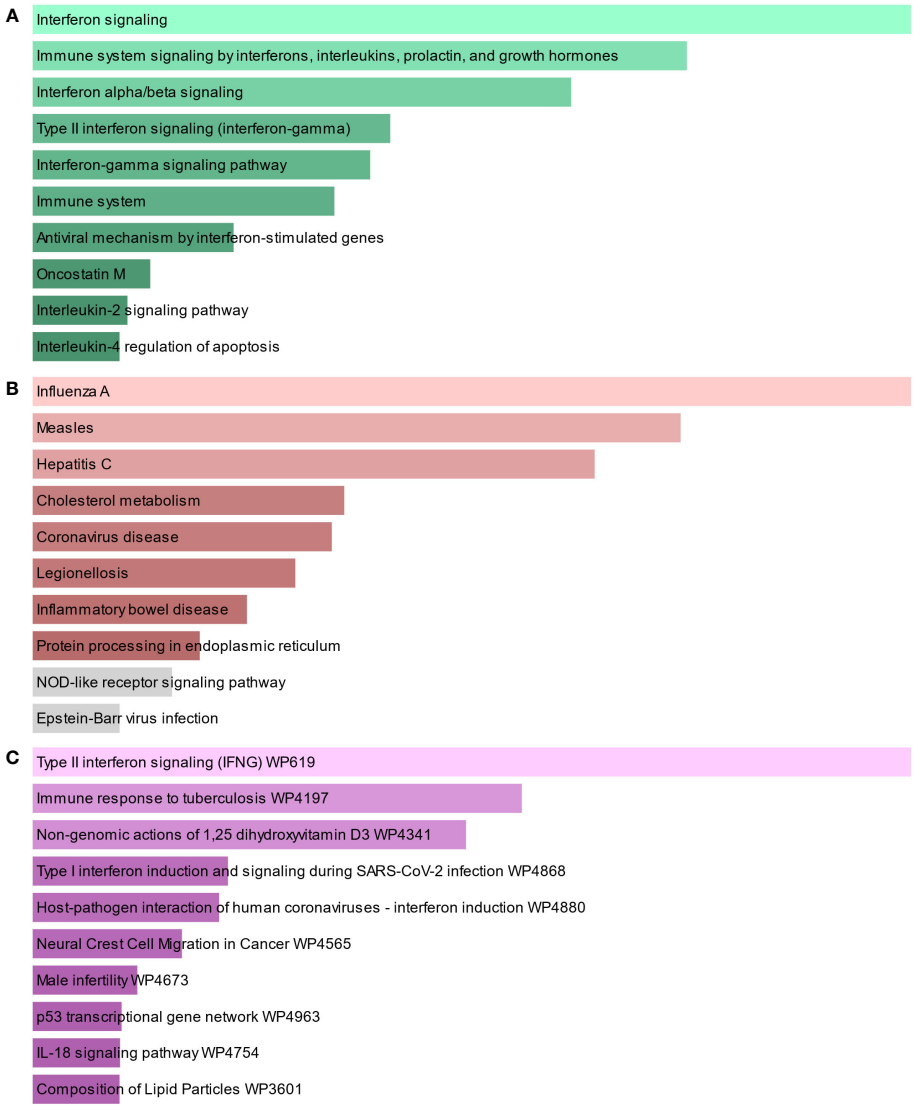

FIGURE 4
The bar graphs of the pathway enrichment of the shared DEGs between TB and COVID-19. **(A)** Bioplanet, **(B)** KEGG, and **(C)** WikiPathways.

between the onset and exacerbation of TB and COVID-19, and likewise, TB is a risk factor for COVID-19 (Fonseca et al., 2021; Gao et al., 2021; Visca et al., 2021). Therefore, it is crucial to explore the common pathogenesis, interaction, and connection between TB and COVID-19.

The enrichment analysis of gene ontology and pathways can help us understand the function and regulation mechanisms of genes in different physiological states. In this study, first of all, 96 common DEGs were identified through the differential analysis of gene expression abundance in transcriptional profiles and the analysis of Venn diagrams, which indicated that there is a certain degree of correlation and similarity between tuberculosis and COVID-19 in their pathogenesis. Subsequently, the functional enrichment analysis of common DEGs was carried out. The results of enrichment analysis showed that these common DEGs were mainly involved in viral genome replication and immune-related pathways. In coronaviruses, the viral genome replication that evades the immunity system may contribute to the viral process (Perlman and Netland, 2009). The negative regulation of viral genome replication is closely tied to the interferon response pathway, and interferon-γ (IFN-γ) is a genome replication negative regulator of SARS-COV-2 (Bhat et al., 2018; Trugilho et al., 2022). SARS-CoV-2 may trigger aggressive proinflammatory reactions in infected cells, including IL-2, IL1-β, IL-4, IL-6, IL-10, IFN-γ, and tumor necrosis factor-α (TNF-α) (Guan et al., 2020). Furthermore, T-cell depletion caused by *M. tuberculosis* affects host immunity, which increases the body's susceptibility to airborne pathogens, making the host more susceptible to COVID-19 infection (Rahman et al., 2009; Tadolini et al., 2020; Mousquer et al., 2021). In addition, elevated levels of the proinflammatory cytokines IL-6 and TNF-α in COVID-19 patients cause damage to the lymphatic system, resulting in immunosuppression, which contributes to the progression of TB (Tan et al., 2020; Hildebrand et al., 2022).

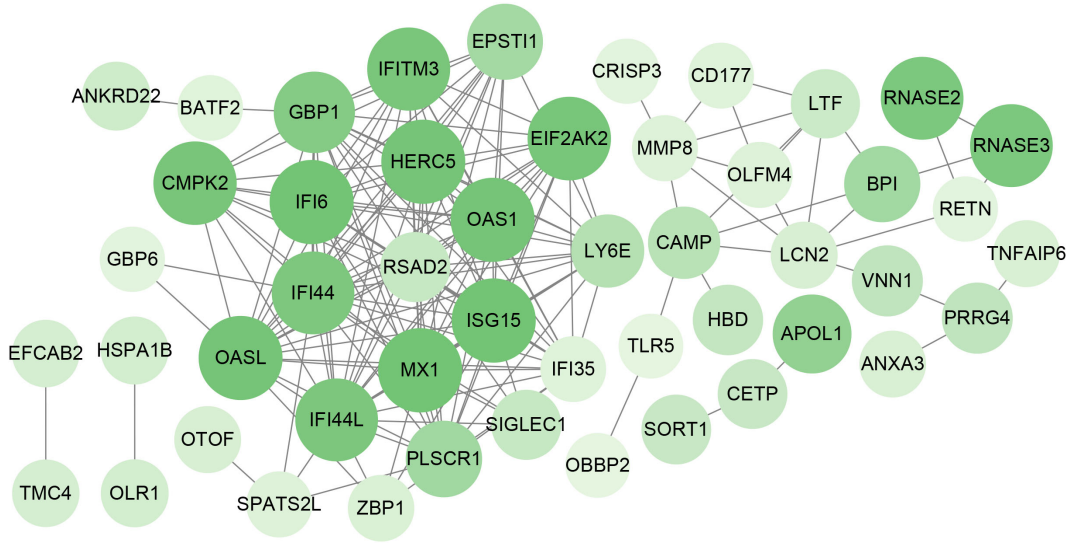

FIGURE 5
PPI network of the mutual DEGs between COVID-19 and TB. The nodes and the edges of the figure represent DEGs and the interactions between the nodes, respectively. The PPI network contains 176 edges and 49 nodes.

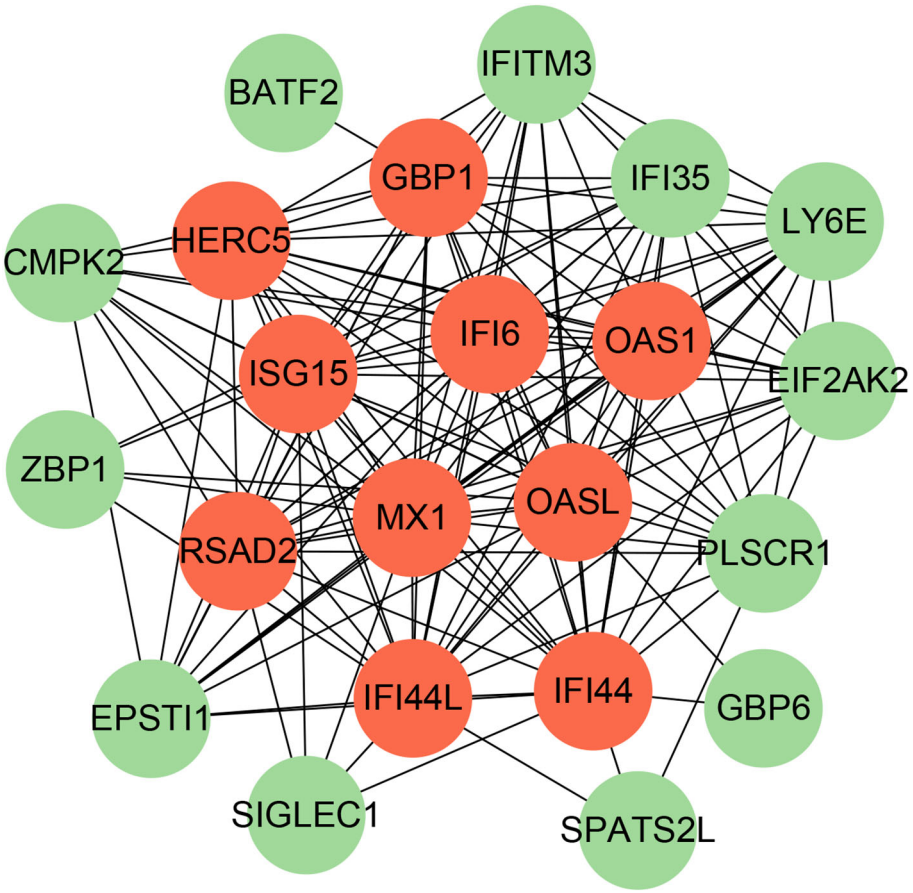

FIGURE 6
The PPI network from all the shared DEGs is constructed by the Cytohubba plugin in Cytosacpe. Red nodes present the selected top 10 hub genes. The network has 22 nodes and 142 edges.

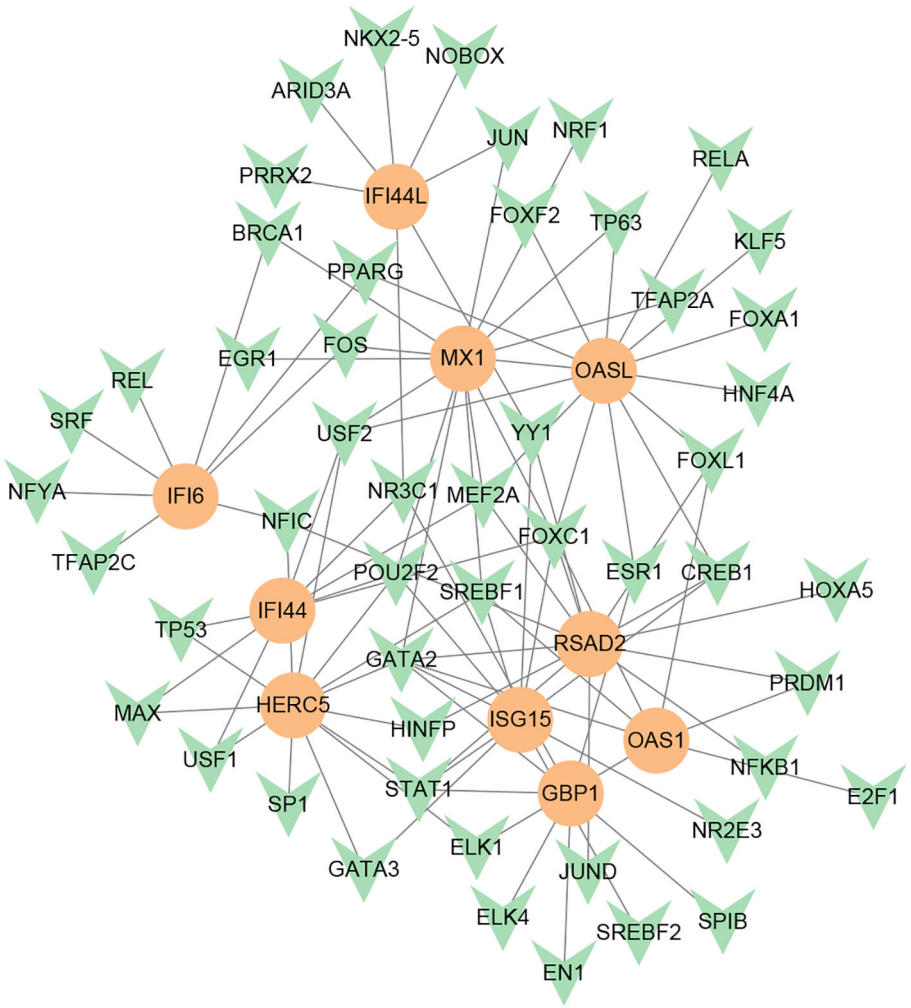

FIGURE 7
DEG-TF interaction network created by the NetworkAnalyst. The orange nodes represent gene symbols interacting with TFs, while the herringbone nodes represent TFs.

The shared DEGs are utilized to construct the PPI network, in which the hub gene is the most significant regulator in the common pathogenetic processes of TB and COVID-19. IFI44L is a potential target for reducing viral replication (Dediego et al., 2019). IFI44L promotes positive regulation and eliminates *M. tuberculosis* from human macrophages, highlighting its potential as a therapeutic target against *M. tuberculosis* infection (Jiang et al., 2021; Deng et al., 2023). IFI44 and IFI44L are antiproliferative factors that independently limit respiratory syncytial virus (RSV) infection (Busse et al., 2020). The expression levels of IFI44L and antiviral genes exhibit alterations during SARS-CoV-2 infection in various human cells, such as liver, respiratory epithelial, and stomach cells (Geerling et al., 2022). IFI44 is situated on human chromosome 1p31.1 and is part of the interferon-stimulated gene (ISG) family, which has a crucial function in regulating immunity and recognizing tumor cells (Lukhele et al., 2019; Boutin et al., 2021; Li et al., 2021a; Li et al., 2021b). IFI44 negatively regulates the IFN signaling pathway, promotes viral replication and bacterial proliferation, and is a crucial molecular target for immune evasion by SARS-CoV-2 (Zheng et al., 2022). Although ISG15 antiviral does not directly hinder the viral life cycle, it restricts viral transmission by joining the host response to modify the immune-metabolic network and restrain the availability of resources for viral amplification (Raso et al., 2020; Gold et al., 2022; Munnur et al., 2022). ISG15 can collaborate with IL-12 to stimulate T and NK cells to produce IFN-γ, which regulates *Mycobacterium tuberculosis* infection through an extracellular cytokine-like pathway (Bogunovic et al., 2012; Kimmey et al., 2017). Mx1 has noteworthy antiviral effects on hematopoietic cells, alongside its recognized antiviral activity on nonhematopoietic cells (Spitaels et al., 2019; Gough et al., 2022). OASL induces amyloid fibrillation in RIPK3, promoting virus-induced necrosis (Lee et al., 2023). OASL is strongly induced upon viral infection to enhance the antiviral IFN response (Leisching et al., 2017; Ghosh et al., 2019). The association between OASL and TB infection has also been validated, and OASL plays a central role in COVID-19 immunopathogenesis (Zhang et al., 2019; Hasankhani et al., 2021; Yi et al., 2021). RSAD2 is the direct suppressor of viral replication and facilitates TLR9- and TLR7-mediated production of IFN-α (Mantovani et al., 2022). The adaptive behavior of NK cells during viral infection is facilitated through STAT1-mediated epigenetic control of RSAD2 (Wiedemann et al., 2020). GBP1 was found to be one of the potential biomarkers of

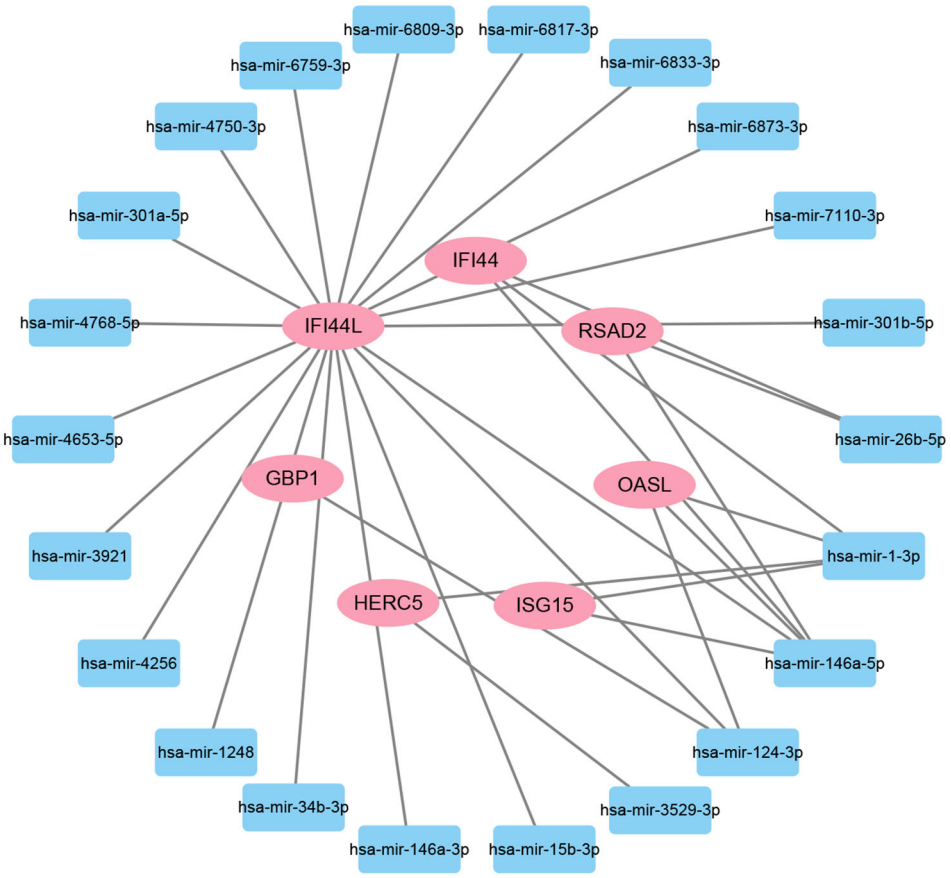

FIGURE 8
The regulatory interaction network of DEG-miRNAs. MiRNAs are presented by the square node, and gene symbols interacting with miRNAs are in an oval shape.

active TB, and its expression was negatively correlated with lymphocyte activity but positively correlated with myeloid and inflammatory cell activity (Perumal et al., 2020; Chen et al., 2022). In severe conditions of COVID-19, there is a high abundance of CXCL10+ and CCL2+ inflammatory macrophages that heavily express the GBP1 inflammatory gene (Zhang et al., 2020). OAS1 acts as a negative regulator of the expression of chemokines and interferon-responsive genes in human macrophages (Lee et al., 2019). Reduced OAS1 expression due to a common haplotype is proven to be related to the severity of COVID-19 (Banday et al., 2022). Genetically regulated loss of OAS1 expression contributes to impaired spontaneous clearance of SARS-CoV-2 and an increased risk of hospitalization for COVID-19 (Banday et al., 2021; Huffman et al., 2022). Compared to normal tissues, IFI6 is markedly upregulated in white blood cells from COVID-19 patients and nasopharyngeal tissues infected with SARS-COV-2 and is associated with antiviral immune modulation and clinical progression (Dong et al., 2022; Sun et al., 2023; Villamayor et al., 2023). The antiviral activity displayed by HERC5 makes them promising drug targets for the development of novel antiviral therapeutics that can augment the host antiviral response (Jacquet et al., 2020; Mathieu et al., 2021).

TFs and miRNAs that act as upstream regulators of these hub genes have also been discovered to better understand the pathological basis of these disease states. Transcription factor GATA2 is associated with hematopoietic dysfunction in severe COVID-19 patients (Wang et al., 2021). Downregulation of GATA2, involved in lymphocyte commitment, is also found in TB (Li et al., 2023). The phosphorylation of STAT1 was reportedly strengthened in severe COVID-19 cases that failed to induce transcription of interferon-stimulated response elements (ISRE) by unbalanced JAK/STAT signaling (Rincon-Arevalo et al., 2022). MiR-26b-5p targeted cyclooxygenase 2 (COX2), leading to a decrease in its expression. Consequently, there were considerable reductions in the levels of proinflammatory mediators such as prostaglandin E2 (PGE2), TNF-α, and IL-6 in retinal artery and human dermal microvascular endothelial cells (HMEC-1). This resulted in an effective inhibition of inflammation (Jiang et al., 2020). MiR-26b-5p was predicted to be regulated by spike, ACE, and histone deacetylation (HDAC) pathways in COVID-19 (Teodori et al., 2020). Although many previous studies have suggested that these TFs and miRNAs may have potential therapeutic effects, these analytical results require further experiments to confirm their effectiveness and authenticity.

Drugs tending to regulate the hub genes were identified from the DSigDB database. The hub genes, which act as regulators of the common pathogenic processes of both diseases and can lead to the simultaneous administration of antiviral and anti-TB drugs, have the potential to provide significant clinical benefit to this

10.3389/fcimb.2023.1280223

TABLE 4 Potential drugs for COVID-19 and TB.

Name	*p*-value	Chemical formula	Structure
Suloctidil HL60 UP	2.19*E*−22	$C_{20}H_{35}NOS$	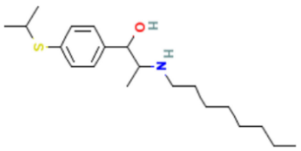
prenylamine HL60 UP	3.45*E*−21	$C_{24}H_{27}N$	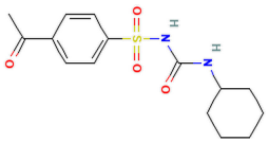
Acetohexamide PC3 UP	1.15*E*−19	$C_{15}H_{20}N_2O_4S$	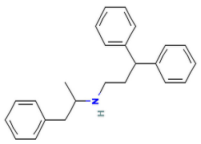
Terfenadine HL60 UP	1.17*E*−13	$C_{32}H_{41}NO_2$	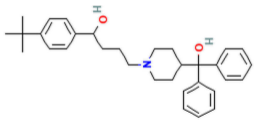
Prochlorperazine MCF7 UP	4.28*E*−11	$C_{20}H_{24}ClN_3S$	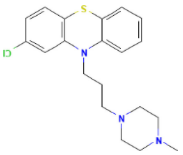
3′-Azido-3′-deoxythymidine CTD 00007047	8.64*E*−11	$C_{10}H_{13}N_5O_4$	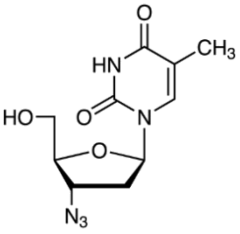
Chlorophyllin CTD 00000324	8.57*E*−10	$C_{34}H_{34}MgN_4O_6$	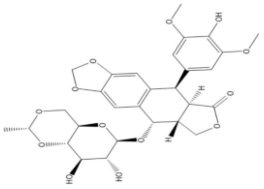
Etoposide HL60 UP	4.90*E*−09	$C_{29}H_{32}O_{13}$	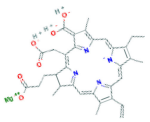
Clioquinol PC3 UP	6.60*E*−09	C_9H_5ClINO	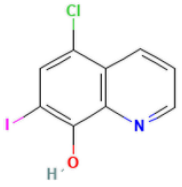
Propofol MCF7 UP	9.84*E*−09	$C_{12}H_{18}O$	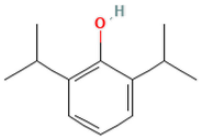

patient population. Some of the drugs identified in this study are proposed by different authors as therapeutics for the treatment of COVID-19 or TB, for example, (1) suloctidil is found to be one of the candidate drugs between COVID-19 and idiopathic pulmonary fibrosis (Chen et al., 2022); (2) acetohexamide is a nucleotide-binding domain (NBD)-binding drug that can be used against COVID-19 by preventing replication and viral attachment to the cell surface binding immunoglobin protein (csBiP) (Zhang et al., 2021); (3) The use of prochlorperazine has been shown to decrease the replication ability of SARS-CoV-2, which is linked to the ACE2 receptor. Also, prochlorperazine is found significant inhibition in lung pathology and lung viral load of SARS-CoV-2-challenged hamsters. Prochlorperazine can bind to G-quadruplexes (G4s), a secondary structure in nucleic acids that is known to impact numerous cellular processes, including viral replication and transcription. This binding can impede SARS-CoV-2 reverse transcription and ultimately reduce the lung viral load (Roy et al., 2023). (4) The application of chlorophyllin and molnupiravir as a specific antiviral drug for SARS-CoV-2 can diminish the detrimental genetic alterations and host cell harm caused by molnupiravir while enhancing the therapeutic effectiveness (Clark et al., 2022).

While the genes we have identified offer fresh perspectives on the creation of potential therapeutic targets for COVID-19 and TB, the validation of these gene targets and drugs requires continued investigation through experimental studies like cellular and animal models. Also, information and methodological biases preclude the full reproduction of potential genetic links using computational biology techniques. Additionally, translating experimental results into clinical applications remains a significant challenge. These are the main limitations of our current study and the focus of our future research.

Conclusion

To help get insights into the common pathogenetic processes between the SARS-CoV2 infection and TB, we utilized transcriptomic data analysis to determine the shared pathways and biomarkers in TB and COVID-19. There are 96 common DEGs of TB and COVID-19 identified by bioinformatics tools. GO terms and signaling pathway enrichment analysis revealed that 96 common DEGs were mainly involved in the regulation of viral genome replication and immune-related pathways. Moreover, through the PPI analysis of DEGs, the top 10 hub genes were extracted, including IFI44L, ISG15, MX1, IFI44, OASL, RSAD2, GBP1, OAS1, IFI6, and HERC5, which may be a therapeutic target for COVID-19 and help to find drug molecules and drug-target interactions. Also, gene–TF and gene–miRNA association were examined to gain a deeper understanding of COVID-19 progression. In addition, several potential drugs were listed for COVID-19 patients with TB treatment, including suloctidil, prenylamine, acetohexamide, terfenadine, prochlorperazine, 3′-azido-3′-deoxythymidine, chlorophyllin, etoposide, clioquinol, and propofol. We hope these findings may provide key perspectives for developing novel and effective medications to combat COVID-19 and TB.

Data availability statement

The original contributions presented in the study are included in the article/Supplementary Material. Further inquiries can be directed to the corresponding authors.

Author contributions

TH: Data curation, Methodology, Supervision, Writing – original draft. JH: Investigation, Supervision, Writing – original draft. XZ: Conceptualization, Project administration, Writing – review & editing. HP: Visualization, Writing – review & editing. FH: Investigation, Writing – review & editing. AD: Project administration, Writing – review & editing. BY: Conceptualization, Writing – original draft. NJ: Conceptualization, Writing – original draft. XL: Project administration, Writing – review & editing. KY: Methodology, Writing – review & editing. ZW: Investigation, Project administration, Writing – original draft.

Funding

The author(s) declare financial support was received for the research, authorship, and/or publication of this article. This work was supported by grants from the Natural Science Foundation of China (82370645, 82270643, 82070644, and 82170621), the National multidisciplinary collaborative diagnosis and treatment capacity building project for major diseases (TJZ202104), the Science and Technology Major Program of Sichuan Province (2022ZDZX0019), and the 1.3.5 project for disciplines of excellence, West China Hospital, Sichuan University (ZYJC18008, ZYGD22006).

Acknowledgments

We thank all of the patients who participated in the study and donated samples, as well as the GEO database, for providing the platform.

Conflict of interest

The authors declare that the research was conducted in the absence of any commercial or financial relationships that could be construed as a potential conflict of interest.

Publisher's note

claim that may be made by its manufacturer, is not guaranteed or endorsed by the publisher.

Supplementary material

The Supplementary Material for this article can be found online at: https://www.frontiersin.org/articles/10.3389/fcimb.2023.1280223/full#supplementary-material

SUPPLEMENTARY TABLE 1
The baseline characteristic of sample in COVID-19 (GSE196822).

SUPPLEMENTARY TABLE 2
The baseline characteristic of sample in TB (GSE126614).

SUPPLEMENTARY TABLE 3
The differential analysis matrix of COVID-19.

SUPPLEMENTARY TABLE 4
The differential analysis matrix of TB.

References

Aggarwal, A. N., Agarwal, R., Dhooria, S., Prasad, K. T., Sehgal, I. S., and Muthu, V. (2021). Active pulmonary tuberculosis and coronavirus disease 2019: A systematic review and meta-analysis. *PloS One* 16 (10), e0259006. doi: 10.1371/journal.pone.0259006

Al-Mustanjid, M., Mahmud, S. M. H., Royel, M. R. I., Rahman, M. H., Islam, T., Rahman, M. R., et al. (2020). Detection of molecular signatures and pathways shared in inflammatory bowel disease and colorectal cancer: A bioinformatics and systems biology approach. *Genomics* 112 (5), 3416–3426. doi: 10.1016/j.ygeno.2020.06.001

Banday, A. R., Stanifer, M. L., Florez-Vargas, O., Onabajo, O. O., Papenberg, B. W., Zahoor, M. A., et al. (2022). Genetic regulation of OAS1 nonsense-mediated decay underlies association with COVID-19 hospitalization in patients of European and African ancestries. *Nat. Genet.* 54 (8), 1103–1116. doi: 10.1038/s41588-022-01113-z

Bardou, P., Mariette, J., Escudié, F., Djemiel, C., and Klopp, C. (2014). jvenn: an interactive Venn diagram viewer. *BMC Bioinf.* 15 (1), 1–7. doi: 10.1186/1471-2105-15-293

Barrett, T., Wilhite, S. E., Ledoux, P., Evangelista, C., Kim, I. F., Tomashevsky, M., et al. (2013). NCBI GEO: archive for functional genomics data sets–update. *Nucleic Acids Res.* 41 (Database issue), D991–D995. doi: 10.1093/nar/gks1193

Behr, M. A., Kaufmann, E., Duffin, J., Edelstein, P. H., and Ramakrishnan, L. (2021). Latent Tuberculosis: Two Centuries of Confusion. *Am. J. Respir. Crit. Care Med.* 204(2), 142–148. doi: 10.1164/rccm.202011-4239PP

Benn, C. S., Netea, M. G., Selin, L. K., and Aaby, P. (2013). A small jab - a big effect: nonspecific immunomodulation by vaccines. *Trends Immunol.* 34 (9), 431–439. doi: 10.1016/j.it.2013.04.004

Bhat, M. Y., Solanki, H. S., Advani, J., Khan, A. A., Keshava Prasad, T. S., Gowda, H., et al. (2018). Comprehensive network map of interferon gamma signaling. *J. Cell Commun. Signal* 12 (4), 745–751. doi: 10.1007/s12079-018-0486-y

Bogunovic, D., Byun, M., Durfee, L. A., Abhyankar, A., Sanal, O., Mansouri, D., et al. (2012). Mycobacterial disease and impaired IFN-γ immunity in humans with inherited ISG15 deficiency. *Science* 337 (6102), 1684–1688. doi: 10.1126/science.1224026

Boutin, S., Hildebrand, D., Boulant, S., Kreuter, M., Rüter, J., Pallerla, S. R., et al. (2021). Host factors facilitating SARS-CoV-2 virus infection and replication in the lungs. *Cell Mol. Life Sci.* 78 (16), 5953–5976. doi: 10.1007/s00018-021-03889-5

Busse, D. C., Habgood-Coote, D., Clare, S., Brandt, C., Bassano, I., Kaforou, M., et al. (2020). Interferon-induced protein 44 and interferon-induced protein 44-like restrict replication of respiratory syncytial virus. *J. Virol.* 94 (18), e00297-20. doi: 10.1128/JVI.00297-20

Callaway, E. (2021). Fast-spreading COVID variant can elude immune responses. *Nature* 589 (7843), 500–501. doi: 10.1038/d41586-021-00121-z

Chakaya, J., Khan, M., Ntoumi, F., Aklillu, E., Fatima, R., Mwaba, P., et al. (2021). Global Tuberculosis Report 2020–Reflections on the Global TB burden, treatment and prevention efforts. *Int. J. Infect. Dis.* 113, S7–S12. doi: 10.1016/j.ijid.2021.02.107

Chan, J. F., Kok, K. H., Zhu, Z., Chu, H., To, K. K., Yuan, S., and Yuen, K. Y. (2020). Genomic characterization of the 2019 novel human-pathogenic coronavirus isolated from a patient with atypical pneumonia after visiting Wuhan. *Emerg. Microbes Infect.* 9 (1), 221–236. doi: 10.1080/22221751.2020.1719902

Chen, L., Hua, J., and He, X. (2022). Coexpression network analysis-based identification of critical genes differentiating between latent and active tuberculosis. *Dis. Markers* 2022, 2090560. doi: 10.1155/2022/2090560

Chen, Y., Guo, Y., Pan, Y., et al. (2020). Structure analysis of the receptor binding of 2019-nCoV. *Biochem. Biophys. Res. Commun.* 525 (1), 135–140. doi: 10.1016/j.bbrc.2020.02.071

Chen, Q., Xia, S., Sui, H., Shi, X., Huang, B., and Wang, T. (2022). Identification of hub genes associated with COVID-19 and idiopathic pu lmonary fibrosis by integrated bioinformatics analysis. *PloS One* 17 (1), e0262737. doi: 10.1371/journal.pone.0262737

Clark, N. F., Taylor-Robinson, A. W., and Heimann, K. (2022). Could chlorophyllins improve the safety profile of beta-d-N4-hydroxycy tidine versus N-hydroxycytidine, the active ingredient of the SARS-CoV -2 antiviral molnupiravir? *Ther. Adv. Drug Saf.* 13. 20420986221107753. doi: 10.1177/20420986221107753

Dediego, M. L., Martinez-Sobrido, L., and Topham, D. J. (2019). Novel functions of IFI44L as a feedback regulator of host antiviral responses. *J. Virol.* 93 (21), e01159-19. doi: 10.1128/JVI.01159-19

Del Rosario, R. C. H., Poschmann, J., Lim, C., Cheng, C. Y., Kumar, P., Riou, C., et al. (2022). Author Correction: Histone acetylome-wide associations in immune cells from individuals with active Mycobacterium tuberculosis infection. *Nat. Microbiol.* 7 (11), 1943. doi: 10.1038/s41564-022-01236-3

Deng, S., Shen, S., Liu, K., El-Ashram, S., Alouffi, A., Cenci-Goga, B. T., et al. (2023). Integrated bioinformatic analyses investigate macrophage-M1-related biomarkers and tuberculosis therapeutic drugs. *Front. Genet.* 14, 1041892. doi: 10.3389/fgene.2023.1041892

Deshpande, S. S., Joshi, A. R., and Shah, A. (2020). Aftermath of pulmonary tuberculosis: computed tomography assessment. *Pol. J. Radiol.* 85, e144–e154. doi: 10.5114/pjr.2020.93714

Dong, Z., Yan, Q., Cao, W., Liu, Z., and Wang, X. (2022). Identification of key molecules in COVID-19 patients significantly correlated with clinical outcomes by analyzing transcriptomic data. *Front. Immunol.* 13, 930866. doi: 10.3389/fimmu.2022.930866

Fonseca, C. A. Jr., Zanetti, G., and Marchiori, E. (2021). Pulmonary tuberculosis in a patient with COVID-19 pneumonia. *Rev. Soc. Bras. Med. Trop.* 54, e03142021. doi: 10.1590/0037-8682-0314-2021

Fornes, O., Castro-Mondragon, J. A., Khan, A., van der Lee, R., Zhang, X., Richmond, P. A., et al. (2020). JASPAR 2020: update of the open-access database of transcription factor binding profiles. *Nucleic Acids Res.* 48 (D1), D87–D92. doi: 10.1093/nar/gkz1001

Gao, Y., Liu, M., Chen, Y., Shi, S., Geng, J., and Tian, J. (2021). Association between tuberculosis and COVID-19 severity and mortality: A rapid systematic review and meta-analysis. *J. Med. Virol.* 93 (1), 194–196. doi: 10.1002/jmv.26311

Geerling, E., Pinski, A. N., Stone, T. E., DiPaolo, R. J., Zulu, M. Z., Maroney, K. J., et al. (2022). Roles of antiviral sensing and type I interferon signaling in the restriction of SARS-CoV-2 replication. *iScience* 25 (1), 103553. doi: 10.1016/j.isci.2021.103553

Gheblawi, M., Wang, K., Viveiros, A., Nguyen, Q., Zhong, J.-C., Turner, A. J., et al. (2020). Angiotensin-converting enzyme 2: SARS-CoV-2 receptor and regulator of the renin-angiotensin system: celebrating the 20th anniversary of the discovery of ACE2. *Circ. Res.* 126 (10), 1456–1474. doi: 10.1161/CIRCRESAHA.120.317015

Ghosh, A., Shao, L., Sampath, P., Zhao, B., Patel, N. V., Zhu, J., et al. (2019). Oligoadenylate-Synthetase-Family Protein OASL Inhibits Activity of the DNA Sensor cGAS during DNA Virus Infection to Limit Interferon Production. *Immunity* 50 (1), 51–63.e5. doi: 10.1016/j.immuni.2018.12.013

Gold, I. M., Reis, N., Glaser, F., and Glickman, M. H. (2022). Coronaviral PLpro proteases and the immunomodulatory roles of conjugated versus free Interferon Stimulated Gene product-15 (ISG15). *Semin. Cell Dev. Biol.* 132, 16–26. doi: 10.1016/j.semcdb.2022.06.005

Gough, M., Singh, D. K., Singh, B., Kaushal, D., and Mehra, S. (2022). System-wide identification of myeloid markers of TB disease and HIV-induced reactivation in the macaque model of Mtb infection and Mtb/SIV co-infection. *Front. Immunol.* 13, 777733. doi: 10.3389/fimmu.2022.777733

Guan, W. J., Ni, Z. Y., Hu, Y., Liang, W. H., Ou, C. Q., He, J. X., et al. (2020). Clinical characteristics of coronavirus disease 2019 in China. *N Engl. J. Med.* 382 (18), 1708–1720. doi: 10.1056/NEJMoa2002032

Hasankhani, A., Bahrami, A., Sheybani, N., Aria, B., Hemati, B., and Fatehi, F. (2021). Differential co-expression network analysis reveals key hub-high traffic genes as potential therapeutic targets for COVID-19 pandemic. *Front. Immunol.* 12, 789317. doi: 10.3389/fimmu.2021.789317

Hildebrand, R. E., Chandrasekar, S. S., Riel, M., Touray, B. J. B., Aschenbroich, S. A., and Talaat, A. M. (2022). Superinfection with SARS-CoV-2 Has Deleterious Effects on Mycobacterium bovis BCG Immunity and Promotes Dissemination of Mycobacterium tuberculosis. *Microbiol. Spectr.* 10 (5), e0307522. doi: 10.1128/spectrum.03075-22

Huang, T., Jiang, N., Song, Y., Pan, H., Du, A., Yu, B., et al. (2023a). Bioinformatics and system biology approach to identify the influences of SARS-CoV2 on metabolic unhealthy obese patients. *Front. Mol. Biosci.* 10, 1274463. doi: 10.3389/fmolb.2023.1274463

Huang, H.-Y., Lin, Y-C-D, Li, J., Huang, K.-Y., Shrestha, S., Hong, H.-C., et al. (2020). miRTarBase 2020: updates to the experimentally validated microRNA–target interaction database. *Nucleic Acids Res.* 48 (D1), D148–D154. doi: 10.1093/nar/gkz896

Huang, T., Yu, B., Zhou, X., Pan, H., Du, A., Bai, J., et al. (2023a). Exploration of the link between COVID-19 and alcoholic hepatitis from the perspective of bioinformatics and systems biology. *MedComm–Future Med.* 2 (2), e42. doi: 10.1002/mef2.42

Huang, T., Zheng, D., Song, Y., Pan, H., Qiu, G., Xiang, Y., et al. (2023b). Demonstration of the impact of COVID-19 on metabolic associated fatty liver disease by bioinformatics and system biology approach. *Medicine* 102 (35), e34570. doi: 10.1097/MD.0000000000034570

Huffman, J. E., Butler-Laporte, G., Khan, A., Pairo-Castineira, E., Drivas, T. G., Peloso, G. M., et al. (2022). Multi-ancestry fine mapping implicates OAS1 splicing in risk of severe COVID-19. *Nat. Genet.* 54 (2), 125–127. doi: 10.1038/s41588-021-00996-8

Jacquet, S., Pontier, D., and Etienne, L. (2020). Rapid evolution of HERC6 and duplication of a chimeric HERC5/6 gene in rodents and bats suggest an overlooked role of HERCs in mammalian immunity. *Front. Immunol.* 11, 605270. doi: 10.3389/fimmu.2020.605270

Jiang, S., Chen, Z., Lai, W., Mai, Q., Chen, D., Sun, S., et al. (2020). Decoction of heat-clearing, detoxifying and blood stasis removing relieves acute soft tissue injury via modulating miR-26b-5p/COX2 axis to inhibit inflammation. *Biosci. Rep.* 40 (12), BSR20201981. doi: 10.1042/BSR20201981

Jiang, H., Tsang, L., Wang, H., and Liu, C. (2021). IFI44L as a forward regulator enhancing host antituberculosis responses. *J. Immunol. Res.* 2021, 5599408. doi: 10.1155/2021/5599408

Jin, Y., Yang, H., Ji, W., Wu, W., Chen, S., Zhang, W., et al. (2020). Virology, epidemiology, pathogenesis, and control of COVID-19. *Viruses* 12 (4), 372. doi: 10.3390/v12040372

Kimmey, J. M., Campbell, J. A., Weiss, L. A., Monte, K. J., Lenschow, D. J., and Stallings, C. L. (2017). The impact of ISGylation during Mycobacterium tuberculosis infection in mice. *Microbes Infect.* 19 (4-5), 249–258. doi: 10.1016/j.micinf.2016.12.006

Kuleshov, M. V., Jones, M. R., Rouillard, A. D., Fernandez, N. F., Duan, Q., Wang, Z., et al. (2016). Enrichr: a comprehensive gene set enrichment analysis web server 2016 update. *Nucleic Acids Res.* 44 (W1), W90–W97. doi: 10.1093/nar/gkw377

Kvam, V. M., Liu, P., and Si, Y. (2012). A comparison of statistical methods for detecting differentially expressed genes from RNA-seq data. *Am. J. Bot.* 99 (2), 248–256. doi: 10.3732/ajb.1100340

Lee, S. A., Chang, L. C., Jung, W., Bowman, J. W., Kim, D., Chen, W., et al. (2023). OASL phase condensation induces amyloid-like fibrillation of RIPK3 to promote virus-induced necroptosis. *Nat. Cell Biol.* 25 (1), 92–107. doi: 10.1038/s41556-022-01039-y

Lee, W. B., Choi, W. Y., Lee, D. H., Shim, H., Kim-Ha, J., and Kim, Y. J. (2019). OAS1 and OAS3 negatively regulate the expression of chemokines and interferon-responsive genes in human macrophages. *BMB Rep.* 52 (2), 133–138. doi: 10.5483/BMBRep.2019.52.2.129

Leisching, G., Wiid, I., and Baker, B. (2017). The association of OASL and type I interferons in the pathogenesis and survival of intracellular replicating bacterial species. *Front. Cell Infect. Microbiol.* 7, 196. doi: 10.3389/fcimb.2017.00196

Li, Y., Liu, Y., Duo, M., Wu, R., Jiang, T., Li, P., et al. (2022). Bioinformatic analysis and preliminary validation of potential therapeutic targets for COVID-19 infection in asthma patients. *Cell Communication Signaling* 20 (1), 1–12. doi: 10.1186/s12964-022-01010-2

Li, F., Ma, Y., Li, X., Zhang, D., Han, J., Tan, D., et al. (2023). Severe persistent mycobacteria antigen stimulation causes lymphopenia through impairing hematopoiesis. *Front. Cell Infect. Microbiol.* 13, 1079774. doi: 10.3389/fcimb.2023.1079774

Li, Y., Qi, J., and Yang, J. (2021a). RTP4 is a novel prognosis-related hub gene in cutaneous melanoma. *Hereditas* 158 (1), 22. doi: 10.1186/s41065-021-00183-z

Li, Y., Zhang, J., Wang, C., Qiao, W., Li, Y., and Tan, J. (2021b). IFI44L expression is regulated by IRF-1 and HIV-1. *FEBS Open Bio* 11 (1), 105–113. doi: 10.1002/2211-5463.13030

Love, M. I., Huber, W., and Anders, S. (2014). Moderated estimation of fold change and dispersion for RNA-seq data with DESeq2. *Genome Biol.* 15 (12), 1–21. doi: 10.1186/s13059-014-0550-8

Lukhele, S., Boukhaled, G. M., and Brooks, D. G. (2019). Type I interferon signaling, regulation and gene stimulation in chronic virus infection. *Semin. Immunol.* 43, 101277. doi: 10.1016/j.smim.2019.05.001

Ma, H., He, Z., Chen, J., Zhang, X., and Song, P. (2021). Identifying of biomarkers associated with gastric cancer based on 11 topological analysis methods of CytoHubba. *Sci. Rep.* 11 (1), 1–11. doi: 10.1038/s41598-020-79235-9

Mantovani, S., Daga, S., Fallerini, C., Baldassarri, M., Benetti, E., Picchiotti, N., et al. (2022). Rare variants in Toll-like receptor 7 results in functional impairment and downregulation of cytokine-mediated signaling in COVID-19 patients. *Genes Immun.* 23 (1), 51–56. doi: 10.1038/s41435-021-00157-1

Mathieu, N. A., Paparisto, E., Barr, S. D., and Spratt, D. E. (2021). HERC5 and the ISGylation pathway: critical modulators of the antiviral immune response. *Viruses* 13 (6), 1102. doi: 10.3390/v13061102

Mousquer, G. T., Peres, A., and Fiegenbaum, M. (2021). Pathology of TB/COVID-19 Co-Infection: The phantom menace. *Tuberculosis (Edinb)* 126, 102020. doi: 10.1016/j.tube.2020.102020

Munnur, D., Banducci-Karp, A., and Sanyal, S. (2022). ISG15 driven cellular responses to virus infection. *Biochem. Soc. Trans.* 50 (6), 1837–1846. doi: 10.1042/BST20220839

Perlman, S., and Netland, J. (2009). Coronaviruses post-SARS: update on replication and pathogenesis. *Nat. Rev. Microbiol.* 7 (6), 439–450. doi: 10.1038/nrmicro2147

Perumal, P., Abdullatif, M. B., Garlant, H. N., Honeyborne, I., Lipman, M., McHugh, T. D., et al. (2020). Validation of differentially expressed immune biomarkers in latent and active tuberculosis by real-time PCR. *Front. Immunol.* 11, 612564. doi: 10.3389/fimmu.2020.612564

Pollard, C. A., Morran, M. P., and Nestor-Kalinoski, A. L. (2020). The COVID-19 pandemic: a global health crisis. *Physiol. Genomics* 52 (11), 549–557. doi: 10.1152/physiolgenomics.00089.2020

Ragab, D., Salah Eldin, H., Taeimah, M., Khattab, R., and Salem, R. (2020). The COVID-19 cytokine storm; what we know so far. *Front. Immunol.* 11, 1446. doi: 10.3389/fimmu.2020.01446

Rahman, S., Gudetta, B., Fink, J., Granath, A., Ashenafi, S., Aseffa, A., et al. (2009). Compartmentalization of immune responses in human tuberculosis: few CD8+ effector T cells but elevated levels of FoxP3+ regulatory t cells in the granulomatous lesions. *Am. J. Pathol.* 174 (6), 2211–2224. doi: 10.2353/ajpath.2009.080941

Raso, M. C., Djoric, N., Walser, F., Hess, S., Schmid, F. M., Burger, S., et al. (2020). Interferon-stimulated gene 15 accelerates replication fork progression inducing chromosomal breakage. *J. Cell Biol.* 219 (8), e202002175. doi: 10.1083/jcb.202002175

Rincon-Arevalo, H., Aue, A., Ritter, J., Szelinski, F., Khadzhynov, D., Zickler, D., et al. (2022). Altered increase in STAT1 expression and phosphorylation in severe COVID-19. *Eur. J. Immunol.* 52 (1), 138–148. doi: 10.1002/eji.202149575

Rivas, M. N., Ebinger, J. E., Wu, M., Sun, N., Braun, J., Sobhani, K., et al. (2021). BCG vaccination history associates with decreased SARS-CoV-2 seroprevalence across a diverse cohort of health care workers. *J. Clin. Invest.* 131 (2), e145157. doi: 10.1172/JCI145157

Roy, S. S., Sharma, S., Rizvi, Z. A., Sinha, D., Gupta, D., Rophina, M., et al. (2023). G4-binding drugs, chlorpromazine and prochlorperazine, repurposed agai nst COVID-19 infection in hamsters. *Front. Mol. Biosci.* 10, 1133123. doi: 10.3389/fmolb.2023.1133123

Rustad, T. R., Minch, K. J., Ma, S., Winkler, J. K., Hobbs, S., Hickey, M., et al. (2014). Mapping and manipulating the Mycobacterium tuberculosis transcriptome using a transcription factor overexpression-derived regulatory network. *Genome Biol.* 15 (11), 1–11. doi: 10.1186/s13059-014-0502-3

Shi, H., Han, X., Jiang, N., Cao, Y., Alwalid, O., Gu, J., et al. (2020). Radiological findings from 81 patients with COVID-19 pneumonia in Wuhan, China: a descriptive study. *Lancet Infect. Dis.* 20 (4), 425–434. doi: 10.1016/S1473-3099(20)30086-4

Smoot, M. E., Ono, K., Ruscheinski, J., Wang, P. L., and Ideker, T. (2011). Cytoscape 2.8: new features for data integration and network visualization. *Bioinformatics* 27 (3), 431–432. doi: 10.1093/bioinformatics/btq675

Song, Y., Huang, T., Pan, H., Du, A., Wu, T., Lan, J., et al. (2023). The influence of COVID-19 on colorectal cancer was investigated using bioinformatics and systems biology techniques. *Front. Med.* 10. doi: 10.3389/fmed.2023.1169562

Spinato, G., Fabbris, C., Polesel, J., Cazzador, D., Borsetto, D., Hopkins, C., et al. (2020). Alterations in smell or taste in mildly symptomatic outpatients with SARS-coV-2 infection. *JAMA* 323 (20), 2089–2090. doi: 10.1001/jama.2020.6771

Spitaels, J., Van Hoecke, L., Roose, K., Kochs, G., and Saelens, X. (2019). Mx1 in hematopoietic cells protects against thogoto virus infection. *J. Virol.* 93 (15), e00193-19. doi: 10.1128/JVI.00193-19

Subramanian, A., Tamayo, P., Mootha, V. K., Mukherjee, S., Ebert, B. L., Gillette, M. A., et al. (2005). Gene set enrichment analysis: a knowledge-based approach for interpreting genome-wide expression profiles. *Proc. Natl. Acad. Sci.* 102 (43), 15545–15550. doi: 10.1073/pnas.0506580102

Sun, Z., Ke, L., Zhao, Q., Qu, J., Hu, Y., Gao, H., et al. (2023). The use of bioinformatics methods to identify the effects of SARS-CoV-2 and influenza viruses on the regulation of gene expression in patients. *Front. Immunol.* 14, 1098688. doi: 10.3389/fimmu.2023.1098688

Szklarczyk, D., Gable, A. L., Lyon, D., Junge, A., Wyder, S., Huerta-Cepas, J., et al. (2019). STRING v11: protein-protein association networks with increased coverage, supporting functional discovery in genome-wide experimental datasets. *Nucleic Acids Res.* 47 (D1), D607–D613. doi: 10.1093/nar/gky1131

Tadolini, M., Codecasa, L. R., García-García, J. M., Blanc, F. X., Borisov, S., Alffenaar, J. W., et al. (2020). Active tuberculosis, sequelae and COVID-19 co-infection: first cohort of 49 cases. *Eur. Respir. J.* 56 (1), 2001398. doi: 10.1183/13993003.01398-2020

Tan, L., Wang, Q., Zhang, D., Ding, J., Huang, Q., Tang, Y. Q., et al. (2020). Lymphopenia predicts disease severity of COVID-19: a descriptive and predictive study. *Signal Transduct Target Ther.* 5 (1), 33. doi: 10.1038/s41392-020-0148-4

Teodori, L., Sestili, P., Madiai, V., Coppari, S., Fraternale, D., Rocchi, M. B.L., et al. (2020). MicroRNAs bioinformatics analyses identifying HDAC pathway as a putative target for existing anti-COVID-19 therapeutics. *Front. Pharmacol.* 11, 582003. doi: 10.3389/fphar.2020.582003

Trugilho, M. R. O., Azevedo-Quintanilha, I. G., Gesto, J. S. M., Moraes, E. C. S., Mandacaru, S. C., Campos, M. M., et al. (2022). Platelet proteome reveals features of cell death, antiviral response and viral replication in covid-19. *Cell Death Discovery* 8 (1), 324. doi: 10.1038/s41420-022-01122-1

Umakanthan, S., Sahu, P., Ranade, A. V., Bukelo, M. M., Rao, J. S., Abrahao-Machado, L. F., et al. (2020). Origin, transmission, diagnosis and management of coronavirus disease 2019 (COVID-19). *Postgraduate Med. J.* 96 (1142), 753–758. doi: 10.1136/postgradmedj-2020-138234

Villamayor, L., Rivero, V., López-García, D., Topham, D. J., Martínez-Sobrido, L., Nogales, A., et al. (2023). Interferon alpha inducible protein 6 is a negative regulator of innate immune responses by modulating RIG-I activation. *Front. Immunol.* 14, 1105309. doi: 10.3389/fimmu.2023.1105309

Visca, D., Ong, C. W. M., Tiberi, S., Centis, R., D'Ambrosio, L., Chen, B., et al. (2021). Tuberculosis and COVID-19 interaction: A review of biological, clinical and public health effects. *Pulmonology* 27 (2), 151–165. doi: 10.1016/j.pulmoe.2020.12.012

Wang, X., Wen, Y., Xie, X., Liu, Y., Tan, X., Cai, Q., et al. (2021). Dysregulated hematopoiesis in bone marrow marks severe COVID-19. *Cell Discovery* 7 (1), 60. doi: 10.1038/s41421-021-00296-9

Wiedemann, G. M., Geary, C. D., Lau, C. M., and Sun, J. C. (2020). Cutting edge: STAT1-mediated epigenetic control of rsad2 promotes clonal expansion of antiviral NK cells. *J. Immunol.* 205 (1), 21–25. doi: 10.4049/jimmunol.2000086

Yi, F., Hu, J., Zhu, X., Wang, Y., Yu, Q., Deng, J., et al. (2021). Transcriptional profiling of human peripheral blood mononuclear cells stimulated by mycobacterium tuberculosis PPE57 identifies characteristic genes associated with type I interferon signaling. *Front. Cell Infect. Microbiol.* 11, 716809. doi: 10.3389/fcimb.2021.716809

Yoo, M., Shin, J., Kim, J., Ryall, K. A., Lee, K., Lee, S., et al. (2015). DSigDB: drug signatures database for gene set analysis. *Bioinformatics* 31 (18), 3069–3071. doi: 10.1093/bioinformatics/btv313

Zhai, W., Wu, F., Zhang, Y., Fu, Y., and Liu, Z. (2019). The immune escape mechanisms of mycobacterium tuberculosis. *Int. J. Mol. Sci.* 20 (2), 340. doi: 10.3390/ijms20020340

Zhang, Y., Greer, R. A., Song, Y., Praveen, H., and Song, Y. (2021). In silico identification of available drugs targeting cell surface BiP to disrupt SARS-CoV-2 binding and replication: Drug repurposing approach. *Eur. J. Pharm. Sci.* 160, 105771. doi: 10.1016/j.ejps.2021.105771

Zhang, Y. W., Lin, Y., Yu, H. Y., Tian, R. N., and Li, F. (2019). Characteristic genes in THP−1 derived macrophages infected with Mycobacterium tuberculosis H37Rv strain identified by integrating bioinformatics methods. *Int. J. Mol. Med.* 44 (4), 1243–1254. doi: 10.3892/ijmm.2019.4293

Zhang, F., Mears, J. R., Shakib, L., Beynor, J. I., Shanaj, S., Korsunsky, I., et al. (2021). IFN- γ and TNF- α drive a CXCL10 + CCL2 + macrophage phenotype expanded in severe COVID-19 and other diseases with tissue inflammation. *Genome Med* 13(1), 64. doi: 10.1186/s13073-021-00881-3

Zheng, Q., Wang, D., Lin, R., Lv, Q., and Wang, W. (2022). IFI44 is an immune evasion biomarker for SARS-CoV-2 and Staphylococcus aureus infection in patients with RA. *Front. Immunol.* 13, 1013322. doi: 10.3389/fimmu.2022.1013322

Zhou, G., Soufan, O., Ewald, J., Hancock, R. E., Basu, N., and Xia, J. (2019). NetworkAnalyst 3.0: a visual analytics platform for comprehensive gene expression profiling and meta-analysis. *Nucleic Acids Res.* 47 (W1), W234–W241. doi: 10.1093/nar/gkz240

Ziegler, C. G. K., Allon, S. J., Nyquist, S. K., Mbano, I. M., Miao, V. N., Tzouanas, C. N., et al. (2020). SARS-coV-2 receptor ACE2 is an interferon-stimulated gene in human airway epithelial cells and is detected in specific cell subsets across tissues. *Cell* 181 (5), 1016–1035 e19. doi: 10.1016/j.cell.2020.04.035

Zou, X., Chen, K., Zou, J., Han, P., Hao, J., and Han, Z. (2020). Single-cell RNA-seq data analysis on the receptor ACE2 expression reveals the potential risk of different human organs vulnerable to 2019-nCoV infection. *Front. Med.* 14 (2), 185–192. doi: 10.1007/s11684-020-0754-0

Frontiers in
Cellular and Infection Microbiology

Investigates how microorganisms interact with their hosts

Explores bacteria, fungi, parasites, viruses, endosymbionts, prions and all microbial pathogens as well as the microbiota and its effect on health and disease in various hosts.

Discover the latest Research Topics

See more →

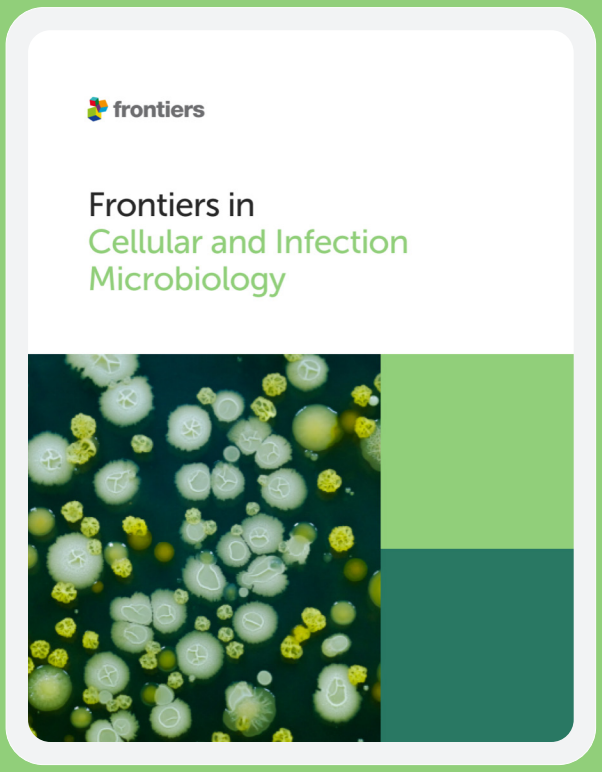

Frontiers

Avenue du Tribunal-Fédéral 34
1005 Lausanne, Switzerland
frontiersin.org

Contact us

+41 (0)21 510 17 00
frontiersin.org/about/contact